UNIVERSIDADE FEDERAL DE MINAS GERAIS

Instituto de Ciências Biológicas

Programa de Pós-Graduação em Bioquímica e Imunologia

Novas Abordagens na Produção de Anticorpos Monoclonais e Caracterização de Epitopos Lineares e Conformacionais de Metaloproteases de Venenos de Serpentes de Classe P-I

Francisco Santos Schneider

Belo Horizonte

2014

FRANCISCO SANTOS SCHNEIDER

Novas Abordagens na Produção de Anticorpos Monoclonais e Caracterização de Epitopos Lineares e Conformacionais de Metaloproteases de Venenos de Serpentes de Classe P-I

Tese apresentada ao Programa de Pós-Graduação em Bioquímica e Imunologia do Instituto de Ciências Biológicas da Universidade Federal de Minas Gerais como pré-requisito para obtenção do título de Doutor em Bioquímica.

ORIENTADOR: Prof. Dr. CARLOS D. CHÁVEZ OLÓRTEGUI

COORIENTADORES: Dr. ELÁDIO O. FLORES SANCHEZ

Dr. FRANCK MOLINA

Belo Horizonte

2014

Francisco Santos Schneider

Novas Abordagens na Produção de Anticorpos Monoclonais e Caracterização de Epitopos Lineares e Conformacionais de Metaloproteases de Venenos de Serpentes de Classe P-I

Tese apresentada ao Departamento de Bioquímica e Imunologia da Universidade Federal de Minas Gerais,
Belo Horizonte, 2014

Dr. Carlos Delfin Chávez Olórtegui

Carlos Delfin Chávez Olórtegui (Orientador) – UFMG

Dra. Ana Maria Moura da Silva

Ana Maria Moura da Silva – Instituto Butantan

Dr. Jonas Enrique Aguilar Perales

Jonas Enrique Aguilar Perales – FIOCRUZ

Dra. Maria Elena de Lima Perez Garcia

Maria Elena de Lima Perez Garcia- UFMG

Dr. Rodrigo Novaes Ferreira

Rodrigo Novaes Ferreira - UFMG

AGRADECIMENTOS

Ao meu orientador, Dr. Carlos Chávez Olórtegui, pela inspiração, pelo incentivo incessante e pelos conselhos sábios;

Ao meu co-orientador, Dr. Eládio O. Flores Sanchez, por me acompanhar e me ensinar, desde os primeiros passos da minha carreira científica;

À mon co-directeur de thèse, Dr. Fanck Molina, pour m'avoir inspiré pendant une année et pour m'avoir montré une vision differente de la science;

Aos colegas de laboratório de Imunoquímica de Proteínas, pela ajuda, incentivo, companheirismo e, como não poderia deixar de ser, pelas boas risadas;

À minha família, sobretudo a meus pais, pelo alicerce bem fundado que possibilitou a caminhada até aqui e, principalmente, por seus esforços imensuráveis para que eu chegasse até aqui;

À Bia, meu amor, pelo companheirismo inabalável, pelo colo nos momentos de dificuldade e por me fazer ver a vida mais colorida;

Aos amigos, Bruna, Filipe, Fábio, Ubá, Conrado e tantos outros, pelos momentos de distração que desanuviaram as pesadas tarefas do dia a dia;

Ao amigo e professor Ricardo, por fazer o trabalho mais leve e mais divertido;

Aux amis du laboratoire SYSDIAG à Montpellier, principalement Christophe, Sandrine, Sandra et Nicolas, qui m'ont très bien reçu et qui ont fait que mon séjour en France a été très plaisant;

Aos amigos do Laboratório de Bioquímica e Química de Proteínas de Fundação Ezequiel Dias, principalmente Gustavo, Siléa e Dário pelos ensinamentos e pela disponibilidade;

A todos aqueles que participaram, direta ou indiretamente, da construção e viabilização deste projeto, incluindo os amigos Dário, Jamil e muitos outros sem os quais não seria possível a realização deste;

Às agencias financiadoras, CAPES, CNPQ e FAPEMIG, por possibilitarem financeiramente a execução deste trabalho.

“Uma coisa que aprendi nessa longa vida: toda nossa ciência, comparada com a realidade, é primitiva e infantil, ainda sim é a coisa mais preciosa que nós temos.”

Albert Einstein

RESUMO

Este trabalho apresenta-se na forma de três artigos publicados em revistas internacionais indexadas. Cada artigo está contido em um capítulo da parte de RESULTADOS. Cada capítulo apresenta seu resumo individualizado. Aqui, faremos a descrição do conteúdo de cada capítulo:

O primeiro artigo (Artigo 1 – The novel metalloproteinase atroxlysin-I from Peruvian *Bothrops atrox* (Jergón) snake venom acts both on blood vessel ECM and platelets) descreve a caracterização bioquímica da primeira metaloprotease de classe P-I do veneno de *Bothrops atrox* a ser purificada.

No segundo capítulo dos RESULTADOS (Artigo 2 – Use of a Synthetic Biosensor for Neutralizing Activity-Biased Selection of Monoclonal Antibodies Against Atroxlysin-I, an Hemorrhagic Metalloproteinase from *Bothrops atrox* Snake Venom), descrevemos a produção de anticorpos monoclonais anti-atroxlisina-I baseada em um novo método funcional de seleção de clones produtores de anticorpos monoclonais neutralizantes, assim como suas caracterizações imunoquímicas, além da identificação de epitopos lineares de atroxlisina-I utilizando o IgG policlonal anti-atr-I.

Finalmente, o terceiro capítulo dos RESULTADOS (Artigo 3 – Mimotopes of mutalysin-II from *Lachesis muta* snake venom induce hemorrhage inhibitory antibodies upon vaccination of rabbits) descreve a caracterização dos epitopos conformacionais reconhecidos pelo anticorpo monoclonal LmmAbB2D4. A identificação de mimotopos de Mutalisina-II foi feita a partir da técnica de phage display aliada à técnica de SPOT síntese.

Cada artigo apresenta sua discussão em separado. Ao final do terceiro artigo uma discussão ampla e integrada dos três artigos é apresentada.

ABSTRACT

This work is presented in format of three published manuscripts in indexed international journals. Each article is located in one separated chapter within RESULTS. Once each paper presents its own ABSTRACT, here we briefly describe the content of the chapters:

The first article (Artigo 1 – The novel metalloproteinase atroxlysin-I from Peruvian *Bothrops atrox* (Jergón) snake venom acts both on blood vessel ECM and platelets) describes for the first time the purification and biochemical characterization of a P-I class metalloproteinase from *Bothrops atrox* venom.

In the second chapter of our RESULTS (Artigo 2 – Use of a Synthetic Biosensor for Neutralizing Activity-Biased Selection of Monoclonal Antibodies Against Atroxlysin-I, an Hemorrhagic Metalloproteinase from *Bothrops atrox* Snake Venom), we produce monoclonal antibodies against atroxlysin-I using a new functional method for the selection of clones able to produce neutralizing monoclonal antibodies, as well as their immunochemical characterization and the identification of continuous epitopes of atroxlysin-I.

Finally, the third manuscript presented in our RESULTS (Artigo 3 – Mimotopes of mutalysin-II from *Lachesis muta* snake venom induce hemorrhage inhibitory antibodies upon vaccination of rabbits) characterizes conformational epitopes recognized by the monoclonal antibody LmmAbB2D4 against mutalysin-II. Mimotopes of mutalysin-II was identified using the phage display and SPOT synthesis techniques.

Every article presents an individual discussion. At the end of the last manuscript a comprehensive and integrative discussion of the three papers is presented.

LISTA DE FIGURAS

Figura 1. Filogenia dos Squamata 12

Figura 2. Posições das presas inoculadoras de veneno..... 14

Figura 3. *Bothrops atrox* e sua distribuição geográfica..... 15

Figura 4. Estimativa global de acidentes ofídicos por região..... 17

Figura 5. Sintomas locais e sistêmicos típicos do envenenamento botrópico..... 18

Figura 6. Composição geral por famílias de proteínas de venenos de *B. atrox* de diferentes localidades amazônicas..... 20

Figura 7. Toxinas de venenos de serpentes atuantes sobre o sistema hemostático 22

Figura 8. Esquema simplificado da classificação das SVMPs de acordo com os motivos apresentados em suas estruturas 25

Figura 9. Sítio ativo das SMVPs 26

Figura 10. Representação esquemática dos diferentes tipos de epítopos 31

Figura 11. Emissão de fluorescência de peptídeos FRET após clivagem proteolítica dos mesmos..... 33

Figura 12. Reatividade do IgG de coelho anti-atr-I frente à sequência primária de atr-I por SPOT..... 59

Figura 13. Regiões reconhecidas de Atr-I pelo IgG de coelho anti-atr-I e sítio catalítico e “met-turn” de atr-I 60

Figura 14. Reconhecimento dos epitopos lineares sintetizados pelo IgG anti-Atr-I..... 61

Figura 15. Alinhamento das sequências primárias de Atr-I e Batroxase..... 73

Figura 16. Alinhamento entre Atroxlisina-I, Mutalisina-II e Neuwiedase, mostrando seus epitopos lineares 77

Figura 17. Alinhamento dos mimotopos de mutalisina-II reconhecidos pelo anticorpo monoclonal LmmAbB2D4. 79

Figura 18. Possíveis resíduos da LHF-II que são mimetizados pelos mimotopos do veneno da serpente *Lachesis muta muta* selecionados por Phage Display..... 80

LISTA DE TABELAS

Tabela 1. Acidentes ofídicos por regiões brasileiras em 2011. 17

Tabela 2. Classificação da gravidade do acidente botrópico. 19

Tabela 3. Efeito do IgG de coelho anti-Atr-I sobre diferentes substratos. 60

LISTA DE SIGLAS E ABREVIATURAS

Abz – Ácido amino-benzóico

Atr-I – Atroxlisina-I

BM – Membrana basal

CRISP – Proteínas Secretadas Ricas em Cisteína

CTLs – Proteínas Semelhantes à Lectina do tipo C

DMC – Dimetil-caseína

ECM – Matriz Extracelular

EDDnp – Etileno-Diamina-Dinitrofenil

ELISA – Enzyme Linked Immunosorbent Assay

FRET – Supressão Intramolecular de Fluorescência

LAO – L-Aminoácido Oxidase

LmmAbB2D4 – Anticorpo Monoclonal anti-mut-II

mAbs – Anticorpos Monoclonais

MABap1 – Anticorpo Monoclonal anti-BaP1

mAbatrs – Anticorpos Monoclonais anti-atr-I

MAJar - Anticorpo Monoclonal anti-jararagina

Mut-I – Mutalisina-I

Mut-II – Mutalisina-II

OMS – Organização Mundial de Saúde

PI-SVMP – Metaloprotease de Venenos de Serpente de Classe P-I

PIII-SVMP – Metaloprotease de Venenos de Serpente de Classe P-III

PLA_2 – Fosfolipase A_2

SerPro – Serino Protease

SVMP – Metaloprotease de Venenos de Serpentes

1. INTRODUÇÃO 12

1.1. FILOGENIA DAS SERPENTES E O SURGIMENTO DO VENENO 12
1.2. A SERPENTE BOTHROPS ATROX *E* LACHESIS MUTA MUTA 14
1.3. OS ACIDENTES OFÍDICOS 16
1.3.1. Epidemiologia 16
1.3.2. Quadro clínico do acidente botrópico 18
1.4. O VENENO DE *BOTHROPS ATROX* 19
1.5. AS METALOPROTEASES DE VENENOS DE SERPENTES 24
1.6. A SOROTERAPIA 27
1.7. EPITOPOS DE METALOPROTEASES DE VENENOS DE SERPENTES 30
1.8. OS ANTICORPOS MONOCLONAIS 31
1.9. PEPTÍDEOS FRET 32

2. OBJETIVOS 34

2.1. OBJETIVO GERAL 34
2.2. OBJETIVOS ESPECÍFICOS 34

3. RESULTADOS 35

3.1. ARTIGO 1 – THE NOVEL METALLOPROTEINASE ATROXLYSIN-I FROM PERUVIAN *BOTHROPS ATROX* (JERGÓN) SNAKE VENOM ACTS BOTH ON BLOOD VESSEL ECM AND PLATELETS 36
3.2. ARTIGO 2 – USE OF A SYNTHETIC BIOSENSOR FOR NEUTRALIZING ACTIVITY-BIASED SELECTION OF MONOCLONAL ANTIBODIES AGAINST ATROXLYSIN-I, AN HEMORRHAGIC METALLOPROTEINASE FROM *BOTHROPS ATROX* SNAKE VENOM 49
3.2.1. Resultados não publicados 59
3.3. ARTIGO 3 – MIMOTOPES OF MUTALYSIN-II FROM *LACHESIS MUTA* SNAKE VENOM INDUCE HEMORRHAGE INHIBITORY ANTIBODIES UPON VACCINATION OF RABBITS 63

4. DISCUSSÃO 72

5. CONCLUSÕES 81

6. PERSPECTIVAS 83

7. REFERÊNCIAS 84

8. ANEXOS – OUTROS TRABALHOS PUBLICADOS 95

1. Introdução

1.1. Filogenia das serpentes e o surgimento do veneno

Os répteis da Ordem Squamata estão entre os animais de maior sucesso adaptativo, estando presente em praticamente todo o globo. Apesar da sistemática e da filogenia dos Squamatas não estar totalmente esclarecida, estudos morfológicos e moleculares recentes sugerem que dentro de Squamata o clado monofilético Toxicofera abranja as Subordens das Serpentes, Anguimorpha e Iguania (Figura 1) [1-11].

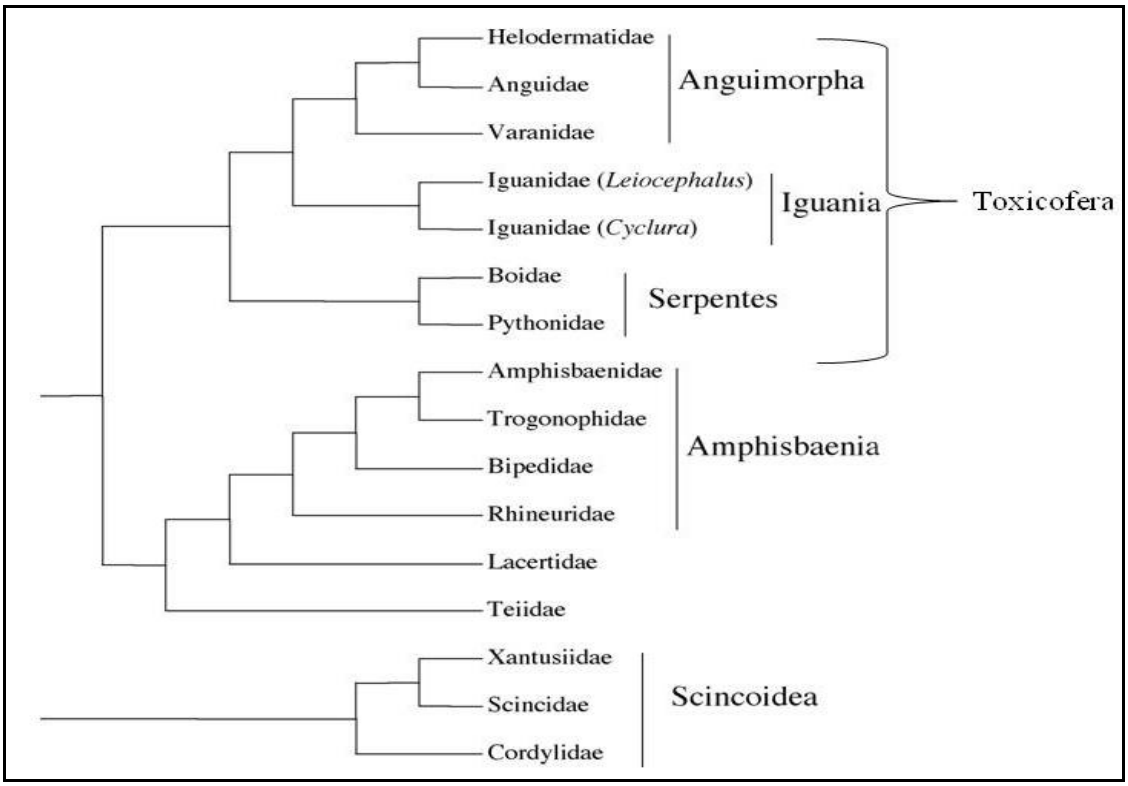

Figura 1. Filogenia dos Squamata. Fonte: Adaptado de Figuras suplementares de Fry, et al. (2006) [11].

O veneno surge cedo na história evolutiva das Squamatas – cerca de 200 milhões de anos atrás [11-13] – e, apesar de ser uma característica comum e ancestral para todos os representantes Toxicofera, é, principalmente, no grupo das Serpentes que o veneno torna-se mais complexo e passa a ter papel chave na evolução e diversificação deste grupo [1,11-15].

Evolutivamente, o veneno é uma secreção produzida em uma glândula especializada de um animal e injetada em outro, promovendo distúrbios em processos fisiológicos e/ou bioquímicos de modo a facilitar o processo de alimentação e defesa do animal produtor [16]. A peçonha pode atuar pela ação de substâncias que auxiliam nas funções enzimáticas da digestão, assim como na imobilização e captura das presas [11,12,16].

Aparentemente, proteínas ancestrais secretadas com diferentes atividades biológicas e envolvidas em processos fisiológicos comuns de diversos tecidos originaram as toxinas dos venenos dos Toxicofera. A duplicação gênica destas moléculas ancestrais, aliada à subsequente expressão específica destas moléculas em um novo tecido, resultou na criação de famílias multigênicas específicas das glândulas de veneno [12,15,17]. A repetição de novos processos de duplicação gênica seguidos de intensa diversificação destes genes (via mutação randômica, conversão gênica e crossing-over desigual, por exemplo) acarretou no processo de neofuncionalização das toxinas, com surgimento de atividades biológicas derivadas e manutenção do gene original da proteína ancestral [12-15,17]. A surpreendente variabilidade inter e intraespecífica encontrada na composição dos venenos de serpentes [18-21] é resultado de forte seleção natural positiva e adaptação a dietas específicas de cada grupo/espécie/população de serpente [22].

A diversificação do veneno teve papel central na impressionante evolução ocorrida na subordem das Serpentes durante a Era Cenozoica [13,14]. Atualmente, a subordem das Serpentes é formada por aproximadamente 3.400 espécies [9], encontradas em todos os continentes, exceto na Antártica e nos oceanos Pacífico e Índico [10].

Mais de 80% das espécies viventes de serpentes (~ 2720 espécies) formam o clado Caenophidia (*sensu* [5]), o qual inclui todas as espécies de serpentes peçonhentas conhecidas [1]. Os representantes dos Caenophidia são conhecidos como “serpentes modernas” e a grande maioria de representantes deste grupo utiliza o veneno em conjunto com a constrição para abater suas presas [4,5]. De acordo Pyron e colaboradores (2011)[23], as serpentes modernas podem ser divididas em sete famílias: Colubridae, Elapidae, Homalopsidae, Lamprophiidae, Pareatidae, Viperidae, e Xenodermatidae.

Nessas famílias, associados à glândula produtora de veneno podem existir dentes modificados (presas) especializados na inoculação do veneno [14,24,25]. Quando existentes, o par de presas inoculadoras de veneno fixa-se na maxila (uma presa de cada lado da maxila) e pode localizar-se rostral (anterior) ou caudalmente (posteriormente) (Figura 2) [14,15,24].

Serpentes com dentição áglifa não possuem qualquer tipo de dentição especializada na inoculação de veneno [14,15]. Nas serpentes opistóglifas, as presas inoculadoras de veneno se localizam caudalmente na maxila e a dentição especializada em inocular o veneno é fixa e de pequeno porte (Figura 2). As presas caudais podem, ou não, apresentar um canal/sulco para a passagem do veneno. As serpentes que possuem os tipos de dentição áglifa e opistóglifa são consideradas não peçonhentas (do ponto de vista antropocêntrico) e não representam interesse médico.

Nas serpentes que possuem o sistema de injeção de veneno rostral, as presas inoculadoras são ocas, possuindo um canal central por onde o veneno passa antes de ser injetado no alvo da serpente. As presas inoculadoras rostrais podem ser fixas e de pequeno tamanho (dentição proteróglifa, típica da família Elapidae - e.g. corais verdadeiras, gênero *Micrurus*) ou retráteis e de maior tamanho (dentição solenóglifa, típica da família Viperidae - e.g. jararacas, cascavéis, e surucucus – família Viperídae) (Figura 2) [14,15]. Estas serpentes são consideradas de importância médica, sendo responsáveis por quase a totalidade de acidentes acometendo humanos.

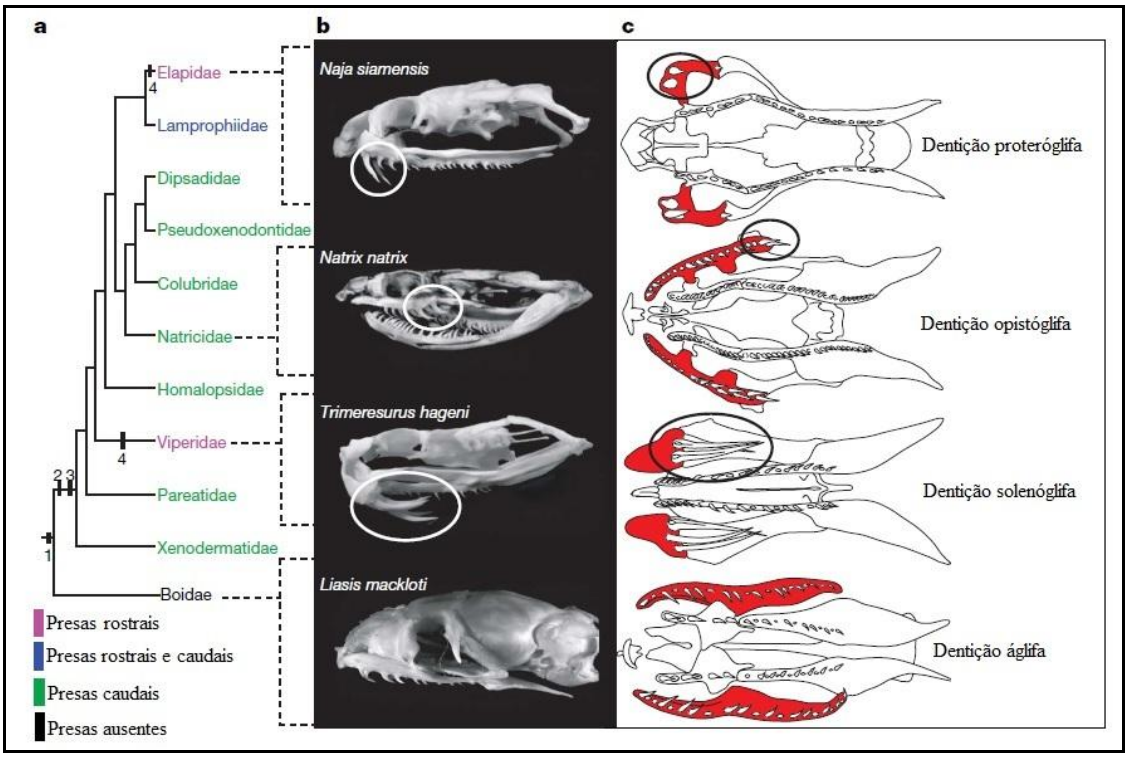

Figura 2. Posições das presas inoculadoras de veneno. (a) Filogenia sugerida por Vidal *et al.* (2007)[5]; (b) Vista lateral de crânios de serpentes; (c) Vista ventral esquemática do palato (maxila em vermelha, presas circuladas) (Tipos de dentição - de cima para baixo: dentição do tipo proteróglifa; opistóglifa, solenóglifa e áglifa, respectivamente). As apomorfias estão indicadas pelos números nos nodos da árvore filogenética: (1) Lâmina dental maxilar contínua, sem regiões especializadas – condição ancestral dos Caenophidia; (2) Evolução da lâmina dental maxilar rostral – desenvolvimento independente da dentição rostral e caudal; (3) Começo da diferenciação da dentição caudal juntamente com a glândula de veneno; (4) Perda da lâmina dental rostral e desenvolvimento das presas rostrais. Fonte: Adaptado de Vonk *et al.* (2008)[24].

1.2. As serpentes *Bothrops atrox* e *Lachesis muta muta*

A família Viperidae é composta por três subfamílias: Azemiopinae, Viperinae e Crotalinae, sendo os representantes da última subfamília os viperídeos encontrados nas Américas [10,23].

Bothrops atrox é um viperídeo vivíparo da subfamília Crotalinae facilmente encontrada nas florestas equatoriais de terras baixas em toda a América do Sul a leste da cordilheira dos

Andes (Figura 3) [26-28]. Esta serpente de hábitos terrestre e, preferencialmente, noturnos pode chegar a 1,80 metros de comprimento. De coloração acinzentada com tons marrons e oliva, indivíduos desta espécie se camuflam facilmente no solo das florestas tropicais. Possui uma cabeça triangular em formato de lança, típica dos viperídeos (Figura 3) [26]. O indivíduo jovem se alimenta de lagartos e artrópodes, enquanto o adulto caça, preferencialmente, pequenos mamíferos. Jovem e adulto forrageiam utilizando a tática "senta e espera" (emboscada) [26].

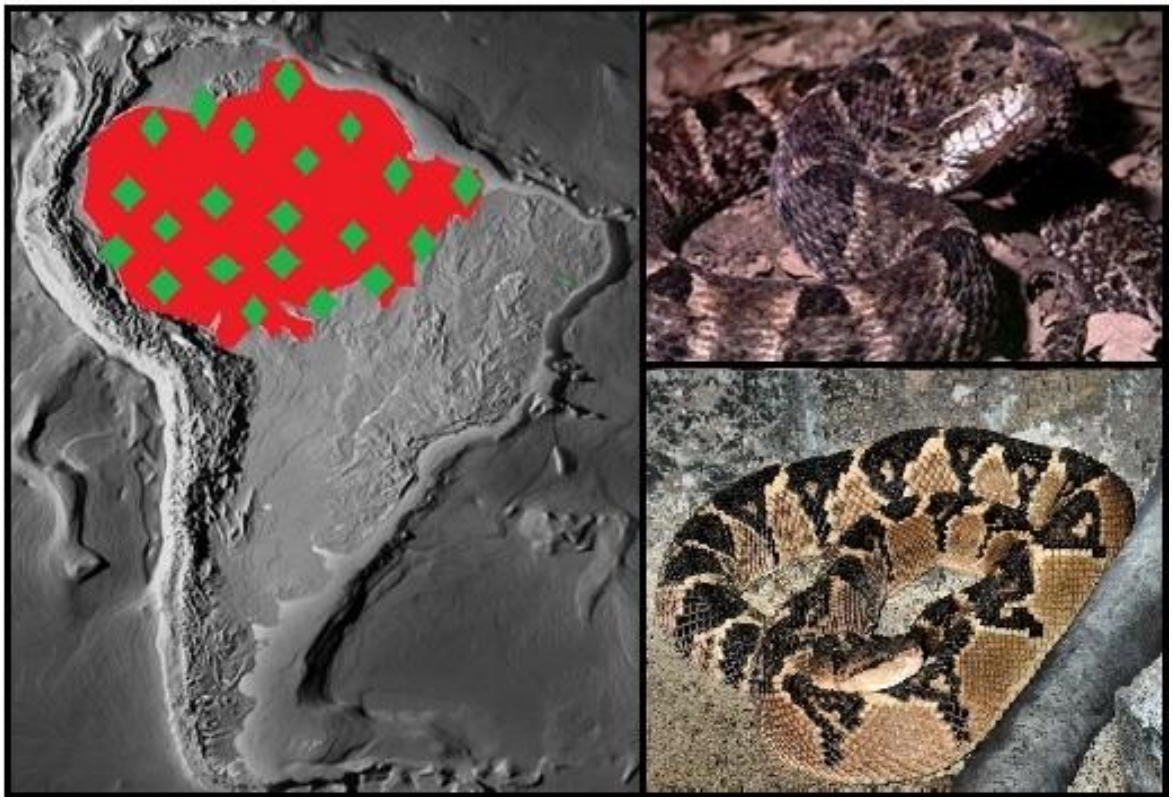

Figura 3. *Bothrops atrox* e Lachesis muta muta e suas distribuições geográficas. À esquerda, as regiões habitadas pelas serpentes *B. atrox* (em vermelho) e por *Lachesis muta muta* (losangos verdes). À direita acima *B. atrox* e à direita abaixo *L. muta muta.* Fonte: Adaptado de http://www.toxinology.com

Coabitando a mesma região amazônica da América do Sul que *Bothrops atrox*, encontram-se indivíduos da subespécie *Lachesis muta muta*, considerado o maior viperídeo do mundo, podendo chegar a mais de 3,5 metros. De coloração que varia do amarelado ao verde escuro, estas serpentes apresentam um padrão típico de triângulos laterais invertidos de coloração escura em seu dorso (Figura 3). A serpente *L. muta muta* vibra sua cauda quando em estado de alerta, mas não possui guizo. Apresenta hábitos diurnos, e é encontrada em matas primárias, secundárias, ou ainda em campos abertos. Estes animais não se adaptam bem ao cativeiro, sendo de difícil manutenção o que ocasiona escassez de veneno para a produção de antissoros específicos para esta serpente [29,30].

Assim como todos os viperídeos sul-americanos, ambos apresentam dentição solenóglifa, sendo de grande importância médica na América do Sul, onde, juntos, pode representar até 95% dos acidentes ofídicos [31-34].

1.3. Os acidentes ofídicos

1.3.1. Epidemiologia

Acidentes causados por animais peçonhentos são um grave problema de saúde pública [35]. A incidência destes acidentes varia de país para país e, dentro de um mesmo país, entre suas regiões, sendo influenciada por fatores como clima, parâmetros ecológicos e biodiversidade das espécies envolvidas, distribuição das serpentes peçonhentas, densidade populacional humana, atividades econômicas exercidas, tipo de habitação da população humana, entre outros [36]. A mortalidade e morbidade associadas aos acidentes ofídicos estão diretamente relacionadas à falta de investimentos públicos em saúde [37].

Apesar do sistema de notificações de acidentes ofídicos ser deficitário, estima-se que em 2007 mais de 1,8 milhões de casos de acidentes ofídicos tenham acontecido em todo o mundo [38]. A grande maioria destes acidentes acomete regiões tropicais e em desenvolvimento ao redor do globo (Figura 4), afetando principalmente trabalhadores rurais de comunidades subsistentes (80-90% dos casos) e fazendo com que possa ser considerado como um risco laboral diário para esses trabalhadores [31,36-39]. Desta forma, desde 2009 a Organização Mundial de Saúde (OMS) considera o acidente ofídico como uma Condição Tropical Negligenciada [38,39].

A mortalidade também pode variar muito entre países e/ou entre regiões de um país. Entre os principais fatores que influenciam as diferenças de taxas de mortalidade, podemos citar: (1) a espécie envolvida no acidente; (2) variabilidade intraespecífica na composição dos venenos – relacionados a parâmetros como idade, tamanho, sexo, dieta e habitat do espécime; (3) tempo entre o acidente e a transferência do paciente para um centro médico; (4) disponibilidade de recursos terapêuticos e de soros antiofídicos apropriados; e (5) fatores etnoantropológicos – e.g. procura por tratamentos tradicionais, típicos de certas comunidades [36].

No Brasil, cerca de 30 mil acidentes ocorrem anualmente, o que representa uma incidência de aproximadamente 16 casos/100 mil habitantes/ano, número muito similar àqueles encontrados em diversos países latino-americanos [36,38,40-42]. No entanto, se levarmos em consideração somente a região norte do país, onde se encontra a Amazônia brasileira, mais de

nove mil casos de acidentes ofídicos ocorrem anualmente, com incidência de até 57 casos/100 mil habitantes/ano, número três vezes e meia maior que aquele encontrado quando consideramos o Brasil como um todo [40] (Tabela 1). Em algumas áreas remotas do estado do Amazonas, uma em cada duas residências de comunidades ribeirinhas possui histórico de acidentes com serpentes [34].

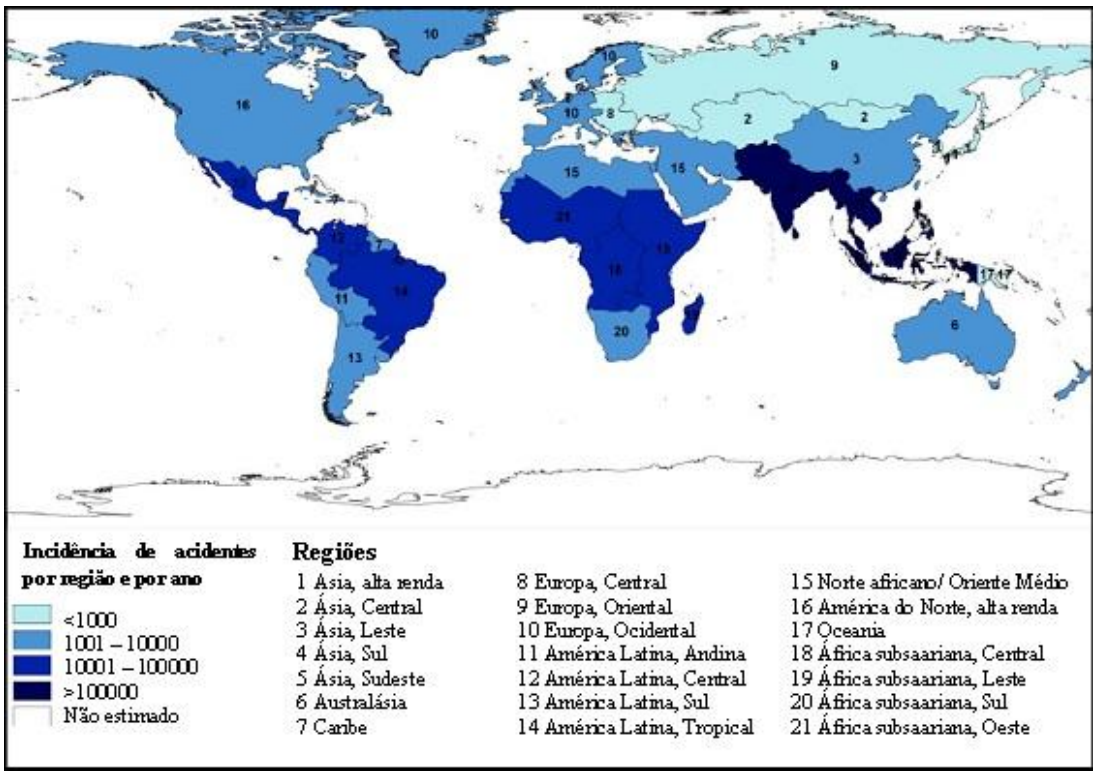

Figura 4. Estimativa global de acidentes ofídicos por região. Fonte: Adaptado de Kasturiratne, *et al* (2008) [38].

Tabela 1. Acidentes ofídicos por regiões brasileiras em 2011.

Região	Nº de casos	Incidência (100.000 hab)	Mortes	Mortalidade (%)
Região Norte	9.309	57,8	48	0.52
Região Nordeste	8.081	15,1	44	0.54
Região Sudeste	7.439	9,3	24	0.32
Região Sul	2.668	9,7	7	0.26
Região Centro-Oeste	3.285	23,1	20	0.61
Brasil	30.836	16,0	143	0.46

Fonte: Adaptado de Sinan/SVS/MS - atualizado em 21/06/2012

Em todo o Brasil, as serpentes do gênero Bothrops são as principais responsáveis pelos acidentes ofídicos [33,40]. Na região amazônica, a serpente *Bothrops atrox* é a serpente mais comumente envolvida nos envenenamentos, respondendo por até 80% do total de casos registrados nos quais a serpente envolvida é identificada. Por outro lado, a serpente *Lachesis muta muta* corresponde a aproximadamente 15% dos casos nessa mesma região [31-34].

Apesar de apresentar baixa mortalidade (0,3-0,4%) [36,40], na região norte do Brasil o envenenamento botrópico e laquético pode apresentar complicações com sequelas em até 40% dos casos, tendo alto impacto para a saúde pública [43].

1.3.2. Quadro clínico do acidente botrópico e laquético

O envenenamento causado por serpentes possui diversos efeitos potenciais, os quais dependem do tipo de serpente envolvida no acidente, bem como do paciente acometido pelo envenenamento. Os quadros clínicos resultantes dos efeitos de envenenamentos podem ser divididos em seis categorias: (1) paralisia flácida; (2) miólise sistêmica; (3) coagulopatia e hemorragia; (4) falência/insuficiência renal; (5) cardiotoxicidade; (6) dano tecidual local [44,45].

O envenenamento botrópico induz reações locais severas nas vítimas humanas, incluindo formação de edema e inchaço (~95% dos casos), equimose, inflamação e dor. Contudo, os sintomas locais mais graves são a hemorragia (~34%) e dano tecidual local, podendo acarretar em necrose (dermo e mionecrose – ~10%) (Figura 5) [36,44].

Em relação aos sinais locais, a progressão e a extensão do edema, bem como a presença de tecido necrosado, definem a gravidade do envenenamento [36,40] (Tabela 2). Complicações relacionadas ao quadro local podem acontecer em até 40% dos casos, nos quais o frequente dano permanente pode levar à necessidade de amputação de membros [43].

Figura 5. Sintomas locais e sistêmicos típicos do envenenamento botrópico. À esquerda, extensa necrose tecidual após o envenenamento do paciente de 11 anos por *B. asper* no México. À direita no alto, sangramento persistente no local da mordida em paciente apresentando incoagulabilidade sanguínea. À direita abaixo, formação de edema e inchaço em paciente mordido por *B. atrox* no Equador. Fontes: Adaptado de Gutierrez *et al.* (2006) [31]; White (2005) [44]; e Warrell (2010) [45].

Tabela 2. Classificação da gravidade do acidente botrópico.

Classificação do quadro clínico	Sinais Locais	Sinais sistêmicos
Envenenamento Leve	Inchaço envolvendo um ou dois segmentos do membro mordido; sangramento leve ou ausente no local da mordida; necrose ausente.	Sangue normal ou incoagulável; hemorragia sistêmica ausente; sem alterações hemodinâmicas.
Envenenamento Moderado	Inchaço de dois ou três segmentos do membro mordido; sangramento local; necrose ausente; bolhas em alguns casos.	Sangue incoagulável; hemorragia sistêmica, alterações hemodinâmicas e renais ausentes.
Envenenamento Grave	Inchaço extrapolando o membro mordido; bolhas; sangramento local; necrose.	Sangue incoagulável, hemorragias sistêmicas múltiplas, hipotensão ou choque; coagulação intravascular disseminada; falência renal; hemorragia cerebral; falência sistêmica múltipla.

Fonte: Adaptado de Otero-Patiño (2009) [36].

Sistemicamente, pode haver hemorragias (25-30% dos casos – sendo a cerebral, sua manifestação mais grave), coagulação intravascular disseminada, desfibrinogenemia (60-70%) e trombocitopenia (15-30%) acarretando em incoagulabilidade sanguínea, choque hipovolêmico (10-14%) e falência renal [31,36,44-47]. Podem ocorrer ainda infecções de tecidos moles, síndrome compartimental e, em gestantes, aborto [36].

Em relação ao quadro sistêmico, alterações na coagulabilidade sanguínea, hemorragias, choque hipovolêmico e falência renal aguda definem a gravidade do envenenamento (Tabela 2) [36,40]. Aparentemente, o grau de severidade do envenenamento relaciona-se com a quantidade de veneno-antígeno presente no soro dos pacientes – os quais podem variar de oito a 200 ng/mL [36,48]. Somente pacientes com quadro grave de envenenamento apresentam risco de morte ou de desenvolvimento de sequelas [36].

O quadro clínico dos acidentados por serpentes *Lachesis muta muta* é indistinguível dos acidentados por *B. atrox*. Na região Norte do Brasil, é extremamente difícil diferenciar estes dois acidentes sem a captura da serpente responsável pela mordida. Isto dificulta a tomada de decisão dos clínicos em relação a qual soro antiofídico aplicar no paciente, os quais escolhem o soro biespecífico antibotrópico-laquético, reduzindo a eficácia neutralizante do tratamento.

1.4. O veneno de *Bothrops atrox*

Venenos de serpentes são misturas ricas e complexas de peptídeos e proteínas com diferentes propriedades biológicas, os quais correspondem a aproximadamente 90% do peso

seco do veneno [18,28,49-51]. A extensa diversidade de proteínas e peptídeos encontrados nos venenos de serpentes é, no entanto, classificada em algumas poucas famílias proteicas que variam de espécie para espécie [12,17,19,52,53].

Entre os indivíduos de uma mesma espécie, a variabilidade na composição do veneno é um fenômeno já documentado, podendo ser influenciado por idade, sexo, dieta, tamanho dos indivíduos e distribuição geográfica (Figura 6) [18,21,28,36,54,55].

Estudos recentes demonstram uma ampla variação intraespecífica na composição do veneno de *B. atrox* (Figura 6) [18,20,28,55,56]. Apesar desta variabilidade, o veneno de *B. atrox* caracteriza-se, assim como em outros venenos botrópicos, por ser rico em famílias de proteínas com importantes atividades tóxicas no envenenamento, como as fosfolipases A_2 (PLA_2), metaloproteases de venenos de serpentes (SVMPs), L-aminoácido oxidases (LAOs), serinoproteases (SerPro), desintegrinas, proteínas semelhantes a lectinas do tipo C (CTLs) e proteínas secretadas ricas em cisternas (CRISP) (Figura 6) [18,20,28,52,55-62].

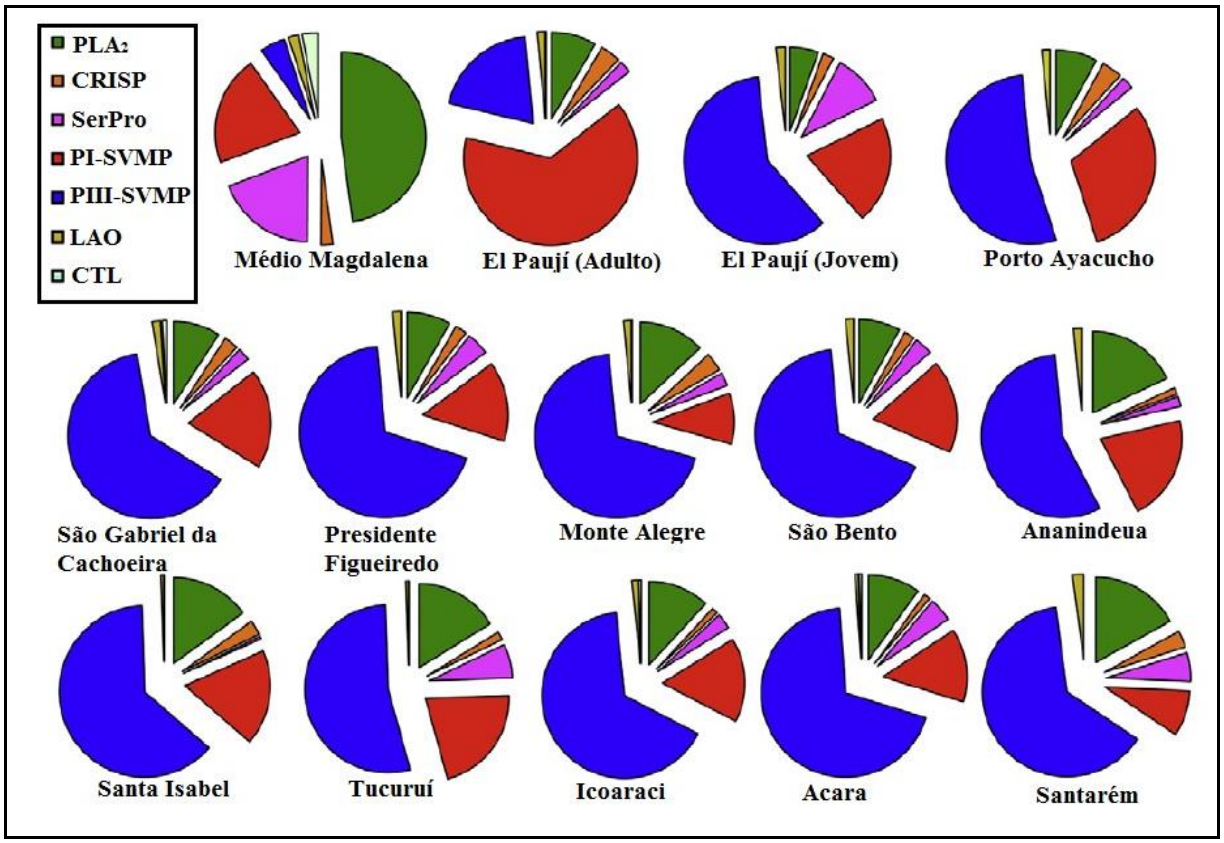

Figura 6. Composição geral por famílias de proteínas de venenos de *B. atrox* de diferentes localidades amazônicas. Fosfolipases A2 (PLA2), Metaloproteases de venenos de serpentes de classe P-I e P-III (PI-SVMP, PIII-SVMP), L-aminoácido oxidases (LAO), serinoproteases (SerPro), proteínas semelhantes a lectinas do tipo C (CTL) e proteínas secretadas ricas em cisteínas (CRISP). Fonte: Traduzido de Calvete (2011) [20].

Dentre essas famílias de proteínas, destacam-se as SVMPs, as quais podem corresponder a mais de 80% do conteúdo proteico do veneno de *B. atrox* [20,28,55,56]. A relação entre os

conteúdos de diferentes classes de SVMPs (classe P-I e classe P-III) é importante na caracterização dos venenos de *B. atrox* [20,28].

Indivíduos jovens possuem veneno com maior letalidade, atividade hemorrágica, edematogênica e procoagulante em relação a indivíduos adultos, os quais possuem maior atividade hemolítica indireta. Estes perfis tóxicos diferentes relacionam-se a diferenças quantitativas e qualitativas de toxinas entre os venenos de indivíduos jovens e adultos. A presença predominante de PIII-SVMPs em relação a SVMPs de classe P-I é característica de indivíduos juvenis, enquanto o perfil oposto é encontrado em adultos [20,28,63].

Esta variação ontogenética é presente em indivíduos presentes na região norte da América do Sul, incluindo Venezuela e Colômbia. Por outro lado, a ocupação de novos habitats ao longo dos Andes e da Floresta Amazônica (no sentido da foz do rio Amazonas) parece relacionar-se à retenção de traços juvenis na composição dos venenos de indivíduos adultos. Espécimes da Amazônia brasileira, do Peru e do Equador apresentam este traço pedomórfico (Figura 6) [20,28,63].

Independentemente das variações intraespecíficas, o envenenamento causado por *B. atrox* caracteriza-se por causar coagulopatias e hemorragias, como dito anteriormente [33,36,44,57,64]. Assim, o sistema hemostático parece ser seu principal alvo, com diversas toxinas capazes de afetar diferentes partes deste sistema, causando, principalmente, (1) consumo de fatores de coagulação e inibição não enzimática de agonistas da cascata de coagulação; e (2) hemorragias pela ação proteolítica direta das SVMPs (Figura 7) [36,44-46,65-69]. Os efeitos nocivos locais (e.g. hemorragia e necrose) são causados, principalmente, pela ação das metaloproteases de venenos de serpentes [44,65-70].

Apesar da grande importância médico-epidemiológica dos acidentes causados por *B. atrox* e embora sejam muitos os estudos sobre seu veneno, poucos foram os trabalhos direcionados à purificação e caracterização de suas toxinas. Até o momento, somente 11 peptídeos/toxinas do veneno de *B. atrox* foram descritas com sequências depositadas na base de dados UniProtKB/Swiss-Prot – sendo elas: (1) batroxobin, uma enzima semelhante a trombina (acesso UniProtKB/Swiss-Prot P04971) [71]; (2) enzima ativadora de protrombina (UniProtKB/Swiss-Prot B3A0N1); (3) *B. atrox* miotoxina I, uma PLA_2(Lys49) secretada (UniProtKB/Swiss-Prot Q6JK69) [72]; (4) BatroxLAAO, uma LAO (UniProtKB/Swiss-Prot P0CC17) [58]; (5) Batroxostatin, um peptídeo semelhante a desintegrina (UniProKB/Swiss-Prot P18618) [73]; (6) Bax12a, um peptídeo potenciador de bradicinina (UniProtKB/Swiss-Prot P86721); (7-9) batroxstatina-1, -2 e -3, três PIII-SVMPs (UniProtKB/Swiss-Prot C5H5D2, C5H5D3 e C5H5D4, respectivamente) [74]; (10) Atroxlisina-I (UniProtKB/Swiss-

Prot P85420) [61]; e (11) Batx-I (UniProtKB/Swiss-Prot P0DJE1) [60]. Além delas, uma décima segunda toxina, nomeada Batroxase, foi descrita recentemente, no entanto sua sequência não foi depositada na base de dados UniProtKB/Swiss-Prot [59].

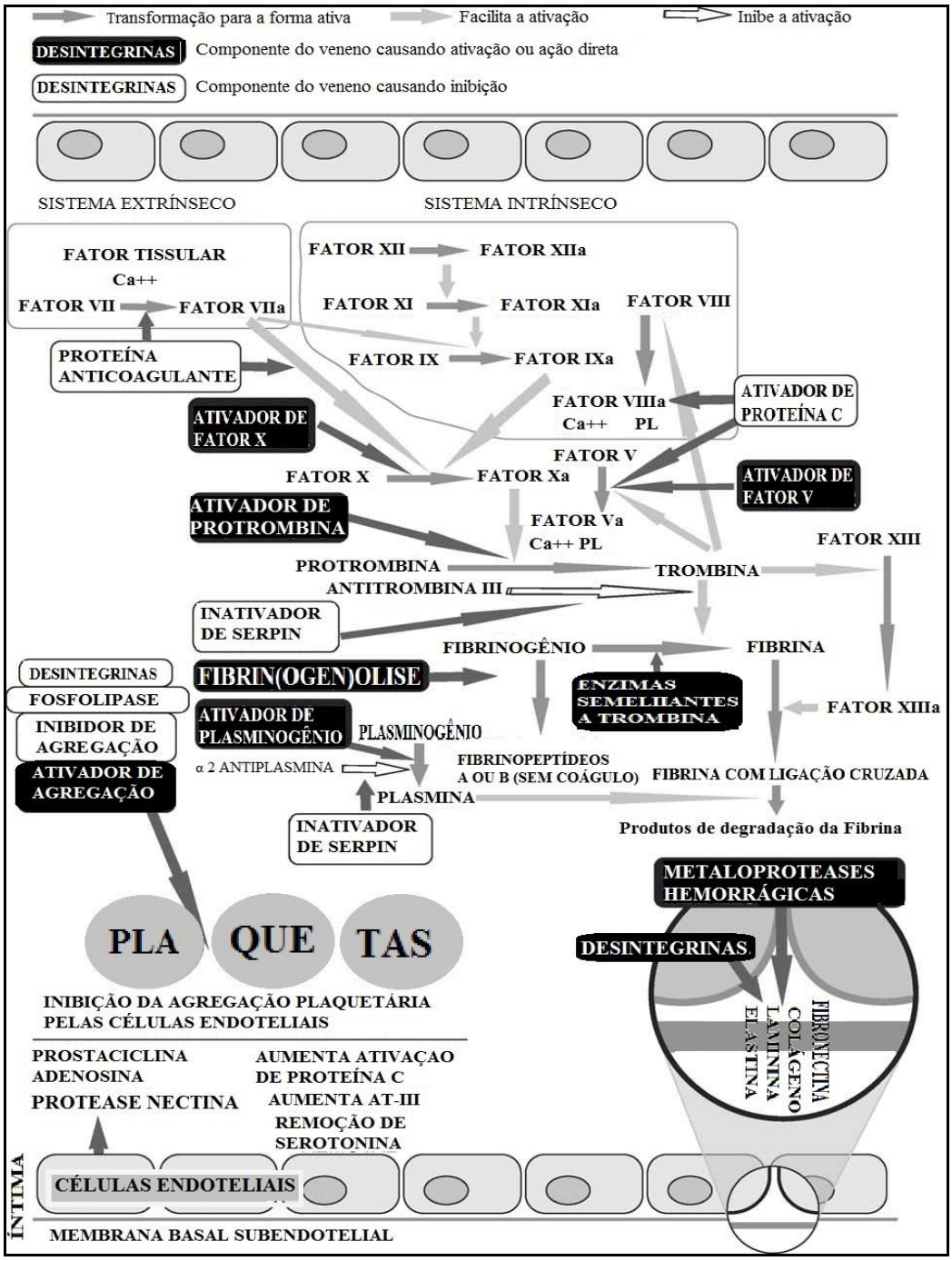

Figura 7. Toxinas de venenos de serpentes atuantes sobre o sistema hemostático. Fonte: Adaptado de White (2005) [44].

As três últimas toxinas (Atroxlisina-I, Batx-I e Batroxase) são metaloproteases de classe P-I isoladas de venenos de *B. atrox* da região amazônica do Peru, Colômbia e Brasil, respectivamente. Mesmo sendo de grande importância na sintomatologia do envenenamento, as primeiras SVMPs de classe P-I só foram isoladas do veneno de *B. atrox* a partir da década

de 2010. A primeira PI-SVMP do veneno de *B. atrox* a ser isolada e caracterizada foi Atroxlisina-I (Atr-I). Ainda em 2010 e depois em 2012, Batx-I e Batroxase foram purificadas caracterizadas. Até o momento, nenhuma PIII-SVMP foi sequenciada nível proteico – batroxstatina-1, -2 e -3 foram caracterizadas a partir de estudos de transcriptômica [59-61,74]. No ano 2000, as atividades edematogênica, proteolítica e hemorrágica de uma PIII-SVMPs de *Bothrops atrox* foram caracterizadas [75].

1.5. O veneno de *Lachesis muta muta*

Assim como o veneno de *B. atrox*, o veneno de *Lachesis muta muta* é rico em toxinas das famílias das fosfolipases A_2 (PLA_2), metaloproteases de venenos de serpentes (SVMPs), L-aminoácido oxidases (LAOs), serinoproteases (SerPro), proteínas semelhantes a lectinas do tipo C (CTLs) e proteínas secretadas ricas em cisternas (CRISP). Além destas, o veneno de *L. muta muta* é rico em peptídeos potenciadores de bradicinina e fatores de crescimento neuronal (Figura 8)[76].

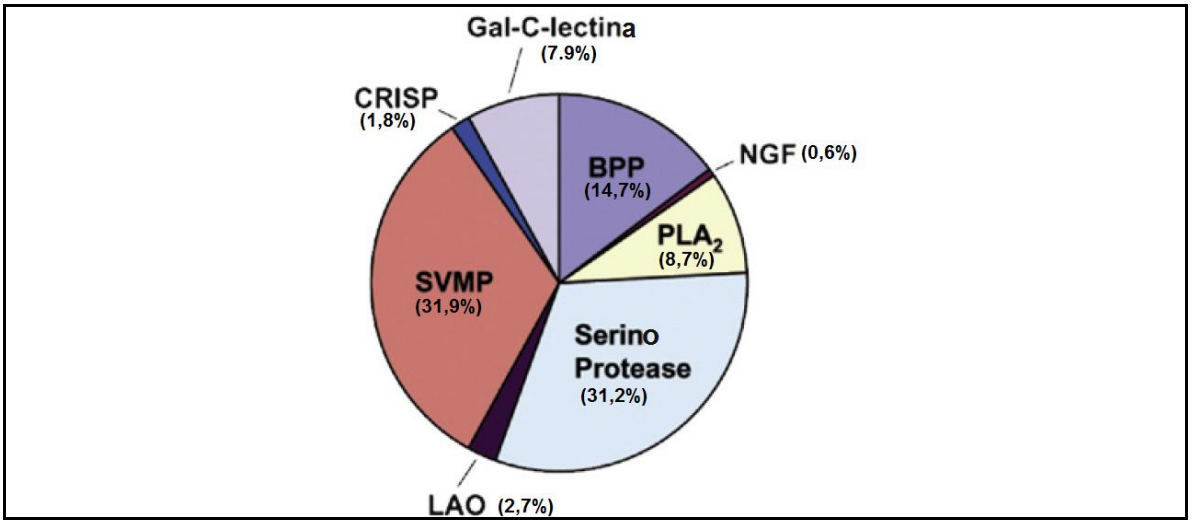

Figura 8. Composição do veneno de Lachesis muta. Principais famílias de toxinas do veneno de Lachesis muta analisados por proteômica. Adaptado de Sanz et al., 2008 [76].

Juntamente com as serinoproteases, as metaloproteases de venenos de serpentes são as toxinas mais abundantes do veneno de *L. muta muta*, correspondendo por cerca de 32% do peso seco do conteúdo do veneno cada [76]. Desta forma, os envenenamentos causados pelas serpentes do gênero Bothrops e Lachesis apresentam sinais e sintomas muito semelhantes entre si [40].

Do veneno de *L. muta muta*, já foram isoladas diversas toxinas, sendo que 12 delas tiveram suas sequências depositadas na base de dados UniProtKB/Swiss-Prot. Dentre elas, a metaloprotease de classe P-I mutalisina-II (mut-II) já foi caracterizada. Mut-II é uma PI-

SVMP de cadeia simples não glicosilada, fibrino(geno)lítica e não-hemorrágica de massa molecular de 22.300 [77,78].

1.6. As Metaloproteases de Venenos de Serpentes

Desde a segunda metade do século XIX, observou-se que o sangue de pacientes vítimas de envenenamentos de serpentes tornava-se incoagulável, o que levou à hipótese que os venenos de serpentes possuíam atividades proteolíticas sobre o fibrinogênio. Um século mais tarde, novos estudos comprovaram que proteases presentes nos venenos de serpentes eram as responsáveis pela atividade anticoalugante dos venenos [79,80].

No começo da década de 1960, com a purificação das primeiras proteases de venenos de serpentes e a descoberta de que suas atividades proteolíticas poderiam ser inibidas por agentes quelantes (i.e. EDTA), sugeriu-se que se tratavam de metaloproteases de venenos de serpentes. Durante a década seguinte, mostrou-se que estas proteases possuíam íons de zinco (Zn^{+2}) em suas moléculas na proporção de 1:1 (proteína:Zn^{+2}) e que a presença do íon era essencial para a atividade enzimática das toxinas. Além disso, verificou-se que a inibição da atividade proteolíticas das SVMPs levava à supressão da hemorragia causada pelo envenenamento [79,80].

Nos últimos anos, centenas de trabalhos a respeito das SVMPs foram publicados com diversas abordagens, os quais ampliaram e enriqueceram, consideravelmente, nosso conhecimento sobre esta família de toxinas, bem como nosso entendimento dos quadros clínicos dos acidentes ofídicos. Atualmente, sabe-se que as SVMPs possuem múltiplas funções no envenenamento, exercendo atividades hemorrágica, fibrino(geno)lítica, ativadora de protrombina, inibidora de agregação plaquetária, pró-inflamatória, necrosante, apoptótica, ativadora de complemento, de cininogenase, entre outras [27,59-61,65-67,70,79,81-89].

Como dito anteriormente, as metaloproteases dos venenos de serpentes são metaloendopeptidases dependentes de Zn^{+2} pertencentes à família M12B das reprolisinas (EC 3.4.24) [79-81,90,91]. Com o advento da transcriptômica, a classificação das SVMPs foi revisada recentemente [79,82]. Hoje em dia são reconhecidas três classes (PI a PIII - Figura 9) e diversas subclasses de SVMPs, as quais são categorizadas de acordo com os domínios apresentados em suas estruturas [79,80,82].

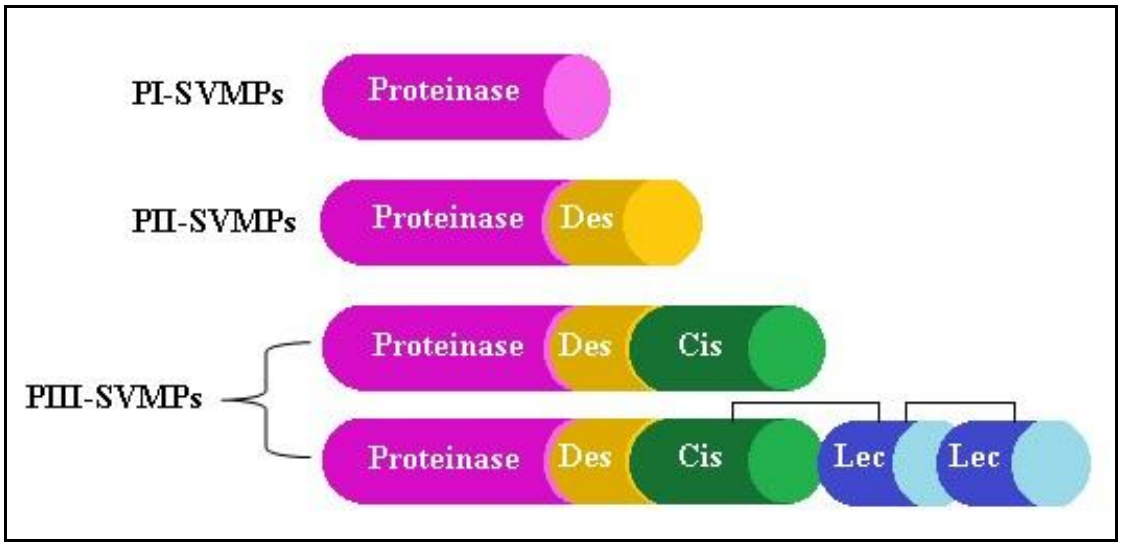

Figura 9. Esquema simplificado da classificação das SVMPs de acordo com os motivos apresentados em suas estruturas. (Des) Domínio desintegrina em PII-SVMPs ou semelhante a desintegrina em PIII-SVMPs, (Cis) domínio rico em cisteína, (Lec) domínio semelhante a lectina do tipo C. Fonte: Adaptado de Fox & Serrano (2008) [82].

PI-SVMPs apresentam unicamente o domínio catalítico dependente de zinco, enquanto as PII-SVMPs apresentam um domínio desintegrina em C-terminal do domínio protease. As PIII-SVMPs possuem um domínio protease e um domínio semelhante à desintegrina ligados a um domínio rico em cisteína (Figura 9) [79-82].

Estas estruturas básicas das PII e PIII-SVMPs podem sofrer modificações pós-traducionais com adição ou remoção de domínios, ou ainda, multimerização de estruturas via pontes dissulfeto, contribuindo para o aumento significativo da complexidade dos venenos e das atividades biológicas das metaloproteases de venenos de serpentes [82]. Estas modificações pós-traducionais determinam as subclasses às quais as SVMPs pertencem. As PII e PIII-SVMPs estão presentes nos venenos de diversas famílias de serpentes (e.g. Viperidae, Elapidae, Atractaspididae), enquanto as PI-SVMPs só foram encontradas em venenos viperídeos[67]. As SVMPs de classe P-II são raramente encontradas intactas em nível proteico, sendo preferencialmente processadas proteoliticamente [81].

Independentemente da classe à qual pertençam, as SVMPs apresentam a sequência consenso do sítio ativo das metaloproteases dependentes de zinco HEXXHXXGXXH (Figura 10). Esta sequência é caracterizada pela presença de três resíduos de histidina (H) responsáveis manutenção e coordenação do íon Zn^{2+} no sítio catalítico na molécula; e um resíduo de ácido glutâmico (E), o qual fixa uma molécula de água responsável pelo ataque nucleofílico nas ligações peptídicas dos substratos. O resíduo Glu age como base catalítica recebendo transitoriamente o próton da molécula de água durante a proteólise [81,92,93].

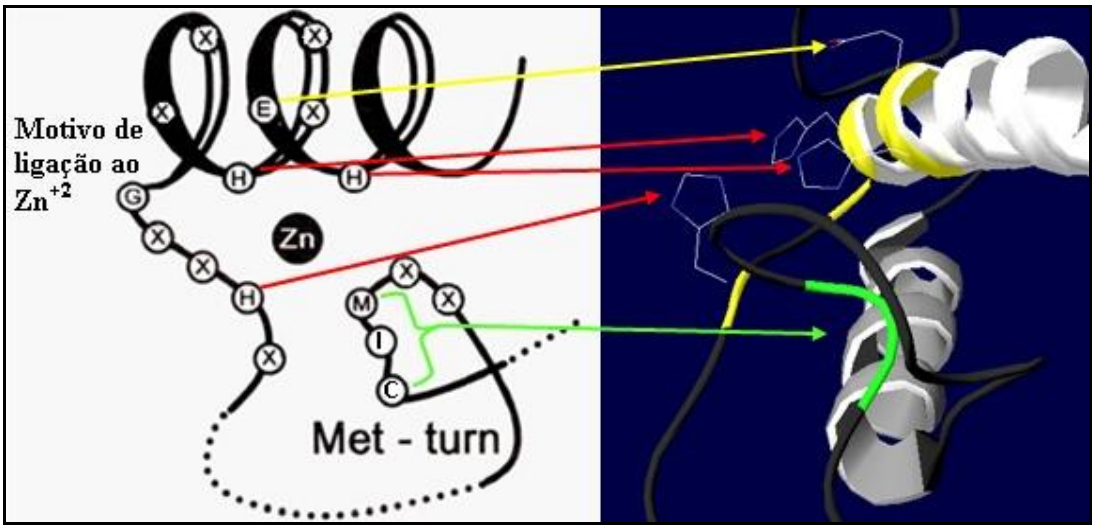

Figura 10. Sítio ativo das SMVPs. À esquerda, figura esquemática do sítio ativo das SMVPs mostrando seus resíduos conservados (HEXXHXXGXXH) e o motivo "Met-Turn" (Adaptado de Stöcker *et al.* (2005)[92]). À direita, modelo tridimensional de atroxlisina-I construído por modelagem. As setas localizam os resíduos conservados no modelo tridimensional. As setas vermelhas localizam as Histidinas, a seta amarela o Ácido glutâmico e a seta verde localiza os resíduos (CIM) que formam o "Met-Turn.

Os dois primeiros resíduos de His e o resíduo de Glu situam-se em uma α-hélice, enquanto a terceira His situa-se em um "loop" adjacente (Figura 10). A glicina conservada (G) exerce importante papel estrutural, pois permite que, ao final da α-hélice, a cadeia peptídica sofra uma abrupta mudança de direção e, assim, a cadeia lateral do terceiro resíduo de His seja direcionada para a α-hélice anterior, contribuindo para a manutenção do Zn^{+2} catalítico [83,92-94].

Ao final do motivo catalítico, as SVMPs apresentam uma região bastante variável envolvida na interação com diferentes substratos, a qual termina se reaproximando do sítio ativo em um "loop" característico e conservado conhecido como "Met-turn". Este motivo é formado por três resíduos: (1) cisteína (C); (2) isoleucina (I)/valina (V); e (3) metionina (M). Esta região é essencial para a manutenção da integridade do sítio catalítico ativo desta família de proteases, pois forma a base hidrofóbica para o íon zinco e as três histidinas do sítio ativo, bem como para a interação com os substratos [92].

Apesar de apresentarem especificidades semelhantes em relação às ligações peptídicas hidrolisadas em seus substratos *in vivo* e *in vitro*, com clara preferência para resíduos de Leu na posição P1' [95], as PIII-SVMPs são, geralmente, hemorraginas mais potentes que as PI-SVMPs [27,59-61,65,79,85,87,96]. Diversos estudos foram realizados na tentativa de se elucidar as determinantes estruturais da hemorragia causada pelas SVMPs (e.g. padrão de pontes dissulfeto, modificações pós-traducionais, hidrofobicidade/hidrofilicidade, presença/ausência de motivos estruturais na sequência primária) [50].

Neste sentido, os domínios adicionais das PIII-SVMPS (semelhante à desintegrina e rico em cisteína) parecem ser importantes por direcionar estas proteases a seus alvos moleculares *in vivo* (e.g. colágenos do tipo IV e tipo I, lamininas, integrinas, nidogênio, perlecano, dentre outros - Figura 6), servindo como potenciais interfaces adesivas proteína-proteína e facilitando a degradação de componentes essenciais à integridade dos endotélios [65-69,97]. A capacidade de se ligarem e hidrolisarem componentes específicos da membrana basal (BM) e da matriz extracelular (ECM) parece, também, determinar a capacidade das PI-SVMPs de causar hemorragia, embora não possuam os domínios adicionais das PIII-SVMPs [67].

Aparentemente, a hidrólise seletiva de proteínas importantes na estabilidade de vasos sanguíneos, encontradas nas BMs de endotélios (e.g. colágeno do tipo IV e perlecano), assim como de alguns substratos presentes na ECM que a circunda (e.g. colágenos do tipo VI e XV), ou ainda de integrinas presentes nas membranas plasmáticas de células endoteliais, levaria ao enfraquecimento da estabilidade mecânica dos capilares, os quais, submetidos às forças biofísicas hemodinâmicas ocasionadas pelo fluxo sanguíneo, poderiam causar o rompimento da integridade do endotélio, culminando no extravasamento de sangue [67]. Além disso, a hidrólise de fatores de coagulação, como o fibrinogênio e a fibrina, e a inibição não enzimática da agregação plaquetária podem possuir ação potencializadora no quadro hemorrágico [67].

A hemorragia ocorre em poucos minutos após a injeção das SVMPs, sendo o principal sintoma local do envenenamento botrópico [67], o qual, juntamente com a necrose tecidual e a atividade pró-inflamatória, representam os principais desafios para os médicos, pois estes efeitos locais parecem não ser bem neutralizados pelo tratamento convencional, utilizando-se o soro comercial antibotrópico [98-101].

1.7. A Soroterapia

Desenvolvida no final do século XIX por Phisalix, Bertrand e Calmette na Europa e trazida ao Brasil por Vital Brazil no ano de 1905, a soroterapia é, ainda hoje, o único tratamento eficaz aprovado pela OMS para os pacientes acometidos pelo envenenamento de serpentes [102]. Os antivenenos são administrados unicamente por profissionais em centros de saúde. Infelizmente, o suprimento de antivenenos é, muitas vezes, escasso, principalmente em áreas rurais remotas de países subdesenvolvidos e em desenvolvimento. Como consequência, em diversas regiões da América Latina, por exemplo, grande parte dos pacientes procura a medicina tradicional em um primeiro atendimento (e.g. extratos de plantas, benzedores, entre outros) [36].

A primeira geração de antivenenos consistia na transferência de soro imune bruto para o acidentado. Posteriormente, a partir do começo da década de 1930, passou-se a purificar as imunoglobulinas do soro dos animais após as imunizações [102]. Atualmente, muitos laboratórios processam os anticorpos a serem utilizados na soroterapia e, assim, três tipos de antivenenos são produzidos em todo o mundo: (1) antivenenos compostos por moléculas inteiras de IgG de cavalo obtidos por meio de fracionamento de plasma; (2) fragmentos $F(ab')_2$ de IgG de cavalos derivados de sua digestão por pepsina; e (3) fragmentos Fab de origem ovina, obtidos pela digestão de moléculas de IgG com papaína [36,102].

A OMS preconiza que o soro antiofídico utilizado em cada país/região seja avaliado em estudos pré-clínicos e que sua capacidade neutralizante seja eficiente contra os principais efeitos tóxicos das serpentes de maior relevância epidemiológica nas regiões onde ele é utilizado [103,104].

Como os soros antiofídicos são eficazes contra os venenos das espécies de serpentes contidos no pool antigênico, os produtores de antivenenos imunizam animais com misturas de venenos na preparação de soros poliespecíficos, garantindo a necessidade clínica neutralizante contra diversos venenos de importância epidemiológica. No entanto, este procedimento aumenta o volume de antiveneno requerido por paciente, aumentando o risco de reações adversas [105].

O pool antigênico utilizado para a produção do soro antibotrópico brasileiro é composto da seguinte maneira: 50% *B. jararaca* e 12,5% de cada um dos seguintes venenos de *B. jararacussu*, *B. neuwiedi*, *B. alternatus* e *B. moojeni* [106]. No Brasil, os soros antivenenos contendo fragmentos $F(ab')_2$ são produzidos pela hiperimunização de cavalos e reações alérgicas podem ocorrer em até 36% dos casos [36,104].

Além dos antivenenos, tratamentos paliativos auxiliares podem ser requeridos para o tratamento de acidentes envolvendo serpentes do gênero *Bothrops* (e.g. uso de antibióticos, correção da hipovolemia, procedimentos cirúrgicos, entre outros) [36].

Os antivenenos antibotrópicos são eficazes em relação à neutralização da sintomatologia sistêmica. Se administrados nas primeiras horas após o acidente, preferencialmente até duas horas após a mordedura, poucas complicações são observadas o que se reflete na taxa de mortalidade relativamente baixa (Tabela 1) [106,107]. O retardo no início do tratamento relaciona-se ao desenvolvimento de quadros de falência renal aguda e hemorragia no sistema nervoso central, podendo acarretar em morte do paciente [36].

Por outro lado, os sintomas locais não são completamente neutralizados pelos soros antibotrópicos, fazendo com que estes sejam clínica e socioeconomicamente de grande

importância, pois, como dito anteriormente, o percentual de pacientes que apresentam algum tipo de sequela nesse tipo de acidente pode chegar a 40% dos casos, sendo que diversas vezes o dano tecidual causado é permanente, com consequente amputação de membros [37,43,99-101]. Estima-se que até 400 mil amputações sejam feitas todos os anos como decorrência de sequelas dos efeitos de envenenamentos de serpentes [108]. Surge-se então, a necessidade de se identificar/desenvolver novas terapias para os efeitos locais hemorrágicos e necrosantes oriundos dos acidentes com serpentes [105].

Além disso, o uso tradicional de venenos inteiros para a produção dos soros antivenenos na imunização de cavalos apresenta desafios para os pesquisadores, produtores de soro e profissionais da saúde, como por exemplo:

- Animais imunizados podem sofrer com problemas de toxicidade, mimetizando o quadro de envenenamento e diminuindo suas expectativas de vida, o que eleva o custo da produção de antivenenos;
- Os animais utilizados na produção de antivenenos vivem em campos abertos, na maioria das vezes, em contato com diversos agentes antigênicos naturais os quais estimulam o sistema imune dos animais produtores, provocando um efeito de diluição do soro – apenas 10% das imunoglobinas dos antisoros são direcionadas a proteínas dos venenos [105];
- Além disso, os componentes não tóxicos, mas imunogênicos, presentes nos venenos, fazem com que dentre os 10% dos anticorpos presentes nos antivenenos dirigidos contra moléculas do veneno, vários possam ser dirigidos a moléculas inócuas dos venenos. Assim, estima-se que somente 5% das moléculas de IgGs que compõem os antivenenos sejam terapêuticos;
- A extensa variabilidade inter e intraespecífica na composição bioquímica de venenos de serpentes pode afetar a eficácia neutralizante dos soros antiofídicos, uma vez que durante a produção de soros antivenenos não são incluídos os venenos de todas as espécies de importância médica.

Sendo assim, é necessária a condução de pesquisas com o intuito de melhorar a eficácia, segurança/confiabilidade e a acessibilidade dos antivenenos. Para tal, torna-se importante a exclusão, ou a não produção de anticorpos obsoletos presentes nos soros antiofídicos, bem como a busca de imunógenos alternativos atóxicos a serem utilizados na produção de antivenenos em animais, como peptídeos sintéticos atóxicos mimetizando epitopos neutralizantes das principais toxinas de cada veneno, ou ainda, a produção de anticorpos

neutralizantes com mínima utilização de animais. Para o desenvolvimento destas novas alternativas de modo eficaz, a utilização de anticorpos monoclonais torna-se uma das ferramentas de extrema importância, assim como a obtenção de informações sobre a estrutura e antigenicidade das principais toxinas presentes nos venenos [105,109-112].

1.8. Epitopos de Metaloproteases de Venenos de Serpentes

Peptídeos realizam diversos papéis na imunologia, sendo o de direcionar a resposta imune adaptativa como os epitopos, o mais importante. Os epitopos peptídicos executam suas funções primárias via interações com complexos principais de histocompatibilidade, no caso de epitopos de células-T, ou via anticorpos, no caso de epitopos de células-B [113].

Por definição, o epitopo de células-B de uma proteína é a porção desta proteína antigênica reconhecida por uma molécula de anticorpo, o qual resulta na ativação da resposta imune [114].

Epitopos podem ser classificados como contínuos/lineares, ou descontínuos/conformacionais. Epitopos contínuos, ou lineares, são aqueles nos quais os aminoácidos reconhecidos por um anticorpo gerado contra a proteína antigênica em sua forma nativa são contíguos na sequência primária do antígeno (Figura 11 A). Já os epitopos descontínuos, ou conformacionais, são aqueles formados por resíduos de aminoácidos não necessariamente adjacentes na estrutura primária do antígeno, mas que se reúnem espacialmente em estrutura terciária, sendo reconhecidos por um anticorpo. Vale ressaltar que epitopos conformacionais podem ser formados por pequenos segmentos de resíduos adjacentes separados por longos trechos na estrutura primária do antígeno (Figura 11 B)[114].

A maioria dos epítopos é do tipo descontínuo e a identificação dos epítopos é de grande importância para compreender e reconhecer molecularmente a proteína analisada. Esses epítopos podem ser úteis em desenvolvimento de testes para diagnóstico de doenças, na formulação de drogas, projetos de vacinas, entre outros [114].

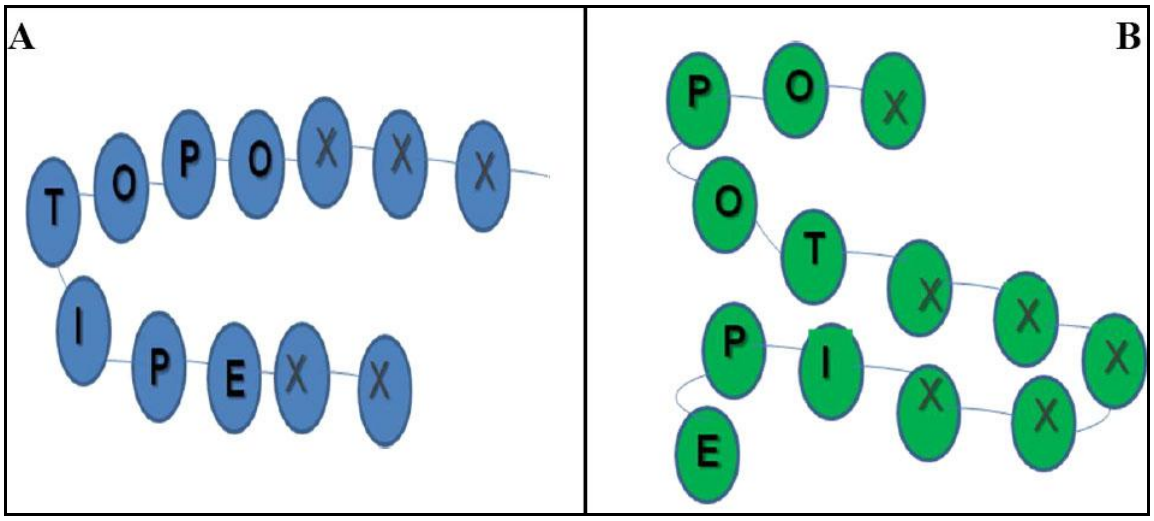

Figura 11. Representação esquemática dos diferentes tipos de epítopos. Cada círculo representa um aminoácido seguindo a seqüência primária da proteína. Os círculos destacados são os aminoácidos que fazem parte do epítopo. 3A mostra a representação esquemática de um epítopo linear e 3B a representação esquemática de um epítopo conformacional

O estudo e a identificação dos principais epitopos de toxinas de venenos animais capazes de induzir a produção de anticorpos neutralizantes podem ser importantes na produção de soros antivenenos possuindo menor percentual de anticorpos obsoletos [105].

Diversas técnicas foram elaboradas para a identificação e predição de epitopos, incluindo: (1) cristalografia de complexos proteínas-anticorpos [115]; (2) phage display [116]; (3) mutagênese sítio-dirigida [117]; (4) ferramentas *in silico* [118,119]; (7) PEPSCAN, incluindo técnica de SPOT e peptídeos solúveis imobilizados em placas de ELISA [113,120,121].

Numerosos estudos de identificação de epitopos neutralizantes de toxinas presentes em venenos de aranhas e escorpiões já foram realizados [105,110,111,122]. Porém, apesar do papel exercido pelas PI-SVMPs no envenenamento botrópico, pouco se sabe sobre suas estruturas antigênicas. Escassos são os trabalhos de identificação de epitopos de células-B de metaloproteases de venenos de serpentes [123-125].

1.9. Os anticorpos Monoclonais

Diversos anticorpos monoclonais têm sido produzidos nas últimas décadas e utilizados com diversos propósitos, como, por exemplo, em estudos de estrutura-função de proteínas [126,127], desenvolvimento de ferramentas biotecnológicas em imunotoxinas [128], kits-diagnóstico [129], ou ainda como agentes terapêuticos [130].

Tradicionalmente, a produção de anticorpos monoclonais utiliza ensaios de detecção de ligação antígeno-anticorpo (i.e. ensaio de ELISA) para a seleção dos clones produtores de anticorpos contra os antígenos de interesse [127,131,132]. No entanto, sabe-se que vários dos

anticorpos capazes de reconhecer seus antígenos não possuem atividade neutralizante frente às atividades tóxicas dos mesmos.

A despeito da importância das PI-SVMPs nos venenos de viperídeos, poucos foram os trabalhos direcionados à produção de mAbs contra essas toxinas. Tanjoni e colaboradores (2003)[127], descrevem a produção de sete mAbs contra a metaloprotease de classe P-III purificada do veneno de *Bothrops jararaca* chamada Jararagina, dos quais somente um (MAJar 3) possui atividade neutralizante contra as atividades proteolítica e hemorrágica dessa toxina. De modo similar, Fernandes (2010) descreve a produção de seis mAbs anti-BaP1, uma SVMP de classe P-I do veneno de *B. asper*, dos quais três (MABaP1-3, 6 e 8) foram capazes de neutralizar a atividade hemorrágica induzida pela toxina purificada [132].

Além disso, a seleção de anticorpos baseada em ensaios de ELISA são processos demorados e laboriosos, os quais consomem uma grande quantidade de antígenos durante o processo de *screening*.

Dessa forma, a metodologia tradicional utilizada na obtenção de anticorpos monoclonais contra as metaloproteases de serpentes não direciona a seleção para os clones produtores de anticorpos neutralizantes, mas sim na obtenção de mAbs que sejam capazes de reconhecer o antígeno estudado.

Assim, a utilização de novas metodologia na seleção de clones produtores de mAbs neutralizantes contra as SVMPs torna-se necessária e útil. Como as principais atividades tóxicas das PI-SVMPS estão relacionadas às suas atividades proteolíticas, o monitoramento da inibição destas atividades por mAbs pode ser utilizado na seleção dos clones de interesse. Para tal, é necessário um método sensível, confiável, rápido e barato. Habitualmente, ensaios colorimétricos e/ou fluorimétricos são utilizados na detecção e determinação das atividades proteolíticas das PI-SVMPs. No entanto, ambos possuem limitações técnicas, como procedimentos laboriosos e baixa sensibilidade. Assim, substratos peptídicos com supressão intramolecular de fluorescência (FRET) tornam-se excelentes candidatos para tais análises.

1.10. Peptídeos FRET

Conceitualmente, peptídeos FRET são aqueles que possuem um grupo doador fluorescente acoplado a uma extremidade de suas sequências de aminoácidos, o qual transfere energia a um aceptor (quencher) localizado na extremidade oposta, no processo denominado de ressonância. É importante destacar que os grupos doador e aceptor possuem o mesmo espectro de emissão e absorção, respectivamente. Os peptídeos FRET exibem absorção intramolecular de fluorescência, quando intactos, no entanto, a quebra de qualquer uma das

ligações peptídicas internas entre o par doador/aceptor proporciona emissão não absorvida de fluorescência, a qual pode ser detectada e quantificada continuamente, como medida da atividade proteolítica (Figura 12) [133,134].

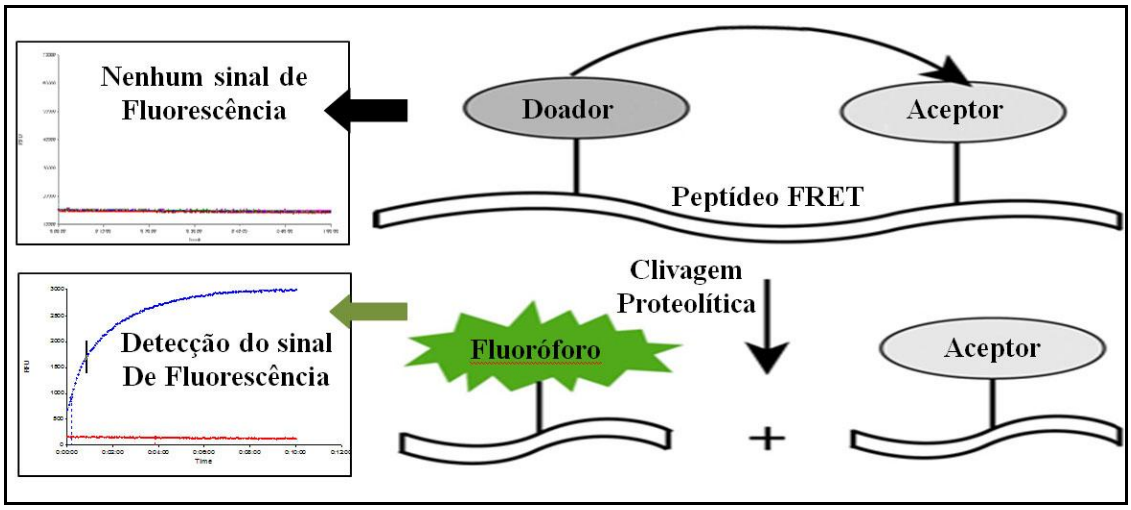

Figura 12. Emissão de fluorescência de peptídeos FRET após clivagem proteolítica dos mesmos. Em situação intacta, o grupo doador fluorescente transfere energia em um determinado comprimento de onda, o qual é absorvido pelo grupo aceptor. Nesta situação, nenhum sinal de fluorescência é detectado. Após a clivagem proteolítica do peptídeo FRET, o aceptor não absorve mais a energia emitida pelo fluorófo, a qual pode ser detectada por um fluorímetro.

As novas gerações de peptídeos FRET, permitem a quantificação de atividade proteolítica de enzimas em concentrações nanomolares e são atualmente utilizados em estudos de determinação de subsítios de especificidade para enzimas [135], medição e detecção de enzimas proteolíticas clinicamente importantes em diagnósticos [136,137], estudos de cinética enzimática e estudos de inibição de atividade enzimática [138,139], os quais podem ser adaptados para a seleção de anticorpos neutralizantes.

Substratos sintéticos utilizando a tecnologia FRET já foram utilizados para determinação da atividade proteolítica e sua inibição em SVMPs de classe P-I [88,89,132]. No entanto, novas abordagens nas quais os substratos peptídicos FRET sejam utilizados no processo funcional de seleção de clones produtores de mAbs nunca foram testadas.

2. OBJETIVOS

2.1. Objetivo Geral

Identificar e caracterizar os epitopos lineares e conformacionais de metaloproteases de venenos de serpentes de classe P-I de *Bothrops atrox* e *Lachesis muta muta*

2.2. Objetivos Específicos

- Purificar e caracterizar a metaloprotease de classe P-I de *Bothrops atrox*, atroxlisina-I;
- Produzir soros policlonais específicos contra atroxlisina-I e mutalisina-II;
- Síntese química de substratos FRET específicos para SVMPs a serem utilizados no *screening* funcional de mAbs;
- Produção de anticorpos monoclonais contra atr-I, utilizando o screening funcional;
- Caracterização dos mAbs produzidos:
    - Purificação e isotipagem dos mAbs;
    - Avaliação do potencial neutralizante *in vivo* e *in vitro* dos mAbs produzidos;
    - Avaliação da afinidade dos mAbs produzidos;
- Mapeamento de epitopos contínuos reconhecidos pelo soro policlonal anti-atroxlisina-I e e descontínuos pelo anticorpo monoclonal LmmAbB2D4, utilizando os métodos de SPOT e Phage Display;
- Síntese química de peptídeos referentes aos epitopos identificados;
- Produção de soros específicos contra os epitopos identificados;
- Avaliação do potencial neutralizante e vacinal induzido pelos epitopos sintéticos produzidos;

3. RESULTADOS

Neste capítulo estão incluídos três artigos, os quais abordam diferentes estudos de caracterização de duas metaloproteases de classe P-I de venenos de serpentes, incluindo a purificação e caracterização bioquímica de Atroxlisina-I (Artigo 1); o desenvolvimento de um novo método a ser utilizado na produção e seleções de anticorpos neutralizantes contra as SVMPs, assim como a caracterização dos anticorpos produzidos (Artigo 2); caracterização de epitopos conformacionais da metaloprotease de serpente Mutalisina-II (Artigo 3).

3.1. Artigo 1 – The novel metalloproteinase atroxlysin-I from Peruvian *Bothrops atrox* (Jergón) snake venom acts both on blood vessel ECM and platelets

(2010) Eladio F. Sanchez, Francisco S. Schneider, Armando Yarleque, Marcia H. Borges, Michael Richardson, Suely G. Figueiredo, Karla S. Evangelista, Johannes A. Eble.

Apesar da importância médico-epidemiológica da serpente *Bothrops atrox,* poucos estudos foram direcionados ao isolamento e caracterização de toxinas presentes em seu veneno. Este primeiro trabalho relata a purificação e caracterização estrutural e funcional da primeira metaloprotease a ser isolada da serpente *Bothrops atrox*.

Atroxlisina-I, uma PI-SVMP de 23kDa de massa molecular, teve sequência de aminoácidos determinada, possuindo 202 resíduos de aminoácidos, os quais possuem alto grau de homologia em relação a outras PI-SVMPs (na descrição deste artigo, é dito que Atroxlysina-I possui 204 resíduos de aminoácidos, sendo que a região central de Atr-I não havia sido completamente sequenciada – resíduos 84 a 90 não foram identificados à época. Esta região foi sequenciada posteriormente e a estrutura primária completa foi depositada no base de dados UNIPROT com 202 resíduos de aminoácidos).

Representando aproximadamente 5% do conteúdo proteico do veneno e possuindo diversas atividades biológicas *in vivo* e *in vitro*, Atroxlisina-I exerce papel importante no envenenamento causado por *B. atrox*. Atr-I é capaz de se ligar a componentes da matriz extracelular (e.g. colágeno do tipo I, fibronectina, laminina e fibrinogênio) e hidrolisar componentes importantes na manutenção da hemostase (e.g. fibrinogênio e fibronectina) e da integridade de vasos sanguíneos (e.g. colágeno do tipo I e IV e integrinas $\alpha_7\beta_1$ e $\alpha_1\beta_1$) o que, possivelmente, relaciona-se à sua atividade hemorrágica *in vivo.* Além disso, é interessante notar que Atr-I exibe inibição não-enzimática da agregação plaquetária, o que sugere a existência de regiões que interajam com receptores de plaquetas.

Archives of Biochemistry and Biophysics 496 (2010) 9–20

Contents lists available at ScienceDirect

Archives of Biochemistry and Biophysics

journal homepage: www.elsevier.com/locate/yabbi

Original paper

The novel metalloproteinase atroxlysin-I from Peruvian *Bothrops atrox* (Jergón) snake venom acts both on blood vessel ECM and platelets

Eladio F. Sanchez [a,*], Francisco S. Schneider [a], Armando Yarleque [b], Marcia H. Borges [a], Michael Richardson [a], Suely G. Figueiredo [c], Karla S. Evangelista [d], Johannes A. Eble [d]

[a] Research and Development Center, Ezequiel Dias Foundation, 30510-010 Belo Horizonte, Brazil
[b] Laboratory of Molecular Biology, University of San Marcos, Peru
[c] Department of Physiological Sciences, Federal University do Espirito Santo, Brazil
[d] Center for Molecular Medicine, Dept. Vascular Matrix Biology, Excellence Cluster Cardio-Pulmonary System, Frankfurt University Hospital, Frankfurt am Main, Germany

ARTICLE INFO

Article history:
Received 6 November 2009
and in revised form 20 January 2010
Available online 25 January 2010

Keywords:
Metalloproteinase
Snake venom
Atroxlysin
Hemostasis
Platelets

ABSTRACT

We report the isolation and structure–function relationship of a 23 kDa metalloproteinase named atroxlysin-I from the venom of the Peruvian *Bothrops atrox* (Jergón). Atroxlysin is a P-I metalloproteinase and contains 204 residues. Its proteolytic activity towards dimethylcasein is enhanced by Ca^{+2} but inhibited by EDTA, dithiothreitol, excessive Zn^{+2} and α2-macroglobulin. Unlike other structurally homologous P-I metalloproteinases, atroxlysin-I causes hemorrhages. To examine its hemorrhagic activity mechanistically, we studied its function *in vitro* and *in vivo*. It cleaved the Ala_{14}–Leu_{15} and Tyr_{16}–Leu_{17} bonds in oxidized insulin B-chain and specifically hydrolyzed the α-chains of fibrin(ogen) in a dose- and time-dependent manner. Atroxlysin-I cleaved plasma fibronectin and other extracellular matrix proteins (collagens I and IV) and the triple-helical fragment CB3 of collagen IV, but did not degrade laminin-111. Complementarily, the laminin and collagen binding integrins $\alpha_7\beta_1$ and $\alpha_1\beta_1$ were cleaved by atroxlysin. Even without catalytic activity atroxlysin-I inhibited collagen- and ADP-triggered platelet aggregation.

© 2010 Elsevier Inc. All rights reserved.

Introduction

Envenomations by *Bothrops* (pit viper) snakes account for most snakebite accidents in the Americas and represent a serious medical problem, particularly among agricultural workers. In Peru, the jergón *Bothrops atrox* is responsible for most envenomations in the rainforest areas with 87.6% of all ophidian accidents reported at the Hospital of Support N°1 of Pucallpa city between 1984 and 1991 [1]. The human envenomations are often characterized by local and systemic hemorrhage, retarded or enhanced blood coagulation and necrosis. Therefore, South American snake venoms have been studied in a search for pro- and anti-thrombotic/coagulant pharmaceuticals [2–5]. Over the last four decades research has clearly indicated that snake venom metalloproteinases (SVMPs)[1] play important roles in snake venom-induced pathogenesis [6]. SVMPs (sub family M12B, the reprolysins) are processed from precursor forms, which have been classified into four classes (P-I to P-IV) [6–8]. Class P-I has a single metalloproteinase domain which is homologous to the matrix metalloproteinases (MMPs) of tissues. Classes P-II through P-IV contain additional C-terminal domains e.g. disintegrin domain and cysteine-rich domain [7–9]. Acting directly on fibrin(ogen) without activating Pg, some P-I SVMPs have become attractive tools as thrombolytic agents [10].

The P-I class SVMPs are further divided into a two subclasses [7,11]. P-IA with hemorrhagic activity e.g. atroxlysin-I (this work) and P-IB with weaker or without hemorrhagic activity (e.g. leuc-a from *Bothrops leucurus*) [12]. Many attempts have been made to find the key molecular features responsible for the hemorrhagic effect of SVMPs. They have included sequence alignments, phylogenetic constructions, disulfide bond patterns and molecular structure comparisons. However, no conclusive results have been obtained, and their exact mechanism of action is still unclear [6,7,9].

The venom of the Peruvian Jergón, is still poorly characterized, except for a thrombin-like enzyme termed Ba III-4, 33 kDa [13]. Additionally, a hemorrhagic metalloproteinase of ~55 kDa (class P-III) is currently being analyzed in structural and functional studies.

The primary aims of this study were the isolation of the Peruvian *B. atrox* venom metalloproteinase named atroxlysin-I, the determination of its amino acid sequence and its structural and

* Corresponding author. Fax: +55 31 3371 1753.
E-mail address: eladiooswaldo@gmail.com (E.F. Sanchez).

[1] *Abbreviations used:* ECM, extracellular matrix; DMC, dimethylcasein; SVMPs, snake venom metalloproteinases; β2-M, β2-macroglobulin; Fg, fibrinogen; Pg, plasminogen; FN, fibronectin; BM, basement membrane; DTT, dithiothreitol; TLCK, Nα-*p*-Tosyl-L-lysine chloromethyl ketone hydrochloride; PMSF, phenylmethanesulfonil fluoride; MHD, minimum hemorrhagic dose; leucurolysin-a (leuc-a) and mutalysin-II (mut-II), P-I metalloproteinases from *Bothrops leucurus* and *Lachesis muta muta*, respectively.

0003-9861/$ - see front matter © 2010 Elsevier Inc. All rights reserved.
doi:10.1016/j.abb.2010.01.010

functional characterization. Since the proteinase exhibits platelet-inhibiting activity we have also attempted to evaluate its effect on hemostasis and to pinpoint the structural elements responsible for the hemorrhagic activity of SVMPs.

Materials and methods

Materials

Lyophilized *B. atrox* venom was from the Amazon rain forest of Ucayali (Perú) Adenosine diphosphate (ADP) and collagen were obtained from Helena Laboratories, TX, USA; bovine and human plasminogen-free fibrinogen, human plasmin, bovine thrombin, and plasma fibronectin from Sigma (St. Louis, USA); human plasminogen and α2-macroglobulin from Calbiochem (San Diego, USA).

Purification of atroxlysin-I and apo-atroxlysin-I

Atroxlysin-I was isolated from jergón venom by two gel filtration chromatographies on Sephacryl S-200 and Sephadex G-50. Fractions were analyzed by SDS–PAGE and for proteolytic activity by using dimethylcasein (DMC) and fibrin as substrates. 1 g of lyophilized venom was dissolved in 6 ml of 50 mM ammonium acetate buffer (pH 7.3), containing 0.3 M NaCl, and centrifuged at 6000*g*. The supernatant solution (781 mg protein) was loaded onto a Sephacryl S-200 column (2.5 × 100 cm) and eluted with the above buffer at 7 ml/h. After being concentrated with a Microcon Centrifugal Filter Units (Millipore Corp.), the active material (101 mg) was applied to a Sephadex G-50 column (1.5 × 100 cm) and eluted with 50 mM Tris–HCl (pH 8.0), 2 mM $CaCl_2$, at 8 ml/h. The purified proteinase, named atroxlysin-I, was concentrated, stored at 4 °C and examined for purity by RP-HPLC on a Vydac C_4 (4.6 × 250 mm) column. To remove divalent cations, atroxlysin was incubated with 20 mM EDTA. Subsequently, the apo-enzyme was separated from the EDTA-chelated cations by gel filtration on a TSKG 4000 SWXL column (Tosoh Bioscience GmbH, Stuttgart, Germany). To determine Zn^{2+}-ions, 2.5 μg of the holo- and apo-enzyme were hydrolyzed in 2 M hydrochloric acid at 95 °C overnight. The lyophilized samples were resuspended in 100 μl in 20 mM Hepes, pH 7.4, 135 mM NaCl buffer and incubated with 2.5 μM Zn^{2+}-indicator FluZin-3 (Molecular Probes, Eugene, OR, USA). Fluorescence with excitation and emission wavelengths of 494 and 516 nm, respectively, were measured in an ELISA reader (Bio Tek, Bad Friedrichshall, Germany). Fluorescence signals were calibrated with Zn^{2+}-solutions ranging from 100 to 800 nM in 20 mM Hepes, pH 7.4, 135 mM NaCl.

Circular Dichroism (CD) spectra analysis

CD spectra of atroxlysin-I and apo-atroxlysin-I were measured at room temperature on Jasco-815 spectrophotometer (Jasco, Japan) in the wavelength range from 188 to 280 nm. The protein sample concentration was 200 μg/ml in ultra-pure water. The spectra were obtained by average of 35 scans with a scan speed of 100 nm/min.

Protein concentration was determined by BCA protein assay (Pierce Chemical, USA). Anti-atroxlysin-I antiserum was raised in a rabbit (New Zealand 2.5 kg) as described [12]. The IgG fraction of immune rabbit serum was purified by affinity chromatography on protein A Sepharose.

Sequence determination

Atroxlysin-I (3.0 mg) was reduced and alkylated with 4-vinyl pyridine as described [14]. One milligram-aliquots of atroxlysin-I were dissolved in 1 ml of 0.1 M Tris–HCl (pH 8.6), 6 M guanidine–HCl. After addition of 30 μl β-mercaptoethanol the samples were incubated first at 50 °C for 4 h under nitrogen, then with 40 μl of 4-vinyl pyridine in the dark at 37 °C for 2 h and subsequently desalted on a Vydac C_4 column with a gradient of 0–65% acetonitrile in 0.1% TFA. The S-pyridylethylated proteins were cleaved with either trypsin (2% w/w, enzyme:substrate in 1 ml of 0.1 M ammonium bicarbonate, pH 7.9) for 3.5 h at 37 °C or cyanogen bromide in 70% TFA under nitrogen for 24 h [14]. The cleavage products were separated on a Vydac C_{18} small pore column (4.6 × 250 mm) in a linear gradient of 0–50% acetonitrile in 0.1% aqueous TFA and sequenced using a Shimadzu PPSQ-21A protein sequencer. The primary structure of atroxlysin-I was compared with the sequences of other related proteins in the SWISS-PROT/TREMBL data bases using the FASTA 3 and BLAST programs.

Enzyme activity of atroxlysin-I

The enzymatic activity of atroxlysin-I was monitored by DMC assay [15] and by the fibrin plate lysis method at a fibrin:enzyme ratio of 1:113 [16].

Effects of proteinase inhibitor on enzymatic activity

Atroxlysin-I (0.5 μg) was incubated with $CaCl_2$, $MgCl_2$ or $ZnCl_2$ (2 mM each) in 50 mM Hepes buffer, pH 7.5, for 30 min at 37 °C before enzymatic activity was tested with DMC. Its proteolytic activity was challenged with various proteinase inhibitors: EDTA, PMSF, TLCK, DTT.

Increasing amounts of α2-M (4.1–32.8 μg) were incubated with a constant concentration of atroxlysin-I (0.5 μg) in 500-μl final volume of 50 mM Hepes buffer, pH 7.5 at 37 °C for 5 min. The molar ratios of α2-M:enzyme varied from 0.25 to 2.0. The products of the enzyme-inhibitor interaction were analyzed by SDS–PAGE. Equal volumes of enzyme (1 μg/ml, final concentration) were incubated for 30 min at 37 °C with human serum, commercial anti-bothropic/lachetic anti-venom (Fundação Ezequiel Dias, FUNED) and horse anti-*B. atrox* serum (all at 1:20 dilution) The residual proteolytic activity of atroxlysin-I was tested with DMC.

Proteolytic cleavage specificity and activity on fibrin(ogen) and fibronectin

The substrate specificity of atroxlysin-I was determined with oxidized insulin B-chain (Sigma) at an enzyme:substrate ratio of 1:200 [12]. The fragments were separated on a Vydac C_{18} (4.6 × 250 mm) column. The amino acid sequences were determined and their positions were deduced from the insulin B-chain sequence. Fibrinogenolytic activity was measured as described in the previous report [16]. Plasma FN (1 mg/ml) was incubated with atroxlysin-I at an enzyme:substrate ratio of 1:100 (w/w).

Immunoblot and enzyme-linked immunoabsorbent assay (ELISA) analysis

Samples for immunoblot analysis were subjected to reducing SDS–PAGE (12% gel), followed by transfer to nitrocellulose membranes according to the manufacturer's (Bio-Rad) instructions. Blotting procedures, using rabbit IgG (4 μg) against atroxlysin-I, were performed according to [17]. For ELISA, multiwell plates were coated overnight with 0.5 μg/well solution of each P-I proteinase (atroxlysin, leuc-a and mut-II) in 0.05 M carbonate buffer, pH 9.6. After washing with 0.05% Tween-saline, a blocking solution (2% casein in phosphate buffered saline, PBS) was added (1 h at room temperature). After two additional washing steps with the same solution, anti-atroxlysin-I IgG diluted in PBS containing 0.25% casein and 0.05% Tween 20 was incubated for 1 h at 37 °C. After six

washes, peroxidase-coupled anti-rabbit antibody (Sigma, diluted 1:12,000) was added for 1 h at room temperature. The wells were washed and 100 µl of peroxidase substrate *o*-phenylenediamine (0.33 mg/ml in citrate buffer, pH 5.2 in the presence of 0.04% hydrogen peroxide) was added and the color reaction developed for 1 h at 37 °C in a dark. Absorbance was read with a micro-plate reader at 492 nm. Tests were performed in triplicate.

Hemorrhagic activity

Hemorrhagic activity was evaluated by a modified skin assay procedure [2] using two animal models, rat and mouse. The MHD was determined in adult male Wistar rats (250–300 g). One MHD was defined as the amount of protein that caused a hemorrhagic lesion of 10 mm in diameter after 24 h. To be sure that bleeding may not be due to other tissue injuries other than a direct action of atroxlysin on blood vessel, the hemorrhagic lesions were also checked up to 3 h after injection. Specific hemorrhagic activity was expressed as U/mg. The experiments reported here were done within the guidelines established by the Brazilian College for Animal Experimentation and approved by FUNED animal Ethics Committee.

Proteolytic activity upon ECM proteins and their integrin recptors

The activity of atroxlysin-I on some ECM proteins and their integrin receptors *in vitro* was determined by incubating laminin-111, type I and IV collagens and the collagen IV fragment CB3 (gifts of R. Timpl and K. Kühn, Max-Planck-Institute for Biochemistry, Martinsried, Germany) and purified recombinant $\alpha_1\beta_1$, $\alpha_2\beta_1$, $\alpha_3\beta_1$ and $\alpha_7\beta_1$ (15 µg) integrins with atroxlysin-I at the enzyme:substrate ratio of 1:50 (w/w) in 25 mM Hepes buffer (pH 7.4) for 1 and 6 h at 37 °C. Digestion products were analyzed by SDS–PAGE. The soluble integrins were generated and purified as previously described [18–20].

Binding of apo-atroxlysin-I to plasma and ECM proteins

Microtiter plates were coated with (0.5 µg/well of each) plasma FN and Fg, collagen type I (bovine Achilles tendon, Sigma) and laminin (human placenta, Calbiochem) by incubation overnight at 4 °C. Excess binding sites on the surface of the wells were blocked with 2% casein in PBS (pH 7.4). Apo-atroxlysin (0.5 µg/well) in blocking solution was applied to the pre-treated wells and incubated at room temperature for 2 h. After washing, the bound apo-enzyme was detected with a 1:500 dilution of rabbit anti-atroxlysin-I IgG

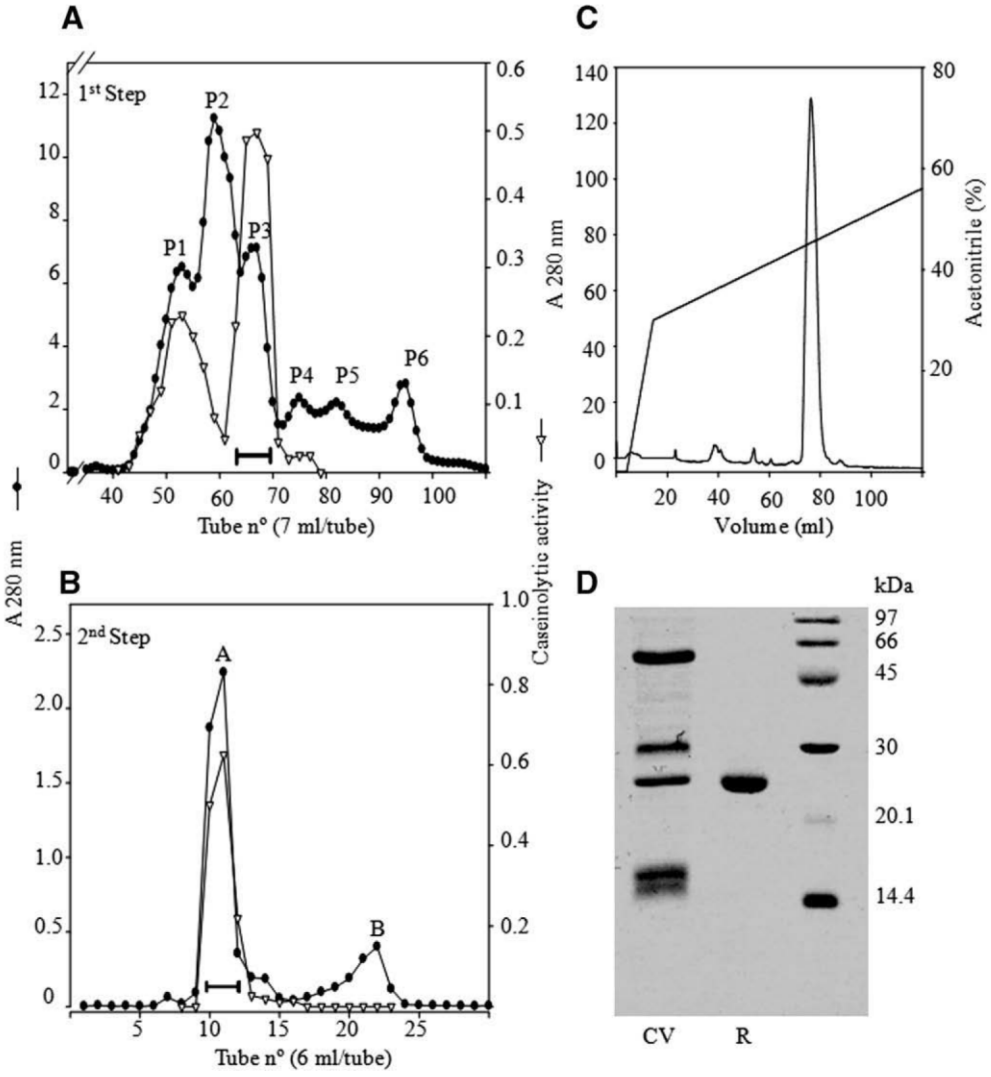

Fig. 1. Purification of atroxlysin-I from *B. atrox* venom. *B. atrox* venom was separated by gel filtration on Sephacryl S-200 (A) and Sephadex G-50 (B) columns. Atroxlysin-I-containing fractions are indicated by bars. Purity of atroxlysin-I was analyzed by RP-HPLC (C) and by SDS–PAGE (D) under reducing (R) conditions. cv denotes crude venom and Mrs. markers are shown on the right.

followed by incubation with anti-rabbit IgG conjugated with peroxidase (diluted 1:12,000, Sigma) for 1 h at 37 °C. Other conditions are as described above (Immunoblot and ELISA section).

Platelet aggregation assay

Aggregation in citrated human platelet-rich plasma (PRP) was measured in a PACKS-4 platelet aggregation system (Helena Laboratories, USA) stirred at 1000 rpm at 37 °C [16]. Inhibition of ADP- or collagen-induced platelet aggregation was monitored by adding atroxlysin-I (0.1–3 μM) or the apo-enzyme 3 min prior to the addition of agonists (10 μM ADP or 5–10 μg/ml collagen). The inhibition of platelet aggregation was normalized to the maximum aggregation in the absence of proteinase. Replicate experiments were conducted with PRP from different drug-free donors.

```
                    1         10         20         30         40         50         60
Atroxlysin-I        ------TPEQ QRYVDLFIVV DHGMFMKYNG NSDKIRRRIH QMVNIMKEAY STMYIDILLT GVEIWSNKDL
BaP1                ---QQR--FS PRYIELAVVA DHGIFTKYNS NLNTIRTRVH EMLNTVNGFY RSVDVHAPLA NLEVWSKQDL
Leucurolysin-a      ----QQ--FS PRYIELVVVA DHGMFKKYNS NLNTIRKWVH EMLNTVNGFF RSMNVDASLV NLEVWSKKDL
Atrolysin-B         ----QN--LP QRYIELVVVA DHRVFMKYNS DLNTIRTRVH EIVNFINGFY RSLNIHVSLT DLEIWSNEDQ
Adamalysin-II       ----QN--LP QRYIELVVVA DRRVFMKYNS DLNIIRTRVH EIVNIINGFY RSLNIDVSLV NLEIWSGQDP
Trimerelysin-II     ----QR--FP QRYIELAIVV DHGMYKKYNQ NSDKIKVRVH QMVNHINEMY RPLNIAISLN RLQIWSKKDL
Mutalysin-II        --------FS QKYIELVVVA DHGMFTKYNG NLNTIRTRVH EIVNTLNGFY RSLNILISLT DLEIWSNQDL
Fibrolase           ----QR--FP QRYVQLVIVA DHRMNTKYNG DSDKIRQWVH QIVNTINEIY RPLNIQFTLV GLEIWSNQDL
Lebetase 2          ---QQR--FE PRYIELVIVA DHAMVTKYNG DLAAITTWVH QLVNNINGFY RDLNVHITLS AVEVWTNGDL
Neuwiedase          ----QQRFFP QRYIELVIVA DRRMYTKYNS DSNKIRTRVH ELVNTVNGFF RSMNVDASLA NLEVWSKKDL
Bilitoxin           -----QRYNP YKYIELFLVV DNRMVTKYNG DLDKIKTRIY ELVNILNEIY RPLYIRVALV GIEFWCNKDL
Insularinase        TPEQQK--FS PRYIELAVVA DHGMFTKYNS NLNTIRTRVH EMVNTLNGFF RSVNVDASLA NLEVWSKKDL
Ussurin             -------TTY QRYVELVVVA DHRMVTKYNG NLIIIRTWVY EIFNTINEIY QRMNIHVALV GLEIWSNGDK
Jerdonitin          -PPE-----Q QRYIELVIVA DHRMYTKYDG DKTEISSKIY ETANNLNEIY RHLKIHVVLI GLEMWSSGEL
Agkistin            -PPDGRIEFL QRYIELVIVA DHRMYTKYDG DKTEISSIIY EIVNILTQNY RPMHIRVALT GLEIWSSGEL
                              :*::* :*: *: :  **: :   *  : :  * :.  :   : :   *  :: *   :

                       70         80         90        100        110        120        130
Atroxlysin-I        INVQPAAPQT LDSFGEWRXX XXXXXKSHDN AQLLTDTDFD QVTINLAYTG SMCDPKRSTG VIQDHSEQDL
BaP1                IKVQKDSSKT LKSFGEWRER DLLPRISHDH AQLLTAVVFD GNTIGRAYTG GMCDPRHSVG VVRDHSKNNL
Leucurolysin-a      IKVEKDSSKT LTSFGEWRER DLLPRISHDH AQLLTVIVFD EETIGIAYTA GMCDLSQSVA VVMDHSKKNL
Atrolysin-B         INIQSASSDT LNAFAEWRET DLLNRKSHDN AQLLTAIELD EETLGLAPLG TMCDPKLSIG IVQDHSPINL
Adamalysin-II       LTIQSSSSNT LNSEGLWREK VLLNKKKKDN AQLLTAIEFK CETLGKAYLN SMCNPRSSVG IVKDHSPINL
Trimerelysin-II     ITVKSASNVT LESFGNWRET VLLKQQNNDC AHLLTATNLN DNTIGLAYKK GMCNPKLSVG LVQDYSPNVF
Mutalysin-II        INVQSAANDT LKTFGEWRER VLLNRISHDN AQLLTAIDLA DNTIGIAYTG GMCYPKNSVG IVQDHSPKTL
Fibrolase           ITVTSVSHDT LASFGNWRET DLLRRQRHDN AQLLTAIDFD GDTVGLAYVG GMCQLKHSTG VIQDHSAINL
Lebetase 2          INVQPAASVT LNLFGEWRER DLLNRRMHDH AQLLTGIDLD DNIIGLAYDD SMCDPRYSVG IVQDHSAIIR
Neuwiedase          IKVEKDSSKT LTSFGEWRER DLLRRKSHDN AQLLTAIDFN GNTIGRAYLG SMCNPKRSVG IVQDHSPINL
Bilitoxin           INVKSASSVT LASFANWRES VLPNRTSHDN AQLLTAIVFN RGVIGSAYPA GMCDPNRSVG TVQDHSEINL
Insularinase        IKVEKDSSKT LTSFGEWRER DLLPRISHDH AQLLTTIVFD QQTIGLAYTA GMCDPRQSVA VVMDHSKKNL
Ussurin             IIVQSSADVT LDLFGTWGEI DLLKRKSHDN AQLLTPTDFD GPTIGLAYVG TMCDPKRSTG VVQDFSPINL
Jerdonitin          SKVTLSADET LDSFGEWRER DLLQRKRHDN AQLLTGMIFN EKIEGRAYKE SMCDPKRSVG IVRDHRTRPH
Agkistin            SNVTLSADDT LDSFGEWRER DLLNRKRHDN AQSLTGMIFS ENIEGRAYKE SMCDLKRSVG IVRDYRTRRH
                      :      *:  *. * *   ** :   *  *  **         .  *:    **     *...: *

                       140        150        160        170        180        190        200
Atroxlysin-I        MVAITMAHEL GHNLGISHDT GSCSCGGYSC IMSPVLSHEP SKYFSDCSYI QCWDFIMKE- -NPQCILNKR
BaP1                WVAVTMAHEL GHNLGIHHDT GSCSCGAKSC IMASVLSKVL SYEFSDCSQN QYETYLTNH- -NPQCILNKP
Leucurolysin-a      RVAVTMAHEL GHNLGMRHDG NQCHCNAPSC IMADTLSKGL SFEFSDCSQN QYQTYLTKH- -NPQCILNKP
Atrolysin-B         LMGVTMAHEL GHNLGMEHDG KDCLRGASLC IMRPGLTKGR SYEFSADSMH YYERFLKQY- -KPQCILNKP
Adamalysin-II       LVAVTMAHEL GHNLGMEHDG KDCLRGASLC IMRPGLTPGR SYEFSDDSMG YYQKFLNQY- -KPQCILNKP
Trimerelysin-II     MVAVTMTHEL GHNLGMEHD- DKDKCKCEAC IMSDVISDKP SKLFSDCSKN DYQTFLTKY- -NPQCILNAP
Mutalysin-II        LIAVTMAHEL GHNLGMKHDE NHCHCSASFC IMPPSISEGP SYEFSDCSKD YYQMFLTKR- -KPQCILNKP
Fibrolase           LVALTMAHEL GHNLGMNHDG NQCHCGANSC VMAAMLSDQP SKLFSDCSKK DYQTFLTVN- -NPQCILNKP
Lebetase 2          LVAVTMAHEL GHNLGMNHDG DQCNCGANGC VMSVVLIEQR SYQFSDCSKN KYQTYLTNR- -NPQCILNQP
Neuwiedase          LVGVTMAHEL GHNLGMEHDG KDCLCGASLC IMSPGLTDGP SYEFSDCSKD YYQTFLTNH- -NPQ------
Bilitoxin           QVAITMAHEI GHNLGMGHDN NSCTCGGYSC IMLPALSDQP SKYFSNCSYI QYRDFIMNQ- -DPQCILNEP
Insularinase        RVAVTMAHEL GHNLGMDHD- DTCTCGAKSC IMASTISKGL SFEFSKCSQN QYQTYLTDH- -NPQCILNKP
Ussurin             LVAVTMAHEI GHNLGMNHDE NYCSCGGFAC IMSPVISPQP SKLFSYCSYI HYWTYINYR- -NPQCILNKP
Jerdonitin          LVANRMAHEL GHNLGFHHDG DSCTCGANSC IMSATVSNEP SSRFSDCSLF QYSSDIIHNP FTSRCLYNEP
Agkistin            FVANIMAHEM GHNLGIDHDR DSCTCDASSC IMSATVSNEP SSRFSDCSLN QYLSDIIHNP LASYCLYNEP
                     :.  ****: *****  **           * :*   :     *  **  *        :         *: *
```

Fig. 2. Alignment of amino acid sequence of atroxlysin-I with other SVMPs: BaP1 (P83512); leuc-a (P84907); atrolysin-B (Q90391); adamalysin-II (P34179); trimerelysin-II (P14530); mut-II (P22796); fibrolase (P28891); lebetase (Q98995); neuwiedase (Q919R4); bilitoxin 1 (P0C6E3); insularinase (Q5XUW8); ussurin (Q7SZD9); jerdonitin (P83912); agkistin (Q8AWX7) by the program ClustalW. Cys residues are highlighted in gray. (*) Identical residues; (:) strongly similar residues; (.) weakly similar residues. The conserved zinc binding motif and the methionine 164 of the Met-turn are marked in boldface. The N-terminal RGD-like RYVD and DKIRRRIHQ sequences are underlined. Unidentified amino acid residues are indicated by X. (–) indicate gaps.

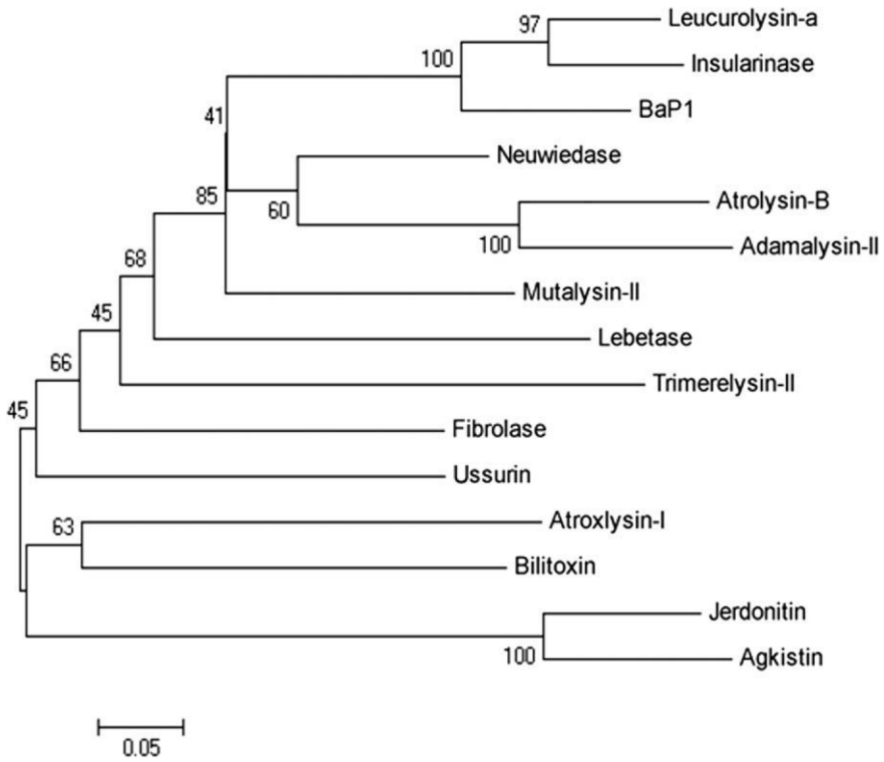

Fig. 3. Phylogenetic tree of P-I and the P-II SVMPs, aligned in Fig. 2. The length of the horizontal scale bar represents 5% divergence.

Results

Purification of atroxlysin-I

Atroxlysin-I was purified by two steps of gel filtration chromatography on Sephacryl S-200 and Sephadex G-50. The purification was monitored by determining the following properties: proteolytic activity on DMC, coagulant activity on human citrated plasma and Fg, amidolytic activity on DL-BAPNA, Tos-Gly-Pro-Lys-pNA, fibrin(ogeno)lytic and hemorrhagic activities. Six major peaks (P1 to P6) were obtained from the crude venom (781 mg) on the Sephacryl S-200 column (Fig. 1A, 1st step). The proteolytic activity on DMC was found in peaks 1 and 3. Peak 1 contained the main hemorrhagic component (P-III SVMP) of ~55 kDa (~52% activity). Peak 3 showed proteolytic (14.8%) and hemorrhagic (8%) activities and included a protein with Mr of ~23 kDa. Further separation of peak 3 (101 mg) on a Sephadex G-50 column resulted in two peaks A and B (Fig. 1B, 2nd step). Peak A had proteolytic activity and appeared homogeneous by RP-HPLC on a C_4 column (Fig. 1C) and by reduced (R) and non-reduced (not shown) SDS–PAGE (Fig. 1D). The purified enzyme was named atroxlysin-I. Its yield was 9.34% with a purification factor of 1.82 with respect to DMC hydrolysis. Atroxlysin-I represented 5.1% (w/w) of the total venom proteins.

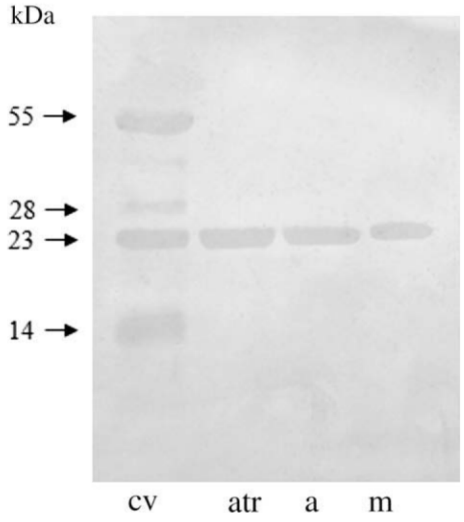

Fig. 4. Reactivity of anti-atroxlysin-I IgG against P-I SVMPs analyzed by western blotting. Immunobloting of anti-atroxlysin-I IgG against crude venom (cv) and purified atroxlysin-I (atr), leuc-a (a) and mut-II (m). The three enzymes are of 23 kDa.

Sequence determination of atroxlysin-I

The primary sequence determination from tryptic or CNBr-derived fragments revealed that atroxlysin-I consists of 204 residues

Table 1
Effect of some reagents on the proteolytic activity of atroxlysin-I.

Compound added	Concentration (mM)	Residual activity (%)
None	–	100
Ca^{2+}	2	117 ± 9
Mg^{2+}	2	90 ± 0.9
Zn^{2+}	2	32 ± 0.3
EDTA	3	0
DTT	2	0
TLCK	1	77 ± 1.4
PMSF	3	100
Apoenzyme + Ca^{2+}	5	0
Apoenzyme + Zn^{2+}	5	15.4 ± 0.1
Human plasma	1:20	72.3 ± 3.6
Anti-bothropic serum	1:20	23.4 ± 6.8
Anti-bothropic/lachetic serum	1:20	59 ± 5

Atroxlysin-I (0.5 μg) was incubated with each compound as described in Materials and methods. The remaining activity was measured with DMC as substrate. Control was performed for each compound (no enzyme). Results are means ± S.D. ($n = 4$).

(Fig. 2) and belongs to the P-I class SVMPs of metzincins [21]. A phylogenetic tree (Fig. 3) was derived by the comparison of the sequence of mature atroxlysin-I with other P-I SVMPs and with the catalytic domain of P-II SVMPs (ussurin, bilitoxin, jerdonitin and agkistin) (Fig. 2) by the MEGA4 program [22] using the Neighbor-Joining method [23]. The phylogenetic tree splits into three branches, however without any correlation of the structural similarity with the hemorrhagic activity of the proteinases. For instance a non-hemorrhagic leuc-a was clustered in the same branch as the hemorrhagic BaP1. Similarly, atroxlysin-I (hemorrhagic) was grouped into the same branch as hemorrhagically less active bilitoxin. The high sequence similarity among P-I enzymes also explain the cross-reactivity of the purified rabbit anti-atroxlysin-I IgG with two related P-I SVMPs from other pit viper species, leuc-a (*B. leucurus*) and mut-II (*Lachesis muta muta*). Immunological cross-reactivity was assessed by western blotting and ELISA. In the crude venom of *B. atrox* (lane cv in Fig. 4), the antibody against atroxlysin-I reacted with protein bands at ~55, 28, 23 and 14 kDa. As the 23 kDa band is the strongest band, it is unlikely that the 23 kDa protease has been generated by (auto)proteolysis that occurs in some P-III type metalloproteases [6]. Therefore, the main form of atroxlysin-I in the venom has a size of 23 kDa, whereas the 55 and the slightly stained 28 kDa bands may correspond to other cross-reacting P-III and P-II class proteinases. Proteins of *B. leucurus* other than SVMPs, such as phospholipase A2, were not recognized by the anti-atroxlysin-I antiserum. However, the antibodies against atroxlysin-I reacted strongly with both leuc-a and mut-II SVMPs from other snake species on immunoblots (Fig. 4) and ELISA (not shown). As the latter metalloproteinase is from a different genus, this cross-reactivity underlines their common structure motifs.

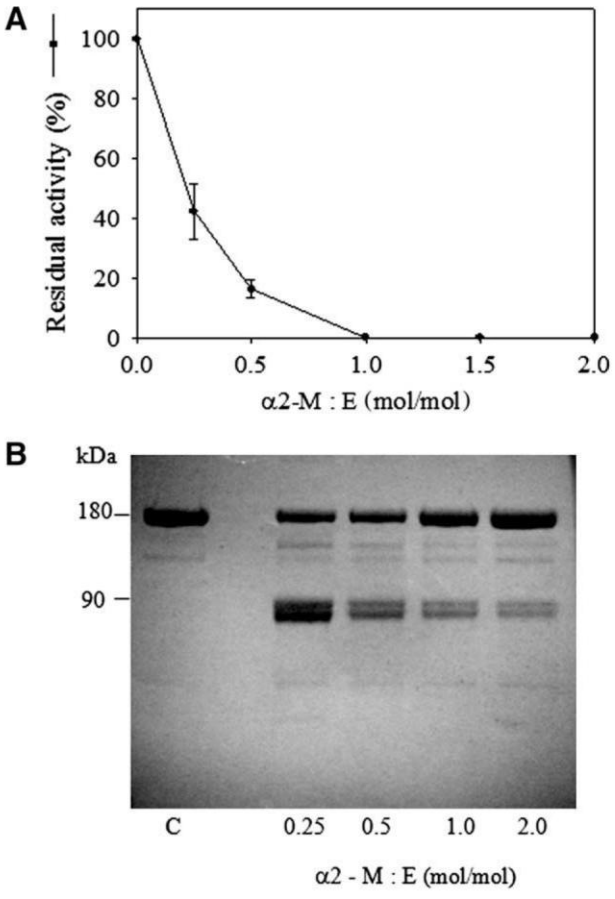

Fig. 5. Interaction of α2-macroglobulin with atroxlysin-I. (A) Stoichiometry of inhibition of atroxlysin-I by α2-M. Atroxlysin-I was incubated with various amounts of α2-M at molar ratios indicated on the abscissa (α2-M/enzyme = 0–2). Proteinase activity in the mixture was measured by DMC assay. The ordinate indicates the remaining activity of the enzyme as a percent of the original activity. Results are means ± S.D. ($n = 4$). (B) Reduced SDS–PAGE pattern of atroxlysin-I incubated with α2-M. Molar ratios of α2-M:enzyme were: 0.25–2.0. From top to bottom: α2-M subunit (180 kDa) and the main cleavage fragments of ~90 kDa are indicated. (C) α2-M control.

Regulation of enzyme activity

The catalytic activity of atroxlysin-I depends on divalent cations and hence was inhibited by EDTA, whereas the serine-reactive PMSF was ineffective (Table 1). Also, typical for metalloproteinases, the internal disulfide bonds of atroxlysin-I were critical for structural integrity and enzymatic activity since incubation with DTT completely inactivated its hydrolyzing activity. The effect of several cations on DMC hydrolysis were also evaluated (Table 1). The activity of atroxlysin-I was slightly enhanced in the presence of Ca^{2+} (117%). However, excessive Zn^{2+} was inhibitory and ~70%

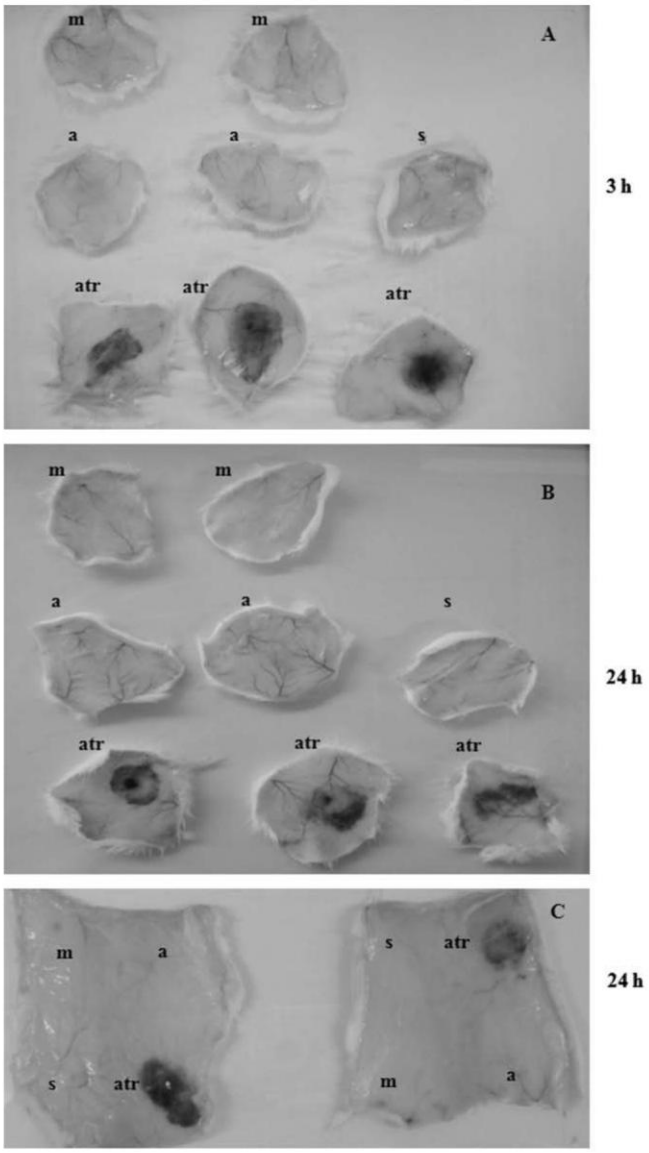

Fig. 6. Hemorrhagic effect of atroxlysin-I. Hemorrhage caused by 50 μg (0.1 ml) of each P-I enzyme: atroxlysin-I (atr), leuc-a (a) and mut-II (m) on the visceral side of removed mice skins after 3 and 24 h (A and B) and in rat skins after 24 h (C) injection, s = saline.

activity was lost after adding 2 mM Zn^{2+}. Anti-bothropic serum showed ~76% inhibition while anti-lachetic/bothropic anti-venom neutralized ~40% of the enzymatic activity (Table 1).

Interaction of atroxlysin-I with α2-M

Pre-incubation of atroxlysin-I with human plasma (1:20 dilution) containing endogenous proteinase inhibitors, e.g. α2-M, abolished ~30% of its enzymatic activity. *In vitro*, the enzymatic activity decreased with increasing α2-M concentrations and was eventually inhibited completely at equimolar stoichiometry. Most remarkably, the180-kDa subunits of α2-M are cleaved into two fragments of ~85 and 100 kDa (Fig. 5B) which frequently run together in SDS–PAGE as the so-called 90-kDa fragment.

Hemorrhagic effect of atroxlysin-I

The local hemorrhagic effect of atroxlysin-I was evaluated in two animal models in comparison with two other P-I SVMPs of the same Mr of 23 kDa and of high sequence similarity: leuc-a (a, *B. leucurus* 67% identity) and mut-II (m, *L. m. muta* 66% identity). Despite their structural similarity, only atroxlysin-I induced local hemorrhage (Fig. 6A–C). Atroxlysin-I (50 μg) directly induced extravascular bleeding on the underside of the mouse skin after 3 and 24 h was shown (Fig. 6A and B), as well as in rat skin after 3 h (not shown) and 24 h (Fig. 6C). The estimated MHD of 19.9 μg/rat, was found to be 1.4 times higher than the crude venom (MHD = 14 μg/rat, [2]).

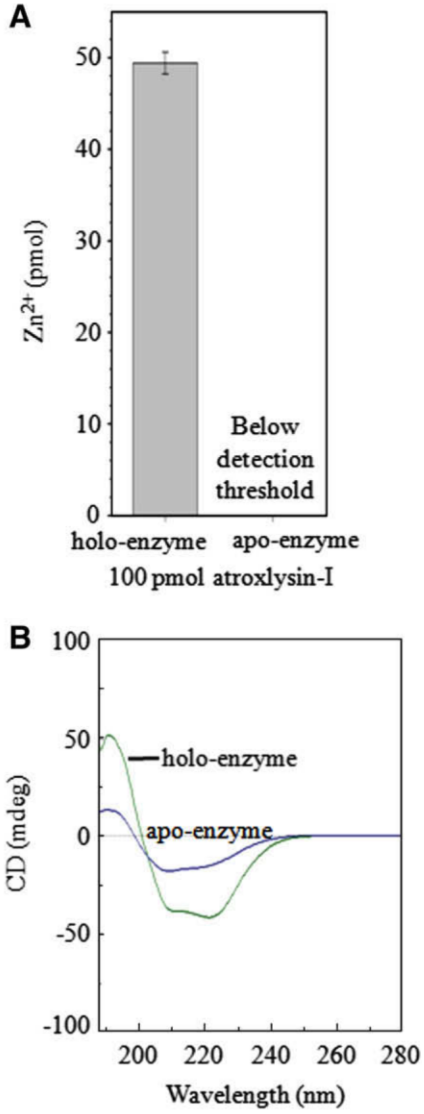

Fig. 7. Zinc determination and CD spectra of holo- and apo-atroxlysin-I. (A) 2.5 μg (100 pmol) atroxlysin and its apo-form were analyzed for their Zn^{2+}-content, using FluoZin-3 indicator. (B) CD spectra were obtained with 200 μg/ml of each sample at room temperature in the wavelength range of 188–280 nm.

Sequence cleavage specificity of atroxlysin-I

To elucidate the mode of action, we determined the peptide bonds which are cleaved by atroxlysin-I and the manner by which the enzyme acts on various plasma and ECM proteins including Fg, FN, type I and IV collagen and laminin-111. As a model substrate the oxidized insulin B-chain was digested with atroxlysin-I. Time-resolved RP-HPLC profiling of the digestion mixture and identification of the digestion products by peptide sequencing revealed that the enzyme rapidly hydrolyzed the peptide bond Ala_{14}–Leu_{15} (first cleavage), followed by Tyr_{16}–Leu_{17} (not shown). Therefore, the X-Leu bond represents the cleavage site within atroxlysin-I's substrate proteins similar to the one of other P-I SVMPs e.g. leuc-a [12].

Fibrin and fibrinogen degradation

The specific activity of purified atroxlysin-I was 6.53 U/mg and 16.8 U/μg with DMC and fibrin as substrates. Irrespective of their hemorrhagic activities, most SVMPs cleave fibrin(ogen). Thus, they keep blood in an anticoagulating state that enables the rapid spread of the other venom components throughout the circulatory system [24]. *In vitro*, atroxlysin-I selectively digests the α-chains of Fg and fibrin dose-(not shown) and time-dependently (Fig. 7A and B). The α-chains of both substrates were completely digested within 30 min. Therefore, atroxlysin-I is an α-fibrinogenase [24]. To examine whether the removal of metal ions (e.g. zinc and calcium) had any impact on the structure and function of the enzyme, we removed the Zn^{2+}-ions from the protein and compared the CD spectra of both, the holo- and apo-enzyme. By using the fluorescent indicator FluoZin-3 we showed that all Zn^{2+} had been removed from the enzyme (Fig. 7A). As result, there is a clear difference between the CD spectrum of holo- and that of the apo-atroxlysin (Fig. 7B). The CD data suggest that apo-atroxlysin undergoes significant conformational change upon removal of metal ions. Yet, the apo-enzyme has a secondary structure distinct from random coil, ruling out a complete unfolding of the enzyme after removal of divalent cations. As EDTA removes any divalent cations, we can not discern the individual effects of Zn^{2+} and Ca^{2+} ions on the conformational stability of atroxlysin-I. Apo-atroxlysin-I failed to hydrolyze the human fibrin α-chains when incubated in a $ZnCl_2$-free buffer solution containing 5 mM $CaCl_2$ (Fig 8B). Its fibrinolytic activity results from the direct interaction with the substrate and is not indirectly causing by activation of Pg. Pg activation was measured by its amidolytic activity on the plasmin substrate Tos-Gly-Pro-Lys-pNA. However, atroxlysin-I failed to activate Pg over a period of 30 min in contrast to the recombinant tissue-type Pg activator (rt-PA) (not shown).

Digestion of fibronectin (FN) and other ECM proteins, as well as integrins by atroxlysin-I

FN is a large multifunctional ECM and plasma glycoprotein that is involved in many cellular processes, including tissue repair and blood clotting [25]. It was degraded by atroxlysin-I resulting in a main degradation product of ~58 kDa which appeared after 1 h

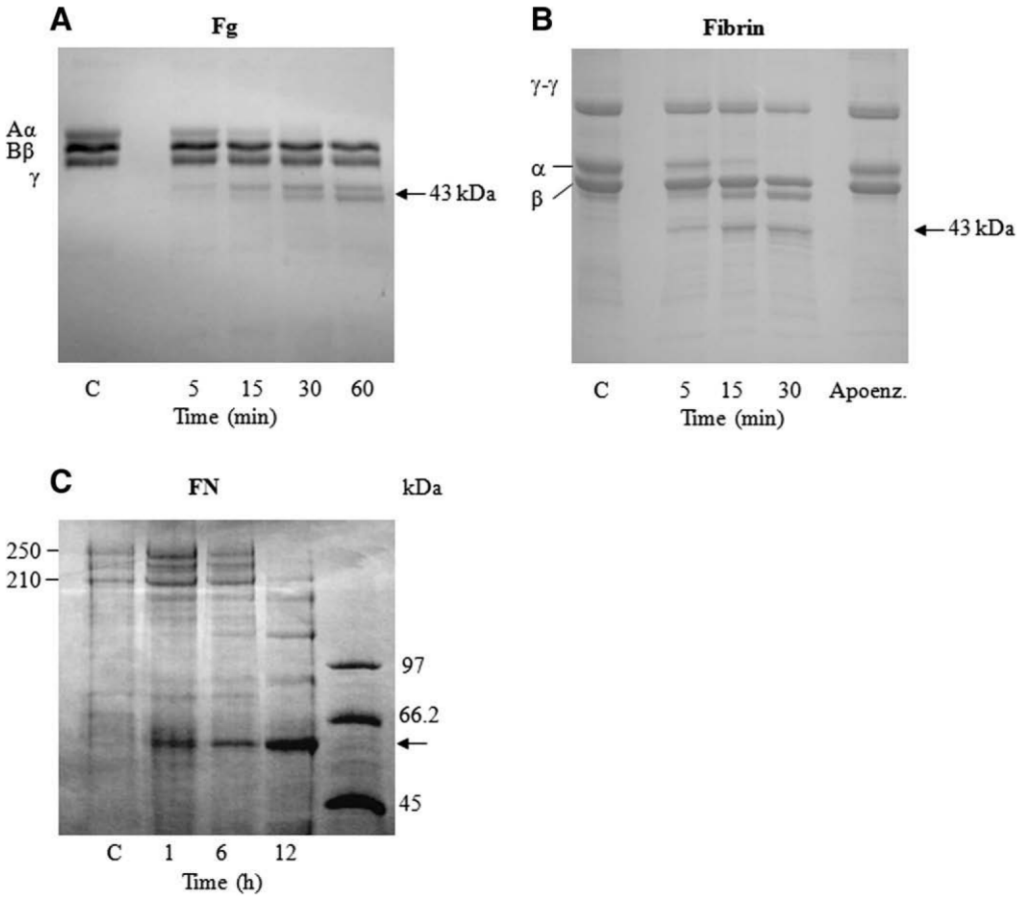

Fig. 8. Proteolytic digestion of Fg, fibrin and FN by atroxlysin-I. Digestion reactions of Fg (A) and fibrin (B) were carried out at a substrate to enzyme ratio of 113:1 (w/w) for the indicated intervals at 37 °C. Aliquots (5 μg) were subjected to reduced SDS–PAGE. Fibrin was also incubated with apo-enzyme (panel B, lane on right) for 30 min under the conditions described in Materials and Methods. As controls (C), Fg and fibrin were incubated without any enzyme for 60 and 30 min respectively. C, plasma FN was incubated with atroxlysin-I at a substrate:enzyme ratio of 100:1. Aliquots of the incubation mixtures were analyzed by reduced SDS–PAGE (7.5% gel). Mr markers are shown on right. Arrows on the right side of the gels indicate the main degradation products.

(Fig. 7C, indicated by an arrow). Hemorrhages can be caused by destruction of the vessel wall. *In vivo* atroxlysin-I disrupts capillary basement membrane (BM), an essential part of the vessel wall. All BMs contain a common set of proteins that include type IV collagen, laminins, heparin sulfate proteoglycans, and enactin/nidogen. Despite the proteolytic resistance due to their triple helices, type I and IV collagens as well as the triple-helical fragment CB3 of collagen IV (not shown) were cleaved by atroxlysin-I within 1 and 6 h (Fig. 9). In contrast, incubation of laminin-111 with atroxlysin-I for 1, 3 and 6 h at 37 °C showed no evidence of digestion (not shown).

Integrins anchor blood vessel cells (endothelial cells, vascular smooth muscle cells) to the underlying BM. Their proteolytic destruction could also cause or contribute to the disintegration of vessels and thus the hemorrhagic effect of atroxlysin-I. The enzyme was able to degrade integrins $\alpha_7\beta_1$ and $\alpha_1\beta_1$ but not $\alpha_2\beta_1$ (Fig. 9) and $\alpha_3\beta_1$ (not shown). Cleavage of $\alpha_7\beta_1$ integrin is in contrast to the proteolytic resistance of its laminin substrate. Integrin $\alpha_7\beta_1$ is abundant in vascular smooth muscle cells and plays diverse roles during the different stages of development [26]. Whereas the collagen binding integrin $\alpha_2\beta_1$ is resistant to atroxlysin-I, the SVMP degrades its collagenous ligands.

Binding assays

The ELISA assay was used to evaluate the binding of apo-atroxlysin-I to plasma FN, Fg as well as collagen I and laminin. After the plasma and ECM proteins were absorbed on the surface of microtiter plate wells, apo-atroxlysin was allowed to interact with the proteins coated on the plate. After thorough washings, bound apo-enzyme molecules on the plasma/ECM proteins-coated surface were detected with anti-atroxlysin-I IgG (0.5 μg) and anti-rabbit IgG conjugated with peroxidase. Fig. 10 illustrates that the apo-enzyme binds to plasma Fg, FN and weakly to collagen I and laminin.

Effect on platelet function

Inhibition of platelet aggregation intensifies bleeding through leaky vessels, thus exacerbating hemorrhages. At micromolar concentrations, atroxlysin-I inhibits ADP- and collagen-induced platelet aggregation in PRP in a dose-dependent manner (Fig. 11A and B). Collagen-induced aggregation (Fig. 11B) showed an initial shape change (increased transmittance) followed by aggregation (decreased transmittance). Atroxlysin-I blocked collagen-triggered aggregation but did not affect shape change. Albeit to a lower extent, the apo-enzyme also inhibits collagen-stimulated aggregation without affecting shape change (Fig. 11B). The IC_{50} values of the holo- and apo-atroxlysin-I were 1.4 and 2.2 μM, respectively (Fig. 11C). This suggests that the inhibition of platelet aggregation by atroxlysin-I is independent of both divalent cations and its metalloproteinase activity.

Discussion

From the *B. atrox* venom we have isolated a novel metalloproteinase named atroxlysin-I. The proteinase is highly homologous to other SVMPs (adamalysins), a subgroup of the metzinzin family

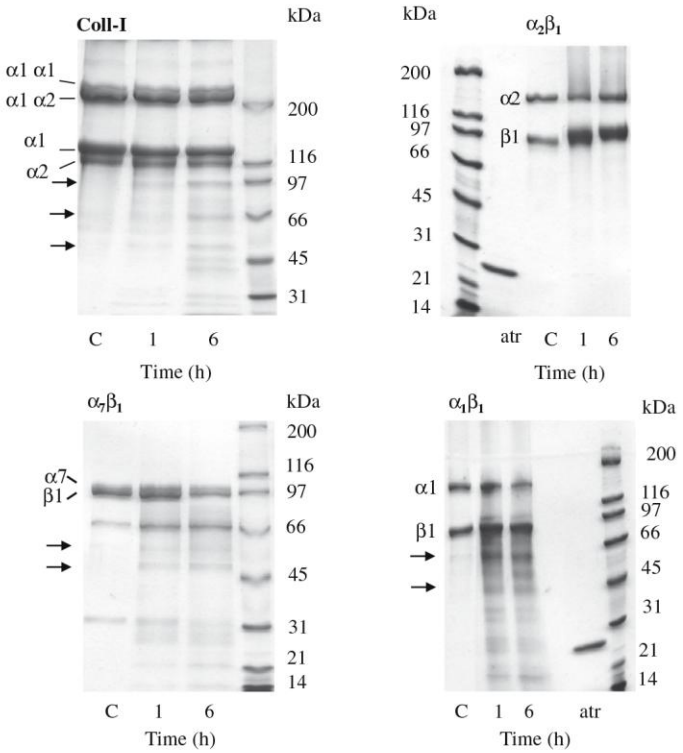

Fig. 9. Proteolytic degradation of ECM and integrin proteins by atroxlysin-I. Type I collagen was incubated with enzyme at a ratio of 1:50 (enzyme:substrate). Aliquots of the incubation mixtures were analyzed by SDS–PAGE under reducing conditions (4.5–10% gels). Typical type I collagen chains (α_1 and α_2) and their naturally cross-linked derivates ($\alpha_1\alpha_1$, $\alpha_1\alpha_2$) are indicated. Integrins $\alpha_7\beta_1$ and $\alpha_1\beta_1$ but not $\alpha_2\beta_1$ are degraded. Arrows on the left indicate the main degradation products. Each integrin was incubated with atroxlysin-I for 1 and 6 h at 37 °C. The digests were examined by SDS–PAGE (7.5–15% gels). Subunits α2, β1 (α2β1), α7, β1 (α7β1) and α1, β1 (α1β1) of each integrin (in parenthesis) are indicated, atr is the control atroxlysin-I. The Mr markers (kDa) were: myosin (200), galactosidase (116), phosphorylase b (97), bovine serum albumin (66), ovalbumin (45), carbonic anhydrase (31), soybean trypsin inhibitor (21) and α-lactalbumin (14.4).

[21]. Typical structural features of the metzincins are the metal-binding consensus HEXXHXXGXXH sequence within the active site and the adjacent Met-turn [21,27]. Atroxlysin-I shows these structural characteristics and loses its proteolytic activity after treatment with EDTA. It also lacks N-linked glycosylation sites (N-X-S/T). Stabilizing the molecular structure, a calcium ion is bound close to the C-terminus opposite to the active site of some SVMPs such as adamalysin-II [28] as well as in leuc-a [29]. The proteolytic activity of atroxlysin-I is activated by calcium, similar to other SVMPs e.g. mut-II and leuc-a [8,12]. Atroxlysin-I harbors a Zn^{2+}-ion in the active site, which is essential for its activity. Nonetheless, an excess of zinc ions inhibited the enzyme, presumably as they bind to allosteric sites and induce an inactivating conformational change.

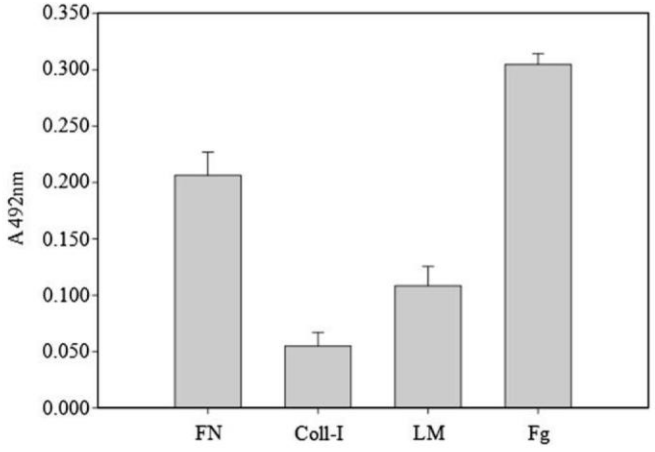

Fig. 10. Binding of atroxlysin-I to FN, Fg, collagen and laminin. Atroxlysin (0.5 μg/well) was incubated in FN-, Fg-, collagen- and laminin-coated microtiter plates. ELISA was used to detect the atroxlysin bound. Results are the mean of triplicates and are expressed as mean ± S.E.

The favored cleavage sites of insulin B-chain by atroxlysin-I were identified as Ala_{14}-Leu_{15} and Tyr_{16}-Leu_{17} within the insulin B-chain. P-I SVMPs e.g. leuc-a [12], fibrolase from *Agkistrodon contortrix contortrix* [24] and lebetase from *Vipera lebetina* [30], mainly split the insulin B-chain at Leu and Phe residues at positions P'_1. However, cleavage specificities of SVMPs are not only influenced by the primary but also tertiary structure of the substrate proteins [24,30].

Here, we demonstrated that atroxlysin-I, is blocked by α2-M, the main proteinase inhibitor in human plasma (720 kDa). Each subunit (180 kDa) of α2-M possesses a bait region which is cleaved by the proteinase. Consequently, α2-M changes its conformation and entraps the proteinase which thus is sterically hindered. This mechanism seems also to occur with atroxlysin-I.

The amino acid sequence of atroxlysin-I contains seven cysteine residues. Six of the cysteines are conserved and likely to be paired as Cys^{117}–Cys^{197}, Cys^{157}–Cys^{181} and Cys^{159}–Cys^{164} in homology to other adamalysins [21,28]. Therefore, atroxlysin-I belongs to the subgroup of P-I class SVMPs which bear three disulfide bridges together with BaP1 [27], acutolysins A and C [11] and leuc-a [12]. The unpaired, free Cys^{186} of atroxlysin-I is located in a hydrophobic core within the C-terminal region of the proteinase domain, similar to the few P-I enzymes e.g. brevilysin L4 from *Glodious halys brevicaudatus* [31] and a P-III bothropasin from *Bothrops jararaca* [32]. It has been suggested [7,9] that the variation in cysteine numbers and an alternative disulfide bridging would lead to different ter-

tiary structures. However, the crystal structures of six P-I SVMPs e.g. adamalysin-II [28], BaP1 [27], acutolysin A [11] and leuc-a [29] show that these proteinases share a common tertiary structure with an upper and lower domain separated by the substrate-binding cleft despite different numbers and patterns of disulfide bonds. Moreover, atroxlysin-I has an equally similar primary structure both to the hemorrhagic P-IA SVMPs such as BaP1 (67% sequence identity) and to the non-hemorrhagic P-IB, such as mut-II and leuc-a (66% and 67% identity, respectively). Thus, the subtle structural differences do not correlate with their (non)hemorrhagic effects in a convincing way. Instead the hemorrhagic potential of P-I SVMPs might be based on their substrate specificity. Atroxlysin-I cleaves not only the hemostasis-relevant proteins fibrin(ogen) α-chains and FN, but also blood vessel components, e.g. collagens and receptors for vessel components such as $\alpha_7\beta_1$ and $\alpha_1\beta_1$ integrins. Cell matrix-interactions within the ves-

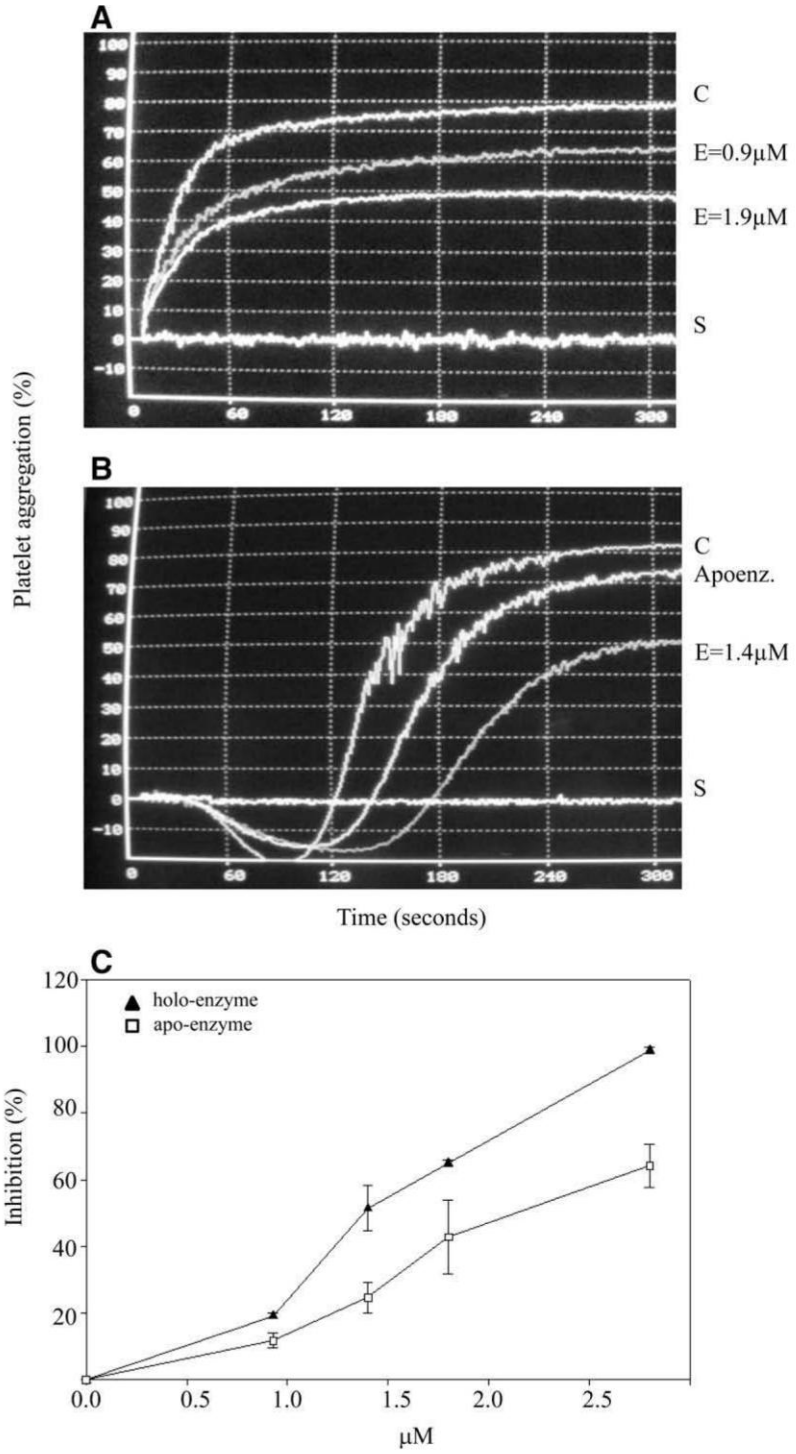

Fig. 11. Effect of atroxlysin-I on ADP- and collagen-induced platelet aggregation. Human PRP was pre-incubated with the indicated concentrations of atroxlysin-I for 3 min at 37 °C before adding 10 μM ADP, (A); or 10 μg/ml collagen, (B). Apo-atroxlysin-I and native enzyme (each at 1.4 μM) were tested to compare the participation of the proteinase activity. C, controls aggregation induced using ADP or collagen; S, PRP incubated with saline (without enzyme). (C) Concentration dependence of holo- (-▲-) and apo-atroxlysin-I (-□-) inhibition of collagen-induced aggregation. Each curve represents the mean of 4–5 individual experiments.

sel wall are disrupted by the proteolytic activity of the SVMPs on specific ECM proteins, among them BM proteins [6,7,12]. Although atroxlysin-I is unable to degrade the characteristic BM protein laminin-111, it cleaves the BM-component type IV collagen and also the protease-resistant type I collagen, which bears tensile forces in the interstitial stromal matrix. Complementary to the ECM proteins, the laminin-binding $\alpha_7\beta_1$ integrin and the collagen binding $\alpha_1\beta_1$ but not $\alpha_2\beta_1$ integrins are degraded by atroxlysin-I. The integrin $\alpha_7\beta_1$ is a predominant integrin receptor of vascular smooth muscle cells with functional importance [33]. By destroying either vessel wall components or their receptors, atroxlysin-I can cause vessel leakiness and hemorrhages.

In the present study we have shown that atroxlysin binds to plasma Fg and FN, which act as ligands for platelet integrins and are involved in platelet adhesion and aggregation. It is known that both Fg and FN bind to the platelet integrins $\alpha_{IIb}\beta_3$ in an activation-dependent manner. Under shear stress in an ex vivo system, platelets adhere with similar efficiencies to surfaces coated with Fg, FN and vWF [34] while adhesion to FN depends on binding to $\alpha_5\beta_1$ and $\alpha_{IIb}\beta_3$ in an RGD-sensitive manner.

Inhibition of platelet aggregation leads to bleeding and contributes to hemorrhage formation through leaky blood vessels. Here, we show that atroxlysin-I can inhibit dose-dependently ADP- or collagen-triggered platelet aggregation at low concentrations in contrast to kistomin, a P-I SVMP from *Calloselasma rhodostoma* [35]. Integrin $\alpha_{IIb}\beta_3$ is a platelet Fg receptor that is critically involved in thrombosis and hemostasis. However, how ligands interact with this integrin has been the subject of much discussion. Ligand-mimetic anti-$\alpha_{IIb}\beta_3$ antibodies that contain the RGD-like RYD sequence in the heavy chain serve as the integrin-binding site in the antibody [36]. Within a natural protein ligands, the tripeptides RGD and RYD exhibit equivalent binding capacity and specificity for the integrin $\alpha_{IIb}\beta_3$ [37]. Moreover, the Gly position can be occupied by a number of different individual amino acids, or even by two residues, in proteins and conformationally restrained peptides, with retention of integrin-binding activity [38]. In this regard, atroxlysin-I contains an RYVD sequence at the N-terminal region (residues 6–10, Fig. 2). Thus, we hypothesized that the RYVD sequence is involved in inhibiting the function of $\alpha_{IIb}\beta_3$ by inducing an allosteric change in the amino terminal portion of αIIb subunit. This mechanism by which ligand binding to integrins is regulated has been proposed for other RGD-containing peptides [39]. In addition, the LDV recognition sequence is an alternatively spliced region of FN [36,37]. In atroxlysin-I the sequence VDL, which is the reverse sequence to the known LDV is found. Furthermore, atroxlysin-I inhibits collagen-induced platelet activation even without its catalytic activity, as the holo- and apo-enzyme inhibit equally well with IC_{50} values of ~1.4 and 2.2 μM, respectively. The high IC_{50} values (μM order) may suggest that the RYVD sequence is not in a cyclic conformation to achieve meaningful impact on inhibiting platelet aggregation. Atroxlysin-I has the sequence DKRRRIHQ close to the N-terminal region, this resembles the sequences TRKSHDNAQ and TRKRHDNAQ in the metalloproteinase domain of the P-III enzymes HR1a from *Trimeresurus flavoviridis* [40] and jararhagin from *B. jararaca*, which recognize the α2I domain and prevent collagen binding to $\alpha_2\beta_1$ integrin [41]. Indeed, the previous studies support the hypothesis that the sequences RYVD and DKIRRRIHQ of atroxlysin-I may be involved in inhibiting platelet aggregation perhaps through interaction with platelet receptors involved in aggregation induced by ADP and collagen. Further investigations together with the crystallization and X-ray diffraction studies that are now in progress will examine this mechanism and may help to clarify its structure–function relationship.

In conclusion, our results indicate that atroxlysin-I belongs to the P-IA class of SVMPs with selective specificity towards the plasma proteins fibrin(ogen) and FN, the vessel wall collagens I and IV the laminin-binding integrin $\alpha_7\beta_1$ and the collagen binding integrin $\alpha_1\beta_1$. The enzyme may play digestive and tissue-degrading roles similar to other SVMPs. Interestingly, its platelet-inhibiting activity is not only caused by its proteolytic activity. It seems that the hemorrhagic potential of a SVMP is less determined by subtle structural characteristics of the enzyme but rather by its pleiotropic effects of both proteolytic destruction of certain substrate proteins involved in blood vessel integrity and non-proteolytic inhibition of platelets.

The amino acid sequence of atroxlysin-I has been deposited in the UNIProtKB (P85420).

Conflict of interest

The authors have declared no conflict of interest.

Acknowledgments

The authors thank to Drs. M.R. Fontes and A.A. Takeda (Dept. of Physics and Biophysics, UNESP, Saõ Paulo, Brazil) for the determination of CD spectra. We also thank Mr. G. Naumann for his technical assistance with zinc analysis. This work was supported by FAPEMIG Grants No: CBB 359/06 and APQ-2673-40.1/07 to E.F.S., J.A.E. receives financial support of the DFG (Grants: SFB 815 project A6, SFB/TR23 project A8 and the Excellence Cluster Cardio-Pulmonary System).

References

[1] H.C. Manrique, D. Chunga, M. Cáceres, E. Espinoza, M.N. Catañeda, Rev. Peruana Enferm. Infecc. Trop. 1 (2001) 1–12.
[2] E.F. Sanchez, T.V. Freitas, D.L. Ferreira-Alves, D.T. Velarde, M.R. Diniz, M.N. Cordeiro, G. Agostini-Cotta, C.R. Diniz, Toxicon 30 (1992) 95–103.
[3] N. Marsh, V. Williams, Toxicon 45 (2005) 1171–1181.
[4] Q. Lu, J.M. Clemetson, K.J. Clemetson, J. Thromb. Haemost. 3 (2005) 1791–1799.
[5] E.F. Sanchez, S. Swenson, Curr. Pharm. Anal. 3 (2007) 147–157.
[6] J.W. Fox, S.M.T. Serrano, J. Proteomics 72 (2009) 200–209.
[7] O.H.P. Ramos, H.S. Selistre-de-Araujo, Toxicon 44 (2004) 529–538.
[8] E.F. Sanchez, Mutalysins, in: A.J. Barrett, N.D. Rawlings, J.F. Woessner (Eds.), Handbook of Proteolytic Enzymes, second ed., Elsevier Academic Press, 2004, pp. 692–694.
[9] J.W. Fox, S.M.T. Serrano, FEBS J. 275 (2008) 3016–3030.
[10] U. Agüero, R.M.E. Arantes, N. Lacerda-Queiroz, O.N. Mesquita, A. Magalhaes, E.F. Sanchez, J. Carvalho-Tavares, Toxicon 50 (2007) 698–706.
[11] W. Gong, X. Zhu, S. Liu, M. Teng, L. Niu, J. Mol. Biol. 283 (1998) 657–668.
[12] C.A. Bello, A.L.N. Hermogenes, A. Magalhaes, S.S. Veiga, L.H. Gremski, M. Richardson, E.F. Sanchez, Biochimie 88 (2006) 189–200.
[13] L.A. Ponce-Soto, V.L. Bonfim, J.C. Novello, R.N. Oviedo, A.Y. Chocas, S. Marangoni, Protein J. 26 (2007) 387–394.
[14] K.J. Wilson, P.M. Yuan, Protein and peptide purification, in: J.B.C. Findlay, M.J. Geisow (Eds.), Protein Sequencing a Practical Approach, IRL Press, Oxford, New York, Tokyo, 1989, pp. 3–41.
[15] E.F. Sanchez, C.I. Santos, A. Magalhaes, C.R. Diniz, S. Figueiredo, J. Gilroy, M. Richardson, Arch. Biochem. Biophys. 378 (2000) 131–141.
[16] M.I. Estevao-Costa, C.R. Diniz, A. Magalhães, F.S. Markland, E.F. Sanchez, Thromb. Res. 99 (2000) 363–376.
[17] H. Towbin, T. Staehlin, G. Gordon, Proc. Natl. Acad. Sci. USA 76 (1979) 4350–4356.
[18] J.A. Eble, K.W. Wucherpfennig, L. Gauthier, P. Dersch, E. Krukonis, R.R. Isberg, M.E. Hemler, Biochemistry 37 (1998) 10945–10955.
[19] J.A. Eble, B. Beermann, H.-J. Hinz, A. Schmidt-Hederich, J. Biol. Chem. 276 (2001) 12274–12284.
[20] J.A. Eble, A. Kassner, S. Niland, M. Mörgelin, J. Grifka, S. Grässel, J. Biol. Chem. 281 (2006) 25745–25756.
[21] W. Stöcker, F. Grams, U. Baumann, P. Reinemer, F.-X. Gomis-Rüth, D.B. McKay, W. Bode, Protein Sci. 4 (1995) 823–840.
[22] K. Tamura, J. Dudley, M. Nei, S. Kumar, Mol. Biol. Evol. 24 (2007) 1596–1599.
[23] N. Saitou, M. Nei, Mol. Biol. Evol. 4 (1987) 406–425.
[24] S. Swenson, C.F. Toombs, L. Pena, J. Johansson, F.S. Markland, Curr. Drug Targets Cardiovas. Haematol. Disord. 4 (2004) 417–434.
[25] S. Beumer, H.F. Heijnen, M.J. Ijsseldijk, E. Orlando, P.G. de Groot, J.J. Sixma, Blood 86 (1995) 3452–3460.
[26] J. Liu, D.J. Burkin, S.J. Kaufman, Am. J. Physiol. Cell Physiol. 294 (2008) C627–C640.

[27] L. Watanabe, J.D. Shannon, R.H. Valente, A. Rucavado, A. Alape-Giron, A.S. Kamiguti, R.D.G. Theakston, J.W. Fox, J.M. Gutierrez, R.K. Arni, Protein Sci. 12 (2003) 2273–2281.
[28] F.X. Gomis-Rüth, F. Kress, W. Bode, EMBO J. 12 (1993) 4151–4157.
[29] R.N. Ferreira, R. Breno, M. Richardson, B.G. Guimaraes, E.F. Sanchez, A.M.C. Pimenta, R.A.P. Nagem, Acta Cryst. 65F (2009) 798–801.
[30] N. Saide, M. Samel, J. Siigur, P.E.H. Jensen, Biochim. Biophys. Acta 1434 (1999) 94–102.
[31] M. Deshimaru, M. Ichihara, T. Hattori, K. Koba, S. Tereda, Toxicon 45 (2005) 571–580.
[32] J.R.C. Muniz, A.L.B. Ambrosio, H.S. Selistre-de Araujo, M.R. Cominetti, A.M. Moura da Silva, G. Oliva, R.C. Garratt, D.H.F. Souza, Toxicon 52 (2008) 807–816.
[33] E.P. Moiseeva, Cardiovasc. Res. 52 (2001) 372–386.
[34] L.K. Lambrecht, B.R. Young, R.E. Stafford, K. Park, R.M. Lambrecht, D.F. Mosher, S.L. Cooper, Thromb. Res. 41 (1986) 99–117.
[35] C.C. Hsu, W.B. Wu, T.F. Huang, J. Thromb. Haemost. 6 (2008) 1578–1585.
[36] W.P. McLaughlin, T. Kamata, Y. Takada, J. Biol. Chem. 275 (2000) 7795–7802.
[37] T.J. Kunicki, K.R. Ely, T.C. Kunicki, Y. Tomiyama, D.S. Annis, J. Biol. Chem. 270 (1995) 16660–16665.
[38] E. Ruoslahti, Annu. Rev. Cell Dev. Biol. 12 (1996) 697–715.
[39] R.B. Basani, G. D'Andrea, N. Mitra, G. Valaire, M. Richberg, M.A. Kowalska, J.S. Bennett, M. Poncz, J. Biol. Chem. 276 (2001) 13975–13981.
[40] M. Kishimoto, T. Takahashi, Toxicon 40 (2002) 1369–1375.
[41] Y. Nymalm, J.S. Puranem, T.K.M. Nyholm, J. Käpylä, H. Kidron, O.T. Pentikäinen, T.T. Airenne, J. Heino, J.P. Slotte, M.S. Johnson, T. Salminen, J. Biol. Chem. 279 (2004) 7962–7970.

3.2. Artigo 2 – Use of a Synthetic Biosensor for Neutralizing Activity-Biased Selection of Monoclonal Antibodies Against Atroxlysin-I, an Hemorrhagic Metalloproteinase from *Bothrops atrox* Snake Venom

(2014) Francisco S. Schneider, Dung Le Nguyen, Karen L. Castro, Sandra Cobo, Ricardo A. Machado de Avila, Nivia de A. Ferreira, Eladio F. Sanchez, Christophe Nguyen, Claude Granier, Pascale Galéa, Carlos Chávez-Olortegui, Franck Molina.

Após a caracterização de Atr-I, propomos neste trabalho a produção de mAbs neutralizantes contra a PI-SVMPs do veneno de *B. atrox* selecionados por meio de uma nova estratégia de screening. Sabendo-se que as principais atividades tóxicas das SVMPs estão relacionadas às suas atividades enzimáticas, elaboramos um protocolo de seleção de hibridomas baseado na neutralização da hidrólise de um substrato peptídico FRET contendo a sequência LVEALYQ. A hidrólise deste substrato foi monitorada por fluorescência e os clones que apresentaram atividades inibitórias contra a atividade proteolítica de Atr-I foram selecionados.

Baseado em nossa nova metodologia, produzimos e caracterizamos seis mAbs. Os três mAbs com maior potencial inibidor da atividade enzimática de Atr-I *in vitro* foram testados *in vivo* contra a atividade hemorrágica de Atr-I. Novamente, os três mAbs inibiram completamente a hemorragia induzida por Atr-I e parcialmente pela veneno bruto de *B. atrox.* Além disso, os mAbs anti-Atr-I mostraram-se extremamente específicos para proteases do veneno de *Bothrops atrox*, não reconhecendo nenhuma das SVMPs provenientes de outros venenos testados, assim como nenhum dos outros diversos venenos de viperídeos sul-americanos. Assim, desenvolvemos uma ELISA sanduíche capaz de diferenciar o envenenamento experimental causado por *Bothrops atrox* de outros acidentes ofídicos.

Esta é a primeira descrição da utilização de um *screening* funcional para a produção de anticorpos neutralizantes contra SVMPs. Vale ressaltar que, apesar de utilizarmos Atr-I como molécula alvo para a produção dos anticorpos monoclonais, esta metodologia pode ser aplicada a diversas SVMPs, tanto de classe P-I quanto de classe P-III, uma vez que várias SVMPs já se mostraram capazes de clivar a ligação peptídica entre Ala e Leu contida na sequência LVEALYQ, referente à cadeia B da insulina.

OPEN ACCESS Freely available online

PLOS | NEGLECTED TROPICAL DISEASES

Use of a Synthetic Biosensor for Neutralizing Activity-Biased Selection of Monoclonal Antibodies against Atroxlysin-I, an Hemorrhagic Metalloproteinase from *Bothrops atrox* Snake Venom

Francisco Santos Schneider[1], Dung Le Nguyen[2], Karen Larissa Castro[1], Sandra Cobo[2], Ricardo Andrez Machado de Avila[1], Nivia de Assis Ferreira[1], Eladio Flores Sanchez[3], Christophe Nguyen[2], Claude Granier[2], Pascale Galéa[2], Carlos Chávez-Olortegui[1]*, Franck Molina[2]

1 Departamento de Bioquímica e Imunologia, Instituto Ciências Biológicas, Universidade Federal de Minas Gerais, Belo Horizonte, Brasil, **2** SysDiag, UMR3145,CNRS/BioRad, Montpellier, France, **3** Departamento de Pesquisa e Desenvolvimento, Fundação Ezequiel Dias, Belo Horizonte, Brasil

Abstract

Background: The snake *Bothrops atrox* is responsible for the majority of envenomings in the northern region of South America. Severe local effects, including hemorrhage, which are mainly caused by snake venom metalloproteinases (SVMPs), are not fully neutralized by conventional serum therapy. Little is known about the immunochemistry of the P-I SVMPs since few monoclonal antibodies (mAbs) against these molecules have been obtained. In addition, producing toxin-neutralizing mAbs remains very challenging.

Methodology/Principal Findings: Here, we report on the set-up of a functional screening based on a synthetic peptide used as a biosensor to select neutralizing mAbs against SVMPs and the successful production of neutralizing mAbs against Atroxlysin-I (Atr-I), a P-I SVMP from *B. atrox*. Hybridomas producing supernatants with inhibitory effect against the proteolytic activity of Atr-I towards the FRET peptide Abz-LVEALYQ-EDDnp were selected. Six IgG1 Mabs were obtained (named mAbatr1 to mAbatr6) and also two IgM. mAbatrs1, 2, 3 and 6 were purified. All showed a high specific reactivity, recognizing only Atr-I and *B. atrox* venom in ELISA and a high affinity, showing equilibrium constants in the nM range for Atr-I. These mAbatrs were not able to bind to Atr-I overlapping peptides, suggesting that they recognize conformational epitopes.

Conclusions/Significance: For the first time a functional screening based on a synthetic biosensor was successfully used for the selection of neutralizing mAbs against SVMPs.

Citation: Schneider FS, Nguyen DL, Castro KL, Cobo S, Machado de Avila RA, et al. (2014) Use of a Synthetic Biosensor for Neutralizing Activity-Biased Selection of Monoclonal Antibodies against Atroxlysin-I, an Hemorrhagic Metalloproteinase from *Bothrops atrox* Snake Venom. PLoS Negl Trop Dis 8(4): e2826. doi:10.1371/journal.pntd.0002826

Editor: José María Gutiérrez, Universidad de Costa Rica, Costa Rica

Received October 2, 2013; **Accepted** March 13, 2014; **Published** April 24, 2014

Copyright: © 2014 Schneider et al. This is an open-access article distributed under the terms of the Creative Commons Attribution License, which permits unrestricted use, distribution, and reproduction in any medium, provided the original author and source are credited.

Funding: This research was supported by Coordenação de Aperfeiçoamento de Pessoal de Nível Superior, Brazil - CAPES (Toxinologia No 23038000825/2011-63), Fundação de Amparo a Pesquisa do Estado de Minas Gerais, Brazil (FAPEMIG), and by funds of the INCTTOX Program of Conselho Nacional de Desenvolvimento Científico e Tecnológico, Brazil (CNPq). The funders had no role in study design, data collection and analysis, decision to publish, or preparation of the manuscript.

Competing Interests: I have read the journal's policy and have the following conflicts: The authors Sandra Cobo and Pascale Galéa are employed by the comercial part (BioRad) of the mix enterprise SysDiag. In addition, mAbatrs are in the patent application process. This does not alter our adherence to all PLOS NTDs policies on sharing data and materials.

* E-mail: olortegi@icb.ufmg.br

Introduction

Snakebites cause up to 1,800 000 envenomations per year, mainly in tropical areas [1–4]. Snakebites might be considered as a daily occupational hazard since rural subsistent farming communities are the main population suffering from this condition [3,4], considered as a Neglected Tropical Condition by WHO (World Health Organization) since 2008 [1]. In Brazil, nearly 30,000 snakebite envenomings occur per year and the incidence is about 14 cases/100,000 people/year, a number as high as those found in many other Latin American countries [1,5–8]. Moreover, in the Brazilian Amazon region, 9,000 snakebites occur per year with an incidence fourfold higher than that found in the rest of Brazil. *Bothrops atrox* is found in tropical lowlands and rainforests in the north of South America and is responsible for the majority of envenomations in this area, causing approximately 80% of snake bites [8–10]. *B. atrox* envenoming is characterized systemically by headache, severe coagulopathy, with consumption of coagulation blood factors, generalized hemorrhage and renal failure. Locally, severe tissue lesions may be observed, including swelling, blisters, inflammatory response, erythema, ecchymosis, local hemorrhage and necrosis [11,12].

Immunotherapy by antivenoms is the only efficacious treatment approved by WHO for snakebite accidents. Antivenoms are produced by hyper immunization of animals (generally horses, sheeps or goats) with a pool of venoms from the most important

Author Summary

In this work, we propose a new screening strategy to produce monoclonal antibodies against Atr-I, a P-I class SVMP from *Bothrops atrox*, which is the snake responsible for the majority of the accidents in South America. SVMPs are the main toxic factors in Bothrops venom causing systemic and local hemorrhage, which may evolve to inflammation and/or necrosis. Since the toxic effects of SVMPs are related to their proteolytic activity, we have produced a peptide which was used as a biosensor for Atr-I hydrolysis. Hydrolysis of this substrate was monitored and the clones possessing inhibitory activity against the proteolytic activity of Atr-I upon the peptide were selected. Using our new approach, we have obtained four monoclonal antibodies highly specific and with neutralizing capacity against the hemorrhagic activity of either Atr-I alone or *Bothrops atrox* whole venom. To the best of the authors' knowledge, this is the first time where a functional screening is used for the selection of neutralizing mAbs against SVMPs. It is also the first description of mAbs anti-Atr-I, with inhibitory potential against its toxic activities which may be useful for diagnosis and treatment in the future.

species of snakes found in each country/region [13]. It is known that serum therapy is effective against several of the systemic noxious effects of snake envenomings, when administered early enough [14–16]. However, the local effects are not fully neutralized, being clinically important [17–20] due to complications related to local hemorrhage and tissue necrosis that can permanently provoke a disability and morbidity among patients, causing a very important socio-economic impact [21].

B. atrox venom is a rich mixture of bioactive components belonging to few protein families [22–24]. Proteomic characterization of toxin composition of *B.* atrox venom used in this study indicates that the main components of this venom are represented by SVMPs (Snake Venom Metalloproteinases) (58.2%), including P-III and P-I classes, SVSP (Snake Venom Serine Proteinases) (11.17%), PLA_2 (Phospholipase A_2) (11.0%) and others [25]. Although these molecules act synergistically in a typical "pit viper envenoming" clinical picture, it is well established that SVMPs are responsible for the most severe local effects (i.e. hemorrhage and its variable consequences) [11,26–31]. SVMPs are zinc-dependent proteinases representing up to 70% of venom dry weight, and can be classified into three classes (P-I to P-III) and several subclasses, according to their domain organization [22–24,32–35]. The P-I class are endopeptidases possessing the metalloproteinase catalytic domain only. The P-II class presents both metalloproteinase and disintegrin domains and the P-III class SVMPs contain disintegrin-like and cysteine-rich domains, in addition to the proteinase domain.

Although no P-III class SVMPs from *B. atrox* have yet been characterized at the protein level, evidence supporting the presence of this class of enzymes has been provided by proteomic and transcriptomic studies [23–25,36]. In addition, three P-I class SVMPs from *B. atrox* venom have already been purified and characterized [37–39]. Atr-I (Atroxlysin-I), Batx-I and Batroxase are P-I enzymes isolated from *B. atrox* venom from the Amazonian regions of Peru, Colombia and Brazil, respectively. They are hemorrhagic and fibrinogenolytic and do not bear any procoagulant activity. These molecules are hemorrhagins that can act proteolytically upon extracellular matrix components, contributing to the local damages following bite. They can also play a systemic role, causing myotoxic effects [38] and inhibition of platelet aggregation [37], which can contribute to hemorrhagic, necrotic and blood-clotting disturbances [37–39].

Considering the important role played by P-I class SVMPs in the *B. atrox* poisoning, polyclonal and monoclonal antibodies against these molecules constitute highly useful tools to investigate the structural determinants of toxicity, for patient diagnosis and may have great potential for the preparation of more efficient antivenoms for passive immunotherapy or even for vaccination. Thus, in this study we used a functional screening based on a synthetic biosensor to produce neutralizing mAbs against Atr-I. Specificity assays of Atr-I using oxidized insulin B-chain as substrate showed that the enzyme cleaves the Ala_{14}-Leu_{15} peptide bond [37]. Inhibition of enzymatic-dependent cleavage of the Atr-I peptide substrate [Abz-LVEALYQ-EDDnp, containing a FRET (Fluorescence Resonance Energy Transfer) system], determined by means of fluorescence emission, was used as a tool to select specific monoclonal antibodies. Four monoclonal antibodies that fully neutralize the proteolytic and hemorrhagic *in vivo* activities of Atr-I and crude *B. atrox* venom were obtained using this functional screening.

Methods

Ethics statement

This study was performed in accordance with the Guide for the Care and Use of Laboratory Animals published by the US National Institutes of Health (NIH Publication No. 85-23, revised 1996) (A5452-01) and were approved by the Animal Experimentation Ethics Committee of the Universidade Federal de Minas Gerais (License number 200/2010).

Animals and venoms

Animals were maintained at the Centro de Bioterismo of the Instituto de Ciências Biológicas of the Federal University of Minas Gerais, Brazil and received water and food under controlled environmental conditions.

Venoms pooled from at least 5–6 adult *B. barnetti*, *B. brazili*, *B. castelnaudi*, *B. chloromelas*, *B. hyoprora*, *B. microphthalmus*, *B. peruvianus*, *B. pictus*, *B.taeniata* and Peruvian *B. atrox* specimens were generously donated by the Instituto Nacional de Salud (Lima, Perú). Venom from Brazilian *B. atrox*, *Lachesis muta muta*, *Crotalus durissus* and *Micrurus frontalis* were ceded by Fundação Ezequiel Dias (FUNED – Belo Horizonte, Brazil).

Atroxlysin-I purification

Atroxlysin-I was purified as described earlier [37], using 1.252 mg of *B. atrox* crude venom collected in the Amazon region of Ucayali – Peru. The purity and the molecular mass of 23 kDa were assessed by SDS-PAGE. BCA Kit (Pierce) was used to determine protein concentration following the manufacturer's instructions.

Production of monoclonal antibodies

Hybridoma production. Atr-I was injected four times subcutaneously in BALB/c mice in order to obtain mice hybridomas. 10 µg of protein were used per dose in complete Freund's adjuvant (Sigma) at the first injection, and incomplete Freund's adjuvant (Sigma) at subsequent inoculations with intervals of 2 weeks between each dose. A booster injection of Atr-I was made 4 weeks after the fourth immunization. Throughout the immunization schedule, mice were bled and the reactivity of immune sera was tested against Atr-I in ELISA assay. Three days after the last injection, spleen cells from hyper immunized mice were fused with Sp2/0 myeloma cells (ATCC).

Functional clone selection and biosensor synthesis. The FRET peptide (Abz-LVEALYQ-EDDnp) was used as a functional biosensor. Supernatants from resulting hybridomas were functionally screened by inhibition of FRET peptide (Abz-LVEALYQ-EDDnp) hydrolysis by Atr-I. For the production of Abz-LVEALYQ-EDDnp, a first step consisting of Fmoc-Glu-EDDnp synthesis was manually done according to a slightly modified version of the method described by Csuhai and colleagues [40]. Next, Fmoc-Glu-EDDnp was immobilized to Rink Amide resin (Novabiochem) by its lateral chain. The subsequent steps of deprotection and coupling of the aminoacids (Abz-LVEALY) were automatically performed by Fmoc chemistry using Multipep robot (Intavis), as previously described [41]. At the end of the synthesis, the rink amide resin liberates a NH_2 group, transforming the Glu into a Gln from the sequence Abz-LVEALYQ-EDDnp.

Fmoc amino acids were acquired from Novabiochem and Boc-2-Abz-OH from Sigma Aldrich. The release from the resin and side-chain deprotection was achieved by treatment with trifluoroacetic acid. The peptide Abz-LVEALYQ-EDDnp was purified and analyzed by reverse-phase HPLC (Waters) on a C-18 column with an acetonitrile gradient (0–60%) (not shown).

To select hybridomas of interest, 40 µL of supernatants from cell cultures were pre-incubated with 11 ng of Atr-I for 30 min at 37°C. Then, 10 µL of Abz-LVEALYQ-EDDnp were added to reach a 47 mM final concentration (1:540 molar ratio enzyme:substrate). The kinetics of FRET peptide hydrolysis was monitored by fluorescence in a Sinergy2 (Biotek) equipment ($\lambda_{ex} = 320$ nm and $\lambda_{em} = 420$ nm) for 60 min at 37°C. Positive controls were made with Sp2/0 supernatants culture and the blank had no Atr-I added. Clones possessing inhibitory effects against the proteolytic activity of Atr-I upon FRET peptide were chosen for subcloning by single-cell limiting dilutions. A second selection round was done and subclones presenting the highest inhibitory effect upon Abz-LVEALYQ-EDDnp cleavage by Atr-I were selected for mAbs production. To determine isotypes of mAbs we used IsoStrip (Roche) according to manufacturer's instructions and purified on a protein A-sepharose column (GE Healthcare). The purity of mAbs was analyzed by a 4%–15% gradient SDS-PAGE (Sodium Dodecyl Sulfate-Polyacrylamide Gel Electrophoresis) in non-reducing conditions.

Molecular characterization of monoclonal antibodies

Indirect ELISA. Purified mAbs were tested against several antigens. Maxisorp plates (Nunc) were coated overnight at 4°C with a 1 µg/mL solution of either Atr-I, BaP1 (from *B. asper*), Leucurolysin-a (Leuc-a, P-I from *B. leucurus* venom), Mutalysin-II (Mut-II, P-I from *Lachesis muta muta* venom) or various bothropic crude venoms (i.e. *B. atrox from* Brazil and Peru, *B. barnetti*, *B. brazili*, *B. castelnaudi*, *B. chloromelas*, *B. hyoprora*, *B. microphthalmus*, *B. peruvianus*, *B. pictus*, *B. taeniata* and *Lachesis muta muta)* in a PBS buffer, pH 7.4, and blocked with PBS-Tween 0.1% containing milk (10 g/L). Antibody binding was detected by horseradish peroxidase conjugated donkey anti-mouse whole-IgG (Jackson ImmunoResearch), followed by addition of TMB solution (Bio-Rad). Washes between steps were done in a Tecan microplate washer. Absorbance values were determined at 450 nm with a Tecan Infinite microplate reader.

Sandwich-ELISA for differentiation between *B. atrox* and L. *muta muta* venom antigens. Pre-immune sera were obtained from female Swiss mice. Maxisorp plates (Nunc) were coated overnight at 4°C with a solution 1:100 of anti-bothropic antivenom (FUNED – Belo Horizonte, Brazil) in coating buffer, pH 9.6, and blocked with PBS-Tween 0.1% containing milk (10 g/L). Then, blocked plates were incubated for 60 min at 37°C with several venoms (i.e. Peruvian *B. atrox*, *Lachesis muta muta*, *Crotalus durissus* and *Micrurus frontalis*) diluted at 10 µg/mL in a solution PBS:mice pre-immune serum (1:1 vol:vol) containing Tween 0.1% and milk (1 g/L). After washing, a mixture of mAbatr1, 2, 3 and 6 (5 µg/mL each) was added to plates. Antibody binding was detected by goat anti-mouse IgG antibody, Peroxidase Conjugated (Milipore) followed by addition of OPD Peroxidase substrate (SIGMAFAST from Sigma-Aldrich). Absorbance values were determined at 450 nm. Positive control was performed using *B. atrox* venom at the same concentration as described above diluted in PBS-Tween 0.1% containing milk (1 g/L). Absorbance from wells containing only PBS:mice pre-immune serum (1:1 vol:vol)-Tween 0.1% and milk (1 g/L) were considered as blank values. To be considered as recognized by mAbatrs, a sample should present an absorbance at least double that obtained from the blank, which was chosen as the threshold signal. Multiple Comparisons versus the *B. atrox* group were carried out using One Way ANOVA applying Holm-Sidak method.

Immunoassay with cellulose-bound peptides. Overlapping pentadecapeptides frameshifted by 3 residues or octopeptides frameshifted by 1 residue covering the entire amino acid sequence of Atr-I were synthesized by Spot synthesis on cellulose membranes, as previously described [42]. A Multipep (Intavis) robot was used for automated peptide synthesis. After an overnight saturation step with 3% BSA (Bovine Serum Albumin), the set of membrane bound peptides was probed by incubation with mAbs anti-Atr-I (1 µg/mL). Antibody binding was detected by using the alkaline–phosphatase conjugated-goat anti-mouse whole IgG (Sigma, diluted 1:2000; 90 min, 37°C). After washing, a phosphatase substrate 5-bromo-4-chloro-3-indolyl phosphate (Sigma) and 3-(4,5-dimethylthiazol-2-yl)-2,5 diphenyltetrazolium bromide (Sigma) was added. Anti-Atr-I IgG produced in rabbits were used as positive controls for the membrane [37]. A blue precipitate was observed on peptides bound by antibodies. To allow the re-use of the membranes, they were sequentially treated with dimethylformamide, then 1% SDS, 0.1% 2-mercapto-ethanol in 8 M urea, followed by ethanol/water/acetic acid (50:40:10 vol/vol/vol) wash and, finally, ethanol so as to remove the precipitated dye and molecules bound to the peptides.

Western blotting. For western blotting, 30 µg of Peruvian *B. atrox* venom were subjected to SDS-PAGE (12%) in non-reducing conditions. The proteins were transferred onto nitrocellulose membranes and blocked with PBS-Tween 0.3% containing 2% casein. The membranes were incubated with mAbatr1, 2, 3 and 6 (50 µg/mL) for one hour at room temperature. Immunoreactive proteins were detected using anti-mouse IgG conjugated with peroxidase (1:3000) from Sigma. After washing three times for 5 minutes with PBS-Tween 0.05%, blots were developed using DAB/chloronaphthol, according to the manufacturer's instructions.

Kinetic interactions between mAbs and Atr-I. Surface Plasmon Resonance (SPR) was used in a ProteOn (Biorad) system to measure association (k_a), dissociation (k_d) and equilibrium (K_D) constants for Atr-I binding to mAbs. Experiments were made following the manufacturer's protocol. Briefly, a sensor chip was activated by a combination of sulfo-NHS and EDC (Ethylene Dichloride). Then, 50 µg of each mAb were dissolved in a 10 mM acetate buffer (pH 4.5) and covalently immobilized on the sensor chip. The chip surface was blocked with ethanolamine 1 M (pH 8.5). Interactions were analyzed at room temperature with different concentrations of Atr-I (200; 100; 50; 25 and 12.5 nM) in PBS buffer (pH 7.5) injected with a flow rate of 30 µL/min.

Neutralizing assays

***In vitro* neutralizing assay.** Purified mAbs were tested for their neutralizing activities upon Abz-LVEALYQ-EDDnp hydrolysis by Atr-I or *B. atrox* whole venom. 60 ng of *B. atrox* venom or 11 ng of Atr-I were pre-incubated with 2 µg of mAbs (molar ratio of

1:28 – Atr-I:antibody) for 30 min at 37°C. Then, the substrate was added in a final concentration of 47 mM. Positive controls were done by pre-incubating Atr-I or *B. atrox* crude venom alone for 30 min at 37°C. The residual activity and neutralizing activity were normalized to the positive control. Enzymatic activity was measured as described above.

***In vivo* neutralizing assay.** Anti-Atr-I mAbs were tested against *B. atrox* venom or Atr-I hemorrhagic activity in Swiss mice as described earlier [43]. One MHD (Minimum Hemorrhagic Dose) of Atr-I (19 µg) [37] or 1.8 MHD of *B. atrox* whole venom (13 µg) [44] was pre-incubated with several amounts of mAbs (12.5; 25.0; 50.0 and 100.0 µg at molar ratios of 10:1, 5:1, 2.5:1 and 1.25:1 – purified Atr-I:antibody; or 2.95:1, 1.48:1, 0.73:1 and 0.37 – estimated quantity [37] of Atr-I in *B. atrox* whole venom: antibody) for 1 hour at 37°C in a final volume of 100 µL. The mixture was inoculated subcutaneously in mice. Alternatively, monoclonal antibodies anti-Atr-I (50 or 100 µg) were subcutaneously injected in PBS solution (100 µL) in mice either before or after experimental envenoming with 1.8 MHD of *B. atrox* venom. In both cases, three hours after Atr-I or venom injection the animals were euthanized in a CO_2 chamber and their skins were removed for evaluation of residual hemorrhage.

List of accession numbers

Atroxlysin-I (UniProtKB/SwissProt P85420); BaP1 (UniProtKB/SwissProt P83512); Batroxstatin-1 (UniProtKB/SwissProt C5H5D2); Batroxstatin-2 (UniProtKB/SwissProt C5H5D3); Batroxstatin-3 (UniProtKB/SwissProt C5H5D4); Batx-I (UniProtKB/SwissProt P0DJE1); *B. atrox* myotoxin I (UniProtKB/SwissProt Q6JK69); Leucurolysin-a (UniProtKB/SwissProt P84907); Mutalysin-II (formely named LHF-II – UniProtKB/SwissProt P22796) were used/cited in this work.

Results

Production and molecular characterization of mAbs

To try to bias the selection of mAbs towards antibodies with Atr-I neutralizing activity, we devised an hybridoma screening assay based on the capacity of hybridoma supernatants to block the proteolytic activity of Atr-I towards the synthetic substrate Abz-LVEALYQ-EDDnp (Figure 1).

After immunization of BALB/c mice with Atr-I, a panel of twenty-one anti-Atr-I secreting hybridomas was selected on the basis of their capacity to neutralize Abz-LVEALYQ-EDDnp hydrolysis by Atr-I. Only hybridomas that presented at least 50% of inhibition of the Atr-I proteolytic activity were selected. These clones were then subcloned and a new round of selection was performed. Eight clones presenting the highest inhibition of the proteolytic activity of Atr-I were finally chosen for production, of which six were IgG1 (named mAbatr1 to mAbatr6) and two were IgM. mAbatr1 to 6 were purified on a protein A-Sepharose column and appeared as homogeneous bands on SDS-PAGE (Figure 2).

The eventual cross-reactivity of the selected mAbatrs with several P-I SVMPs (i.e. Atr-I, BaP1, Leuc-a and Mut-II) and *B. atrox* crude venom was tested in an ELISA format. Figure 3A shows that mAbatrs were not able to recognize the heterologous P-I SVMPs tested. On the other hand, mAbatr1, 2, 3 and 6 presented a high reactivity against Atr-I and a moderate reactivity with *B. atrox* whole venom. mAbatr4 weakly recognized Atr-I and presented low reactivity against the crude venom, while mAbatr5 reacted neither with Atr-I nor *B. atrox* venom. mAbatr1, 2, 3 and 6 were also tested against several South American snake venom antigens (Figure 3B). All mAbs tested showed high specific reactivity against *B. atrox* venom in our ELISA conditions. The other venoms used as antigens coated to ELISA plates were not recognized by the mAbatrs.

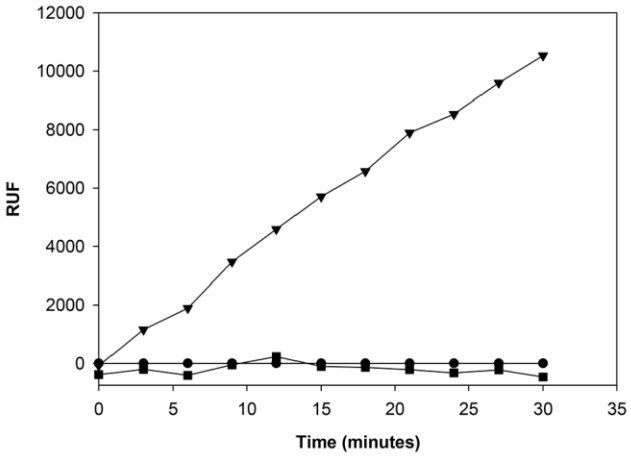

Figure 1. Enzymatic hydrolysis of Abz-LVEALYQ-EDDnp by Atr-I. Cleavage of Abz-LVEALYQ-EDDnp by Atr-I results in a fluorescent emission dependent of the Atr-I enzymatic activity. Hydrolysis of the substrate was assessed after incubation of 11 ng of Atr-I alone (▼) or mixed with EDTA 2 mM (■) with the FRET substrate for 30 minutes at 37°C. Abz-LVEALYQ-EDDnp alone was used as negative control (●).
doi:10.1371/journal.pntd.0002826.g001

Based on the specificity of mAbatrs1, 2, 3 and 6, we decided to evaluate their potential application as diagnostic tools for *B. atrox* simulating experimental envenoming. In sandwich ELISA using plates coated with polyspecific anti-bothropic antivenom from FUNED (Brasil), mAbatrs recognized *B. atrox* venom exclusively with an absorbance signal significantly higher ($p<0.001$) compared to all other venoms tested (Figure 3C).

mAbatr1, 2, 3 and 6 were also tested against *B. atrox* venom in Western Blot. All mAbatrs tested recognized four bands around 15, 23, 30 and 55 kDa (Figure 4).

In an attempt to understand mAbatrs epitope recognition on Atr-I, octa- and pentadecapeptides frameshifted by 1 or 3 residues, respectively, covering the amino acid sequence of Atr-I were synthesized by the SPOT technique and tested either with mAbatr1, 2, 3 and 6 (Figure 5) or IgG anti-Atr-I from rabbit as

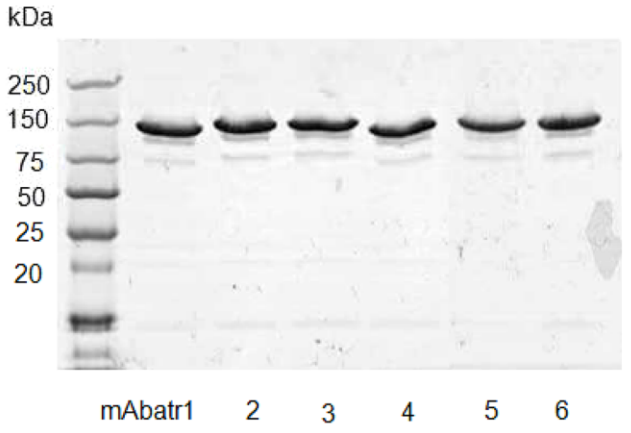

Figure 2. SDS-PAGE of purified mAbatrs. Six anti-Atr-I monoclonal antibodies, isotyped as IgG1, were purified on a protein A-Sepharose column. They appear as homogeneous fractions on SDS-PAGE using a gradient gel (4–15%) in non-reducing conditions.
doi:10.1371/journal.pntd.0002826.g002

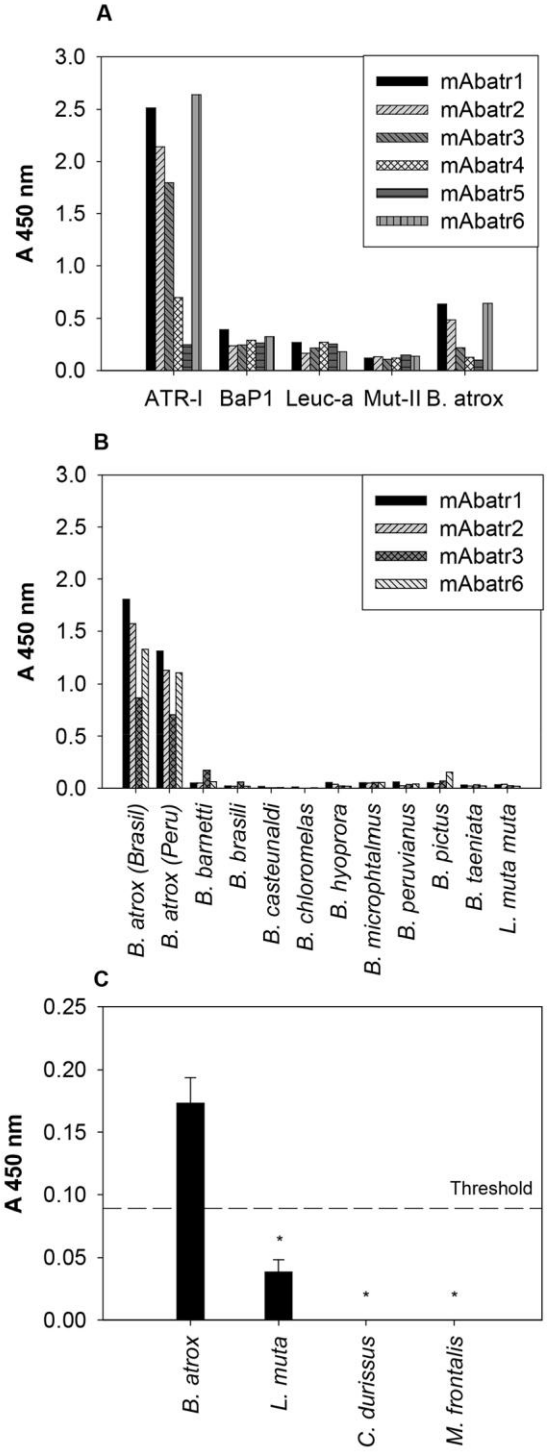

Figure 3. Antigenic reactivity of selected monoclonal antibodies (mAbatrs). (A) Reactivity of purified mAbatrs (5 μg/mL) against several P-I SVMPs and *B. atrox* venom and BSA (negative control-not shown) was measured by ELISA. (B) Reactivity of mAbatr1, 2, 3 and 6 against *B. atrox* (from Brazil and Peru), *B. barnetti*, *B. brasili*, *B. casteunaldi*, *B. chloromelas*, *B. hyoprora*, *B. microphtalmus*, *B. peruvianus*, *B. pictus*, *B. taeniata* e *Lachesis muta muta* venoms (40 μg/mL) was accessed by ELISA. (C) Reactivity of polled mAbatr1, 2, 3 and 6 in sandwich ELISA against Peruvian *B. atrox* venom, *L. muta muta*, *C. durissus* and *M. frontalis* venoms (10 μg/mL) diluted in mice sera simulating experimental envenoming. Positive controls were performed using diluting *B. atrox* venom at the same concentration diluted in a PBS buffer (not shown). Threshold absorbance is represented as at least double that obtained from the blank wells. (*$p<0.001$). Results are expressed as mean of the absorbance value of triplicates.
doi:10.1371/journal.pntd.0002826.g003

positive control. None of the mAbatrs was capable of reacting with the linear peptides covering the Atr-I primary sequence. However, rabbit anti-Atr-I polyclonal IgGs exhibited reactivity against linear epitopes of Atr-I (not shown - manuscript in preparation), suggesting that epitope recognition by mAbs requires folding of Atr-I into its native structure.

The kinetic parameters of mAbatrs interaction with Atr-I were measured on a ProteOn system (BioRad). This equipment measures up to 36 interactions simultaneously, allowing comparisons of affinity among mAbatrs, since they are tested at the same time. Association (k_a), dissociation (k_d) and equilibrium (K_D) constants for Atr-I binding to mAbs are shown in figure 6. mAbatr1, 2 and 6 showed high affinity to Atr-I with equilibrium constants in the 10^{-9} M range, whilst mAbatr3 and mAbatr4 showed slightly lower affinities ($K_D = 9.67\times10^{-8}$ M and 9.40×10^{-8} M). mAbatr5 was not able to react with Atr-I, corroborating the ELISA's results. The interaction of BaP1, Leucurolysin-a and Mutalysin-II with mAbatr1, 2, 3 and 6 were also tested on ProteOn, but no binding was detected (not shown).

Neutralizing assays

The mAbatrs were tested both *in vitro* and *in vivo* in order to assess their neutralizing ability against purified Atr-I or *B. atrox* whole venom. Inhibition of the proteolytic activity of Atr-I or *B. atrox* crude venom on Abz-LVEALYQ-EDDnp substrate cleavage is shown in figure 7. mAbatr1 and 6 exhibited around 85% neutralization of the maximal effect (mAbatr1 – 83.56%±0.40; mAbatr6 – 84.67%±0.78). mAbatr2 showed a weaker blocking of

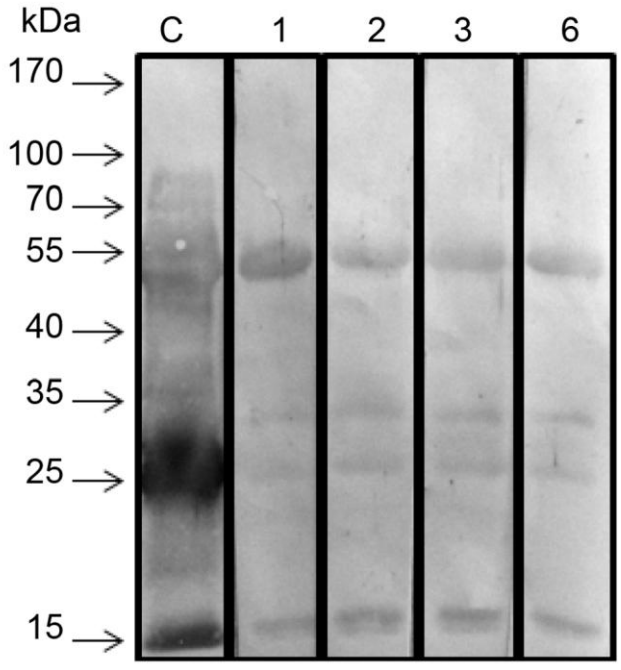

Figure 4. Cross-reactivity of mAbatrs with different toxins from *B. atrox* venom analyzed by western blotting. *B. atrox* crude venom was transferred to a nitrocellulose membrane and incubated with rabbit polyclonal anti-Atr-I serum (**C**) as control, or mAbatr1 (**1**), mAbatr2 (**2**), mAbatr3 (**3**) or mAbatr6 (**6**). All mAbatrs recognized bands around 55, 30, 23 and 15 kDa.
doi:10.1371/journal.pntd.0002826.g004

Figure 5. Molecular pattern of mAbatrs recognition. Reactivity of 8-mer overlapping peptides derived from the amino acid sequence of Atr-I. Peptides were prepared by the Spot method on cellulose membranes and binding of mAbatrs (1 μg/mL) to cellulose-bound peptides was detected by an alkaline phosphatase-conjugated anti-mouse antibody (diluted 1:1000). None of mAbatrs showed reactivity against linear sequence of Atr-I.
doi:10.1371/journal.pntd.0002826.g005

Atr-I activity (75.30%±1.5) and mAbatr-3 only demonstrated a moderate neutralizing effect (37.55%±3.67). When tested against *B. atrox* whole venom *in vitro*, mAbatr1, 2, 3 and 6 presented a weaker neutralization ability (51.24%±0.01; 43.63%±1.62; 29.79%±0.93 and 39.58%±4.45, respectively). On the other hand, mAbatr4 and 5 did not neutralize enzymatic proteolysis of the synthetic substrate induced by Atr-I in the tested conditions.

To reduce testing in living animals, only the three strongest *in vitro* neutralizing antibodies (mAbatr1, 2 and 6) were tested against Atr-I or *B. atrox* venom induced hemorrhage. One MHD of Atr-I was pre-incubated with mAbatrs at different concentrations and then injected subcutaneously in mice. mAbatr1 and 6 fully neutralized the hemorrhagic activity induced by atr-I at a molar ratio of 5:1 (Atr-I : mAbatr), while mAbatr2 only neutralized the

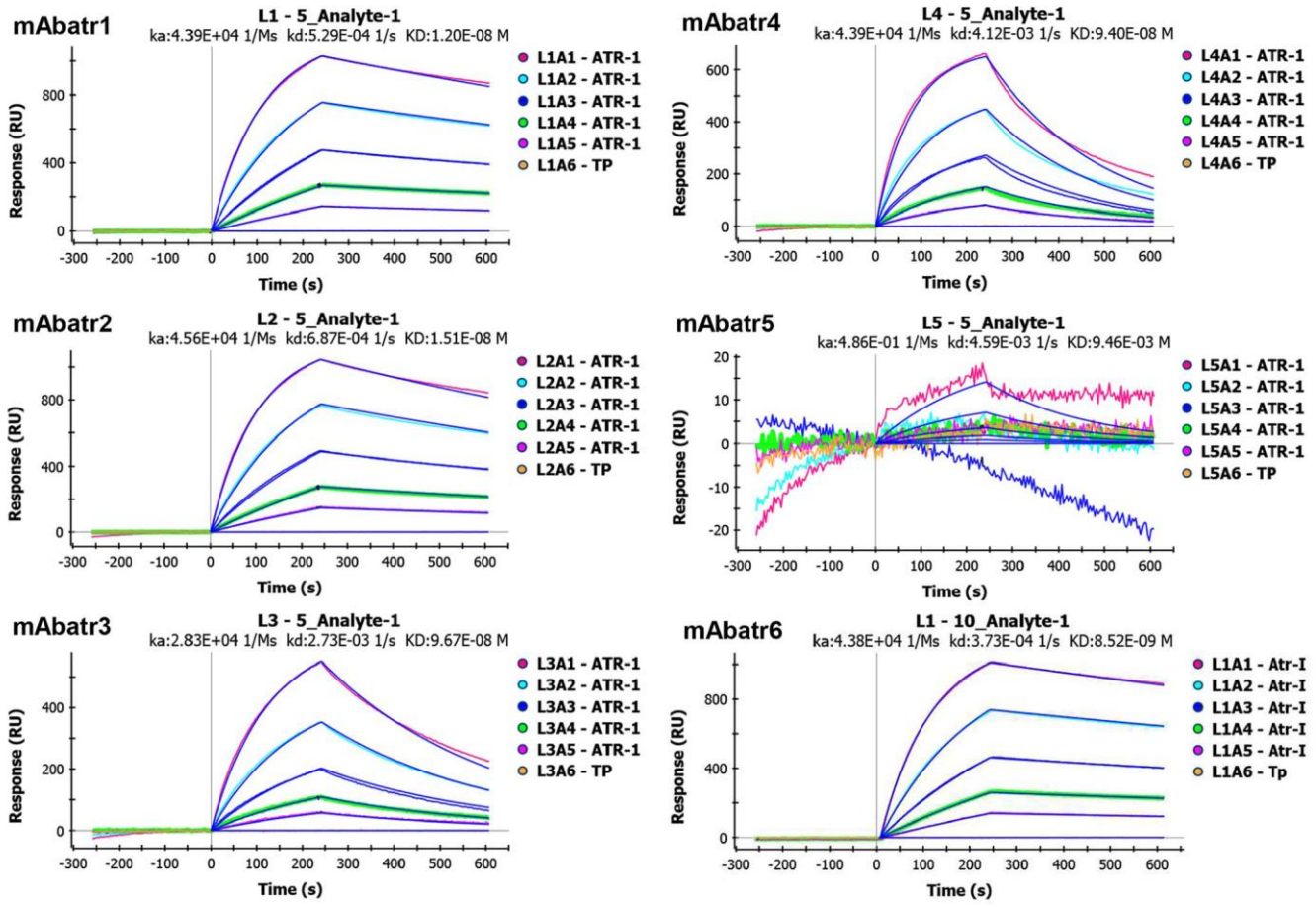

Figure 6. mAbatrs affinity to Atr-I. Kinetic parameters were measured in a ProteOn system. mAbatrs were immobilized on a chip and different concentrations of Atr-I were injected in a flow of 30 μL/min. Binding was evaluated at room temperature.
doi:10.1371/journal.pntd.0002826.g006

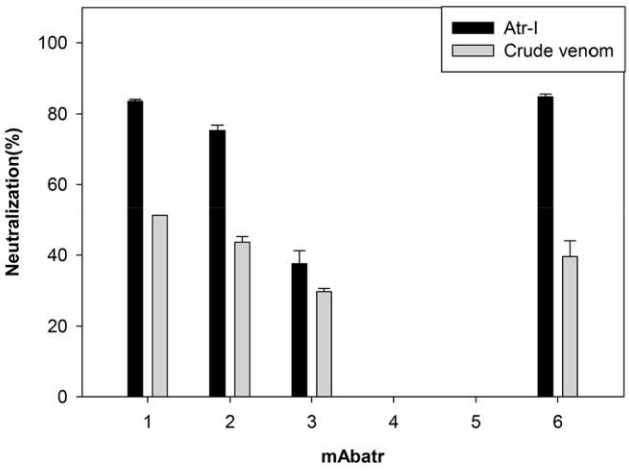

Figure 7. Neutralization of Atr-I or *B. atrox* venom enzymatic activities on Abz-LVEALYQ-EDDnp substrate. Purified mAbatrs were pre-incubated with Atr-I or *B. atrox* venom at 37°C for 30 minutes previously to addition of the FRET substrate. Results are normalized to Atr-I or *B. atrox* venom alone (positive control) and represent means ±S.D. of triplicates.
doi:10.1371/journal.pntd.0002826.g007

hemorrhage at a 2.5:1 molar ratio or higher (Atr-I : mAbatr2) (Figure 8A). 1.8 MHD of *B. atrox* crude venom was completely neutralized by mAbatr1 at 50 µg (0.73:1 molar ratio Atr-I: mAbatr1) or higher, while mAbatr2 and 6 inhibited *B. atrox* hemorrhagic activity at 100 µg (0.37:1 molar ratio Atr-I: mAbatr) (figure 8B).

However, when injected without preincubation with *B. atrox* venom, none of the mAbatrs was able to neutralize hemorrhage induced by *B. atrox* venom at any dose tested (not shown).

Discussion

The bothropic envenoming induces severe local symptoms in human victims, including hemorrhage and tissue necrosis. Complications arise in up to 40% of the cases, in which permanent damage can necessitate the amputation of limbs. The local noxious effects of bothropic venoms (e.g. hemorrhage and necrosis) are mainly due to the action of SVMPs [11,26–30], which seem to be not well neutralized by current therapeutic anti-bothropic antivenoms [17–20]. In this present work, we describe a new rational and functional method to produce neutralizing monoclonal antibodies against P-I SVMPS, using as hybridoma selection criterion the capability of mAbs to block the proteolysis induced by SVMPs.

Atr-I, a 22.3 kDa P-I class SVMP isolated from the Peruvian *B. atrox* venom, is able to hydrolyze the peptide bond between ala_{14} and leu_{15} present in insulin B-chain [37], as well in the fluorogenic peptide (Abz- LVEALYQ-EDDnp). We decided to synthesize this peptide sequence coupled to a fluorescent donor and its respective quencher and to use the FRET technique to measure the inhibition of Atr-I-induced hydrolysis of this biosensor by mAbs. Hybridoma supernatants abolishing fluorescent emission were selected as potentially neutralizing mAbs. Based on this method, we have obtained six IgG1 and two IgM monoclonal antibodies against Atr-I.

mAbs previously produced against BaP1 or Mut-II were selected by ELISA and presented cross-reactivity against heterologous venoms and P-I class SVMPs [45–47]. Although our mAbatrs were not selected on an antigen-binding capacity basis, they showed a very high specificity to Atr-I and *B. atrox* venom. We demonstrated that they do not recognize either other P-I SVMPs from Latin American pit viper venoms that present high degrees of similarity to Atr-I (i.e. Mut-II and BaP1, 57% of identity and Leuc-a, 52% of identity), or any other South American whole venoms from species that share the Amazonia forest as habitat with *B. atrox*.

In the Amazonian forest, the snake *Lachesis muta muta* is responsible for approximately 10% of all snakebites, and the symptoms of this accident are very similar to *B. atrox* envenoming. Currently, there is no laboratory diagnostic able to differentiate *B. atrox* from *L. muta muta* envenoming. Therefore, we have developed a simple test for discriminating *B. atrox* envenoming from envenoming caused by other genera. To avoid unnecessary animal suffering, we have bled Swiss mice and prepared a mixture of their sera with different venoms, simulating experimental envenoming. ELISA plates were coated with polyspecific anti-bothropic antivenom (FUNED – Brasil) to capture antigens from different venoms. Using a pool of mAbatrs, only antigens from *B. atrox* venom were recognized, presenting an absorbance signal double that of pre-immune sera, suggesting that our mAbatrs could be useful in the development of a differential diagnostic for *B. atrox* envenoming.

Western blot assays using mAbatr and purified Atr-I or *B. atrox* venom were done under reducing (not shown) and non-reducing conditions. Under reducing conditions, no reactivity was observed. In non-reducing conditions, mAbatr1, 2, 3 and 6 recognized four

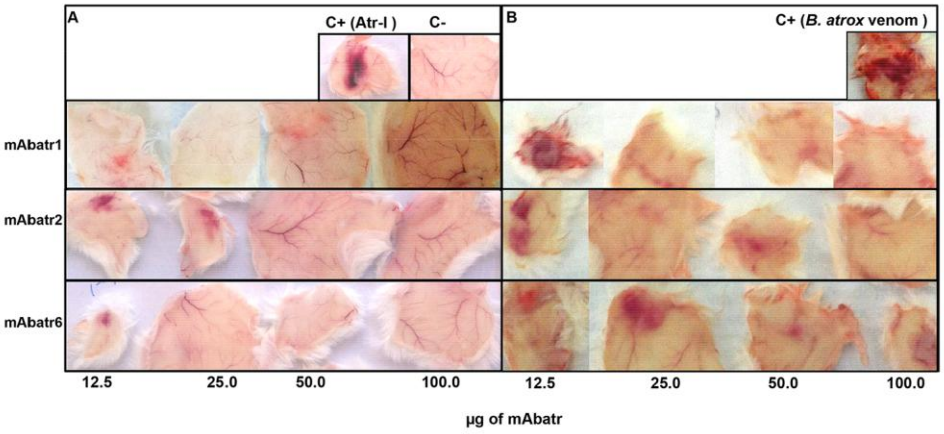

Figure 8. Neutralization of Atr-I-induced hemorrhage in mice. Residual hemorrhage was evaluated after incubating mAbatr1, mAbatr2 or mAbatr3 with 1 MHD of Atr-I (**A**) or 1.8 MHD of *B. atrox* crude venom (**B**) and injecting subcutaneously in mice. After 3 hours mice were euthanized and skins removed. Negative control was saline and positive controls were Atr-I or *B. atrox* venom alone.
doi:10.1371/journal.pntd.0002826.g008

bands at approximately 15, 23, 30 and 55 kDa. Earlier works have shown the presence of several toxins in *B. atrox* venom [23,24,48,49], including: *B. atrox* myotoxin I, a secreted Lys49 PLA_2 with an calculated MW of 13,826 [50], which possesses 37% of identity compared to Atr-I; a P-I SVMP named Batroxase [39], which contains 90% of identical residues compared to Atr-I; as well as three SVMPs from P-III class, called batroxstatin-1, -2 and -3, which possess up to 60% of identity at the proteinase domain compared to Atr-I [36,39]. Due to the likely evolution of toxins by gene duplication and diversification, some epitopes may be kept unchanged during evolution [24,51,52] and common epitopic motifs recognized by mAbatrs might be shared by some different classes of SVMPs in *B. atrox* venom, which could explain the cross-reacting bands around 30 and 55 kDa in Western Blot assay, as observed before [46,47,53,54]. However, the recognition of the band at ~15 kDa is probably not the result of an interaction between mAbatrs and PLA_2 since the overall shape of PLA_2 molecules differ from SVMPs structures. Thus it is reasonable to assume that the reacting band at 15 kDa might be either an artifact or result of SVMPs autolysis/degradation.

None of our mAbatrs recognized overlapping synthetic peptides from the Atr-I primary sequence, confirming that the conformation of Atr-I is very important in recognition by mAbatrs and suggesting that all mAbatrs bind to conformational epitopes. Few works have reported on the molecular interaction of monoclonal antibodies with their respective epitopes in SVMPs. Apparently, neutralizing mAbs against P-I SVMPs interact predominantly via conformational structures [45–47]. Further studies are necessary to better characterize the functional epitopes recognized by mAbatrs and to clarify their role in the biological activity of Atr-I. However, recognition of loops adjacent to the methionine-turn near to the catalytic region, which is an important region for the catalytic activity and determines substrate specificity, might explain the neutralizating activities of mAbatrs. Moreover, this region presents the highest variability in SVMPs, which could account to the high mAbatrs' specificity for Atr-I [55,56].

mAbatr6 ($K_D = 8.52 \times 10^{-9}$ M), mAbatr1 ($K_D = 12.0 \times 10^{-9}$ M) and mAbatr2 ($K_D = 15.1 \times 10^{-9}$ M), showed the highest affinities for Atr-I. Despite the fact that the hybridoma selection method we designed was based on function and not on binding, mAbatrs presented nanomolar equilibrium constants for their binding to Atr-I. This affinity is in the same range as that found in mAbs against others SVMPs, which were selected through affinity-based ELISA assays. When selected conventionally by binding assays, mAbs against SVMPs do not present a correlation between affinity and inhibitory action [45,47]. However, it is interesting to note that there is a clear correlation between the measured affinity of mAbatrs to Atr-I and their neutralizing efficacy.

Three mAbs (mAbatr1, mAbatr2 and mAbatr6) efficiently neutralized proteolysis induced by both Atr-I and *B. atrox* venom upon Abz-LVEALYQ-EDDnp. As hemorrhagic activity of SVMPs is dependent on their enzymatic activities, we decided to test whether mAbatr1, 2 and 6 could prevent hemorrhage induced by either Atr-I or *B. atrox* venom *in vivo*. Although mAbatr1, mAbatr2 and mAbatr6 presented a slightly weaker inhibitory activity on synthetic substrate compared to anti-BaP1 monoclonal antibodies MABaP1-3 and MABaP1-6; mAbtr1, 2 and 6 fully neutralized *in vivo* hemorrhage induced by Atr-I isolated or *B. atrox* whole venom when preincubations with mAbs were performed.

Brazilian and Peruvian *B. atrox* venoms are composed mainly by SVMPs, including P-I and P-III classes [21–25], which are the main molecules responsible for the hemorrhagic activity in *B. atrox* envenoming. The possible cross-reactivity against some other SVMPs present in *B. atrox* venom, but not all of them, may play a key role in neutralization of *B. atrox* whole venom in hemorrhage and could explain the weaker neutralizing ability of mAbatrs against *B. atrox* whole venom tested *in vitro*. The neutralization of other bothropic South American venoms was not tested, since all mAbatrs were very specific and recognized only *B. atrox* venom.

Currently, the standard procedure used, even for monoclonal antibodies, to measure the neutralization capacity of an antivenom against the hemorrhagic activity of snake venoms consists in the preparation of a mixture of venom and antivenom, followed by injection of this preincubated mixture in animals [45,46,53,57,58]. Thus, it is reasonable to assume that once mAbatrs bind to Atr-I and/or Atr-I-like molecules in preincubation step of our hemorrhagic assay these hemorrhagins are sterically hindered and not able to bind to their *in vivo* molecular targets, leading to the abolishment of hemorrhage. On the other hand, when mAbatrs are not preincubated with *B. atrox* venom, hemorrhage is still observed, suggesting that when hemorrhagins are first injected in animals, they bind to and degrade their *in vivo* molecular targets and become inaccessible to mAbatrs. Further studies are needed to clarify the efficacy of preincubation steps of mabs and SVMPs in studies of neutralization of hemorrhage induced by SVMPs.

In conclusion, we developed an efficient method for functional antibody screening, based on a synthetic biosensor to produce mAbs specifically neutralizing P-I SVMPs *in vitro* and *in vivo*. To the best of our knowledge, this is the first time that a functional screening has been used in order to select monoclonal antibodies able to block the toxic effects of SVMPs. It is also the first description of mAbs against Atr-I, isolated from *B. atrox* venom, with inhibitory potential against toxic activities of purified Atr-I and *B. atrox* crude venom. It is still unknown where neutralizing mAbatrs bind to Atr-I. Further, mAbatrs are highly specific to *B. atrox* antigens and may be useful as diagnostic tools for *B. atrox* envenoming. These very encouraging results open the way for a wider utilization of synthetic biosensors in functional screening aiming at the production of neutralizing monoclonal antibodies for further therapeutic approaches or diagnostic assays against *B. atrox* envenoming.

Acknowledgments

We thank Dr. Alexandra Rucavado for providing BaP1 and Dr. M. Richardson for critical reading of the manuscript.

Author Contributions

Conceived and designed the experiments: FSS DLN PG CCO FM. Performed the experiments: FSS DLN KLC SC RAMdA NdAF CN. Analyzed the data: FSS KLC SC RAMdA NdAF EFS CN CG PG CCO FM. Contributed reagents/materials/analysis tools: DLN EFS PG CCO FM. Wrote the paper: FSS DLN RAMdA EFS CN CG PG CCO FM.

References

1. Kasturiratne A, Wickremasinghe AR, de Silva N, Gunawardena NK, Pathmeswaran A, et al. (2008) The Global Burden of Snakebite: A Literature Analysis and Modelling Based on Regional Estimates of Envenoming and Deaths. Plos Medicine 5: 1591–1604.
2. Gutierrez JM, Theakston RDG, Warrell DA (2006) Confronting the neglected problem of snake bite envenoming: The need for a global partnership. Plos Medicine 3: 727–731.
3. Williams D, Gutierrez JM, Harrison R, Warrell DA, White J, et al. (2010) The Global Snake Bite Initiative: an antidote for snake bite. Lancet 375: 89–91.
4. Harrison RA, Hargreaves A, Wagstaff SC, Faragher B, Lalloo DG (2009) Snake Envenoming: A Disease of Poverty. Plos Neglected Tropical Diseases 3: e569.
5. Brasil. Ministério da Saúde. Secretaria de Vigilância em Saúde. Departamento de Vigilância E (2010) Guia de vigilância epidemiológica. Brasília. 816–816 p.

6. Hansson E, Cuadra S, Oudin A, de Jong K, Stroh E, et al. (2010) Mapping Snakebite Epidemiology in Nicaragua - Pitfalls and Possible Solutions. Plos Neglected Tropical Diseases 4: e896.
7. Otero-Patino R (2009) Epidemiological, clinical and therapeutic aspects of Bothrops asper bites. Toxicon 54: 998–1011.
8. Hansson E, Sasa M, Mattisson K, Robles A, Gutierrez JM (2013) Using Geographical Information Systems to Identify Populations in Need of Improved Accessibility to Antivenom Treatment for Snakebite Envenoming in Costa Rica. Plos Neglected Tropical Diseases 7: e2009.
9. Vidal N, Hedges SB (2005) The phylogeny of squamate reptiles (lizards, snakes, and amphisbaenians) inferred from nine nuclear protein-coding genes. Comptes Rendus Biologies 328: 1000–1008.
10. *Bothrops atrox*. Clinical Toxinology Resources. In: http://www.toxinology.com/fusebox.cfm?fuseaction = main.snakes.display&id = SN0389. Acessed in 03/20/2013
11. White J (2005) Snake venoms and coagulopathy. Toxicon 45: 951–967.
12. Warrell DA (2010) Snake bite. Lancet 375: 77–88.
13. Espino-Solis GP, Riano-Umbarila L, Becerril B, Possani LD (2009) Antidotes against venomous animals: State of the art and prospectives. Journal of Proteomics 72: 183–199.
14. Camey KU, Velarde DT, Sanchez EF (2002) Pharmacological characterization and neutralization of the venoms used in the production of Bothropic antivenom in Brazil. Toxicon 40: 501–509.
15. Schneider FS, Starling MC, Duarte CG, de Avila RM, Kalapothakis E, et al. (2012) Preclinical testing of Peruvian anti-bothropic anti-venom against Bothrops andianus snake venom. Toxicon 60: 1018–1021.
16. Otero R, Nunez V, Osorio RG, Gutierrez JM, Giraldo CA, et al. (1995) Ability of 6 Latin-American antivenoms to neutralize the venom of Mapana-equis (*Bothrops atrox*) from Antioquia and Choco (Colombia). Toxicon 33: 809–815.
17. Moreira V, Teixeira C, da Silva HB, D'Imperio Lima MR, Dos-Santos MC (2013) The crucial role of the MyD88 adaptor protein in the inflammatory response induced by Bothrops atrox venom. Toxicon 67: 37–46.
18. Muniz EG, Maria WS, Estevao-Costa MI, Buhrnheim P, Chavez-Olortegui C (2000) Neutralizing potency of horse antibothropic Brazilian antivenom against Bothrops snake venoms from the Amazonian rain forest. Toxicon 38: 1859–1863.
19. Battellino C, Piazza R, da Silva AMM, Cury Y, Farsky SHP (2003) Assessment of efficacy of bothropic antivenom therapy on microcirculatory effects induced by Bothrops jararaca snake venom. Toxicon 41: 583–593.
20. Zamuner SR, da Cruz-Hofling MA, Corrado AP, Hyslop S, Rodrigues-Simioni U (2004) Comparison of the neurotoxic and myotoxic effects of Brazilian Bothrops venoms and their neutralization by commercial antivenom. Toxicon 44: 259–271.
21. Queiroz GP, Pessoa LA, Portaro FCV, Furtado MdFD, Tambourgi DV (2008) Interspecific variation in venom composition and toxicity of Brazilian snakes from Bothrops genus. Toxicon 52: 842–851.
22. Lopez-Lozano JL, de Sousa MV, Ricart CAO, Chavez-Olortegui C, Sanchez EF, et al. (2002) Ontogenetic variation of metalloproteinases and plasma coagulant activity in venoms of wild Bothrops atrox specimens from Amazonian rain forest. Toxicon 40: 997–1006.
23. Nunez V, Cid P, Sanz L, De La Torre P, Angulo Y, et al. (2009) Snake venomics and antivenomics of Bothrops atrox venoms from Colombia and the Amazon regions of Brazil, Peru and Ecuador suggest the occurrence of geographic variation of venom phenotype by a trend towards paedomorphism. Journal of Proteomics 73: 57–78.
24. Calvete JJ, Sanz L, Perez A, Borges A, Vargas AM, et al. (2011) Snake population venomics and antivenomics of Bothrops atrox: Paedomorphism along its transamazonian dispersal and implications of geographic venom variability on snakebite management. Journal of Proteomics 74: 510–527.
25. Kohlhoff M, Borges MH, Yarleque A, Cabezas C, Richardson M, et al. (2012) Exploring the proteomes of the venoms of the Peruvian pit vipers Bothrops atrox, B. barnetti and B. pictus. Journal of Proteomics 75: 2181–2195.
26. Gutierrez JM, Rucavado A, Escalante T, Diaz C (2005) Hemorrhage induced by snake venom metalloproteinases: biochemical and biophysical mechanisms involved in microvessel damage. Toxicon 45: 997–1011.
27. Moura-da-Silva AM, Ramos OHP, Baldo C, Niland S, Hansen U, et al. (2008) Collagen binding is a key factor for the hemorrhagic activity of snake venom metalloproteinases. Biochimie 90: 484–492.
28. Escalante T, Rucavado A, Fox JW, Gutierrez JM (2011) Key events in microvascular damage induced by snake venom hemorrhagic metalloproteinases. Journal of Proteomics 74: 1781–1794.
29. Baldo C, Jamora C, Yamanouye N, Zorn TM, Moura-da-Silva AM (2010) Mechanisms of Vascular Damage by Hemorrhagic Snake Venom Metalloproteinases: Tissue Distribution and In Situ Hydrolysis. Plos Neglected Tropical Diseases 4: e727.
30. Terra RMS, Pinto AFM, Guimaraes JA, Fox JW (2009) Proteomic profiling of snake venom metalloproteinases (SVMPs): Insights into venom induced pathology. Toxicon 54: 836–844.
31. Eble JA (2010) Matrix biology meets toxinology. Matrix Biology 29: 239–247.
32. Stocker W, Grams F, Baumann U, Reinemer P, Gomisruth FX, et al. (1995) The Metzincins – Topological and Sequential Relations Between the Astacins, Adamalysins, Serralysins, and Matrixins (Collagenases) Define a Superfamily of Zinc-Peptidases. Protein Science 4: 823–840.
33. Fox JW, Serrano SMT (2005) Structural considerations of the snake venom metalloproteinases, key members of the M12 reprolysin family of metalloproteinases. Toxicon 45: 969–985.
34. Markland FS, Jr., Swenson S (2013) Snake venom metalloproteinases. Toxicon 62: 3–18.
35. Fox JW, Serrano SMT (2009) Timeline of key events in snake venom metalloproteinase research. Journal of Proteomics 72: 200–209.
36. Tavares NAC, Correia JM, Guarnieri MC, Lima-Filho JL, Prieto-da-Silva ARB, et al. (2008) Expression of mRNAs coding for VAP1/crotastatin-like metalloproteases in the venom glands of three South American pit vipers assessed by quantitative real-time PCR. Toxicon 52: 897–907.
37. Sanchez EF, Schneider FS, Yarleque A, Borges MH, Richardson M, et al. (2010) The novel metalloproteinase atroxlysin-I from Peruvian Bothrops atrox (Jergon) snake venom acts both on blood vessel ECM and platelets. Archives of Biochemistry and Biophysics 496: 9–20.
38. Patiño AC, Pereañez JA, Núñez V, Benjumea DM, Fernandez M, et al. (2010) Isolation and biological characterization of Batx-I, a weak hemorrhagic and fibrinogenolytic PI metalloproteinase from Colombian Bothrops atrox venom. Toxicon 56: 936–943.
39. Cintra ACO, De Toni LGB, Sartim MA, Franco JJ, Caetano RC, et al. (2012) Batroxase, a new metalloproteinase from B. atrox snake venom with strong fibrinolytic activity. Toxicon 60: 70–82.
40. Csuhai E, Juliano MA, St Pyrek J, Harms AC, Juliano L, et al. (1999) New fluorogenic substrates for N-arginine dibasic convertase. Analytical Biochemistry 269: 149–154.
41. Gausepohl H, Boulin C, Kraft M, Frank RW (1992) Automated multiple peptide synthesis. Pept Res 5: 315–320.
42. Laune D, Molina F, Ferrieres G, Villard S, Bes C, et al. (2002) Application of the Spot method to the identification of peptides and amino acids from the antibody paratope that contribute to antigen binding. Journal of Immunological Methods 267: 53–70.
43. Kondo H, Kondo S, Ikezawa H, Murata R (1960) Studies on the quantitative method for determination of hemorrhagic activity of Habu snake venom. Jpn J Med Sci Biol 13: 43–52.
44. Laing GD, Yarleque A, Marcelo A, Rodriguez E, Warrell DA, et al. (2004) Preclinical testing of three south American antivenoms against the venoms of five medic ally-important Peruvian snake venoms. Toxicon 44: 103–106.
45. Fernandes I, Assumpcao GG, Silveira CRF, Faquim-Mauro EL, Tanjoni I, et al. (2010) Immunochemical and biological characterization of monoclonal antibodies against BaP1, a metalloproteinase from Bothrops asper snake venom. Toxicon 56: 1059–1065.
46. Estevao-Costa MI, Martins MS, Sanchez EF, Diniz CR, Chavez-Olortegui C (2000) Neutralization of the hemorrhagic activity of Bothrops and Lachesis snake venoms by a monoclonal antibody against mutalysin-II. Toxicon 38: 139–144.
47. Tanjoni I, Butera D, Bento L, Della-Casa MS, Marques-Porto R, et al. (2003) Snake venom metalloproteinases: structure/function relationships studies using monoclonal antibodies. Toxicon 42: 801–808.
48. Kanashiro MM, Escocard RDM, Petretski JH, Prates MV, Alves EW, et al. (2002) Biochemical and biological properties of phospholipases A(2) from Bothrops atrox snake venom. Biochemical Pharmacology 64: 1179–1186.
49. Lomonte B, Gutierrez JM, Furtado MF, Otero R, Rosso JP, et al. (1990) Isolation of basic myotins from *Bothrops moojeni* and *Bothrops atrox* snake venoms. Toxicon 28: 1137–1146.
50. Nunez V, Arce V, Gutierrez JM, Lomonte B (2004) Structural and functional characterization of myotoxin I, a Lys49 phospholipase A(2) homologue from the venom of the snake Bothrops atrox. Toxicon 44: 91–101.
51. Fry BG, Wuster W (2004) Assembling an arsenal: Origin and evolution of the snake venom proteome inferred from phylogenetic analysis of toxin sequences. Molecular Biology and Evolution 21: 870–883.
52. Fry BG, Vidal N, Norman JA, Vonk FJ, Scheib H, et al. (2006) Early evolution of the venom system in lizards and snakes. Nature 439: 584–588.
53. Tanjoni I, Butera D, Spencer PJ, Takehara HA, Fernandes I, et al. (2003) Phylogenetic conservation of a snake venom metalloproteinase epitope recognized by a monoclonal antibody that neutralizes hemorrhagic activity. Toxicon 42: 809–816.
54. Lomonte B (2012) Identification of linear B-cell epitopes on myotoxin II, a Lys49 phospholipase A(2) homologue from Bothrops asper snake venom. Toxicon 60: 782–790.
55. Ramos OHP, Selistre-de-Araujo HS (2004) Comparative analysis of the catalytic domain of hemorrhagic and non-hemorrhagic snake venom metallopeptidases using bioinformatic tools. Toxicon 44: 529–538.
56. Akao PK, Tonoli CCC, Navarro MS, Cintra ACO, Neto JR, et al. (2010) Structural studies of BmooMP alpha-I, a non-hemorrhagic metalloproteinase from Bothrops moojeni venom. Toxicon 55: 361–368.
57. Morine N, Matsuda S, Terada K, Eto A, Ishida I, et al. (2008) Neutralization of hemorrhagic snake venom metalloproteinase HR1a from Protobothrops flavoviridis by human monoclonal antibody. Toxicon 51: 345–352.
58. Frauches TS, Petretski JH, Arnholdt ACV, Lasunskaia EB, de Carvalho ECQ, et al. (2013) Bothropic antivenom based on monoclonal antibodies, is it possible? Toxicon 71: 49–56.

3.2.1. Resultados não publicados

Além dos resultados publicados, testamos também a membrana de SPOT utilizada neste artigo incubando-a com o IgG de coelho anti-Atr-I purificado do soro policlonal produzido em coelho anti-Atr-I citado no capítulo anterior (Artigo 1 – The novel metalloproteinase atroxlysin-I from Peruvian *Bothrops atrox* (Jergón) snake venom acts both on blood vessel ECM and platelets) visando a caracterização dos epitopos lineares de Atr-I. O protocolo utilizado neste ensaio foi o mesmo descrito no Artigo 2 – Use of a Synthetic Biosensor for Neutralizing Activity-Biased Selection of Monoclonal Antibodies Against Atroxlysin-I, an Hemorrhagic Metalloproteinase from *Bothrops atrox* Snake Venom.

Após a revelação, os SPOTs reativos foram analisados manualmente, sendo que duas regiões foram fortemente reconhecidas pelo IgG de coelho anti-atr-I (Spots 419 a 423 e 455 a 457)(Figura 13).

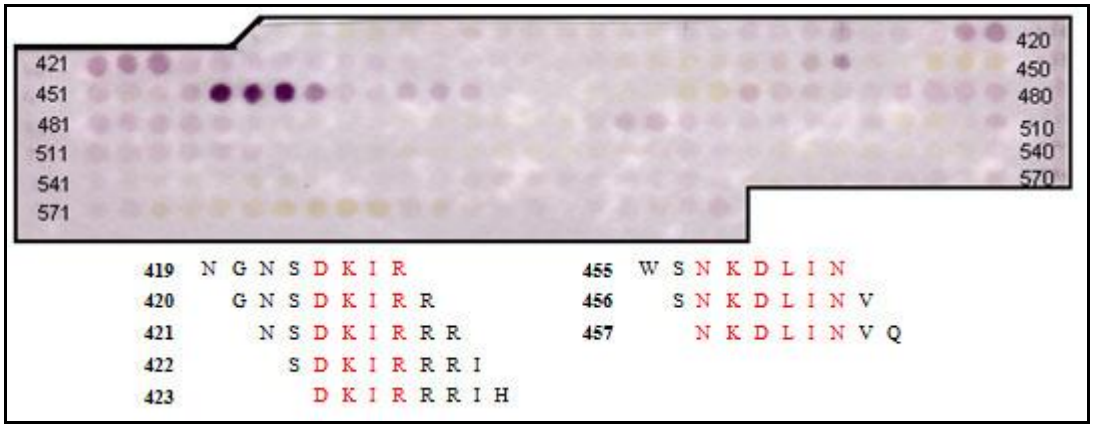

Figura 13. Reatividade do IgG de coelho anti-atr-I frente à sequência primária de atr-I por SPOT. Acima, os spots reativos tornam-se azulados após a revelação. Abaixo, a análise manual dos resíduos comuns encontrados em cada uma das regiões reativas. Os epitopos sugeridos para as regiões um (spots 419 a 423) e dois (spots 455 a 457) são, respectivamente, DKIR e NKDLIN.

Foram identificadas, então, as sequências comuns dentro de cada uma dessas regiões como possíveis epitopos lineares de Atr-I, sendo o primeiro formado pelos resíduos ^{27}DKIR^{30} e o segundo pelos resíduos ^{61}NKDLIN^{66}.

As regiões contendo estes resíduos foram identificadas em um modelo tridimensional de Atr-I. A sequência ^{61}NKDLIN^{66} localiza-se em um loop entre a folha-β 2 e a terceira α-hélice; já a região ^{27}DKIR^{30} é encontrada no final de uma primeira α-hélice e seguindo em seu loop adjacente, anterior à segunda α-hélice. Ambas as regiões situam-se distantes dos resíduos conservados do sítio catalítico das SVMPs (HEXXHXXGXXH), assim como dos resíduos que formam o "met-turn" (Figura 14).

O IgG de coelho anti-atr-I é capaz de inibir a hidrólise de substratos macromoleculares *in vitro*, como a dimetil-caseína (DMC), e ainda a hemorragia induzida por Atr-I *in vivo*. No entanto, mostrou-se ineficaz na inibição da clivagem do peptídeo FRET Abz- LVEALYQ-EDDnp (Tabela 3). A interação enzima-substrato é uma etapa prévia importante à quebra das ligações peptídicas dos substratos. Devido ao seu pequeno tamanho é provável que o peptídeo Abz-LVEALYQ-EDDnp interaja unicamente com resíduos presentes na região hidrofóbica presente na fenda catalítica de Atr-I. Desta forma, anticorpos que reconheçam epitopos localizados distantes espacialmente do sítio ativo podem ser incapazes de neutralizar a hidrólise do substrato FRET por Atr-I. No entanto, estes mesmos anticorpos podem gerar um impedimento estérico das etapas de interação entre atr-I e seus substratos, sendo capazes de inibir a hidrólise de substratos macromoleculares, como a DMC.

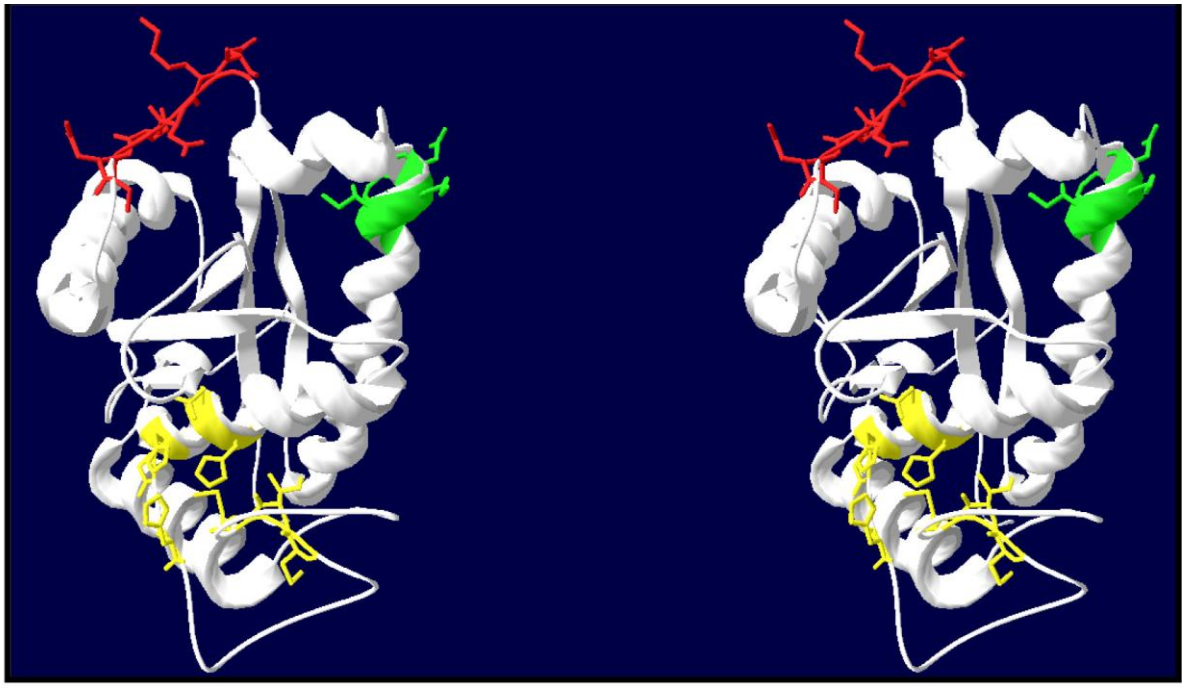

Figura 14. Regiões reconhecidas de Atr-I pelo IgG de coelho anti-atr-I e sítio catalítico e "met-turn" de atr-I. Em verde são mostrados os resíduos ^{27}DKIR^{30} e em vermelho os resíduos ^{61}NKDLIN^{66} reconhecidos pelo IgG de coelho anti-Atr-I em SPOT. Em amarelo estão mostrados os resíduos conservados do sítio catalítico das SVMPs (HEXXHXXGXXH), assim como os resíduos que formam o "met-turn".

Tabela 3. Efeito do IgG de coelho anti-Atr-I sobre diferentes substratos.

Substrato	Relação enzima:anticorpo (mol/mol)	Inibição (%)
DMC	1:1	100±0
Abz-LVEALYQ-EDDnp	1:20	15,8±2,3

Além disso, estes epitopos lineares reconhecidos podem não ser os responsáveis pela indução dos anticorpos neutralizantes frente à hidrólise de DMC, uma vez que é possível que

haja outros epitopos conformacionais reconhecidos por anticorpos presentes no IgG de coelho anti-Atr-I não identificados pelo método de SPOT.

Ainda assim, quatro peptídeos contendo as sequências epitôpicas lineares de Atr-I foram sintetizados (i.e. KDLIN; WSN**KDLIN**VQ; DKIR e NGNS**DKIR**RRIH). Os peptídeos KDLIN e DKIR não foram reconhecidos em ELISA pelo IgG de coelho anti-Atr-I e, por isso, nenhum outro ensaio adicional foi realizado com estes peptídeos. Por outro lado, os peptídeos WSNKDLINVQ e NGNSDKIRRRIH foram reconhecidos em ELISA pelo IgG anti-Atr-I e, desta maneira, foram usados em etapas subsequentes (Figura 15 A). Para se confirmar que o resultado de ELISA não se tratava de um reconhecimento inespecífico por parte do IgG anti-Atr-I, uma nova ELISA de competição foi realizada (Figura 15 B).

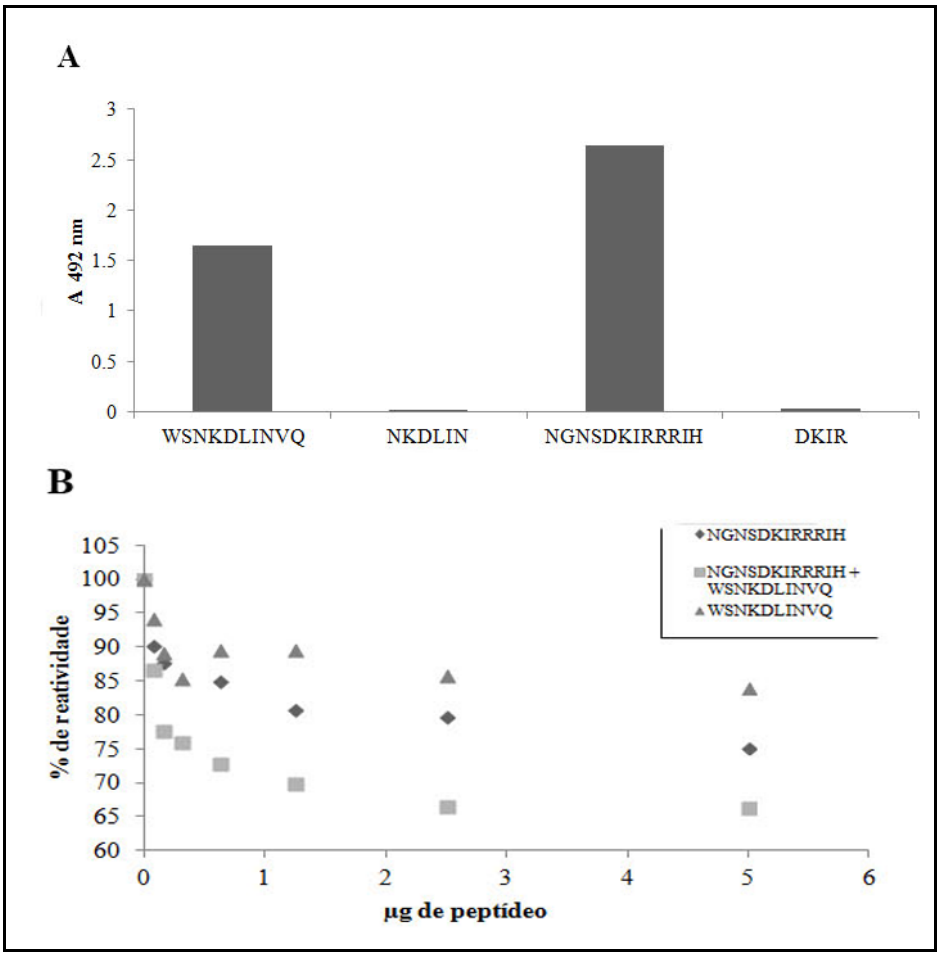

Figura 15. Reconhecimento dos epitopos lineares sintetizados pelo IgG anti-Atr-I. (**A**) Reconhecimento em ensaio de ELISA, no qual os quatro peptídeos sintetizados foram utilizados na sensibilização da placa (100 µg/mL) e incubados com IgG de coelho anti-Atr-I. Somente os peptídeos WSNKDLINVQ e NGNSDKIRRRIH foram reconhecidos pelo IgG anti-Atr-I (20 µg/mL). (**B**) ELISA de competição entre os peptídeos reconhecidos pelo IgG anti-Atr-I e Atroxlisina-I. IgG de coelho anti-Atr-I (10 µg/mL) foi pré-incubado com cada um dos peptídeos isoladamente, ou com uma mistura dos dois peptídeos em diversas concentrações diferentes

Neste ensaio, IgG anti-Atr-I (10 µg/mL) foi pré-incubado com diferentes concentrações de cada peptídeo isoladamente ou simultaneamente (0,78; 1.56; 3,13; 6,25; 12,5; 25,0 e 50,0

µg/mL). Em todos os casos testados houve redução dose-dependente do reconhecimento de Atroxlisina-I pelo IgG anti-Atr-I. Além disso, é possível observar o efeito cumulativo da competição na pré-incubação simultânea dos peptídeos WSNKDLINVQ e NGNSDKIRRRIH com o IgG anti-Atr-I, sugerindo que as regiões reconhecidas são reconhecidas especificamente pelo IgG anti-Atr-I, tratando-se, possivelmente, de epitopos de atroxlisina-I. Estes peptídeos sintetizados foram, também, utilizados como imunógenos em estudos de produção de soros neutralizantes. No entanto, até o momento nenhum protocolo testado foi capaz de gerar quantidades detectáveis de anticorpos. No momento, novos protocolos estão sendo utilizados na tentativa de gerar uma melhor resposta imune.

3.3. Artigo 3 – Mimotopes of mutalysin-II from *Lachesis muta* snake venom induce hemorrhage inhibitory antibodies upon vaccination of rabbits

(2011) Ricardo A. Machado de Avila, Stephanie Stransky, Mariana Velloso, Paula Castanheira, Francisco S. Schneider, Evanguedes Kalapothakis, Eladio F. Sanchez, Christophe Nguyen, Franck Molina, Claude Granier, Carlos Chávez-Olórtegui.

Mutalisina-II (mut-II), isolada do veneno de *Lachesis muta muta,* é uma PI-SVMP não hemorrágica. No entanto, o anticorpo monoclonal LmmAbB2D4 anti-mut-II, produzido previamente por Estêvão-Costa e colaboradores [131], demonstrou ser capaz de reconhecer mutalisina-I (mut-I é uma PIII-SVMP hemorrágica purificada do mesmo veneno) inibindo a atividade hemorrágica desta enzima purificada, ou do veneno bruto de *L. muta muta*.

É interessante notar que anticorpos produzidos contra uma SVMP não hemorrágica sejam capazes de neutralizar outras metaloproteases hemorrágicas. Outros grupos de trabalho sugerem que os domínios adicionais das PIII-SVMPs (e.g. semelhante a desintegrina) podem ser importantes na determinação da atividade hemorrágica das SVMPs [127]. Levando-se em consideração que mut-II apresenta somente o domínio catalítico, o estudo dos epitopos reconhecidos pelo anticorpo monoclonal LmmAbB2D4 torna-se importante no entendimento da relação estrutura-função das SVMPs.

Além disso, é interessante notar que, comparado aos mAbs produzidos contra Atr-I (Artigo 2 – Use of a Synthetic Biosensor for Neutralizing Activity-Biased Selection of Monoclonal Antibodies Against Atroxlysin-I, an Hemorrhagic Metalloproteinase from *Bothrops atrox* Snake Venom), LmmAbB2D4 possui uma grande promiscuidade de reconhecimento de antígenos, o que torna útil o estudo do padrão de reconhecimento deste anticorpo monoclonal no intuito de se identificar regiões comuns entre as SVMPs importantes no exercício de suas atividades tóxicas.

Tendo em vista a alta incidência de acidentes envolvendo as serpentes *Bothrops atrox* e *Lachesis muta muta* na região norte da América do Sul, aliado à falta de um diagnóstico laboratorial capaz de diferenciar estes acidentes, a comparação entre os epitopos reconhecidos pelos mAbAtrs (anti-Atroxlisina-I) e LmmAbB2D4 (anti-mut-II) pode elucidar determinantes antigênicas diferenciais entre Atr-I e mut-II eficientes no desenvolvimento de testes diagnósticos capazes de diferenciar os acidentes envolvendo essas serpentes.

Assim, neste trabalho, utilizamos as técnicas de Phage Display e SPOT para determinar mimotopos conformacionais reconhecidos pelo LmmAbB2D4. Alguns dos mimotopos identificados foram capazes de induzir resposta imune em coelhos, os quais geraram

anticorpos capazes de neutralizar a atividade hemorrágica de mut-I isolada ou do veneno inteiro de *Lachesis muta muta*.

Peptides 32 (2011) 1640–1646

Contents lists available at ScienceDirect

Peptides

journal homepage: www.elsevier.com/locate/peptides

Mimotopes of mutalysin-II from *Lachesis muta* snake venom induce hemorrhage inhibitory antibodies upon vaccination of rabbits

R.A. Machado de Avila[a], S. Stransky[a], M. Velloso[a], P. Castanheira[a], F.S. Schneider[a], E. Kalapothakis[b], E.F. Sanchez[c], C. Nguyen[d], F. Molina[d], C. Granier[d], C. Chávez-Olórtegui[a,*]

[a] *Departamento de Bioquímica e Imunologia, Instituto de Ciências Biológicas, Universidade Federal de Minas Gerais, CEP 31270-901, Belo Horizonte-MG, Brazil*
[b] *Biologia Geral, Instituto de Ciências Biológicas, Universidade Federal de Minas Gerais, CEP 31270-901, Belo Horizonte-MG, Brazil*
[c] *Centro de Pesquisa e Desenvolvimento, Fundação Ezequiel Dias (FUNED), Rua Conde Pereira Carneiro 80, 30510-010, Belo Horizonte, MG, Brazil*
[d] *CNRS UMR 3145 BIO-RAD, Cap Delta/Parc Euromédecine, 1682 rue de la Valsière, CS 61003, 34184 Montpellier Cedex 4, France*

ARTICLE INFO

Article history:
Received 8 April 2011
Received in revised form 29 June 2011
Accepted 29 June 2011
Available online 6 July 2011

Keywords:
Lachesis muta venom
Antivenom
Phage-display
Synthetic peptides
Mimotope
Monoclonal antibody

ABSTRACT

Mutalysin-II (mut-II) from *Lachesis muta* snake venom is an endopeptidase with hemorrhagic activity. A mAb against mutalysin-II that neutralized the hemorrhagic effect was produced previously. To identify the mAb epitopes, sets of 15-mer overlapping peptides covering the mut-II amino acid sequence were synthesized using the SPOT method and tested but failed to react with the mAb. Using a phage-display approach seventeen clones reactive with mAb were identified. Additional immunoassays with the peptides and mAb identified the QCTMDQGRLRCR, TCATDQGRLRCT, HCFHDQGRVRCA, HCTMDQGRLRCR and SCMLDQGRSRCR sequences as possible epitopes. Immunization of rabbits with these peptides induced antibodies that recognize mut-II and protected against the hemorrhagic effects of *Lachesis* venom.
© 2011 Elsevier Inc. All rights reserved.

1. Introduction

Snake bites are an important public health problem in Brazil. Approximately 20,000 cases are reported annually, with a mortality rate of 0.5%. Envenomation due to *Bothrops* sp. and *Lachesis muta* accounts for more than 80% of cases [30]. Local or invasive hemorrhage is a major complication of *Bothrops* and *Lachesis* envenomation; this results from the action of hemorrhagic metalloproteinases, also referred to as reprolysins [4]. In addition, there are secondary factors which are involved in blood coagulation disorders, kinin release and also neurotoxic components [22,23].

Metalloproteinases from viperid snake venoms (SVMPs) disrupt the vascular basement membrane resulting in typical hemorrhage [4,33]. As observed in other snakes, envenoming by the bushmaster snake (*L. muta muta*) leads to the development of both local and systemic bleeding. Two hemorrhagic factors characterized as metalloproteinases were named LHF-I and LHF-II (*Lachesis* hemorrhagic factor I and II), and correspond to mutalysin-I and mutalysin-II (mut-II), respectively [35]. Mutalysin-I is a large peptidase (100 kDa) with restricted substrate specificity and has the strongest hemorrhagic activity (approximately 30 times higher than mut-II). Mut-II is a 22.5 kDa single chain protein with broad substrate specificity and traces of hemorrhagic effects [35,36]. As for other SVMPs, mutalysins proteolytically degrade not only fibrinogen, but also other extracellular matrix components such as laminin, fibronectin, type IV collagen or gelatin [34,35]. In addition, mutalysin-I selectively inhibits collagen-induced aggregation of human platelets [12].

We have previously reported that the monoclonal antibody LmmAbB2D4 [11] and rabbit polyclonal antibodies [39] against mut-II show cross-reactivity against mutalysin-I and efficiently neutralize the hemorrhagic effects of whole *L. muta muta* venom and certain *Bothrops* venoms (i.e. *B. alternatus*, *B. atrox*, *B. itapetiningae*, *B. jararaca* and *B. neuwiedii*). Identifying the epitope of this neutralizing antibody could aid in the preparation of immunogens for therapeutic serum development or vaccination approaches. In the present investigation, the peptide phage-display method [20,40], and the SPOT synthesis technique [17,26,31] were used together to identify the epitope recognized by LmmAbB2D4. Rabbits immunized with defined synthetic mimotopes encapsulated in liposomes produced an antibody response capable of efficiently neutralizing the hemorrhagic effect of *L. muta* crude venom.

* Corresponding author. Tel.: +55 31 3409 2625; fax: +55 31 3441 5963.
E-mail address: olortegi@icb.ufmg.br (C. Chávez-Olórtegui).

0196-9781/$ – see front matter © 2011 Elsevier Inc. All rights reserved.
doi:10.1016/j.peptides.2011.06.028

2. Materials and methods

2.1. Animals, L. muta muta snake venom and antibodies

Eight- to nine-week-old New Zealand rabbits were maintained at the Centro de Bioterismo, ICB-UFMG (Belo Horizonte, MG, Brazil), and received water and food under controlled environmental conditions. Treatment and handling of all animals used in the experiments followed the requirements of the Ethics Committee of Animal Experimentation (CETEA) of UFMG. The *L. muta muta* venom was obtained by milking specimens captured near Manaus, Amazonas, Brazil and raised at the serpentarium of Fundação Ezequiel Dias (FUNED), Belo Horizonte, Brazil. Mut-II was isolated as previously described by Sanchez et al. [36]. The neutralizing monoclonal antibody (LmmAbB2D4) and the polyclonal antibodies against mut-II were produced as described by Estêvão-Costa et al. [11] and Souza et al. [39], respectively.

2.2. Spot synthesis

Overlapping synthetic peptides corresponding to the mut-II amino acid sequence (GenBank accession number AAQ16123) were prepared using the SPOT technique [17]. Two series of membrane-bound peptides were synthesized according to the procedure described by Laune et al. [26] as 15-mer peptides frameshifted by three residues. After synthesis, non-specific binding sites of the membranes were blocked by incubation with blocking buffer (Roche, Germany) overnight at 4 °C, and further probed with rabbit serum against mut-II (diluted 1:400) or with LmmAbB2D4 (1 or 10 μg/ml in blocking buffer) for 90 min at room temperature. Antibody binding to spots was revealed by incubation (90 min at room temperature) with alkaline phosphatase-conjugated goat anti-rabbit or goat anti-mouse antibodies and 5-bromo-4-chloro-3-indolyl phosphate (BCIP) plus 3-(4,5-dimethylthiazol-2-yl)-2,5-diphenyltetrazolium bromide (MTT) as substrate. The membrane was stripped by sequential treatment with dimethylformamide, 1% SDS, 0.1% 2-mercaptoethanol in 8 M urea, ethanol/water/acetic acid (50:40:10, v/v/v) and, finally, methanol to remove the precipitated dye and molecules bound to the peptides.

2.3. Isolation of phage clones binding to LimAb7

Four different M13 phage libraries expressing 15-mer (X_{15}), 30-mer (X_{30}), 17-mer including a fixed cysteine residue (X_8CX_8), and 12-mer peptides including two fixed cysteine residues (XCX_8CX) were employed [40]. Biopannings were performed as described previously [40] with some modifications. Briefly, 96-well microtiter plates (Becton Dickinson, Oxnard, CA) were incubated overnight at 4 °C with 100 μl LmmAbB2D4 at 5 μg/ml for the first two biopannings and 0.5 μg/ml for the last one, in 0.1 M $NaHCO_3$, pH 8.6. The plates were then washed with 0.05% Tween 20 in 50 mM Tris-buffered saline, pH 7.5 (TBS-T) and blocked with 3% BSA in TBS-T at 37 °C for 2 h. For the first biopanning, 1.5×10^{11} transducing units (TU) of phages expressing linear 15-mer (X15), 17-mer (X_8CX_8) and 30-mer (X_{30}) peptides and 2.5×10^{10} TU of phages expressing constrained 12-mer (XCX_8CX) peptides were incubated in TBS-T with the immobilized LmmAbB2D4 overnight at 4 °C. Unbound phages were removed by washing with TBS-T. Bound phages were eluted with 0.1 M glycine, 1 mg/ml bovine serum albumin (pH 2.2) and neutralized with 2 M Tris–HCl, pH 9.0. *Escherichia coli* K91 cells were infected with the eluted phages and grown overnight at 37 °C. Phage particles were precipitated with 20% PEG 8000, 2.5 M NaCl overnight on ice, resuspended in 0.05 M Tris–HCl, 0.15 M NaCl, pH 7.5 and used for the next round of biopanning (2×10^{11} TU). After three rounds, phage clones were isolated and submitted to screening ELISA.

2.4. Sandwich ELISA screening assay

Microtiter plate wells (Falcon) were coated with 100 μl sheep anti-M13 polyclonal antibody (10 μg/ml) in 0.1 M $NaHCO_3$, pH 8.6, overnight at 4 °C. Plates were washed with 0.1% Tween 20-PBS (PBS-T) and blocked with 2% non-fat dry milk in PBS-T for 1 h at 37 °C. The wells were washed, and phages, diluted 1:1 in PBS-T, were incubated for 90 min at 37 °C. Phages able to bind LmmAbB2D4 at 10 μg/ml were detected by a horseradish peroxidise (HRP)-conjugated rabbit anti-mouse antibody (Sigma, St. Louis, MO, USA). The clones selected by LmmAbB2D4 were used in a new ELISA plate configuration to verify their reactivity with the monoclonal antibody. Plates were sensitized with 5 μg/ml LmmAbB2D4 in coating buffer, washed and blocked as described previously and incubated with phages at 1×10^{11} to 1×10^{6} pfu/ml diluted in 0.05% Tween 20-PBS for 2 h at 37 °C. Binding was detected using a HRP-conjugated anti-M13 antibody (Sigma) diluted 1:3000 in blocking buffer.

2.5. DNA sequencing, peptides synthesis on cellulose membranes and immunoassay

The single-stranded DNA was purified using the QIAprep Spin M13 protocol (Qiagen). Sequencing reactions were carried out according to the dideoxy chain termination method using the ABI Prism Kit using the ABI PRISM 377 (both from PE Applied Biosystems). The reverse primer 5′-TCGGCAAGCTCTTTTAGG-3′ was used for sequencing. The sequences obtained were translated and seventeen dodecapeptides corresponding to the XCX_8CX library were identified. A cellulose membrane containing the seventeen peptides was prepared, blocked and probed with LmmAbB2D4 (10 μg/ml) as described in Section 2.2.

2.6. Synthesis, chromatography and mass spectrometry of soluble peptide

Based on the results of immunoassay with cellulose-bound peptides, the peptides recognized by LmmAbB2D4 (QCTMDQGRLRCR, TCATDQGRLRCT, HCFHDQGRVRCA, HCTMDQGRLRCR and SCMLDQGRSRCR) were synthesized manually by Fmoc chemistry [18]. The peptides were deprotected and released from the resin by trifluoroacetic acid (TFA) treatment in the presence of the appropriate scavengers. The peptides were lyophilized and their purity assessed by HPLC and their mass confirmed by mass spectrometry. The synthetic peptides (20 mg of each) were diluted in 1 ml of PBS and used for immunogen preparation. The peptides were purified by high performance liquid chromatography (HPLC) on a C18 reverse phase column (flow rate 1.0 mL/min; Vydac). The column was equilibrated with 0.1% aqueous TFA, and was eluted by a linear gradient of 0.1% TFA in acetonitrile. The peaks were then submitted to MALDI-TOF-TOF analyses. MS and tandem MS analysis were performed using a MALDI-TOF-TOF AutoFlex III (Bruker Daltonics) instrument in positive/reflector mode controlled by the FlexControl software. Instrument calibration was achieved by using Peptide Calibration Standard II (Bruker Daltonics) as reference and α-cyano-4-hydroxycinnamic acid was used as the matrix.

2.7. Liposome preparation and peptide incorporation

The individual peptides were encapsulated in liposomes using the dehydration–rehydration method [24]. Briefly, multilamellar

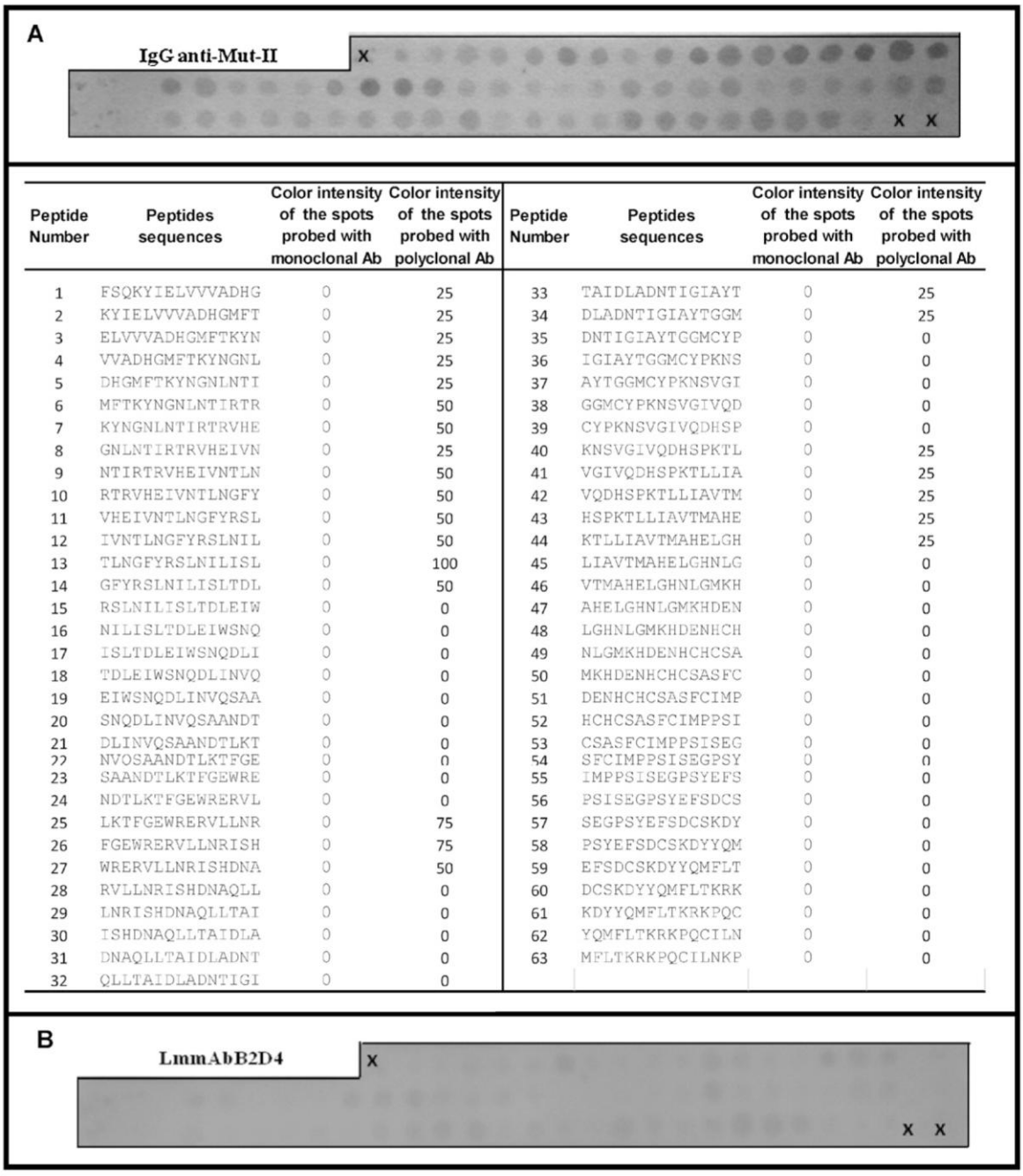

Peptide Number	Peptides sequences	Color intensity of the spots probed with monoclonal Ab	Color intensity of the spots probed with polyclonal Ab	Peptide Number	Peptides sequences	Color intensity of the spots probed with monoclonal Ab	Color intensity of the spots probed with polyclonal Ab
1	FSQKYIELVVVADHG	0	25	33	TAIDLADNTIGIAYT	0	25
2	KYIELVVVADHGMFT	0	25	34	DLADNTIGIAYTGGM	0	25
3	ELVVVADHGMFTKYN	0	25	35	DNTIGIAYTGGMCYP	0	0
4	VVADHGMFTKYNGNL	0	25	36	IGIAYTGGMCYPKNS	0	0
5	DHGMFTKYNGNLNTI	0	25	37	AYTGGMCYPKNSVGI	0	0
6	MFTKYNGNLNTIRTR	0	50	38	GGMCYPKNSVGIVQD	0	0
7	KYNGNLNTIRTRVHE	0	50	39	CYPKNSVGIVQDHSP	0	0
8	GNLNTIRTRVHEIVN	0	25	40	KNSVGIVQDHSPKTL	0	25
9	NTIRTRVHEIVNTLN	0	50	41	VGIVQDHSPKTLLIA	0	25
10	RTRVHEIVNTLNGFY	0	50	42	VQDHSPKTLLIAVTM	0	25
11	VHEIVNTLNGFYRSL	0	50	43	HSPKTLLIAVTMAHE	0	25
12	IVNTLNGFYRSLNIL	0	50	44	KTLLIAVTMAHELGH	0	25
13	TLNGFYRSLNILISL	0	100	45	LIAVTMAHELGHNLG	0	0
14	GFYRSLNILISLTDL	0	50	46	VTMAHELGHNLGMKH	0	0
15	RSLNILISLTDLEIW	0	0	47	AHELGHNLGMKHDEN	0	0
16	NILISLTDLEIWSNQ	0	0	48	LGHNLGMKHDENHCH	0	0
17	ISLTDLEIWSNQDLI	0	0	49	NLGMKHDENHCHCSA	0	0
18	TDLEIWSNQDLINVQ	0	0	50	MKHDENHCHCSASFC	0	0
19	EIWSNQDLINVQSAA	0	0	51	DENHCHCSASFCIMP	0	0
20	SNQDLINVQSAANDT	0	0	52	HCHCSASFCIMPPSI	0	0
21	DLINVQSAANDTLKT	0	0	53	CSASFCIMPPSISEG	0	0
22	NVQSAANDTLKTFGE	0	0	54	SFCIMPPSISEGPSY	0	0
23	SAANDTLKTFGEWRE	0	0	55	IMPPSISEGPSYEFS	0	0
24	NDTLKTFGEWRERVL	0	0	56	PSISEGPSYEFSDCS	0	0
25	LKTFGEWRERVLLNR	0	75	57	SEGPSYEFSDCSKDY	0	0
26	FGEWRERVLLNRISH	0	75	58	PSYEFSDCSKDYYQM	0	0
27	WRERVLLNRISHDNA	0	50	59	EFSDCSKDYYQMFLT	0	0
28	RVLLNRISHDNAQLL	0	0	60	DCSKDYYQMFLTKRK	0	0
29	LNRISHDNAQLLTAI	0	0	61	KDYYQMFLTKRKPQC	0	0
30	ISHDNAQLLTAIDLA	0	0	62	YQMFLTKRKPQCILN	0	0
31	DNAQLLTAIDLADNT	0	0	63	MFLTKRKPQCILNKP	0	0
32	QLLTAIDLADNTIGI	0	0				

Fig. 1. Anti-mut-II antibody reactivity with membrane bound 15-mer overlapping linear peptides derived from the mut-II amino acid sequence. The 15-mer overlapping linear peptides were probed by rabbit polyclonal anti mut-II at a dilution of 1:400 (A) and with LmmAbB2D4 at 10 μg/ml (B). Antibodies were detected with alkaline phosphatase-coupled anti-rabbit or anti mouse antibodies (1:1000).

vesicles (MLVs) were prepared in water from an equimolar mixture of cholesterol (CHOL; Sigma) and egg yolk phosphatidylcholine (EPC, 100%; Lipoid) at a 135 g/L final lipid concentration, through the film hydration method. Small unilamellar vesicles (SUVs) were obtained by submitting the MLVs suspension to three 5 min-cycles of ultrasonication using a probe-sonicator (Misonix) under argon and in an ice-cold bath. After filtration through a sterile 0.22 μm membrane, the SUVs suspension was mixed with the peptide solution at a 64:1 lipid-to-peptide mass ratio and the mixture was immediately frozen in liquid nitrogen and then dried overnight (freeze-dryer, 4.5 L; Labconco, UK). Dehydration–rehydration vesicles (DRVs) were obtained through rehydration of the dried powder at 25 °C as follows: one-tenth of the original SUVs volume of deionized water was added, vortexed and incubated for 30 min; 0.1 volume of PBS (0.15 M NaCl, 0.01 M phosphate, pH 7.2) was added, and the mixture was vortexed prior to the addition of 0.8 volume of PBS, and then vortexed again and incubated for 30 min. A parallel preparation of empty (PBS-loaded) DRVs was also obtained. The fraction of peptide entrapped in liposomes was determined indirectly by centrifugation (43,000 × *g*; 30 min; 4 °C) and peptide titration in the supernatant.

2.8. Immunization protocols

Adult female New Zealand white rabbits (2.0–2.5 kg) were used for the production of anti-peptide antibodies. After collection of

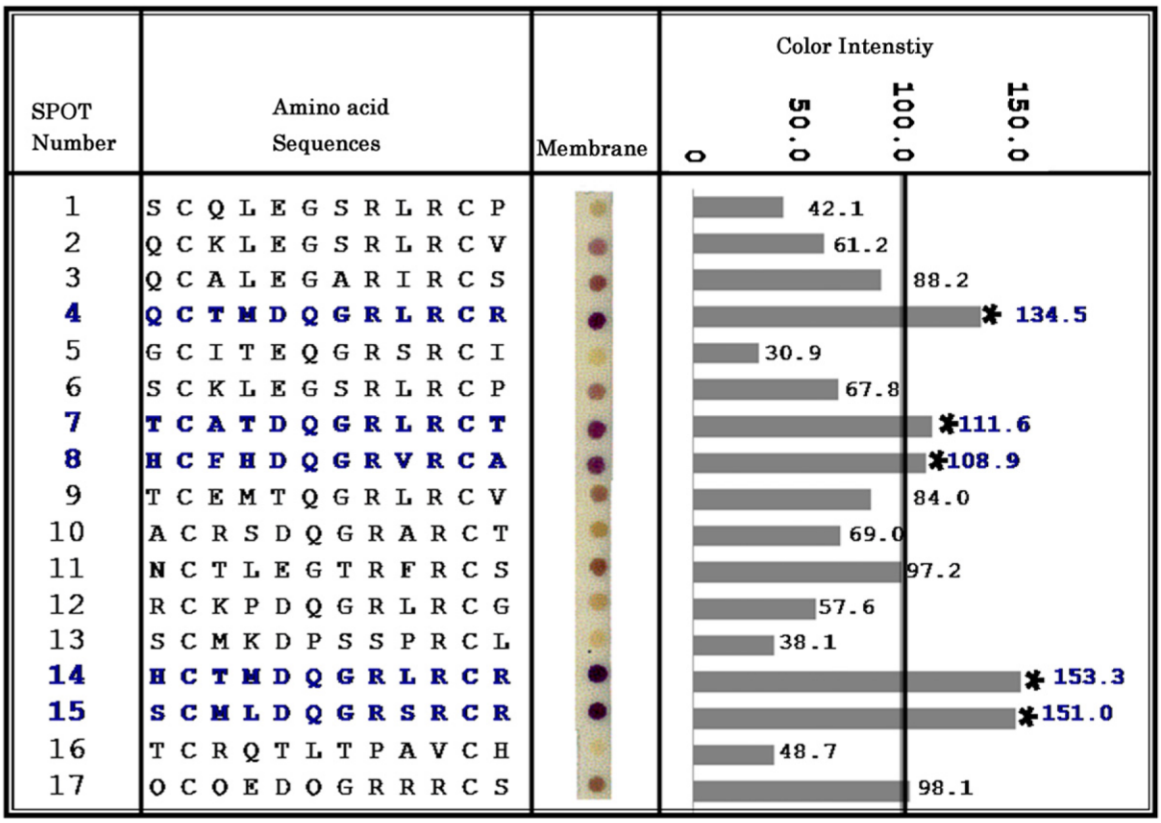

Fig. 2. Reactivity of peptides selected by phage display on a SPOT membrane. LmmAbB2D4 reactivity with cellulose-bound phage-display identified peptides was detected with an alkaline-phosphatase coupled anti-mouse antibody. Spot intensities were measured with the Scion Image software.

pre-immune sera, each animal received an initial subcutaneous injection of 100 μg liposome-trapped synthetic peptide in aluminum hydroxide (day 1). Five similar booster injections were made 21, 36, 51, 66 and 76 days later. Blood samples were drawn 1 week after the last injection. As a control, rabbits were also immunized with liposomes not containing synthetic peptides, prepared as described previously [9].

2.9. Indirect ELISA for the determination of anti-peptide antibodies

Falcon flexible microtitration plates (Becton Dickinson France S.A.) were coated overnight at 4 °C with 5 μg/ml mut-II or *L. muta muta* whole venom in 0.02 M $NaHCO_3$ buffer, pH 9.6, as described previously [3]. Absorbance values were determined at 492 nm with a Titertek Multiscan spectrophotometer. Tests were done in triplicate and the values represent means of experiments. Standard deviations are represented by error bars. Results were evaluated by Student's *t*-test using Sigma Plot 10.0. In all cases, differences were considered significant at $P < 0.05$.

2.10. Toxicity assays

Hemorrhagic activity was assayed using the Kondo method [25] and adapted by Sanchez et al. [36]. Aliquots of *L. muta muta* venom in 100 μl physiological saline, or saline alone, were injected into the dorsal shaved skin of the non-immunized rabbits. Twenty-four hours later, the rabbits were euthanized and the back skin was totally removed in order to photograph and measure the hemorrhagic lesions. One minimum hemorrhagic dose (MHD) was defined as the dose which causes a hemorrhagic lesion 10 mm in diameter. The MHD of *L. muta* venom used throughout this study was 20 μg. For the *in vivo* neutralization assays of the hemorrhagic activity of *L. muta* venom, the immunized and control rabbits were challenged with *L. muta* venom 30 days after the last immunization by intradermal injection of an amount equivalent to 1 MND/kg.

3. Results

3.1. Epitope mapping

In order to map the epitope recognized by the neutralizing monoclonal antibody LmmAbB2D4, membrane-bound peptides of 15 amino acids, spanning the entire sequence of mut-II, were probed with LmmAbB2D4. Only background reactivity was observed at the highest concentration of the polyclonal antibody (10 μg/ml; Fig. 1B – lower panel). As a control for peptide quality, the 15-mer peptides (Fig. 1A – upper panel) were reactive when probed with a rabbit polyclonal antiserum produced against mut-II.

The phage-display system of expression of randomly generated peptides can identify peptides mimicking discontinuous epitopes (mimotopes). To identify peptides that would bind to LmmAbB2D4, four different phage libraries were screened, two of which expressed linear peptides of either 15 (X15) or 30 amino acids (X30), whereas the other two displayed peptides including either one or two fixed cysteines and whose sizes were 17 (XCX15) or 12 amino acids (XCX8CX). A significant enrichment of phage binding to the target antibodies was obtained after three rounds of biopanning (data not shown). Of approximately one hundred phage clones randomly picked from the third round of selection, seventeen clones were selected. The DNA sequence and the deduced amino acid sequence were determined (Fig. 2A), showing that the peptides were selected from the (XCX8CX) library. Another cellulose membrane containing the seventeen peptides

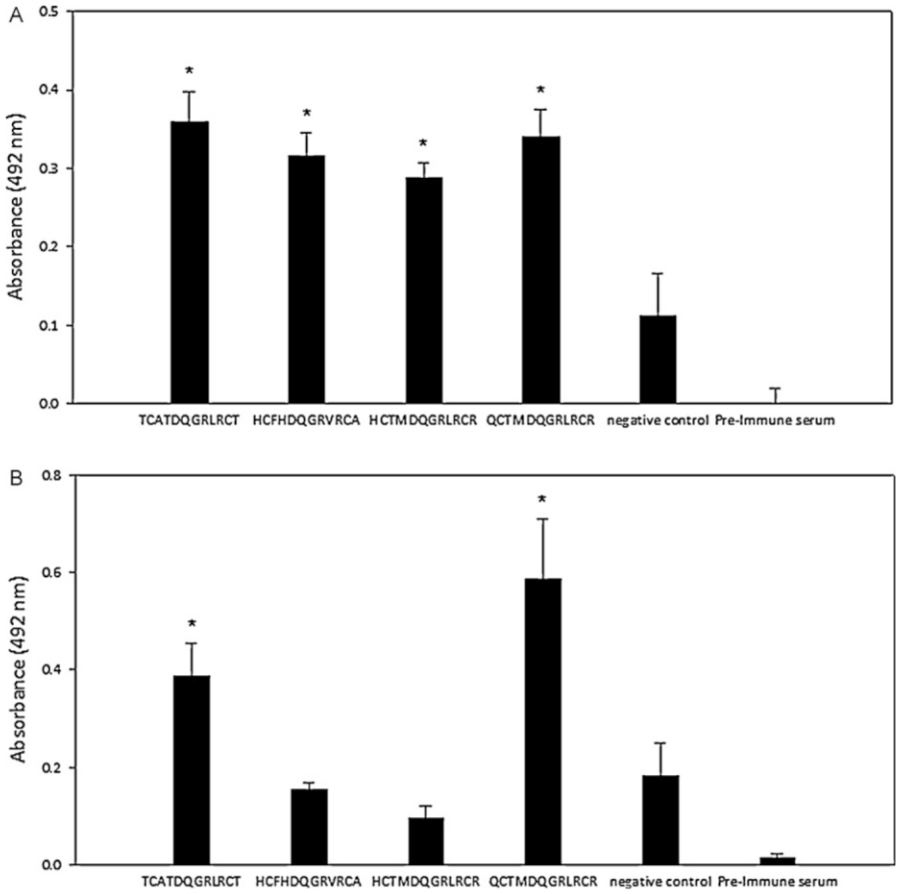

Fig. 3. Immune response of peptide-immunized rabbits evaluated by ELISA. Reactivity of peptide-immunized rabbit sera with *L. muta* whole venom (A) and mut-II (B) were diluted from 1 to 100. The pre-immune sera (control) were used as a negative control. Experiments were performed in triplicate; the values are the means of the experiments. Standard deviations are represented by error bars. $^{*}P < 0.05$ compared with the negative control.

were prepared, blocked and probed with LmmAbB2D4 (10 μg/ml). As shown in Fig. 2B, the peptides recognized by LmmAbB2D4 were peptide 4 (QCTMDQGRLRCR), peptide 7 (TCATDQGRLRCT), peptide 8 (HCFHDQGRVRCA), peptide 14 (HCTMDQGRLRCR) and peptide 15 (SCMLDQGRSRCR). Analysis of these sequences revealed no obvious homology between the mimotopes and the mut-II sequence.

3.2. Neutralizing ability of anti-peptide antibodies

Based on the results of immunoassay with cellulose-bound peptides, the peptides (QCTMDQGRLRCR, TCATDQGRLRCT, HCFHDQGRVRCA and HCTMDQGRLRCR) were synthesized in a soluble form, trapped in liposomes and used as immunogens in rabbits. One week after the sixth injection, sera from rabbits were tested in an indirect ELISA for their reactivity toward the peptides, the *L. muta* whole venom and the cognate mut-II protein. The sera from rabbits immunized with peptides show marginal reactivity against the peptides coated to plates, likely due to low adsorption of peptides to the microtiter plates (data not shown). However, ELISA reactivity was observed when the antigens were *L. muta* crude venom and mut-II (Fig. 3A and B). The strongest reactivity toward Mut-II was obtained with the serum of rabbits immunized with peptides TCATDQGRLRCT and QCTMDQGRLRCR (Fig. 3B). The serum of rabbits immunized with the peptides HCFHDQGRVRCA and HCTMDQGRLRCR reacted poorly with the Mut-II protein, even lower that the serum of mock-liposomes immunized rabbits.

The neutralizing properties of the anti-peptide antibodies raised in rabbits were assessed *in vivo* by testing the hemorrhagic inducing activity of *L. muta* venom in animals immunized with the four target peptides. The rabbits immunized with the peptide-mimotopes TCATDQGRLRCT and QCTMDQGRLRCR were completely protected (Fig. 4A and B). The rabbits immunized with the HCFHDQGRVRCA and HCTMDQGRLRCR peptides were partially protected (about 62% and 37% protection, respectively). The animal from the group that received the empty liposome (without peptides) as negative control liposome was not protected.

4. Discussion

Snake venoms are a cocktail of biologically active molecules, including toxins with enzymatic and non-enzymatic activities that have evolved to assist in the capture and digestion of prey, as well as defense against predators. Human systemic envenomation is associated with a number of adverse effects, the nature and severity of which depends on the species of snake, the quantity of venom injected and the time period between envenomation and the administration of appropriate medical treatment. These effects may include paralysis, myolysis, blood coagulation disturbances and renal damage [7,41]. Bushmaster snake envenomation is characterized by serious hemorrhage, blood coagulation disorders, and renal failure; hemorrhage is the major complication resulting from envenomation by the pit vipers *Bothrops* and *Lachesis* snakebites [22]. Hemorrhagic metalloproteinases are important contributors to local and systemic hemorrhage in human snakebite victims. Two of these metalloproteinases, originally called *Lachesis* hemorrhagic factors I and II (LHF-I and LHF-II; corresponding to mutalysin-I and mut-II), were previously purified and characterized [37]. Mut-II is a P-I class SVMP single chain protein of 22.5 kDa with broad substrate specificity and a minor hemorrhagic effect [38].

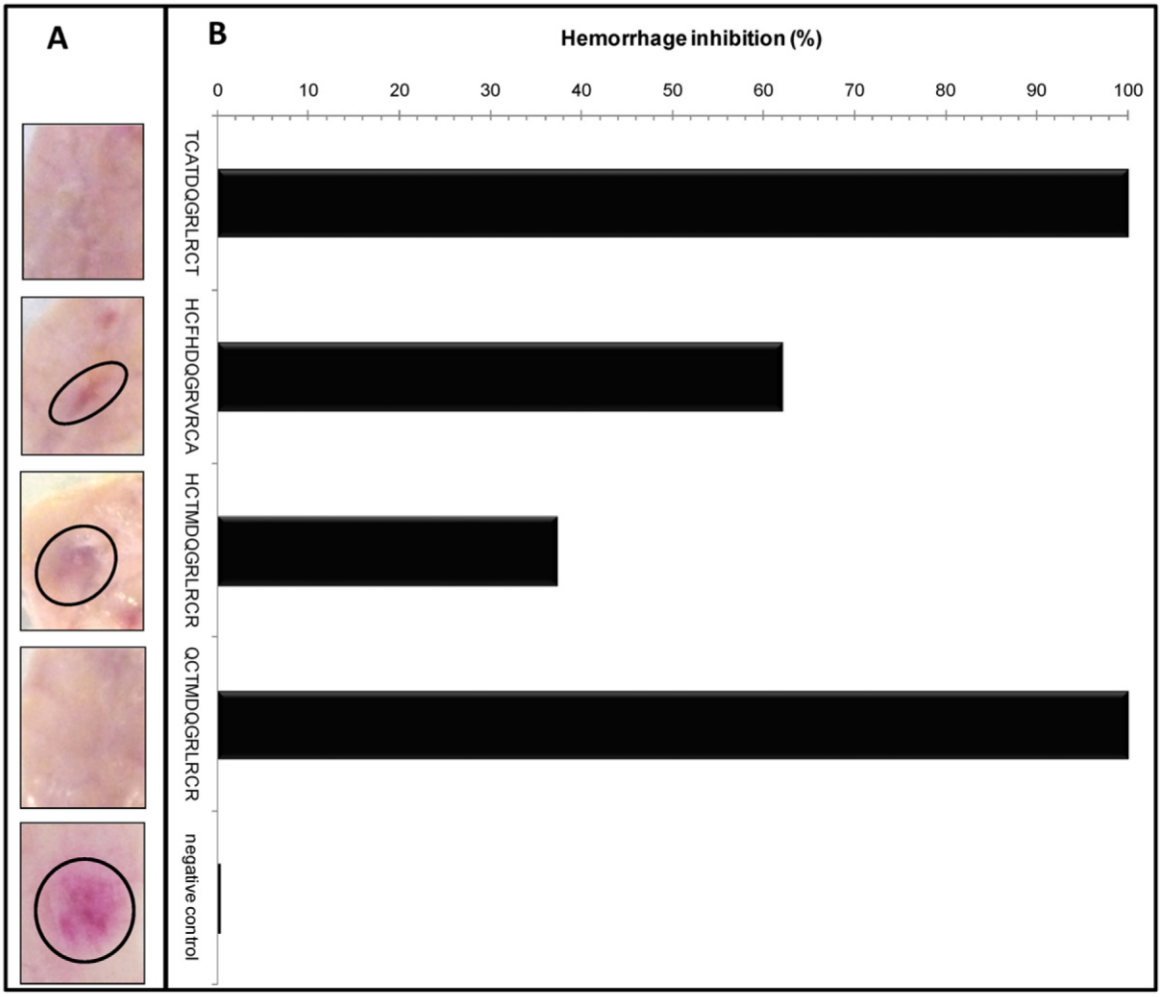

Fig. 4. Neutralization of the *L. muta muta* venom hemorrhagic effect measured *in vivo* in peptide-immunized rabbits. Hemorrhage was assessed on the visceral side of the immunized rabbit skin samples taken 24 h after exposure to *L. muta* venom (A) and inhibition percentage of hemorrhage lesion (B) measured was calculated as the percentage of the control hemorrhage. Control animals were immunized with empty liposomes.

Our previous results showed that the neutralizing monoclonal antibody LmmAbB2D4, produced against *L. muta muta* venom, recognizes mut-II and neutralizes the hemorrhagic effect of *L. muta* and several *Bothrops* crude venoms [11,39]. However, the ability of LmmAbB2D4 to neutralize the whole venom is likely due to the recognition of several venom proteins that share the same epitopic region [11]. Since several continuous antigenic regions of mut-II were previously identified [15], herein we mapped the mut-II epitope recognized by LmmAbB2D4 to determine if it corresponds to known antigenic regions. We first used the peptide scanning method to map continuous and discontinuous epitopes [2,6,10,14,27,28]. Sets of 15-mer overlapping peptides covering the mut-II amino acid sequence were chemically synthesized by the SPOT method of multiple peptide synthesis [26,31]. Such linear peptides were, however, not recognized, indicating that the epitope is likely discontinuous. Consequently, the phage-display technique was used. Although libraries of filamentous phages have often led to the identification of peptides with high homology to the wild type sequence of the epitope [8,13,32], we have identified, like others [1,16,19], peptides (mimotopes) mimicking discontinuous components of the epitope. All seventeen identified peptides contain two cysteine residues. Thus, the peptides must be constrained to be recognized, suggesting that the antibody is sensitive to conformation. We note, however, that the peptides QCTMDQGRLRCR, TCATDQGRLRCT, HCFHDQGRVRCA, HCTMDQGRLRCR and SCMLDQGRSRCR were able to bind LmmAbB2D4 when prepared as synthetic replicas of the phage-born sequences. This can be due to the different conformations the peptide adopts in the cellulose membranes when it is prepared as a synthetic peptide, compared to the conformations it adopts when displayed on phage surface [29]. The amino acid sequences of the phage-selected peptides had no homology with the sequence of Mut-II protein, and thus are considered mimotopes.

Phage-display peptide libraries have identified mimotopes of toxins from scorpion and snake venoms. Such peptides stimulate the production of neutralizing antibodies [5,19,21]. Our results show, for the first time, the usefulness of peptide mimotopes for the neutralization of hemorrhagic activity induced in animals by bushmaster snake venom. Given that synthetic epitopes derived from mut-II sequences permit the development of efficient mut-II antivenom [15] and that two mimotopes are capable of inducing a significant neutralizing humoral response against *L. muta muta* snake venom, these synthetic immunogens will allow for therapeutic serum development or for vaccination approaches.

Acknowledgments

This research was supported by Fundação de Amparo a Pesquisa do Estado de Minas Gerais (FAPEMIG), the INCTTOX PROGRAM of Conselho Nacional de Desenvolvimento Científico e Tecnológico (CNPq) and Coordenação de Aperfeiçoamento de Pessoal de Nível

Superior/Comité Français d'evaluation de la Cooperation Universitaire avec le Brésil (CAPES/COFECUB-Brazil/France). We thank Dr. J. Scott for the gift of phage libraries and the Núcleo de Estudo de Estrutura e Função de Biomoléculas (Departamento de Bioquímica e Imunologia, Instituto de Ciências Biológicas, Universidade Federal de Minas Gerais Belo Horizonte, Minas Gerais, Brasil) for technical support for mass spectrometry.

References

[1] Adda CG, Tilley L, Anders RF, Foley M. Isolation of peptides that mimic epitopes on a malarial antigen from random peptide libraries displayed on phage. Infect Immun 1999;67(9):4679–88.
[2] Alvarenga LM, Machado de Avila RA, Amim PR, Martins MS, Kalapothakis E, de Lima ME, et al. Molecular characterization of a neutralizing murine monoclonal antibody against *Tityus serrulatus* scorpion venom. Toxicon 2005;46(6):664–71.
[3] Alvarenga LM, Martins MS, Moura JF, Kalapothakis E, Oliveira JC, Mangili OC, et al. Production of monoclonal antibodies capable of neutralizing dermonecrotic activity of *Loxoceles intermedia* spider venom and their use in a specific immunometric assay. Toxicon 2003;42(7):725–31.
[4] Bjarnason JB, Fox JW. Hemorrhagic metalloproteinases from snake venoms. Pharmacol Ther 1994;62(3):325–72.
[5] Cardoso R, Homsi-Brandeburgo MI, Rodrigues VM, Santos WB, Souza GL, Prudencio CR, et al. Peptide mimicking antigenic and immunogenic epitope of neuwiedase from *Bothrops neuwiedi* snake venom. Toxicon 2009;53(2):254–61.
[6] Chavez-Olortegui C, Molina F, Granier C. Molecular basis for the cross-reactivity of antibodies elicited by a natural anatoxin with alpha- and beta-toxins from the venom of *Tityus serrulatus* scorpion. Mol Immunol 2002;38(11):867–76.
[7] Chippaux JP, Goyffon M. Venoms, antivenoms and immunotherapy. Toxicon 1998;36(6):823–46.
[8] Choulier L, Laune D, Orfanoudakis G, Wlad H, Janson J, Granier C, et al. Delineation of a linear epitope by multiple peptide synthesis and phage display. J Immunol Methods 2001;249(1–2):253–64.
[9] Dias-Lopes C, Guimarães G, Felicori L, Fernandes P, Emery L, Kalapothakis E, et al. A protective immune response against lethal, dermonecrotic and hemorrhagic effects of *Loxosceles intermedia* venom elicited by a 27-residue peptide. Toxicon 2010;55(2–3):481–7.
[10] Duarte CG, Alvarenga LM, Dias-Lopes C, Machado-de-Avila RA, Nguyen C, Molina F, et al. In vivo protection against *Tityus serrulatus* scorpion venom by antibodies raised against a discontinuous synthetic epitope. Vaccine 2010;28(5):1168–76.
[11] Estêvão-Costa MI, Martins MS, Sánchez EF, Diniz CR, Chávez-Olórtegui C. Neutralization of the hemorrhagic activity of *Bothrops* and *Lachesis* snake venoms by a monoclonal antibody against mutalysin-II. Toxicon 2000;38(1):139–44.
[12] Estêvão-Costa MI, Diniz CR, Magalhaes A, Markland FS, Sanchez EF. Action of metalloproteinases mutalysin I and II on several components of the hemostatic and fibrinolytic systems. Thromb Res 2000;99:363–76.
[13] Felici F, Luzzago A, Folgori A, Cortese R. Mimicking of discontinuous epitopes by phage-displayed peptides. II. Selection of clones recognized by a protective monoclonal antibody against the *Bordetella pertussis* toxin from phage peptide libraries. Gene 1993;128(1):21–7.
[14] Felicori L, Araujo SC, Machado de Avila RA, Sanchez EF, Granier C, Kalapothakis E, et al. Functional characterization and epitope analysis of a recombinant dermonecrotic protein from *Loxosceles intermedia* spider. Toxicon 2006;48(5):509–19.
[15] Ferreira RN, Machado de Avila RA, Sanchez EF, Maria WS, Molina F, Granier C, et al. Antibodies against synthetic epitopes inhibit the enzymatic activity of mutalysin II, a metalloproteinase from bushmaster snake venom. Toxicon 2006;48(8):1098–103.
[16] Forster-Waldl E, Riemer AB, Dehof AK, Neumann D, Bramswig K, Boltz-Nitulescu G, et al. Isolation and structural analysis of peptide mimotopes for the disialoganglioside GD2, a neuroblastoma tumor antigen. Mol Immunol 2005;42(3):319–25.
[17] Frank R. Spot-synthesis: an easy technique for the positionally addressable, parallel chemical synthesis on a membrane support. Tetrahedron 1992;48(42):9217–32.
[18] Gausepohl H, Boulin C, Kraft M, Frank RW. Automated multiple peptide synthesis. Pept Res 1992;5:315–20.
[19] Gazarian T, Selisko B, Hérion P, Gazarian K. Isolation and structure–functional characterization of phage display library-derived mimotopes of noxiustoxin, a neurotoxin of the scorpion *Centruroides noxius* Hoffmann. Mol Immunol 2000;37(12–13):755–66.
[20] Hell RC, Amim P, de Andrade HM, Machado de Avila RA, Felicori L, Oliveira AG, et al. Immunodiagnosis of human neurocysticercosis using a synthetic peptide selected by phage-display. Clin Immunol 2009;131(1):129–38.
[21] Hernández R, Gazarian TG, Hérion PS, Gazarian KG. Molecular localization and crossreactivity of two epitopes of noxiustoxin from scorpion *Centruroides noxius*, identified by a panel of monoclonal antibodies and peptide mimotopes. Immunol Lett 2002;80(2):97–103.
[22] Jorge MT, Sano-Martins IS, Tomy SC, Castro SC, Ferrari RA, Ribeiro LA, et al. Snakebite by the bushmaster (*Lachesis muta*) in Brazil: case report and review of the literature. Toxicon 1997;35(4):545–54.
[23] Kamiguti AS, Zuzel M, Theakston RD. Snake venom metalloproteinases and disintegrins: interactions with cells. Braz J Med Biol Res 1998;31(7):853–62.
[24] Kirby CJ, Gregoriadis G. Preparation of liposomes containing factor VIII for oral treatment of haemophilia. J Microencapsul 1984;1(1):33–45.
[25] Kondo H, Kondo S, Ikezawa H, Murata R. Studies on the quantitative method for determination of hemorrhagic activity of Habu snake venom. Jpn J Med Sci Biol 1960;13:43–52.
[26] Laune D, Molina F, Ferrieres G, Villard S, Bes C, Rieunier F, et al. Application of the Spot method to the identification of peptides and amino acids from the antibody paratope that contribute to antigen binding. J Immunol Methods 2002;267(1):53–70.
[27] Machado de Avila RA, Alvarenga LM, Tavares CA, Molina F, Granier C, Chávez-Olórtegui C. Molecular characterization of protective antibodies raised in mice by *Tityus serrulatus* scorpion venom toxins conjugated to bovine serum albumin. Toxicon 2004;44(3):233–41.
[28] Maria WS, Velarde DT, Alvarenga LM, Nguyen C, Villard S, Granier C, et al. Localization of epitopes in the toxins of *Tityus serrulatus* scorpions and neutralizing potential of therapeutic antivenoms. Toxicon 2005;46(2):210–7.
[29] Martin L, Messmer B, Thaler D. Synthetic peptide analogs compared with phage display. American Peptide Symposia 2002;6(4):172–3.
[30] Ministério Da Saúde Do Brasil. Manual de diagnóstico e tratamento de acidentes por animais peçonhentos. Brasília: Fundação Nacional De Saúde; 1990.
[31] Molina F, Laune D, Gougat C, Pau B, Granier C. Improved performances of spot multiple peptide synthesis. Pept Res 1996;9(3):151–5.
[32] Murthy KK, Shen SH, Banville D. Epitope mapping of SHP-1 monoclonal antibodies using peptide phage display. Biochem Biophys Res Commun 1998;248(1):69–74.
[33] Ownby CL, Bjarnason J, Tu AT. Hemorrhagic toxins from rattlesnake (*Crotalus atrox*) venom. Pathogenesis of hemorrhage induced by three purified toxins. Am J Pathol 1978;93(1):201–18.
[34] Rucavado A, Flores-Sánchez E, Franceschi A, Magalhães A, Gutiérrez JM. Characterization of the local tissue damage induced by LHF-II, a metalloproteinase with weak hemorrhagic activity isolated from *Lachesis muta muta* snake venom. Toxicon 1999;37(9):1297–312.
[35] Sanchez EF, Cordeiro MN, De Oliveira EB, Juliano L, Prado ES, Diniz CR. Proteolytic specificity of two hemorrhagic factors, LHF-I and LHF-II, isolated from the venom of the bushmaster snake (*Lachesis muta muta*). Toxicon 1995;33(8):1061–9.
[36] Sanchez EF, Diniz CR, Richardson M. The complete amino acid sequence of the hemorrhagic factor LHFII, a metalloproteinase isolated from the venom of the bushmaster snake (*Lachesis muta muta*). FEBS Lett 1991;282:178–82.
[37] Sanchez EF, Magalhães A, Diniz CR. Purification of a hemorrhagic factor (LHF-I) from the venom of the bushmaster snake, *Lachesis muta muta*. Toxicon 1987;25(6):611–9.
[38] Sanchez EF, Souza CT, Bello CA, Richardson M, Oliveira EB, Magalhães A. Resolution of isoforms of mutalysin II, the metalloproteinase from bushmaster snake venom. Toxicon 2003;41(8):1021–31.
[39] Souza CT, Moura MB, Magalhaes A, Heneine LG, Olortegui CC, Diniz CR, et al. Inhibition of mutalisyn II, a metalloproteinase from bushmaster snake venom by human a 2-macroglobulin and rabbit immunoglobulin. Comp Biochem Physiol 2001;130:155–68.
[40] Villard S, Lacroix-Desmazes S, Kieber-Emmons T, Piquer D, Grailly S, Benhida A, et al. Peptide decoys selected by phage display block in vitro and in vivo activity of a human anti-FVIII inhibitor. Blood 2003;102(3):949–52.
[41] Warrell DA. Clinical features of envenoming from snake bites. In: Bon C, Goyffon M, editors. Envenomings and their treatments. Lyon: Fondation Marcel Merieux; 1996. p. 63–76.

4. Discussão

Neste capítulo serão abordados de maneira integrativa temas adicionais e complementares àqueles já discutidos em cada um dos artigos.

Nas últimas décadas, centenas de trabalhos foram publicados acerca das metaloproteases de serpentes e estes estudos recentes permitiram muitos avanços em relação ao nosso entendimento sobre esta importante família de toxinas. No entanto, diversos desafios ainda se apresentam neste campo, incluindo, por exemplo: (1) o entendimento das determinantes estruturais que diferenciam as PI-SVMPs hemorrágicas e não hemorrágicas; (2) o mecanismo completo da hemorragia causada por essas toxinas; (3) o processo completo pós-traducional e processamento das pró-peptidases até a formação das formas maduras destas toxinas, bem com suas determinantes estruturais; (4) o papel sinergístico das SVMPs em estudos sistêmico-integrativos do quadro do envenenamento; e, por último, (5) um entendimento detalhado dos determinantes antigênicos das SVMPs, no intuito de possibilitar o desenvolvimento de ferramentas diferenciais de diagnóstico, ou de melhorias na qualidade e eficiências dos soros antiofídicos produzidos.

Outro desafio na área da toxinologia consiste no fato de diversas serpentes continuarem sem ter seus venenos caracterizados, mesmo que somente em nível de estudos pré-clínicos para a avaliação dos potenciais neutralizantes dos antivenenos comerciais disponíveis nos centros de saúde contra as principais atividades tóxicas destes venenos, como preconizado pela OMS [103,104,140-142].

Até o ano de 2010, vários trabalhos haviam sido publicados em relação ao veneno de *Bothrops atrox*, os quais descrevem: variações ontogenéticas e geográficas na composição dos venenos de diferentes espécimes de *B. atrox* [28,55,63]; análise e avaliação da neutralização de efeitos tóxicos causados pelo veneno desta espécie, utilizando-se diferentes antivenenos [28,106,107,141,143]; desenvolvimento de testes na tentativa de diferenciar o envenenamento causado por *Bothrops atrox* daquele causado por *Lachesis muta muta* [144,145]; e descrição do isolamento de algumas toxinas [58,62,72,73,146]. Neste trabalho, descrevemos no Artigo 1 – The novel metalloproteinase atroxlysin-I from Peruvian *Bothrops atrox* (Jergón) snake venom acts both on blood vessel ECM and platelets – a purificação e caracterização de uma metaloprotease do veneno da serpente *Bothrops atrox,* chamada Atroxlisina-I.

Apesar da importância das SVMPs nos venenos de viperídeos, Atroxlisina-I foi a primeira SVMP do veneno de *B. atrox* a ser purificada e caracterizada. Outras duas PI-SVMPs, Batx-I

e Batroxase, foram isoladas subsequentemente por outros grupos [59,60]. Como dito anteriormente, até o momento, nenhuma PIII-SVMP foi isolada e estudada em nível proteico.

Atr-I, Batx-I e Batroxase são PI-SVMPs hemorrágicas e fibrin(ogen)olíticas, sem atividade procoagulante, isoladas de venenos de espécimes de *B. atrox* da região amazônica do Peru, Colômbia e Brasil, respectivamente [59-61]. Atroxlisina e Batroxase são capazes de degradar componentes da matriz extracelular (incluindo fibronectina e colágeno tipo I e IV), contribuindo para a sintomatologia e dano tecidual local, bem como o quadro hemorrágico seguido ao envenenamento [59]. Além disso, as PI-SVMPs de *Bothrops atrox* podem exercer também papel sistêmico no envenenamento, agindo como miotoxinas [60] e inibidoras de agregação plaquetária [61], o que poderia contribuir e acentuar os efeitos hemorrágico e necrótico, bem como potencializar a incoagulabilidade sanguínea.

Embora Batx-I possua somente um pequeno fragmento de 24 resíduos de aminoácidos sequenciado, Atr-I e Batroxase foram completamente sequenciadas, cada uma possuindo 202 aminoácidos com 90% de identidade entre si (Figura 16).

```
Atr-I     TPEQQRYVDLFIVVDHGMFMKYNGNSDKIRRRIHQMVNIMKEAYSTMYIDILLTGVEIWSNKDLINVQPAAPQTLDSFGE  80
Batroxase TPEQQRYVELLIVVGHGMFMKYNGNSPKIIRRIHQMVNIMKEAYTVMYIDILLTGVEIWSNKDLINVQPAAPQTLTSFGE  80
          ******** * *** *********** ** **************  ****************************** ****

Atr-I     WRKTDLLNRKSHDNAQLLTSTDFNGPTIGLAYVGSMCDPKRSTGVIQDHSEQDLMVAITMAHELGHNLGISHDTGSCSCG  160
Batroxase WRETDLLNRKSHDNAQLLTATDLDQETLGLAYLGTMCDPKLSIGVIQDHSEQDLMVAITMAHELGHNLGISHDTGSCSCG  160
          **+***************** **    * **** * ***** * ************************************

Atr-I     GYSCIMSPVLSHEPSKYFSDCSYIQCWDFIMKENPQCILNKR  202
Batroxase GYSCIMSPVLSHEPSKYFSDCSYIQCWDFIMRENPQCILNKR  202
          ****************************** **********
```

Figura 16. Alinhamento das sequências primárias de Atr-I e Batroxase. Resíduos são representados pela abreviatura padrão de uma letra. Resíduos em vermelhos são idênticos entre as sequências (*).

Estudos de venômica e antivenômica sugerem que os venenos de serpentes da espécie *B. atrox* encontrados no Peru possuam perfis bioquímico e imunológico muito semelhantes aos de indivíduos encontrados em território brasileiro, enquanto espécimes colombianos partilham maior similaridade fenotípica com o veneno da espécie *B. asper*, encontrada na América Central e extremo norte da América do Sul. O fragmento sequenciado de Batx-I parece corroborar tal fato, uma vez que possui 100% de identidade com BaP1 (PI-SVMP isolada do veneno de *B. asper*) enquanto compartilha somente 54% e 53% com Atr-I e Batroxase, respectivamente [20,28,60]. Comparado com mutalisina-II – PI-SVMP de *Lachesis muta muta*, serpente que compartilha o habitat norte amazônico com *B. atrox* –, Atr-I apresenta 66% de identidade em sua sequência primária, como discutido no Artigo 1 – The novel metalloproteinase atroxlysin-I from Peruvian *Bothrops atrox* (Jergón) snake venom acts both on blood vessel ECM and platelets.

Além disso, Atroxlisina-I apresenta habilidade de se ligar (i.e. fibrinogênio, fibronectina, laminina e colágeno do tipo I) e hidrolisar (i.e. colágenos do tipo I e IV, fibrinogênio, fibronectina, e as integrinas $\alpha_7\beta_1$ e $\alpha_1\beta_1$) componentes importantes na manutenção da hemostase e da integridade de vasos sanguíneos. Estas observações poderiam explicar a atividade hemorrágica exercida por Atr-I, uma vez que se ligando a certos componentes importantes da membrana basal de endotélios e da matriz extracelular, esta toxina se localizaria próximo às paredes de vasos sanguíneos e hidrolisaria proteínas mantenedoras da estabilidade dos capilares, os quais estariam sujeitos às forças biofísicas geradas pelo fluxo sanguíneo e resultaria em extravasamento de sangue, assim como proposto anteriormente [67-69,147].

Por se tratar de uma PI-SVMP, Atr-I não apresenta os domínios semelhante a desintegrina e rico em cisteína. Portanto, regiões intrínsecas ao domínio protease podem exercer função de ligação a alvos moleculares importantes na indução da hemorragia e da inibição da agregação plaquetária (a qual ocorre mesmo sob ação da apo-atroxlisina-I). Sendo assim, estudos de estrutura-função da molécula de Atr-I podem servir como modelo para um melhor entendimento das PI-SVMPs.

Além disso, a determinação de estruturas antigênicas de atroxlisina-I (e batroxase) pode ser importante no desenvolvimento de testes laboratoriais capazes de distinguir o envenenamento causado por *B. atrox* dos demais. Por último, a caracterização e desenvolvimento de novas de novas técnicas e ferramentas imunoquímicas podem ser úteis no aperfeiçoamento da soroterapia disponível atualmente.

Sendo assim, desenvolvemos um novo método de seleção de hibridomas produtores de anticorpos neutralizantes contra SVMPs para produção de anticorpos monoclonais anti-atr-I, os quais serão chamados mAbatrs deste ponto em diante (Artigo 2 – Use of a Synthetic Biosensor for Neutralizing Activity-Biased Selection of Monoclonal Antibodies Against Atroxlysin-I, an Hemorrhagic Metalloproteinase from *Bothrops atrox* Snake Venom).

Atroxlisina-I, assim como outras PI-SVMPs, hidrolisa a cadeia B da insulina preferencialmente entre as ligações peptídicas Ala^{14}-Leu^{15} e Tyr^{16}-Leu^{15}, sendo a ligação Ala^{14}-Leu^{15} rompida mais rapidamente e dentro de poucos minutos. Este padrão está de acordo com a especificidade de sequência de clivagem de substratos proposto para as SVMPs, onde, na sequência do substrato, o aminoácido na posição P1’ (P4-P3-P2-P1-P1’-P2’-P3’-P4’) normalmente é um aminoácido hidrofóbico (Leu ou Phe, preferencialmente) [79].

Estudos anteriores demonstraram que peptídeos FRET apresentando a sequência LVEALYQ, contida na cadeia B da insulina e possuindo a ligação Ala^{14}-Leu^{15} (numeração

referente à cadeia B da insulina), podem ser usados na avaliação da atividade proteolítica de SVMPs [132]. Como as atividades tóxicas mais pronunciadas das SVMPS, incluindo a hemorrágica, são dependentes das atividades proteolíticas das mesmas, decidimos sintetizar quimicamente o peptídeo Abz-LVEALYQ-EDDnp e usá-lo como biossensor da atividade neutralizante de anticorpos monoclonais anti-atr-I.

Basicamente, nossa seleção de clones produtores de mAbs neutralizantes contra as SVMPs funcionou da seguinte maneira: o sobrenadante de cultura celular dos hibridomas foi pré-incubado com Atr-I por 30 minutos a 37ºC. Em seguida, o peptídeo Abz-LVEALYQ-EDDnp foi adicionado à mistura em uma placa de 96 poços, a qual teve a emissão de fluorescência monitorada por uma hora. Presumimos que nos poços onde a emissão de fluorescência foi detectada, não havia a presença de anticorpos neutralizantes contra Atr-I, de tal maneira que os clones presentes nos poções de onde foram retirados estes sobrenadantes não foram selecionados. Por outro lado, assumimos que a ausência ou a diminuição de fluorescência detectável deu-se pela neutralização total/parcial da atividade proteolítica de Atr-I, ocasionada pela presença de mAbs neutralizantes. Sendo assim, os clones que produziram os sobrenadantes neutralizantes foram selecionados.

Este processo mostrou-se eficiente na seleção de clones produtores de anticorpos neutralizantes contra as atividades tóxicas das SVMPs. Uma vez que nossa metodologia é composta por somente duas etapas (incubação do sobrenadante com a enzima de interesse, seguida pela adição do substrato), este processo mostrou-se extremamente rápido e menos laborioso, além de muito sensível (11ng de Atr-I foram utilizados para cada hibridoma testado) em relação ao processo de *screening* convencional por ELISA.

Apesar da metodologia escolhida para a produção dos anticorpos monoclonais, os mAbatrs mostraram-se extremamente específicos para Atr-I e para o veneno de *B. atrox* em ELISA, não reconhecendo nenhum dos outros antígenos testados.

Por outro lado, e como esperado, os mAbatrs purificados dos sobrenadantes de cultura celular foram capazes de neutralizar a atividade proteolítica de Atr-I sobre o substrato sintético Abz-LVEALYQ-EDDnp. Além disso, os mAbtrs com maior atividade neutralizante *in vitro* (mAbatr1, 2 e 6) foram capazes de neutralizar a hemorragia induzida por Atroxlisina-I *in vivo*.

É importante ressaltar que a sequência dos subsítios dos substratos determinantes para a especificidade de clivagem das SVMPs de classe P-I não parece ser um fator determinante em relação à atividade hemorrágica, visto que enzimas com atividade não hemorrágica (e.g. leucurolisina-a) e enzimas com atividade hemorrágica (e.g. atroxlisina-I e BaP1) apresentam o

mesmo padrão de especificidade para a sequência de clivagem (X-Leu) [95]. Deve-se levar em consideração que, além da sequência de aminoácidos do substrato, a estrutura terciária dos substratos também influencia a especificidade enzimática das SVMPs, uma vez que interações moleculares prévias são requeridas para que ocorra quebra das ligações peptídicas dos substratos.

Desta forma, e devido ao fato de nenhum dos mAbatrs ser capaz de reconhecer Atr-I desnaturada em western blot ou na sequência linear de Atr-I no ensaio de SPOT, sugerimos que os mAbatrs reconhecem epitopos conformacionais localizados em regiões próximas ao sítio catalítico de Atr-I, pois estes mabs são capazes de inibir a hidrólise de pequenos substratos, como o peptídeo FRET, além de substratos macromoleculares, como aqueles envolvidos na indução da hemorragia *in vivo*.

No entanto, o motivo consenso do sítio ativo (HEXXHXXGXXH) e o "Met-turn" das SVMPs são regiões altamente conservadas nas SVMPs, o que não explicaria a especificidade dos mAbatrs para atroxlisina-I. Sendo assim, propomos que os mAbatrs reconhecem epitopos localizados no "loop" posicionado entre as duas regiões supracitadas. Este "loop" parece ser a região de maior variabilidade entre as PI-SVMPs e uma maior rigidez/flexibilidade nesta região parece ser um fator importante para a determinação da capacidade de induzir hemorragias *in vivo* nas PI-SVMPs [27,50,67,132].

Por outro lado, o IgG anti-atr-I purificado do soro policlonal produzido em coelhos, capaz de inibir a hidrólise de DMC e a atividade hemorrágica de Atr-I, mas inócuo em relação à proteólise de atroxlisina sobre o peptídeo FRET, reconhece dois epitopos de Atroxlisina-I – ^{59}WSNKDLINVQ^{68} e ^{23}NGNSDKIRRRIH^{34}. Estes epitopos localizam-se em regiões espacialmente distantes do sítio ativo de Atr-I, sendo o primeiro epitopo localizado em um loop entre a folha-β 2 e a terceira α-hélice; já o epitopo ^{23}NGNSDKIRRRIH^{34} está posicionado no final da primeira α-hélice e segue em seu loop adjacente, anterior à segunda α-hélice (Figura 14).

Em 2006, Ferreira e colaboradores [125] identificaram várias regiões epitôpicas de mutalisina-II utilizando-se do soro policlonal de coelhos anti-Mut-II, previamente produzido [148]. Este soro anti-Mut-II possui ampla reatividade cruzada e potencial neutralizante contra a atividade hemorrágica de diversos venenos, incluindo os de *Lachesis muta muta* e *Bothrops atrox* [148].

Das regiões identificadas por Ferreira (2006) [125], três delas foram sintetizadas e utilizadas em conjunto na imunização de coelhos (i.e. ^{10}VVADHGMFTKYN^{21}, ^{73}LKTFGEWRERVL^{84} e ^{168}SEGPSYEFSDCS^{179} – numeração referente à cadeia de

mutalisina-II). Apesar de estas regiões localizarem-se distantes do sítio ativo de mut-II, os IgGs anti-peptídeo purificados foram capazes de inibir a fibrinogenólise e a degradação de DMC induzida por mut-II, sugerindo um impedimento estérico que impossibilitaria o acesso dos resíduos catalíticos ao substrato [125].

Além das três regiões sintetizadas por Ferreira (2006) [125], uma quarta região altamente reativa com o soro de coelho anti-Mut-II foi identificada (^{25}NTIRTRVHEIVN^{36}). Esta região é adjacente ao epitopo ^{10}VVADHGMFTKYN^{21} e, em conjunto, se sobrepõem no alinhamento de mutalisina-II e atroxlisina-I ao epitopo linear de Atr-I (^{23}NGNSDKIRRRIH^{34}), identificado no capítulo 3.2.1 (Resultados não publicados). Estas regiões de mutalisina-II e Atr-I estão próximas à região identificada como possível epitopo de da PI-SVMP da *Bothrops neuwiedi*, Neuwiedase (^{40}NTVNGFFRSMN^{50}), por Cardoso e colaboradores (2009)[123] (Figura 17).

```
Atr-I     TPE--QQRYVDLFIVVDHGMFMKYNGNSDKIRRRIHQMVNIMKEAYSTMYIDILLTGVEI
Mut-II    ----FSQKYIELVVVADHGMFTKYNGNLNTIRTRVHEIVNTLNGFYRSLNILISLTDLEI
Neu       QQRFFPQRYIELVIVADRRMYTKYNSDSNKIRTRVHELVNTVNGFFRSMNVDASLANLEV
                 * *  *  * *  *  ***     ** * *  **               *   *

Atr-I     WSNKDLINVQPAAPQTLDSFGEWRKTDLLNRKSHDNAQLLTSTDFNGPTIGLAYVGSMCD
Mut-II    WSNQDLINVQSAANDTLKTFGEWRERVLLNRISHDNAQLLTAIDLADNTIGIAYTGGMCY
Neu       WSKKDLIKVEKDSSKTLTSFGEWRERDLLRRKSHDNAQLLTAIDFNGNTIGRAYLGSMCN
          **  *** *      **  *****   ** * *********  *    *** ** * **

Atr-I     PKRSTGVIQDHSEQDLMVAITMAHELGHNLGISHDTGSCSCGGYSCIMSPVLSHEPSKYF
Mut-II    PKNSVGIVQDHSPKTLLIAVTMAHELGHNLGMKHDENHCHCSASFCIMPPSISEGPSYEF
Neu       PKRSVGIVQDHSPINLLVGVTMAHELGHNLGMEHDGKDCLCGASLCIMSPGLTDGPSYEF
          ** * *  ****   *    **********  **   * *    *** *     **  *

Atr-I     SDCSYIQCWDFIMKENPQCILNKR
Mut-II    SDCSKDYYQMFLTKRKPQCILNKP
Neu       SDCSKDYYQTFLTNHNPQ------
          ****      *     **
```

Figura 17. Alinhamento entre Atroxlisina-I, Mutalisina-II e Neuwiedase, mostrando seus epitopos lineares. Na sequência de atroxlisina-I os epitopos identificados estão em vermelho. Em mutalisina-II, os epitopos identificados e sintetizados estão em verde e um terceiro epitopo identificado e não sintetizado encontra-se em laranja. Os epitopos identificados de Neuwiedase estão em azul.

No Artigo 1 – The novel metalloproteinase atroxlysin-I from Peruvian *Bothrops atrox* (Jergón) snake venom acts both on blood vessel ECM and platelets – sugerimos que a sequência ^{27}DKIRRRIHQ^{35} de Atr-I, presente no epitopo identificado, se assemelha às sequências TRKSHDNAQ e TRKRHDNAQ presente no domínio proteinase de HR1 e jararagina, PIII-SVMPs de *Trimeresurus flavoviridis* e *Bothrops jararaca*, respectivamente. Em HR1 e jararagina, estas regiões são responsáveis pela ligação ao domínio α_2I da integrina $\alpha_2\beta_1$, impedindo a interação entre o colágeno e seu receptor. Desta forma, a região localizada

entre o final da primeira α-hélice e o começo da segunda, incluindo o loop que as conecta, parece ser uma região importante para as atividades tóxicas das SVMPs, provavelmente direcionando estas toxinas a seus alvos moleculares.

Além disso, a alta conservação desta região na molécula de mutalisina-II e Atr-I, pode explicar a promiscuidade de ambos IgGs (anti-Mut-II e anti-atr-I). Apesar da baixa similaridade entre mut-II, Atr-I e Neuwiedase na região epitôpica da identificada utilizando-se soro policlonal anti-Neuwiedase por Cardoso e colaboradores (2006) na metaloprotease de *B. neuwiedi*, o epitopo (^{40}NTVNGFFRSMN^{50}) parece corroborar a importância antigênica desta região para as SVMPs.

Se, por um lado, a identificação de regiões específicas de interação antígeno-anticorpo pode ser útil no desenvolvimento de diagnósticos diferenciais entre envenenamentos, como dito anteriormente, por outro lado, a identificação de regiões comuns e importantes para a atividade tóxica das SVMPs é uma importante etapa para o desenvolvimento de novos imunógenos com potencial de induzir resposta imune de ampla reatividade cruzada.

Desta forma, decidimos estudar o padrão de reconhecimento do anticorpo monoclonal LmmAbB2D4 anti-Mutalisina-II.

No Artigo 3 – Mimotopes of mutalysin-II from *Lachesis muta* snake venom induce hemorrhage inhibitory antibodies upon vaccination of rabbits – utilizamos a técnica de SPOT associada à técnica de phage display para identificar epitopos de mutalisina-II.

Primeiramente, a técnica de SPOT foi utilizada na avaliação de reconhecimento da estrutura primária de mut-II por LmmAbB2D4. No entanto, o anticorpo monoclonal LmmAbB2D4 reconhece unicamente epitopos conformacionais, uma vez que os peptídeos lineares cobrindo a sequência primária de mut-II não foram reconhecidos.

Desta forma, a técnica de phage display foi utilizada na identificação dos mimotopos de mut-II. Mimotopos são sequências peptídicas que mimetizam epitopos de proteínas nativas reconhecidas por anticorpos específicos. Diversos trabalhos reportam o uso da técnica de phage display para a identificação de mimotopos de toxinas, incluindo a identificação dos epitopos lineares de Neuwiedase, descritos acima [123]. No entanto, esta é a primeira vez que a técnica de phage display é utilizada para a identificação de epitopos/mimotopos reconhecidos por um anticorpo monoclonal anti-SVMP.

Das quatro bibliotecas de fagos testadas, somente peptídeos da biblioteca XCX8CX foram selecionados. Na superfície dos fagos, estes peptídeos estão, provavelmente, ciclizados, corroborando a importância da conformação dos antígenos para o reconhecimento de LmmAbB2D4.

Após a seleção de 17 sequências, somente cinco foram reativas em uma nova membrana sintetizada (QCTMDQGRLRCR, TCATDQGRLRCT, HCFHDQGRVRCA, HCTMDQGRLRCR e SCMLDQGRSRCR). Nenhuma das cinco sequências reativas possuiu homologia à sequência primária de mut-II. A análise do alinhamento dos mimotopos reativos permite, no entanto, visualizar que o motivo XCXXDQGRXRCX é conservado em todos os cinco mimotopos (Figura 18).

```
Pep 4          QCTMDQGRLRCR
Pep 7          TCATDQGRLRCT
Pep 8          HCFHDQGRVRCA
Pep 14         HCTMDQGRLRCR
Pep 15         SCMLDQGRSRCR
                *  **** **
```

Figura 18. Alinhamento dos mimotopos de mutalisina-II reconhecidos pelo anticorpo monoclonal LmmAbB2D4.

É interessante notar que todos os resíduos conservados localizam-se entre as duas cisteínas, sugerindo que a ciclização dos peptídeos é uma característica realmente importante na interação LmmAbB2D4-mimotopos. Levando em consideração este traço dos mimotopos e sabendo que epitopos estão geralmente localizados em regiões flexíveis e expostos na superfície dos antígenos [149], sugerimos que na molécula nativa de mut-II, o epitopo reconhecido por LmmAbB2D4 pode estar localizado em um "loop" de mutalisina-II.

Além disso, o programa de bioinformática MIMOP [118] foi utilizado na tentativa de localização dessas sequências no modelo tridimensional de mut-II. MIMOP é um programa que, a partir da sequência e estrutura 3D da proteína utiliza-se de metodologias diferentes para analisar os mimotopos, encontrando regiões de consensos entre eles. Estes consensos são então examinados na estrutura 3D da proteína, sugerindo-se, assim, os resíduos na proteína que foram mimetizados pelos mimotopos.

De acordo com as análises feitas por MIMOP, diversos resíduos foram selecionados como possíveis regiões mimetizadas pelos peptídeos (Figura 19).

A região com maior concentração de resíduos indicados por MIMOP (Figura 19), localiza-se na região N-terminal de mutalisina-II, entre a primeira e a segunda α-hélices, passando pelo "loop" que as conecta, se sobrepondo às regiões sugeridas anteriormente (^{10}VVADHGMFTKYN^{21} e ^{25}NTIRTRVHEIVN^{36}).

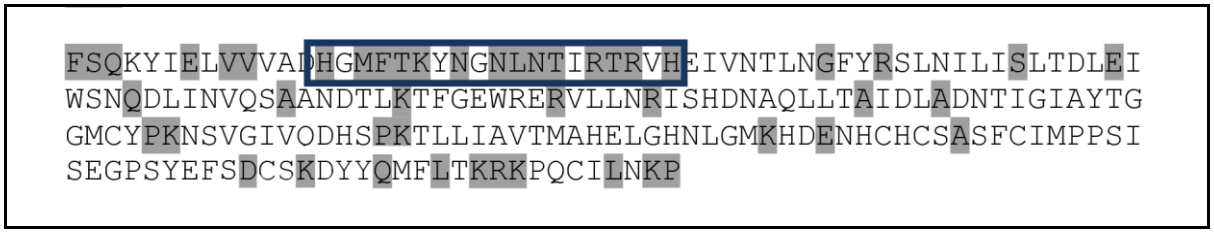

Figura 19. Possíveis resíduos da LHF-II que são mimetizados pelos mimotopos do veneno da serpente *Lachesis muta muta* selecionados por Phage Display. Em destaques, os resíduos possivelmente mimetizados sugeridos por MIMOP. A região marcada pelo retângulo azul apresenta a maior concentração de resíduos identificados, sugerindo uma possível região epitôpica.

Assim como os soros policlonais anti-mut-II, anti-atr-I e anti-Neuwiedase, o anticorpo monoclonal LmmAbB2D4 e o anticorpo monoclonal anti-BaP1(PI-SVMP de *Bothrops asper*) [132] apresentam alta reatividade cruzada com diversas SVMPs e diversos venenos. A duplicação gênica seguida de diversificação de sequências relaciona-se também à manutenção de certos motivos proteicos durante o processo evolutivo [12,16,17], o qual parece ter papel essencial na conservação de estruturas antigênicas que conferem alta promiscuidade aos anticorpos anti-toxinas [150].

Vale ressaltar que os mAbatrs (anti-atr-I), apesar de específicos para o veneno de *Bothrops atrox*, também reconhecem bandas em torno de 55, 30, 23 e 15 kDa do veneno de B. atrox em western blot. Portanto, em relação às SVMPs, a alta similaridade entre suas sequências de aminoácidos e a manutenção da estrutura terciária típica, parece favorecer respostas imunes com amplo espectro de reconhecimento.

Desta forma, novos trabalhos são requeridos para a caracterização dos epitopos conformacionais de Atr-I reconhecidos pelos mAbatrs, os quais poderiam clarificar os mecanismos envolvidos no reconhecimento específico destes anticorpos monoclonais.

5. Conclusões

Este trabalho, dividido em três partes, descreve a caracterização bioquímica e imunoquímica da atroxlisina-I, purificada do veneno de *Bothrops atrox*. A molécula de atroxlisina-I é um ótimo modelo para estudos de estrutura-função das SVMPs, uma vez que possui diversas atividades biológicas, incluindo a atividade hemorrágica, inibitória da agregação plaquetária, além de conseguir se ligar a alguns de seus alvos moleculares.

Sabendo da importância médico-epidemiológica de *Bothrops atrox* e do papel exercido pelas SVMPs em seu envenenamento, criamos um novo método funcional para a produção de anticorpos monoclonais neutralizantes. Este método mostrou-se confiável, rápido e pouco dispendioso, tanto economicamente quanto em relação ao consumo do antígeno alvo na produção dos mAbs. Os anticorpos monoclonais produzidos por esta metodologia mostraram-se neutralizantes contra Atr-I e *Bothrops atrox in vitro* e *in vivo.* Além disso, apresentaram alta especificidade frente às SVMPs de *Bothrops atrox*, fato que nos permitiu desenvolver um ensaio capaz de diferenciar o envenenamento experimental de *Bothrops atrox* de todos os outros testados, incluindo L*achesis muta muta*.

No intuito de se entender melhor os mecanismos de ação de Atr-I, bem como o padrão de reconhecimento dos mAbatrs, decidimos entender a estrutura imunoquímica e antigênica de atroxlisina-I. Apesar de não termos identificado os epitopos conformacionais reconhecidos pelos mAbatrs, sugerimos que estes podem reconhecer o alça localizada entre a α-hélice que contém o sítio ativo das SVMPs e o motivo conservado “Met-turn”. O reconhecimento desta região satisfaria tanto a alta especificidade dos mAbatrs pelas SVMPs de *Bothrops atrox*, pois esta região apresenta a maior variabilidade no domínio protease das moléculas de SVMPs, quanto a capacidade neutralizante destes anticorpos monoclonais.

Utilizando-se o IgG policlonal anti-atr-I, identificamos dois epitopos lineares. Apesar de se localizarem em regiões espacialmente distantes do sítio ativo de Atr-I, sendo o epitopo ^{59}WSNKDLINVQ^{68} localizado em um loop entre a folha-β 2 e a terceira α-hélice; já o epitopo ^{23}NGNSDKIRRRIH^{34} está posicionado no final da primeira α-hélice e segue em seu loop adjacente, anterior à segunda α-hélice. Este último parece representar uma região imunodominante das SVMPs, visto que tanto o soro policlonal anti-mut-II, quanto o soro anti-Neuwiedase reconhecem regiões muito próximas ao identificado em nosso trabalho.

Além disso, esta região parece ser importante para as atividades biológicas das SVMP, visto que resíduos localizados nesta região podem estar relacionados à interação entre estas

enzimas e seus alvos moleculares. Anticorpos produzidos contra epitopos desta região induzem resposta neutralizante contra as SVMPs.

Da mesma forma, estudamos o padrão de reconhecimento do anticorpo neutralizante e inespecífico anti-mut-II, LmmAbB2D4. Pela primeira vez a técnica de phage display foi utilizada para a caracterização de mimotopos de SVMPs reconhecidos por um anticorpo monoclonal. LmmAbB2D4 reconhece cinco mimotopos de mutalisina-II, os quais foram usados como imunógenos e geraram resposta neutralizante anti-mut-II e anti-veneno total de *L. muta muta*. A sequência consenso destes mimotopos (XCXXDQGRXRCX) foi utilizada no programa MIMOP, o qual sugeriu diversos resíduos de aminoácidos como sendo possíveis resíduos mimetizados pelos mimotopos. De acordo com o MIMOP, a região localizada entre as duas primeiras α-hélices podem representar o epitopo reconhecido por LmmAbB2D4.

Novos estudos são necessários para se avaliar a importância desta região nas atividades biológicas das SVMPs, assim como novos trabalhos serão feitos no intuito de se confirmar os epitopos reconhecidos pelas mAbatrs.

6. Perspectivas

- Confirmar o papel das sequências ^{27}DKIRRRIHQ^{35} e ^{6}RYVD^{10} nas atividades biológicas exercidas por Atr-I por meio de estudos de mutagênese sítio-dirigida;
- Identificar os epitopos conformacionais reconhecidos pelos mAbatrs por phage display ou cristalografia de proteínas e entender mecanismo responsável pela neutralização e pela especificidade destes anticorpos monoclonais;
- Produzir anticorpos monoclonais contra outras SVMPs utilizando-se do método funcional desenvolvido no intuito de se confirmar sua ampla aplicabilidade;
- Realizar ensaios de envenenamento experimental em outros modelos animais, visando o desenvolvimento de um kit diagnóstico para o envenenamento causado por *Bothrops atrox*;
- Validar experimentalmente os epitopos lineares identificados em Atr-I (^{59}WSNKDLINVQ^{68} e ^{23}NGNSDKIRRRIH^{34}) por meio da produção de anticorpos específicos contra estes peptídeos que reconheçam a molécula nativa de atroxlisina-I;
- Desenvolver anticorpos específicos para a região localizada entre a primeira e a segunda α-hélices e utilizá-los em estudos futuros de estrutura-função das PI-SVMPs, buscando a compreensão da importância desta região na atividade das SVMPs;
- Validar a região proposta pelo programa MIMOP como sendo mimetizada pelas mimotopos de mutalisina-II.

7. Referências

1. Vidal N, Hedges SB (2002) Higher-level relationships of caenophidian snakes inferred from four nuclear and mitochondrial genes. Comptes Rendus Biologies 325: 987-995.

2. Townsend TM, Larson A, Louis E, Macey JR (2004) Molecular phylogenetics of Squamata: The position of snakes, Amphisbaenians, and Dibamids, and the root of the Squamate tree. Systematic Biology 53: 735-757.

3. Vidal N, Hedges SB (2004) Molecular evidence for a terrestrial origin of snakes. Proceedings of the Royal Society B-Biological Sciences 271: S226-S229.

4. Vidal N, Hedges SB (2005) The phylogeny of squamate reptiles (lizards, snakes, and amphisbaenians) inferred from nine nuclear protein-coding genes. Comptes Rendus Biologies 328: 1000-1008.

5. Vidal N, Delmas A-S, David P, Cruaud C, Coujoux A, et al. (2007) The phylogeny and classification of caenophidian snakes inferred from seven nuclear protein-coding genes. Comptes Rendus Biologies 330: 182-187.

6. Wiens JJ, Kuczynski CA, Townsend T, Reeder TW, Mulcahy DG, et al. (2010) Combining Phylogenomics and Fossils in Higher-Level Squamate Reptile Phylogeny: Molecular Data Change the Placement of Fossil Taxa. Systematic Biology 59: 674-688.

7. Gauthier JA, Kearney M, Maisano JA, Rieppel O, Behlke AR (2012) Assembling the Squamate Tree of Life: Perspectives from the Phenotype and the Fossil Record. Bulletin of the Peabody Museum of Natural History 53: 3-308.

8. Losos JB, Hillis DM, Greene HW (2012) Who Speaks with a Forked Tongue? Science 338: 1428-1429.

9. Uetz P (2013) The Reptile Database.

10. Pyron RA, Burbrink FT, Wiens JJ (2013) A phylogeny and revised classification of Squamata, including 4161 species of lizards and snakes. Bmc Evolutionary Biology 13.

11. Fry BG, Vidal N, Norman JA, Vonk FJ, Scheib H, et al. (2006) Early evolution of the venom system in lizards and snakes. Nature 439: 584-588.

12. Fry BG, Wuster W (2004) Assembling an arsenal: Origin and evolution of the snake venom proteome inferred from phylogenetic analysis of toxin sequences. Molecular Biology and Evolution 21: 870-883.

13. Fry BG, Casewell NR, Wuester W, Vidal N, Young B, et al. (2012) The structural and functional diversification of the Toxicofera reptile venom system. Toxicon 60: 434-448.

14. Vidal N (2002) Colubroid systematics: Evidence for an early appearance of the venom apparatus followed by extensive evolutionary tinkering. Journal of Toxicology-Toxin Reviews 21: 21-41.

15. Fry BG, Vidal N, van der Weerd L, Kochva E, Renjifo C (2009) Evolution and diversification of the Toxicofera reptile venom system. Journal of Proteomics 72: 127-136.

16. Fry BG, Roelants K, Champagne DE, Scheib H, Tyndall JDA, et al. (2009) The Toxicogenomic Multiverse: Convergent Recruitment of Proteins Into Animal Venoms. Annual Review of Genomics and Human Genetics 10: 483-511.

17. Fry BG, Scheib H, van der Weerd L, Young B, McNaughtan J, et al. (2008) Evolution of an arsenal. Molecular & Cellular Proteomics 7: 215-246.

18. Queiroz GP, Pessoa LA, Portaro FCV, Furtado MdFD, Tambourgi DV (2008) Interspecific variation in venom composition and toxicity of Brazilian snakes from Bothrops genus. Toxicon 52: 842-851.

19. Calvete JJ, Sanz L, Angulo Y, Lomonte B, Maria Gutierrez J (2009) Venoms, venomics, antivenomics. Febs Letters 583: 1736-1743.

20. Calvete JJ, Sanz L, Perez A, Borges A, Vargas AM, et al. (2011) Snake population venomics and antivenomics of Bothrops atrox: Paedomorphism along its transamazonian dispersal and implications of geographic venom variability on snakebite management. Journal of Proteomics 74: 510-527.

21. Maria Gutierrez J, Sanz L, Flores-Diaz M, Figueroa L, Madrigal M, et al. (2010) Impact of Regional Variation in Bothrops asper Snake Venom on the Design of Antivenoms: Integrating Antivenomics and Neutralization Approaches. Journal of Proteome Research 9: 564-577.

22. Barlow A, Pook CE, Harrison RA, Wuester W (2009) Coevolution of diet and prey-specific venom activity supports the role of selection in snake venom evolution. Proceedings of the Royal Society B-Biological Sciences 276: 2443-2449.

23. Pyron RA, Burbrink FT, Colli GR, Montes de Oca AN, Vitt LJ, et al. (2011) The phylogeny of advanced snakes (Colubroidea), with discovery of a new subfamily and comparison of support methods for likelihood trees. Molecular Phylogenetics and Evolution 58: 329-342.

24. Vonk FJ, Admiraal JF, Jackson K, Reshef R, de Bakker MAG, et al. (2008) Evolutionary origin and development of snake fangs. Nature 454: 630-633.

25. Wuster W, Peppin L, Pook CE, Walker DE (2008) A nesting of vipers: Phylogeny and historical biogeography of the Viperidae (Squamata: Serpentes). Molecular Phylogenetics and Evolution 49: 445-459.

26. *Bothrops atrox*. Clinical Toxinology Resources. In: http://www.toxinology.com/fusebox.cfm?fuseaction=main.snakes.display&id=SN0389. Acessed in 03/20/2013

27. Akao PK, Tonoli CCC, Navarro MS, Cintra ACO, Neto JR, et al. (2010) Structural studies of BmooMP alpha-I, a non-hemorrhagic metalloproteinase from Bothrops moojeni venom. Toxicon 55: 361-368.

28. Nunez V, Cid P, Sanz L, De La Torre P, Angulo Y, et al. (2009) Snake venomics and antivenomics of Bothrops atrox venoms from Colombia and the Amazon regions of Brazil, Peru and Ecuador suggest the occurrence of geographic variation of venom phenotype by a trend towards paedomorphism. Journal of Proteomics 73: 57-78.

29. Patterson D (2008) Serpentes. In: Patterson D, editor. Encyclopedia of Life. http://eol.org/pages/2815988/details.

30. (2014) *Lachesis muta*. http://www.toxinology.com/fusebox.cfm?fuseaction=main.snakes.display&id=SN0356.

31. Gutierrez JM, Theakston RDG, Warrell DA (2006) Confronting the neglected problem of snake bite envenoming: The need for a global partnership. Plos Medicine 3: 727-731.

32. Struchiner CJ Epidemiologia dos acidentes ofídicos nos últimos 100 anos no Brasil : uma revisão Snake bite epidemiology in the last 100 years in Brazil : a review. Medicina 19: 7-16.

33. Borges CC, Sadahiro M, dos-Santos MC (1999) Aspectos epidemiológicos e clínicos dos acidentes ofídicos ocorridos nos municípios do Estado do Amazonas Epidemiological and clinical aspects of snake accidentes in the municipalities of the State of Amazonas , Brazil. Revista da Sociedade Brasileira de Medicina Tropical 32: 637-646.

34. Waldez F, Vogt RC Aspectos ecológicos e epidemiológicos de acidentes ofídicos em comunidades ribeirinhas do baixo rio. 39: 681-692.

35. Chippaux J-P (2008) Estimating the Global Burden of Snakebite Can Help To Improve Management. Plos Medicine 5: 1538-1539.

36. Otero-Patino R (2009) Epidemiological, clinical and therapeutic aspects of Bothrops asper bites. Toxicon 54: 998-1011.

37. Harrison RA, Hargreaves A, Wagstaff SC, Faragher B, Lalloo DG (2009) Snake Envenoming: A Disease of Poverty. Plos Neglected Tropical Diseases 3.

38. Kasturiratne A, Wickremasinghe AR, de Silva N, Gunawardena NK, Pathmeswaran A, et al. (2008) The Global Burden of Snakebite: A Literature Analysis and Modelling Based on Regional Estimates of Envenoming and Deaths. Plos Medicine 5: 1591-1604.

39. Williams D, Gutierrez JM, Harrison R, Warrell DA, White J, et al. (2010) The Global Snake Bite Initiative: an antidote for snake bite. Lancet 375: 89-91.

40. Brasil. Ministério da Saúde. Secretaria de Vigilância em Saúde. Departamento de Vigilância E (2010) Guia de vigilância epidemiológica. Brasília. 816-816 p.

41. Hansson E, Cuadra S, Oudin A, de Jong K, Stroh E, et al. (2010) Mapping Snakebite Epidemiology in Nicaragua - Pitfalls and Possible Solutions. Plos Neglected Tropical Diseases 4.

42. Hansson E, Sasa M, Mattisson K, Robles A, Gutierrez JM (2013) Using Geographical Information Systems to Identify Populations in Need of Improved Accessibility to Antivenom Treatment for Snakebite Envenoming in Costa Rica. Plos Neglected Tropical Diseases 7.

43. de Souza ARB, Tavares AM, Bührnheim PF Acidentes por animais peçonhentos. Fundação de Medicina Tropical Doutor Heitor Vieira Dourado.

44. White J (2005) Snake venoms and coagulopathy. Toxicon 45: 951-967.

45. Warrell DA (2010) Snake bite. Lancet 375: 77-88.

46. Sanchez EF, Swenson S (2007) Proteases from South American snake venoms affecting fibrinolysis. Current Pharmaceutical Analysis 3: 147-157.

47. Cruz LS, Vargas R, Lopes AA (2009) SNAKEBITE ENVENOMATION AND DEATH IN THE DEVELOPING WORLD. Ethnicity & Disease 19: 42-46.

48. Franca FOS, Barbaro KC, Fan HW, Cardoso JLC, Sano-Martins IS, et al. (2003) Envenoming by Bothrops jararaca in Brazil: association between venom antigenaemia and severity at admission to hospital. Transactions of the Royal Society of Tropical Medicine and Hygiene 97: 312-317.

49. Markland FS (1998) Snake venoms and the hemostatic system. Toxicon 36: 1749-1800.

50. Ramos OHP, Selistre-de-Araujo HS (2004) Comparative analysis of the catalytic domain of hemorrhagic and non-hemorrhagic snake venom metallopeptidases using bioinformatic tools. Toxicon 44: 529-538.

51. Bieber AL (1979) Metal and Nonprotein Constituents in Snake Venoms. In: Lee C-Y, editor. Snake Venoms: Springer Berlin Heidelberg. pp. 295-306.

52. Calvete JJ (2013) Snake venomics: From the inventory of toxins to biology. Toxicon 75: 44-62.

53. Calvete JJ, Juarez P, Sanz L (2007) Snake venomics. Strategy and applications. Journal of Mass Spectrometry 42: 1405-1414.

54. Escoubas P, Quinton L, Nicholson GM (2008) Venomics: unravelling the complexity of animal venoms with mass spectrometry. Journal of Mass Spectrometry 43: 279-295.

55. Lopez-Lozano JL, de Sousa MV, Ricart CAO, Chavez-Olortegui C, Sanchez EF, et al. (2002) Ontogenetic variation of metalloproteinases and plasma coagulant activity in venoms of wild Bothrops atrox specimens from Amazonian rain forest. Toxicon 40: 997-1006.

56. Kohlhoff M, Borges MH, Yarleque A, Cabezas C, Richardson M, et al. (2012) Exploring the proteomes of the venoms of the Peruvian pit vipers Bothrops atrox, B. barnetti and B. pictus. Journal of Proteomics 75: 2181-2195.

57. Calvete JJ, Borges A, Segura A, Flores-Diaz M, Alape-Giron A, et al. (2009) Snake venomics and antivenomics of Bothrops colombiensis, a medically important pitviper of the Bothrops atrox-asper complex endemic to Venezuela: Contributing to its taxonomy and snakebite management. Journal of Proteomics 72: 227-240.

58. Alves RM, Antonucci GA, Paiva HH, Cintra ACO, Franco JJ, et al. (2008) Evidence of caspase-mediated apoptosis induced by L-amino acid oxidase isolated from Bothrops atrox snake venom. Comparative Biochemistry and Physiology a-Molecular & Integrative Physiology 151: 542-550.

59. Cintra ACO, De Toni LGB, Sartim MA, Franco JJ, Caetano RC, et al. (2012) Batroxase, a new metalloproteinase from B. atrox snake venom with strong fibrinolytic activity. Toxicon 60: 70-82.

60. Patino AC, Pereanez JA, Nunez V, Benjumea DM, Fernandez M, et al. (2010) Isolation and biological characterization of Batx-I, a weak hemorrhagic and fibrinogenolytic PI metalloproteinase from Colombian Bothrops atrox venom. Toxicon 56: 936-943.

61. Sanchez EF, Schneider FS, Yarleque A, Borges MH, Richardson M, et al. (2010) The novel metalloproteinase atroxlysin-I from Peruvian Bothrops atrox (Jergon) snake venom acts both on blood vessel ECM and platelets. Archives of Biochemistry and Biophysics 496: 9-20.

62. Kanashiro MM, Escocard RDM, Petretski JH, Prates MV, Alves EW, et al. (2002) Biochemical and biological properties of phospholipases A(2) from Bothrops atrox snake venom. Biochemical Pharmacology 64: 1179-1186.

63. Guercio RAP, Shevchenko A, Shevchenko A, Lopez-Lozano JL, Paba J, et al. (2006) Ontogenetic variations in the venom proteome of the Amazonian snake Bothrops atrox. Proteome Science 4.

64. Luna KPO, da Silva MB, Pereira VRA (2011) Clinical and immunological aspects of envenomations by Bothrops snakes. Journal of Venomous Animals and Toxins Including Tropical Diseases 17: 130-141.

65. Escalante T, Shannon J, Moura-da-silva AM, María J, Fox JW (2006) Novel insights into capillary vessel basement membrane damage by snake venom hemorrhagic metalloproteinases : A biochemical and immunohistochemical study. Electrophoresis 455: 144-153.

66. Gutierrez JM, Rucavado A, Escalante T, Diaz C (2005) Hemorrhage induced by snake venom metalloproteinases: biochemical and biophysical mechanisms involved in microvessel damage. Toxicon 45: 997-1011.

67. Escalante T, Rucavado A, Fox JW, Gutierrez JM (2011) Key events in microvascular damage induced by snake venom hemorrhagic metalloproteinases. Journal of Proteomics 74: 1781-1794.

68. Baldo C, Jamora C, Yamanouye N, Zorn TM, Moura-da-Silva AM (2010) Mechanisms of Vascular Damage by Hemorrhagic Snake Venom Metalloproteinases: Tissue Distribution and In Situ Hydrolysis. Plos Neglected Tropical Diseases 4.

69. Moura-da-Silva AM, Ramos OHP, Baldo C, Niland S, Hansen U, et al. (2008) Collagen binding is a key factor for the hemorrhagic activity of snake venom metalloproteinases. Biochimie 90: 484-492.

70. Terra RMS, Pinto AFM, Guimaraes JA, Fox JW (2009) Proteomic profiling of snake venom metalloproteinases (SVMPs): Insights into venom induced pathology. Toxicon 54: 836-844.

71. Itoh N, Tanaka N, Mihashi S, Yamashina I (1987) MOLECULAR-CLONING AND SEQUENCE-ANALYSIS OF CDNA FOR BATROXOBIN, A THROMBIN-LIKE SNAKE-VENOM ENZYME. Journal of Biological Chemistry 262: 3132-3135.

72. Nunez V, Arce V, Gutierrez JM, Lomonte B (2004) Structural and functional characterization of myotoxin I, a Lys49 phospholipase A(2) homologue from the venom of the snake Bothrops atrox. Toxicon 44: 91-101.

73. Rucinski B, Niewiarowski S, Holt JC, Soszka T, Knudsen KA (1990) BATROXOSTATIN, AN ARG-GLY-ASP-CONTAINING PEPTIDE FROM BOTHROPS-ATROX, IS A POTENT INHIBITOR OF PLATELET-AGGREGATION AND CELL-INTERACTION WITH FIBRONECTIN. Biochimica Et Biophysica Acta 1054: 257-262.

74. Tavares NAC, Correia JM, Guarnieri MC, Lima-Filho JL, Prieto-da-Silva ARB, et al. (2008) Expression of mRNAs coding for VAP1/crotastatin-like metalloproteases in the venom glands of three South American pit vipers assessed by quantitative real-time PCR. Toxicon 52: 897-907.

75. Petretski JH, Kanashiro MM, Rodrigues FR, Alves EW, Machado OLT, et al. (2000) Edema induction by the disintegrin-like/cysteine-rich domains from a Bothrops atrox hemorrhagin. Biochemical and Biophysical Research Communications 276: 29-34.

76. Sanz L, Escolano J, Ferretti M, Biscoglio MJ, Rivera E, et al. (2008) Snake venomics of the South and Central American Bushmasters. Comparison of the toxin composition of Lachesis muta gathered from proteomic versus transcriptomic analysis. Journal of Proteomics 71: 46-60.

77. Sanchez EF, Magalhaes A, Mandelbaum FR, Diniz CR (1991) PURIFICATION AND CHARACTERIZATION OF THE HEMORRHAGIC FACTOR-II FROM THE VENOM OF THE BUSHMASTER SNAKE (LACHESIS-MUTA-MUTA). Biochimica Et Biophysica Acta 1074: 347-356.

78. Sanchez EF, Diniz CR, Richardson M (1991) THE COMPLETE AMINO-ACID-SEQUENCE OF THE HEMORRHAGIC FACTOR LHFII, A METALLOPROTEINASE ISOLATED FROM THE VENOM OF THE BUSHMASTER SNAKE (LACHESIS-MUTA-MUTA). Febs Letters 282: 178-182.

79. Fox JW, Serrano SMT (2009) Timeline of key events in snake venom metalloproteinase research. Journal of Proteomics 72: 200-209.

80. Markland FS, Jr., Swenson S (2013) Snake venom metalloproteinases. Toxicon 62: 3-18.

81. Fox JW, Serrano SMT (2005) Structural considerations of the snake venom metalloproteinases, key members of the M12 reprolysin family of metalloproteinases. Toxicon 45: 969-985.

82. Fox JW, Serrano SMT (2008) Insights into and speculations about snake venom metalloproteinase (SVMP) synthesis, folding and disulfide bond formation and their contribution to venom complexity. Febs Journal 275: 3016-3030.

83. Ramos OHP, Selistre-De-Araujo HS (2006) Snake venom metalloproteases - structure and function of catalytic and disintegrin domains. Comparative Biochemistry and Physiology C-Toxicology & Pharmacology 142: 328-346.

84. Kamiguti AS, Markland FS, Zhou Q, Laing GD, Theakston RDG, et al. (1997) Proteolytic cleavage of the beta(1) subunit of platelet alpha(2)beta(1), integrin by the metalloproteinase jararhagin compromises collagen-stimulated phosphorylation of pp72(syk). Journal of Biological Chemistry 272: 32599-32605.

85. Sanchez EF, Gabriel LM, Gontijo S, Gremski LH, Veiga SS, et al. (2007) Structural and functional characterization of a P-III metalloproteinase, leucurolysin-B, from Bothrops leucurus venom. Archives of Biochemistry and Biophysics 468: 193-204.

86. Swenson S, Toombs CF, Pena L, Johansson J, Markland FS (2004) Alpha-fibrinogenases. Curr Drug Targets Cardiovasc Haematol Disord 4: 417-435.

87. Takacs Z, Retzios AD, Markland FS (1992) A hemorrhagic (basement membrane degrading) zinc metalloproteinase from southern copperhead venom. Matrix Suppl 1: 101-103.

88. Pidde-Queiroz G, Magnoli FC, Portaro FCV, Serrano SMT, Lopes AS, et al. (2013) P-I Snake Venom Metalloproteinase Is Able to Activate the Complement System by Direct Cleavage of Central Components of the Cascade. Plos Neglected Tropical Diseases 7.

89. Okamoto DN, Kondo MY, Oliveira LCG, Honorato RV, Zanphorlin LM, et al. (2014) P-I class metalloproteinase from Bothrops moojeni venom is a post-proline cleaving peptidase with kininogenase activity: Insights into substrate selectivity and kinetic behavior. Biochimica et biophysica acta 1844: 545-552.

90. Bjarnason JB, Fox JW (1994) METALLOPROTEINASES FROM SNAKE-VENOMS (REPROLYSINS), STRUCTURE, FUNCTION, AND RELATIONSHIP TO MAMMALIAN REPRODUCTIVE PROTEINS. Journal of Cellular Biochemistry: 151-151.

91. Bjarnason JB, Fox JW (1995) SNAKE-VENOM METALLOENDOPEPTIDASES - REPROLYSINS. Proteolytic Enzymes: Aspartic and Metallo Peptidases 248: 345-368.

92. Stocker W, Grams F, Baumann U, Reinemer P, Gomisruth FX, et al. (1995) The Metzincins – Topological and Sequential Relations Between the Astacins, Adamalysins, Serralysins, and Matrixins (Collagenases) Define a Superfamily of Zinc-Peptidases. Protein Science 4: 823-840.

93. Gomis-Ruth FX, Kress Lf Fau - Bode W, Bode W First structure of a snake venom metalloproteinase: a prototype for matrix metalloproteinases/collagenases.

94. Bolger MB, Swenson S, Markland FS (2001) Three-dimensional structure of fibrolase, fibrinolytic enzyme from southern copperhead venom, modeled from the X-ray structure of adamalysin II and atrolysin C. Aaps Pharmsci 3.

95. Paes Leme AF, Escalante T, Pereira JGC, Oliveira AK, Sanchez EF, et al. (2011) High resolution analysis of snake venom metalloproteinase (SVMP) peptide bond cleavage specificity using proteome based peptide libraries and mass spectrometry. Journal of Proteomics 74: 401-410.

96. Bello CA, Hermogenes ALN, Magalhaes A, Veiga SS, Gremski LH, et al. (2006) Isolation and biochemical characterization of a fibrinolytic proteinase from Bothrops leucurus (white-tailed jararaca) snake venom. Biochimie 88: 189-200.

97. Takeda S, Igarashi T, Mori H, Araki S (2006) Crystal structures of VAP1 reveal ADAMs' MDC domain architecture and its unique C-shaped scaffold. Embo Journal 25: 2388-2396.

98. Moreira V, Teixeira C, da Silva HB, D'Imperio Lima MR, Dos-Santos MC (2013) The crucial role of the MyD88 adaptor protein in the inflammatory response induced by Bothrops atrox venom. Toxicon 67: 37-46.

99. Muniz EG, Maria WS, Estevao-Costa MI, Buhrnheim P, Chavez-Olortegui C (2000) Neutralizing potency of horse antibothropic Brazilian antivenom against Bothrops snake venoms from the Amazonian rain forest. Toxicon 38: 1859-1863.

100. Battellino C, Piazza R, da Silva AMM, Cury Y, Farsky SHP (2003) Assessment of efficacy of bothropic antivenom therapy on microcirculatory effects induced by Bothrops jararaca snake venom. Toxicon 41: 583-593.

101. Zamuner SR, da Cruz-Hofling MA, Corrado AP, Hyslop S, Rodrigues-Simioni U (2004) Comparison of the neurotoxic and myotoxic effects of Brazilian Bothrops venoms and their neutralization by commercial antivenom. Toxicon 44: 259-271.

102. Espino-Solis GP, Riano-Umbarila L, Becerril B, Possani LD (2009) Antidotes against venomous animals: State of the art and prospectives. Journal of Proteomics 72: 183-199.

103. OMS (2010) WHO Guidelines for the Production Control and Regulation of Snake Antivenoms Immunoglobulins.

104. Theakston RD, Warrell DA, Griffiths E (2003) Report of a WHO workshop on the standardization and control of antivenoms. Toxicon 41: 541-557.

105. Harrison RA, Cook DA, Renjifo C, Casewell NR, Currier RB, et al. (2011) Research strategies to improve snakebite treatment: Challenges and progress. Journal of Proteomics 74: 1768-1780.

106. Camey KU, Velarde DT, Sanchez EF (2002) Pharmacological characterization and neutralization of the venoms used in the production of Bothropic antivenom in Brazil. Toxicon 40: 501-509.

107. Otero R, Nunez V, Osorio RG, Gutierrez JM, Giraldo CA, et al. (1995) Ability of 6 Latin-American antivenoms to neutralize the venom of Mapana-equis (*Bothrops atrox*) from Antioquia and Choco (Colombia). Toxicon 33: 809-815.

108. Maria Gutierrez J, Williams D, Fan HW, Warrell DA (2010) Snakebite envenoming from a global perspective: Towards an integrated approach. Toxicon 56: 1223-1235.

109. Calderonaranda ES, Olamendiportugal T, Possani LD (1995) THE USE OF SYNTHETIC PEPTIDES CAN BE A MISLEADING APPROACH TO GENERATE VACCINES AGAINST SCORPION TOXINS. Vaccine 13: 1198-1206.

110. Mendes TM, Oliveira D, Figueiredo LFM, Machado-de-Avila RA, Duarte CG, et al. (2013) Generation and characterization of a recombinant chimeric protein (rCpLi) consisting of B-cell epitopes of a dermonecrotic protein from Loxosceles intermedia spider venom. Vaccine 31: 2749-2755.

111. Alvarenga L, Moreau V, Felicori L, Nguyen C, Duarte C, et al. (2010) Design of anti body-reactive peptides from discontinuous parts of scorpion toxins. Vaccine 28: 970-980.

112. Frauches TS, Petretski JH, Arnholdt ACV, Lasunskaia EB, de Carvalho ECQ, et al. (2013) Bothropic antivenom based on monoclonal antibodies, is it possible? Toxicon 71: 49-56.

113. Flower DR (2013) Designing immunogenic peptides. Nature Chemical Biology 9: 748-752.

114. Van Regenmortel MHV (2001) Antigenicity and immunogenicity of synthetic peptides. Biologicals 29: 209-213.

115. Rynkiewicz MJ, Lu Z, Hui JH, Sharon J, Seaton BA (2012) Structural Analysis of a Protective Epitope of the Francisella tularensis O-Polysaccharide. Biochemistry 51: 5684-5694.

116. Zhou M, Meyer T, Koch S, Koch J, von Briesen H, et al. (2013) Identification of a new epitope for HIV-neutralizing antibodies in the gp41 membrane proximal external region by an Env-tailored phage display library. European Journal of Immunology 43: 499-509.

117. Kong R, Li H, Georgiev I, Changela A, Bibollet-Ruche F, et al. (2012) Epitope Mapping of Broadly Neutralizing HIV-2 Human Monoclonal Antibodies. Journal of Virology 86: 12115-12128.

118. Moreau V, Granier C, Villard S, Laune D, Molina F (2006) Discontinuous epitope prediction based on mimotope analysis. Bioinformatics 22: 1088-1095.

119. Moreau V, Fleury C, Piquer D, Nguyen C, Novali N, et al. (2008) PEPOP: Computational design of immunogenic peptides. Bmc Bioinformatics 9.

120. Gausepohl H, Boulin C, Kraft M, Frank RW (1992) Automated Multiple Peptide-Synthesis. Peptide Research 5: 315-320.

121. Frank R (2002) The SPOT synthesis technique - Synthetic peptide arrays on membrane supports - principles and applications. Journal of Immunological Methods 267: 13-26.

122. Dias-Lopes C, Guimaraes G, Felicori L, Fernandes P, Emery L, et al. (2010) A protective immune response against lethal, dermonecrotic and hemorrhagic effects of Loxosceles intermedia venom elicited by a 27-residue peptide. Toxicon 55: 481-487.

123. Cardoso R, Homsi-Brandeburgo MI, Rodrigues VM, Santos WB, Souza GLR, et al. (2009) Peptide mimicking antigenic and immunogenic epitope of neuwiedase from Bothrops neuwiedi snake venom. Toxicon 53: 254-261.

124. Tanjoni I, Butera D, Spencer PJ, Takehara HA, Fernandes I, et al. (2003) Phylogenetic conservation of a snake venom metalloproteinase epitope recognized by a monoclonal antibody that neutralizes hemorrhagic activity. Toxicon 42: 809-816.

125. Ferreira RN, de Avila RAM, Sanchez EF, Maria WS, Molina F, et al. (2006) Antibodies against synthetic epitopes inhibit the enzymatic activity of mutalysin II, a metalloproteinase from bushmaster snake venom. Toxicon 48: 1098-1103.

126. Buschiazzo A, Muia R, Larrieux N, Pitcovsky T, Mucci J, et al. (2012) Trypanosoma cruzi trans-Sialidase in Complex with a Neutralizing Antibody: Structure/Function Studies towards the Rational Design of Inhibitors. Plos Pathogens 8.

127. Tanjoni I, Butera D, Bento L, Della-Casa MS, Marques-Porto R, et al. (2003) Snake venom metalloproteinases: structure/function relationships studies using monoclonal antibodies. Toxicon 42: 801-808.

128. Shapira A, Benhar I (2010) Toxin-Based Therapeutic Approaches. Toxins 2: 2519-2583.

129. Waldmann TA (1991) MONOCLONAL-ANTIBODIES IN DIAGNOSIS AND THERAPY. Science 252: 1657-1662.

130. Nieri P, Donadio E, Rossi S, Adinolfi B, Podesta A (2009) Antibodies for Therapeutic Uses and the Evolution of Biotechniques. Current Medicinal Chemistry 16: 753-779.

131. Estevao-Costa MI, Martins MS, Sanchez EF, Diniz CR, Chavez-Olortegui C (2000) Neutralization of the hemorrhagic activity of Bothrops and Lachesis snake venoms by a monoclonal antibody against mutalysin-II. Toxicon 38: 139-144.

132. Fernandes I, Assumpcao GG, Silveira CRF, Faquim-Mauro EL, Tanjoni I, et al. (2010) Immunochemical and biological characterization of monoclonal antibodies against BaP1, a metalloproteinase from Bothrops asper snake venom. Toxicon 56: 1059-1065.

133. Forster T (1948) *ZWISCHENMOLEKULARE ENERGIEWANDERUNG UND FLUORESZENZ. Annalen Der Physik 2: 55-75.

134. Carmona AK, Juliano MA, Juliano L (2009) The use of Fluorescence Resonance Energy Transfer (FRET) peptides for measurement of clinically important proteolytic enzymes. Anais Da Academia Brasileira De Ciencias 81: 381-392.

135. Kaman WE, Voskamp-Visser I, de Jongh DMC, Endtz HP, van Belkum A, et al. (2013) Evaluation of a D-amino-acid-containing fluorescence resonance energy transfer peptide library for profiling prokaryotic proteases. Analytical Biochemistry 441: 38-43.

136. Kaman WE, El Arkoubi-El Arkoubi N, Roffel S, Endtz HP, van Belkum A, et al. (2013) Evaluation of a FRET-Peptide Substrate to Predict Virulence in Pseudomonas aeruginosa. Plos One 8.

137. Song E, Cheng D, Song Y, Jiang M, Yu J, et al. (2013) A graphene oxide-based FRET sensor for rapid and sensitive detection of matrix metalloproteinase 2 in human serum sample. Biosensors & Bioelectronics 47: 445-450.

138. Noe F, Wu H, Prinz J-H, Plattner N (2013) Projected and hidden Markov models for calculating kinetics and metastable states of complex molecules. Journal of Chemical Physics 139.

139. Razzaghi-Asl N, Firuzi O, Hemmateenejad B, Javidnia K, Edraki N, et al. (2013) Design and synthesis of novel 3,5-bis-N-(aryl/heteroaryl) carbamoyl-4-aryl-1,4-dihydropyridines as small molecule BACE-1 inhibitors. Bioorganic & Medicinal Chemistry 21: 6893-6909.

140. Laing GD, Yarleque A, Marcelo A, Rodriguez E, Warrell DA, et al. (2004) Preclinical testing of three south American antivenoms against the venoms of five medic ally-important Peruvian snake venoms. Toxicon 44: 103-106.

141. Rojas E, Quesada L, Arce V, Lomonte B, Rojas G, et al. (2005) Neutralization of four Peruvian Bothrops sp snake venoms by polyvalent antivenoms produced in Peru and Costa Rica: preclinical assessment. Acta Tropica 93: 85-95.

142. Schneider FS, Starling MC, Duarte CG, de Avila RM, Kalapothakis E, et al. (2012) Preclinical testing of Peruvian anti-bothropic anti-venom against Bothrops andianus snake venom. Toxicon 60: 1018-1021.

143. Otero R, Nunez V, Gutierrez JM, Robles A, Estrada R, et al. (1997) Neutralizing capacity of a new monovalent anti-Bothrops atrox antivenom: Comparison with two commercial antivenoms. Brazilian Journal of Medical and Biological Research 30: 375-379.

144. Chavez-Olortegui C, Lopes CS, Cordeiro FD, Granier C, Diniz CR (1993) An Enzyme-Linked-Immunosorbent-Assay (ELISA) That Dsicriminates Between *Bothrops atrox* and *Lachesis muta muta* Venoms. Toxicon 31: 417-425.

145. Colombini M, Fernandes I, Cardoso DF, Moura-da-Silva AM (2001) Lachesis muta muta venom: immunological differences compared with Bothrops atrox venom and importance of specific antivenom therapy. Toxicon 39: 711-719.

146. Lomonte B, Gutierrez JM, Furtado MF, Otero R, Rosso JP, et al. (1990) Isolation of basic myotoxins from *Bothrops moojeni* and *Bothrops atrox* snake venoms. Toxicon 28: 1137-1146.

147. Escalante T, Ortiz N, Rucavado A, Sanchez EF, Richardson M, et al. (2011) Role of Collagens and Perlecan in Microvascular Stability: Exploring the Mechanism of Capillary Vessel Damage by Snake Venom Metalloproteinases. Plos One 6.

148. Souza CT, Moura MB, Magalhaes A, Heneine LGD, Olortegui CC, et al. (2001) Inhibition of mutalysin II, a metalloproteinase from bushmaster snake venom by human alpha 2-macroglobulin and rabbit immunoglobulin. Comparative Biochemistry and Physiology B-Biochemistry & Molecular Biology 130: 155-168.

149. Getzoff ED, Geysen HM, Rodda SJ, Alexander H, Tainer JA, et al. (1987) MECHANISMS OF ANTIBODY-BINDING TO A PROTEIN. Science 235: 1191-1196.

150. Harrison RA, Wuster W, Theakston RDG (2003) The conserved structure of snake venom toxins confers extensive immunological cross-reactivity to toxin-specific antibody. Toxicon 41: 441-449.

8. Anexos – Outros Trabalhos Publicados

OUTROS TRABALHOS PUBLICADOS DURANTE O DOUTORADO

Toxicon 60 (2012) 1018–1021

Contents lists available at SciVerse ScienceDirect

Toxicon

journal homepage: www.elsevier.com/locate/toxicon

Short communication

Preclinical testing of Peruvian anti-bothropic anti-venom against *Bothrops andianus* snake venom

Francisco S. Schneider [a], Maria C. Starling [a], Clara G. Duarte [a], Ricardo Machado de Avila [a], Evanguedes Kalapothakis [a], Walter Silva Suarez [b], Benigno Tintaya [b], Karin Flores Garrido [b], Silvia Seraylan Ormachea [b], Armando Yarleque [c], César Bonilla [b], Carlos Chávez-Olórtegui [a,*]

[a] *Departamento de Bioquímica e Imunologia, Instituto de Ciências Biológicas, Universidade Federal de Minas Gerais, Av. Antonio Carlos 6627, CP: 486, CEP: 31270-901, Belo Horizonte, Minas Gerais, Brazil*
[b] *Instituto Nacional de Salud, Lima, Peru*
[c] *Universidad Nacional Mayor de San Marcos, Lima, Peru*

ARTICLE INFO

Article history:
Received 3 April 2012
Received in revised form 20 June 2012
Accepted 28 June 2012
Available online 14 July 2012

Keywords:
Bothrops andianus
Andean snake
Venom
Anti-venom
Toxicity

ABSTRACT

Bothrops andianus is a venomous snake found in the area of Machu Picchu (Peru). Its venom is not included in the antigenic pool used for production of the Peruvian anti-bothropic anti-venom. *B. andianus* venom can elicit many biological effects such as hemorrhage, hemolysis, proteolytic activity and lethality. The Peruvian anti-bothropic anti-venom displays consistent cross-reactivity with *B. andianus* venom, by ELISA and Western Blotting and is also effective in neutralizing the venom's toxic activities.

© 2012 Elsevier Ltd. All rights reserved.

Snake bites represent an important health problem in Peru, especially to the east of the Andes in the High Forest (600–3500 m altitude) and Tropical Rain Forest (<600 m altitude) (Ministério de Salúd Peru, 2004). These regions are known for containing the major Peruvian snake species and most diversified ophidian population. The Instituto Nacional de Salud (INS), located in Lima, Peru has been producing commercial anti-venoms since 1978 (Ministério de Salúd Peru, 2004). The Peruvian anti-bothropic polyvalent anti-venom (PABA), used to treat envenomations involving Bothrops complex (*Bothrops* and *Bothrocophias* genera), is a whole IgG preparation produced from horse plasma previously immunized with an antigenic pool consisting of *Bothrops atrox* (50%), *Bothrops pictus*, *Bothrops barnetti*, *Bothrops brazili* and *Bothrocophias hyoprora* (12.5% each) venoms (Laing et al., 2004; Rojas et al., 2005; Theakston and Warrell, 1991). Besides neutralizing the most severe toxic effects induced by envenomation involving snakes from the antigenic pool, (Laing et al., 2004; Rojas et al., 2005) the preclinical assessment of anti-venom's efficacy against venoms from other medically important species would be useful in Latin America for improving anti-venom production (Gutierrez et al., 2009). This work describes the preclinical evaluation of the neutralizing capacity of PABA against lethality, hemorrhagic, proteolytic, and PLA_2 effects of *Bothrops andianus*' venom. *B. andianus* is a venomous snake found in the southern mountains of Peru and Bolivia and its venom is

Abbreviations: INS, Instituto Nacional de Salud; PABA, Peruvian anti-bothropic polyvalent anti-venom; BSA, Bovine serum albumin; PBS, Phosphate buffered saline; LD_{50}, Median lethal dose; MHD, Minimum hemorrhagic dose; MPD, Minimum PLA_2 Dose; DMC, Dimethylcasein; ED_{50}, Median effective dose.

* Corresponding author. Tel.: +55 31 3409 2625; fax: +55 31 3441 5963.
E-mail address: olortegi@icb.ufmg.br (C. Chávez-Olórtegui).

0041-0101/$ – see front matter © 2012 Elsevier Ltd. All rights reserved.
http://dx.doi.org/10.1016/j.toxicon.2012.06.018

not included in PABA production. In Peru, *B. andianus* is found in the areas (departments) of Cuzco and Puno, at elevations of 1800–3300 m (Ministério de Salúd Peru, 2004). Its geographical distribution overlaps Machu Picchu area, a UNESCO World Heritage Site (UNESCO, 2012), which is an important touristic attraction and receives more than 600,000 tourists per year, increasing the risks of accidents involving this snake. In Peru, the snakes of genus *Bothrops* are responsible for 80% of accidents and approximately 6.5% of these accidents are registered in the Cuzco and Puno Departments (Ministério de Salúd Peru, 2004).

For the experiments, male and female Swiss mice (18–22 g) were maintained in the Centro de Bioterismo of Instituto de Ciências Biológicas of Universidade Federal de Minas Gerais (UFMG), Brazil. All animals received water and food *ad libitum* under controlled environmental conditions. The experimental protocols were approved by the Ethics Committee in Animal Experimentation (CETEA/UFMG). PABA, crude venoms from *B. andianus*, and antigenic pool species were provided by INS. Venoms were kept at −20 °C and anti-venom at 4 °C temperature as indicated on their prescription. The protein content in crude venoms and anti-venoms were determined according to Bradford's method (1976) using BSA (Sigma Chemicals) as standard.

Lethality of *B. andianus* venom was assessed by the intra-peritoneal (i.p.) route. Groups of four mice were injected with increasing amounts of venom (34.6 μg–72 μg/mouse), dissolved in 0.5 ml of PBS–BSA 0.01% solution, pH 7.4. Twenty four hours later, deaths were counted and LD_{50} was calculated using Probit analysis (95% confidence) (Finney, 1971).

The hemorrhagic activity was assayed as described in Kondo et al. (1960) and modified by Gutierrez et al. (1985). Five different doses (3.72 μg; 5.2 μg; 7.29 μg; 10.2 μg; 14.28 μg) of crude venom were inoculated subcutaneously into dorsal shaved skin of mice in 0.1 ml NaCl 0.9%. Two hours later, mice were sacrificed by cervical dislocation and back skin was totally removed in order to measure the area of the hemorrhagic lesion. MHD was defined by the dose causing a lesion with a diameter of 10 mm.

PLA_2 activity was measured using an indirect hemolytic assay (Gutierrez et al., 1988). Increasing concentrations of *B. andianus* venom (from 0.004 μg up to 10 μg) were prepared in a final volume of 15 μl in PBS and added to 2 mm wells in agarose gel plates (0.8% in PBS, pH = 8.1, containing 1.2% sheep erythrocytes, 1.2% egg yolk and 100 mM $CaCl_{2)}$. Plates were incubated at 37 °C for 18 h and the diameters of the hemolytic haloes were measured. In controls, 15 μl of PABA was used. One unit (Minimum PLA_2 Doses-MPD) corresponds to a minor concentration of venom which produced a hemolytic halo of 10 mm diameter. Experiments were conducted in triplicate.

Proteolytic activity was measured with dimethylcasein (Sigma) as described in Lin et al. (1969) with the modifications described in Sanchez et al. (2000). Dilutions corresponding to 5, 10, 20 and 40 μg of venom were used and absorbance values were determined at 340 nm. One unit was defined as ΔA 340 nm/min. Activity was expressed relative to protein concentration (mg).

The anti-venom potency was determined by mixing $5LD_{50}$ of *B. andianus* venom with 12.5, 25, 50, 100 or 200 μl of PABA and incubating for 1 h at 37 °C followed by i.p. injection in 5 groups of 4 mice. Median effective dose (ED_{50}) was calculated from the number of deaths within 24 h of injection of the venom/anti-venom mixture using Probit analysis as described above. The ED_{50} was expressed as ml anti-venom/mg of venom needed to prevent death in 50% of the injected mice.

To determine the neutralization of hemorrhagic activity, PABA was incubated with either 3MHD or 5MHD for 30 min at 37 °C according to manufacturer's instructions (1 μL of serum to 2.5 μg of venom) and inoculated in different groups of 3 Swiss male mice (18–22 g) as described above. Positive and negative control groups, each consisting of 2 mice were treated with venom alone (5MHD) or anti-venom, respectively. Two hours later, mice were euthanized and the hemorrhage was measured (Kondo et al., 1960; Sanchez et al., 1992).

Inhibition of PLA_2 activity of *B. andianus* venom by PABA was conducted as described by Gutierrez et al. (1998). Two MPD of venom were incubated with 13, 6.5 and 3.25 μl of anti-venom for 30 min at 37 °C, and 15 μl of each mixture added in triplicate to wells in agarose gels. Neutralization of venom was checked by the absence of halos on the plate's surface.

Inhibition of dimethylcasein hydrolysis by PABA was estimated by incubation (30 min at 37 °C) of a fixed concentration of *B. andianus* venom with increasing amounts of anti-venom (μl). After incubation the mixtures were tested as described before. The neutralizing ability of anti-venom is expressed as the quantity of anti-venom able to neutralize 50% of proteolytic activity obtained by 1 mg of venom.

For the immunological assays (ELISA and Western Blotting assays), Falcon flexible micro titration plates were used (Becton Dickinson France S.A). The plates were coated overnight at 5 °C with 100 μl of a 5 μg/ml solution of the crude venoms (*B. andianus*, *B. atrox*, *B. barnetti*, *B. brazili*, *B. pictus* and *B. hyoprora*) in 0.02 M sodium bicarbonate buffer, pH 9.6. The assays were performed as described previously by Chávez-Olórtegui et al. (1991). Absorbance values were determined at 492 nm with a Biorad 680 Microplate Reader. All measurements were made in triplicate and the results expressed as the median of two assays. For Western Blotting the venoms were subjected to electrophoresis SDS-PAGE (15%) according to Laemmli (1970) in reducing conditions. The proteins were transferred onto nitrocellulose membranes (Towbin et al., 1979) and blocked with PBS-Tween 0.3% containing 2% casein. The membranes were incubated with PABA (1:10,000) for 1 h at room temperature. Immunoreactive proteins were detected using anti-horse Sigma IgG conjugated with peroxidase (1:3000). After washing three times for 5 min with PBS-Tween 0.05%, blots were developed using DAB/chloronaphthol according to the manufacturer's instructions.

The LD_{50} of *B. andianus* venom determined in this paper (57.96 μg, Table 1) is similar to the LD_{50} doses of *B. atrox*, 49.9 μg/mouse; *B. pictus*, 58.91 μg/mouse and *B. Barnetti*, 53.2 μg/mouse (Laing et al., 2004; Rojas et al., 2005). However, *B. brazili* venom was three times more potent in the LD_{50} assay than the other four Peruvian venoms (Laing et al., 2004). PABA was effective in neutralizing lethality

Table 1
Biological activities of *Bothrops andianus* venom and their neutralization by PABA.

Effect	Activity	Neutralization[e] (μl anti-venom/mg venom)
Lethal[a]	LD_{50} = 57.96 μg (36.02–93.26)	200 ± 0.0
Hemorrhagic[b]	MHD = 4.68 μg ± 0.20	187.8 ± 6.0
Proteolytic[c]	68.50 U/mg ± 1.75	500.0 ± 43.0
PLA_2 activity[d]	MPD = 5 μg ± 2.83	350 ± 40.0

Results are presented as mean ± S.D. (n = 4), except in lethality, where 95% confidence limits are included in parentheses.

[a] LD_{50} is expressed as the dose of venom (μg) responsible for causing 50% of death in mice (18–22 g) i.p. injected.

[b] MHD is defined as the amount of venom (μg) causing a 10 mm diameter spot hemorrhage on skin 2 h after injection.

[c] Proteolytic activity is expressed as Units/mg of venom. One unit of specific activity is defined as ΔA 340 nm/min.

[d] Minimum PLA_2 Dose (MPD) is defined as the amount of venom responsible for causing a 10 mm diameter of hemolysis.

[e] Neutralization corresponds to the quantity of anti-venom able to neutralize in 50% lethal, hemorrhagic, proteolytic and PLA_2 activities obtained by 1 mg of venom.

induced by *B. andianus* venom and showed high neutralizing potency (Table 1, ED_{50} of 200 μl anti-venom/mg venom). Furthermore, local hemorrhagic activity of *B. andianus* venom was evaluated in a mouse model. *B. andianus* venom directly induced extra vascular bleeding on the underside of the skin 2 h after injection. The estimated MHD is 4.68 μg ± 0.20 (Table 1). The results obtained concerning the capacity of PABA to neutralize the hemorrhagic effect of *B. andianus* are shown in Table 1. This anti-venom was efficient in neutralizing the hemorrhagic activity. MPD using an indirect hemolytic assay and inhibition of PLA_2 activity by PABA were measured. PLA_2 activity was dose dependent (data not shown) and the MPD determined in this study was 5.0 μg (S.D. ± 2.83 μg) (Table 1). PABA was also able to neutralize *B. andianus* PLA_2 activity with a potency of 350 ± 40.0 (μl anti-venom/mg venom). The proteolytic activity of *B. andianus* venom was expressed as DMC units (Δ340 nm) hydrolyzed per mg of venom per minute and was found to be 68.5 U/mg min ± 1.75 (Table 1). PABA was able to neutralize *B. andianus* proteolytic activity with a potency of 200 ± 11.4 (μl anti-venom/mg venom).

Immunological cross-reactivity of PABA against *Bothrops* venoms was assessed by both ELISA and western blotting. For ELISAs, reactivity at different serum dilutions can be seen in Fig. 1A. Importantly, cross-reactivity with *B. andianus* venom and reactivity with *B. atrox*, *B. barnetti* and *B. pictus* was observed. In this experiment, a weaker reactivity was observed against the venoms from *B. pictus* and *B. hyoprora*. Fig. 1B shows the results of the Western Blot assay. PABA was able to recognize all of the analyzed venoms. Regarding *B. andianus* venom, reactivity against bands at ~14, 25, 50 kDa and higher masses were observed. There was remarkable reactivity with the ~14 kDa protein compared to the others.

B. andianus venom has toxicological and electrophoretic profiles similar to those of other Peruvian *Bothrops* sp. venoms used in the anti-venom production. The

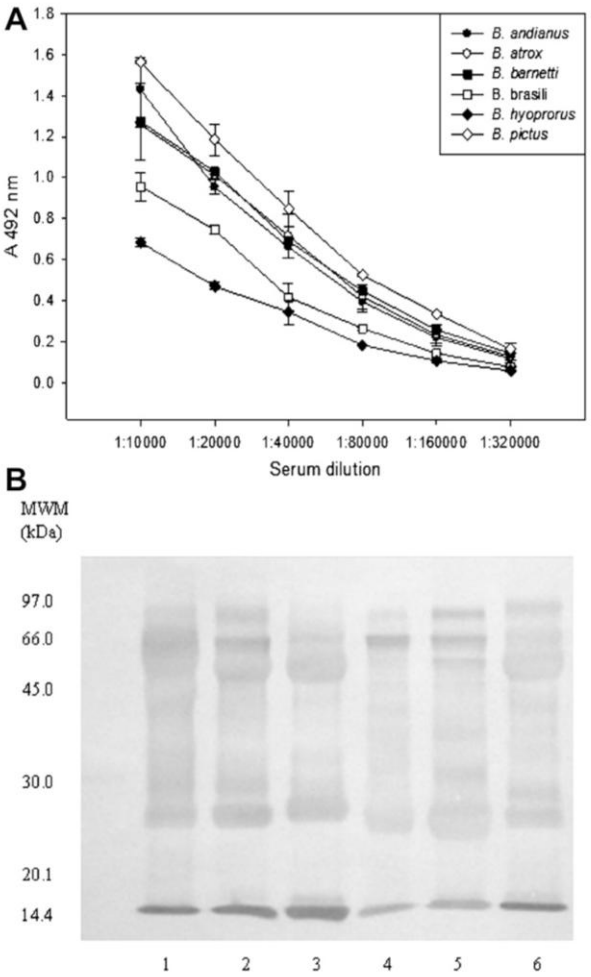

Fig. 1. (A) ELISA reactivity of Peruvian anti-bothropic serum against *Bothrops andianus*, *B. atrox*, *B. barnetti*, *B. brazili*, *B. hyoprora* and *B. pictus* venoms. Plates were coated with 0.5 μg of each venom per well and cross-reactivity tested against anti-bothropic anti-venom using serial dilution from 1:2000 to 1:256,000. Antibodies were detected with anti-horse Sigma IgG conjugated with peroxidase (1:3000), OPD and H_2O_2 in citrated buffer. (B) Western Blotting analysis of *Bothrops* venoms. 20 μg of each of the venoms were analyzed by SDS-PAGE under reducing conditions. Lanes correspond to: (1) *B. andianus*, (2) *B. atrox*, (3) *B. barnetti*, (4) *B. brazili*, (5) *Bothrocophias hyoprora*, (6) *B. pictus*. The venoms were analyzed against anti-bothropic anti-venom (1:10,000) and revealed with DAB/chloronaphthol.

toxicological profile is also common to Bothropic envenomations characterized by local tissue damage and by systemic manifestations (White, 2005). The symptoms observed in animals experimentally envenomed by *B. andianus* venom were very similar to other Peruvian *Bothrops* venoms (Laing et al., 2004; Rojas et al., 2005). Our observations find that PABA is effective in neutralizing the most important toxic activities induced by *B. andianus* venoms when using an experimental protocol based on pre-incubation of venom and anti-venom before testing in experimental systems (Gutierrez et al., 1990; Otero et al., 1995). Thus, despite the fact that *B. andianus* venom is not included in the antigenic pool used in Peru, PABA is

effective against this venom. Our preclinical observations are in agreement with the report of Rojas et al. (2005), which shows the efficacy of Peruvian anti-venom in neutralizing many snake venoms found in Peru.

Acknowledgments

This research was supported by Coordenação de Aperfeiçoamento de Pessoal de Nível Superior, Brazil – CAPES (TOXINOLOGIA No 23038000825/2011-63), Fundação de Amparo a Pesquisa do Estado de Minas Gerais, Brazil (FAPEMIG) and by funds of the INCTTOX PROGRAM of Conselho Nacional de Desenvolvimento Científico e Tecnológico, Brazil (CNPq). The authors gratefully acknowledge the financial support and assistance of the Instituto Nacional de Salud (Lima, Peru) without which it would not have been possible to carry out this study. We would like to express our gratitude to Dr. Michael Richardson and Jessica McCormack for revising this manuscript.

Conflict of interest statement

The authors declare that there are no conflicts of interest.

References

Bradford, M.M., 1976. A rapid and sensitive method for the quantitation of microgram quantities of protein utilizing the principle of protein-dye binding. Anal. Biochem. 72, 248–254.

Chavez-Olortegui, C., Amara, D.A., Rochat, H., Diniz, C., Granier, C., 1991. In vivo protection against scorpion toxins by liposomal immunization. Vaccine 9, 907–910.

Finney, D.J., 1971. Probit Analysis, third ed. Cambridge University Press, Cambridge.

Gutierrez, J.M., Gene, J.A., Rojas, G., Cerdas, L., 1985. Neutralization of proteolytic and hemorrhagic activities of Costa Rican snake venoms by a polyvalent antivenom. Toxicon 23, 887–893.

Gutierrez, J.M., Avila, C., Rojas, E., Cerdas, L., 1988. An alternative in vitro method for testing the potency of the polyvalent antivenom produced in Costa Rica. Toxicon 26, 411–413.

Gutierrez, J.M., Rojas, G., Lomonte, B., Gene, J.A., Chaves, F., Alvarado, J., Rojas, E., 1990. Standardization of assays for testing the neutralizing ability of antivenoms. Toxicon 28, 1127–1129. author reply 1129–1132.

Gutierrez, J.M., Leon, G., Rojas, G., Lomonte, B., Rucavado, A., Chaves, F., 1998. Neutralization of local tissue damage induced by Bothrops asper (terciopelo) snake venom. Toxicon 36, 1529–1538.

Gutierrez, J.M., Lomonte, B., Leon, G., Alape-Giron, A., Flores-Diaz, M., Sanz, L., Angulo, Y., Calvete, J.J., 2009. Snake venomics and antivenomics: proteomic tools in the design and control of antivenoms for the treatment of snakebite envenoming. J. Proteomics 72, 165–182.

Kondo, H., Kondo, S., Ikezawa, H., Murata, R., 1960. Studies on the quantitative method for determination of hemorrhagic activity of Habu snake venom. Jpn. J. Med. Sci. Biol. 13, 43–52.

Laemmli, U.K., 1970. Cleavage of structural proteins during the assembly of the head of bacteriophage T4. Nature 227, 680–685.

Laing, G.D., Yarleque, A., Marcelo, A., Rodriguez, E., Warrell, D.A., Theakston, R.D., 2004. Preclinical testing of three South American antivenoms against the venoms of five medically-important Peruvian snake venoms. Toxicon 44, 103–106.

Lin, Y., Means, G.E., Feeney, R.E., 1969. The action of proteolytic enzymes on N, N-dimethyl proteins. Basis for a microassay for proteolytic enzymes. J. Biol. Chem. 244, 789–793.

Ministério de Salúd, Peru, 2004. Norma Técnica sobre Prevencion y Tratamiento de Acccidentes por Animales Ponzoñosos.

Otero, R., Nunez, V., Osorio, R.G., Gutierrez, J.M., Giraldo, C.A., Posada, L.E., 1995. Ability of six Latin American antivenoms to neutralize the venom of mapana equis (Bothrops atrox) from Antioquia and Choco (Colombia). Toxicon 33, 809–815.

Rojas, E., Quesada, L., Arce, V., Lomonte, B., Rojas, G., Gutierrez, J.M., 2005. Neutralization of four Peruvian Bothrops sp. snake venoms by polyvalent antivenoms produced in Peru and Costa Rica: preclinical assessment. Acta Trop. 93, 85–95.

Sanchez, E.F., Freitas, T.V., Ferreira-Alves, D.L., Velarde, D.T., Diniz, M.R., Cordeiro, M.N., Agostini-Cotta, G., Diniz, C.R., 1992. Biological activities of venoms from South American snakes. Toxicon 30, 95–103.

Sanchez, E.F., Santos, C.I., Magalhaes, A., Diniz, C.R., Figueiredo, S., Gilroy, J. , Richardson, M., 2000. Isolation of a proteinase with plasminogen-activating activity from *Lachesis muta muta* (bushmaster) snake venom. Arch. Biochem. Biophys. 378, 131–141.

Theakston, R.D., Warrell, D.A., 1991. Antivenoms: a list of hyperimmune sera currently available for the treatment of envenoming by bites and stings. Toxicon 29, 1419–1470.

Towbin, H., Staehelin, T., Gordon, J., 1979. Electrophoretic transfer of proteins from polyacrylamide gels to nitrocellulose sheets: procedure and some applications. Proc. Natl. Acad. Sci. U S A 76, 4350–4354.

Unesco, 2012. Historic Sanctuary of Machu Picchu. http://whc.unesco.org/en/list/274/. 16 March 2012.

White, J., 2005. Snake venoms and coagulopathy. Toxicon 45, 951–967.

Toxins **2013**, *5*, 1780-1798; doi:10.3390/toxins5101780

OPEN ACCESS

toxins

ISSN 2072-6651
www.mdpi.com/journal/toxins

Article

Molecular Characterization of Lys49 and Asp49 Phospholipases A_2 from Snake Venom and Their Antiviral Activities against *Dengue virus*

Alzira B. Cecilio [1], Sergio Caldas [1], Raiana A. De Oliveira [1], Arthur S. B. Santos [1], Michael Richardson [2], Gustavo B. Naumann [2], Francisco S. Schneider [2],Valeria G. Alvarenga [2], Maria I. Estevão-Costa [2,3], Andre L. Fuly [4], Johannes A. Eble [3] and Eladio F. Sanchez [2,*]

[1] Laboratory of Biotechnology and Health, Research and Development Center, Ezequiel Dias Foundation, Belo Horizonte 30510-010, MG, Brazil; E-Mails: alzira.cecilio@funed.mg.gov.br (A.B.C.); sergio.caldas@funed.mg.gov.br (S.C.); oliveira.raiana@hotmail.com (R.A.D.O.); arthursander8@yahoo.com.br (A.S.B.S.)

[2] Laboratory of Biochemistry of Proteins from Animal Venoms, Research and Development Center, Ezequiel Dias Foundation, Belo Horizonte 30510-010, MG, Brazil; E-Mails: mmikeana@yahoo.com (M.R.); gnaumann@funed.mg.gov.br (G.B.N.); schneider@yahoo.com (F.S.S.); valeria.alvarenga@funed.mg.gov.br (V.G.A.); maria.inacia@funed.mg.gov.br (M.I.E.-C.)

[3] Center for Molecular Medicine, Dept. Vascular Matrix Biology, Frankfurt University Hospital, Frankfurt am Main 60590, Germany; E-Mail: eble@med.uni-frankfurt.de

[4] Department of Cellular and Molecular Biology, Federal University Fluminense, RJ 24220-008, Brazil; E-Mail: andfuly@uff.br

* Author to whom correspondence should be addressed; E-Mail: eladio.flores@funed.mg.gov.br; Tel.: +55-31-3314-4335; Fax: +55-31-3314-4768.

Received: 2 August 2013; in revised form: 11 September 2013 / Accepted: 26 September 2013 / Published: 15 October 2013

Abstract: We report the detailed molecular characterization of two PLA_2s, Lys49 and Asp49 isolated from *Bothrops leucurus* venom, and examined their effects against *Dengue virus* (DENV). The *Bl*-PLA_2s, named *Bl*K-PLA_2 and *Bl*D-PLA_2, are composed of 121 and 122 amino acids determined by automated sequencing of the native proteins and peptides produced by digestion with trypsin. They contain fourteen cysteines with p*Is* of 9.05 and 8.18 for *Bl*K- and *Bl*D-PLA_2s, and show a high degree of sequence similarity to homologous snake venom PLA_2s, but may display different biological effects. Molecular masses of 13,689.220 (Lys49) and 13,978.386 (Asp49) were determined by mass

spectrometry. DENV causes a prevalent arboviral disease in humans, and no clinically approved antiviral therapy is currently available to treat DENV infections. The maximum non-toxic concentration of the proteins to LLC-MK2 cells determined by MTT assay was 40 µg/mL for *Bl*-PLA$_2$s (pool) and 20 µg/mL for each isoform. Antiviral effects of *Bl*-PLA$_2$s were assessed by quantitative Real-Time PCR. *Bl*-PLA$_2$s were able to reduce DENV-1, DENV-2, and DENV-3 serotypes in LLC-MK2 cells infection. Our data provide further insight into the structural properties and their antiviral activity against DENV, opening up possibilities for biotechnological applications of these *Bl*-PLA$_2$s as tools of research.

Keywords: svPLA$_2$s; *Bothrops leucurus*; *Dengue virus*; antiviral effect; Real-Time PCR

1. Introduction

Snake venoms have been regarded for long as excellent sources for drug discovery given their structural diversity and wide variety of biological activities [1–4]. Due to the broad range of pharmacological functions, these active components have been the subject of hundreds of scientific papers in different research fields. Snake venom PLA$_2$s (svPLA$_2$s) are secreted enzymes (EC 3.1.1.4) that, despite their conserved structure, these molecules have been associated with a variety of pharmacological effects [5]. They form a family of enzymes, which require Ca^{2+} and catalyze the hydrolysis of glycerophospholipids at the sn-2 position of the glycerol backbone to produce free fatty acids and lysophospholipids [6]. In addition, svPLA$_2$s are small (approximately. 14 kDa), extremely stable due to the presence of seven disulphide bridges in the globular structure and have an active site histidine. These enzymes are classified into different groups based on their structural homology, disulphide pattern, catalytic specificity, and site of expression [7]. Group I of svPLA$_2$s includes, the proteins mainly found in the venom of elapid and colubrid snakes (Group IA), and pancreatic svPLA$_2$s (Group IB), while group II is found abundantly in the venom of viperidae snakes [5,7]. The latter group is similar to the mammalian nonpancreatic, inflammatory enzymes and are the major toxic proteins of the venom. Thus, they have a relevant role in immobilization and capture of the prey by interfering with physiological processes of victims. On the other hand, group II differs from group I in having an extended *C*-terminal tail [6,8].

In vitro, the svPLA$_2$s can also modulate cell adhesion and cell proliferation and have anti-angiogenic properties [9–11]. Furthermore, a number of studies describe the anti-microbial properties of several svPLA$_2$s against Gram negative [12] and Gram positive bacteria [13]. The readers are also referred to the recent review [5]. In addition, some svPLA$_2$s or their products have been shown to interfere with viral infection, mainly by inhibiting the replication of HIV-1 and HIV-2 [14,15].

Over the last forty years, dengue disease has become recognized as the world's most important mosquito-borne viral disease. Likely due to the climate change, the mosquito and the dengue virus expands into countries, which had been considered disease-free. Moreover, the virus re-emerges in countries where the disease used to be once under medical control [16]. It is the most rapidly spreading arboviral disease that is caused by four related and antigenically distinct viruses, which are named

Dengue virus (DENV) 1–4, and belong to the *Flaviviridae* family. Dengue infection ranks in fifth position in the list of neglected tropical diseases in the Americas in terms of disability-adjusted life years (DAYLs) [17]. An estimated 2.5 billion people live in approximately 100 endemic countries and are at risk of acquiring dengue viral infection [18]. DENV is generally transmitted in a cycle involving humans and mosquito vectors, mainly *Aedes aegypti*. DENV causes a wide range of diseases in humans, from the acute febrile illness of dengue fever (DF) to life-threatening dengue haemorrhagic fever/dengue shock syndrome (DHF/DSS) [19] that can occur in hyperendemic areas with multiple circulating serotypes. Several factors such as uncontrolled urbanization and inadequate basic urban infrastructure (e.g., unreliable water supply leading householders to store water in containers close to homes) have combined to produce epidemiological conditions in developing countries in tropics and subtropics that favor viral transmission by the mosquito vector. Consequently, the number of cases of severe dengue disease continues to grow in endemic areas of Central and South America, Southeast Asia, and other subtropical regions. Children have the highest risk of developing severe disease manifestations, further underscoring the need for effective care. The total economic burden of dengue disease in the Americas was estimated to be approx. US$ 2.1 billion per year on average [20]. Since there is no specific drug therapy for DENV, the development of an effective vaccine remains a global public health priority [21].

The pit viper *B. leucurus* (white-tailed-jararaca) is a common venomous snake which inhabits restricted areas of the northeast of Brazil including the states of Ceará and Bahia to Espírito Santo in the southeast [22], where snakebite envenomations represent a relevant public health problem, *B. leucurus* is a leading cause of human accidents [23]. In a previous study, we reported the isolation and partial characterization of two svPLA$_2$s from the venom of *B. leucurus*. One enzyme contains lysine at position 49 (*Bl*K-PLA$_2$), and the other, an aspartic acid in this position (*Bl*D-PLA$_2$). We showed that *Bl*K-PLA$_2$ exhibited negligible levels of phospholipase activity as compared to that of *Bl*D-PLA$_2$. In addition, *Bl*D-PLA$_2$ did not affect platelet aggregation induced by ADP, collagen, and arachidonic acid, but strongly inhibited coagulation and was able to stimulate Erlich tumor growth, but not angiogenesis [24]. The absence of direct correlation between catalytic activity and biological effects has led to the hypothesis that specific effects of svPLA$_2$s are due to the presence of pharmacological sites/domains on the enzyme surface [5]. The magnitude and severity of cases of the dengue disease, which acerbates with every new epidemic, spur the search for novel bioactive compounds with antiviral activities. Several studies dedicated to molecular mechanisms and structure-function relationships reported the toxicities of svPLA$_2$s and their neutralization. However, little is known about the antiviral properties of these enzymes. A few reports indicate that some components of snake venoms, including svPLA$_2$s, and the enzymes from bee venom have potential anti-viral activity [25]. At present, there are still no antiviral drugs being tested against dengue infection in any clinical trial. Many endeavors to develop DENV specific antiviral derivatives have been undertaken, and include the development and design of a low-cost rapid diagnostic tool, as well as the identification of safe compounds, which target multiple serotypes and are effective even after the onset of severe clinical disease [26]. In this regard, an alternative approach is to evaluate bioactive compounds such as the svPLA$_2$s that could ultimately allow the advancement of lead structures for the development of a new antiviral agent against DENV. We therefore examined whether *Bl*-PLA$_2$s have antiviral properties against DENV. The antiviral effects of *Bl*-PLA$_2$s detected against DENV-1,

DENV-2, and DENV-3 serotypes on cells in culture could be due to enzymatic activity or perhaps due to the presence of pharmacological domains on the enzyme surface, or may be due to both, that is specific protein-protein interaction and enzymatic activity. This is a topic that is under investigation by us. A model of the molecular mechanism of action of the neurotoxic svPLA$_2$ ammodytoxin (AtxA) from *Vipera ammodytes ammodytes*, which includes specific protein-protein interaction, and enzymatic activity has been recently reported [27].

In this study, our primary objective was to determine the structural properties of *Bl*K- and *Bl*D-PLA$_2$s and more closely investigate the potential of these molecules as antiviral agents against dengue virus 1–3 serotypes. Due to their binding properties, small size and high stability, the *Bl*-PLA$_2$s may represent a convenient tool for proving interactions between cell surfaces.

2. Results and Discussion

2.1. Mass Spectrometry Analysis and Sequence Determination

Snake venoms contain PLA$_2$s isoforms exhibiting different physiological activities including antiviral properties [15,25,28]; thus, they could serve beneficial applications in medicine and as tools for biomedical research. Two *Bl*-PLA$_2$s were purified to homogeneity according to the method used in previous study [24]. The MALDI-TOF mass spectrum analysis of these proteins showed - molecular masses of 13,978.386 for *Bl*D-PLA$_2$ and 13,689.220 for *Bl*K-PLA$_2$, respectively (Figure 1), which fall in the typical range of svPLA$_2$s. A great number of svPLA$_2$s share similar structural features. The complete amino acid sequences of both enzymes have been determined (Figure 2), and deposited in the UniProt (accession numbers: P86974 for D49-PLA$_2$ and P86975 for K49-PLA$_2$). Sequence alignment of the isoforms was made by ClustalW program [29]. They contain 121 (*Bl*K-PLA$_2$) and 122 (*Bl*D-PLA$_2$) amino acid residues determined by automated Edman degradation of the reduced and pyridylethylated proteins and of peptides produced by digestion with trypsin (data not shown). Both polypeptides display a large amino acid sequence similarity between each other and to the members of Viperidae svPLA$_2$s (Figure 2), including the positions of the 14 cysteine residues that may form seven disulfide bridges to stabilize the tertiary structure as proposed for homologous svPLA$_2$s [5,30]. Irrespective of any enzymatic activity the overall structures of both isoforms are very similar except for the extended *C*-terminal region. The presence of two short clusters of hydrophobic/basic amino acids residues 61–71 and 105–117 (Figure 2, this work) is observed in *Bl*K49 isoform that may be the membrane-destabilizing elements as reported for Lys49 myotoxin-II from *B. asper* [31] and others. The significantly more positive surface observed for *Bl*K49- compared to the *Bl*D49-PLA$_2$ isoform is in line with the higher penetrability of most basic svPLA$_2$s compared to acidic and neutral enzymes [32].

Figure 1. Mass spectrometry analysis of native *Bl*D-PLA$_2$ and *Bl*K-PLA$_2$ from *B. leucurus* venom (top and bottom panels, respectively) performed in Matrix assisted desorption/ionization-time-of flight (MALDI-TOF-MS).

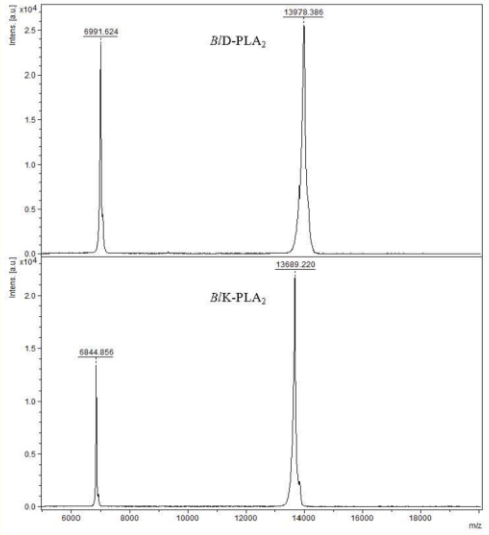

2.2. Biochemical and Immunochemical Properties

Separated proteins of the crude venom by 2D-electrophoresis (2-DE) showed two protein spots at approx. 14 kDa (at alkaline pH), with *pI*s of 8.18 and 9.05, corresponding to *Bl*D- and *Bl*K-PLA$_2$s, respectively (Figure 3A). It is known that *Bl*K49-PLA$_2$s present a high isoelectric point (pI > 9) and a good stability at room temperature. Two main spots that may correspond to both isoforms were immunologically recognized by the antiserum raised against *BlK* isoform (Figure 3B). The SDS-PAGE (15% gel) analysis also showed that crude venom contain a band of 14 kDa (Figure 4A, lane 2) which correspond to the apparent molecular masses (14 kDa) of purified *Bl*K- and *Bl*D-PLA$_2$s under reduced (Figure 4A, lanes 3–4) and non-reduced conditions (not shown). Furthermore, western blotting showed these bands at approx. 14 kDa of the transferred samples *Bl*K- and *Bl*D-PLA$_2$s, which were immunologically recognized by the purified anti-*BlK*-PLA$_2$ IgG (Figure 4B, lanes 3 and 4). In addition, a band at the same Mr (14 kDa) was immunologically detected in the crude venom (Figure 4B, lane 2). A number of svPLA$_2$s interact with other proteins to form complexes or aggregates and others exist as monomers [6]. These additional molecules help svPLA$_2$s to express their biological properties to the greatest potency. For instance, vipoxin, a heterodimeric post-synaptic neurotoxin found in *V. ammodytes meridionalis,* consists of two PLA$_2$ subunits: a basic, highly toxic PLA$_2$ and an acidic, nontoxic and enzymatically inactive PLA$_2$ [33]. Furthermore, when the purified rabbit anti *BlK*-PLA$_2$ IgG was tested against the *Bl*-PLA$_2$s (pool) and with other snake venoms by ELISA, a strong cross-recognition was observed with *Bl*-PLA$_2$s, *B. leucurus* as well as with *B. atrox*. On the other hand, *Crotalus durissus terrificus*, *Bothrops barnetti*, and *B. jararaca* gave only low cross-reactivity signals. Finally, very low cross-reaction was detected with *L.m. muta*, and there was no reaction with *Micrurus lemniscatus* (Elapidae) (Figure 4C).

Figure 2. Multiple amino acid sequence alignment of *Bl*PLA$_2$s with svPLA$_2$s homologous. The one letter code for amino acid nomenclature is used. Proteins compared and their UniProt or GeneBank (GB) accession numbers: K49 (piratoxin II, P82287) from *Bothrops pirajai:* K49 (bthtx I, Q90249) from *B. jararacussu*: K49 (*Bl*K-PLA$_2$, P86975) from *B. leucurus:* K49 (myotoxin II, P24605) from *B. asper:* K49 (myotoxin II, Q91834) from *B. moojeni:* K49 (O57385) from *Deinagkistrodon* (formerly *Agkistrodon) acutus:* R49 (Q28681) from *Protobothrops elegans:* S49 (P48650) from *Echis carinatus*; D49 (*Bl*D-PLA$_2$, P86974) from *B. leucurus*: D49 (vipoxin complex, P04084) from *Vipera ammodytes meridionalis*: D49 (C9E7C4) from *Crotalus durissus cascavella:* D49 (Q7ZTA6) from *C.v.viridis*: D49 (Q2H228) from *B. erythromelas:* D49 (GB/KC544002) from *B. neuwiedi:* D49 (O42191) from *Gloydius* (formerly *Agkistrodon) halys pallas*. (*****) is used for identical residues (:) for conserved ones and (.) for semi-conserved substitutions among all sequences in the alignment. Gaps were introduced to maximize the sequence homology, as indicated in part (**A**) and (**B**), respectively.

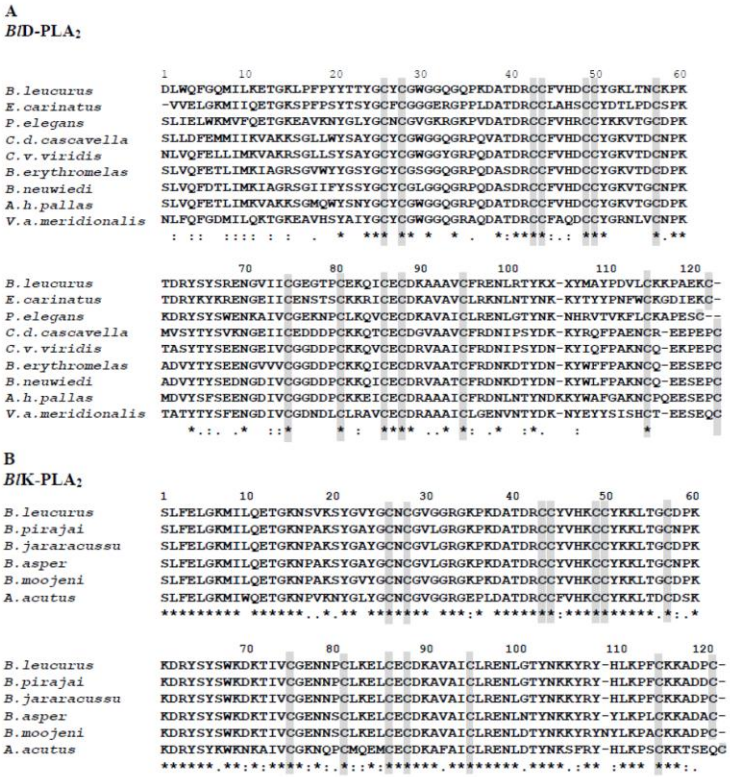

Figure 3. 2-DE SDS-PAGE pattern of venom proteins from *B. leucurus*. (**A**) 60 µg of total proteins were isoelectrically focused (pI range 3–10) followed by separation by SDS-PAGE (15% gel) and Coomassie blue staining. Protein spots of approx. 14 kDa correspond to the position of *Bl*-PLA$_2$ isoforms are indicated by arrows, (**B**) Immunoblotting of venom proteins separated by 2D-SDS-PAGE with anti-*BlK*-PLA$_2$ IgG. Arrows indicates the reactivity of the antibody with the approx. 14 kDa PLA$_2$s.

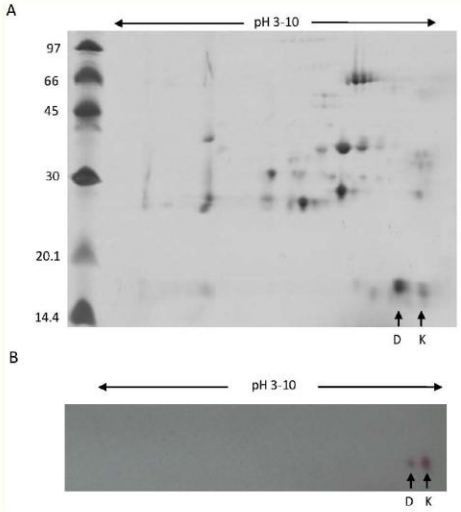

Figure 4. Reactivity of purified rabbit anti *Bl*K-PLA$_2$ IgG against *Bl*D- and *Bl*K-PLA$_2$ isoforms. (**A**) reduced SDS-PAGE (15% gel) of: 1, molecular mass markers; 2, crude venom (20 µg); 3, *Bl*K-PLA$_2$ (5 µg); 4, *Bl*D-PLA$_2$ (5 µg); (**B**) immunoblotting of anti *Bl*K-PLA$_2$ IgG against crude venom (1), *Bl*K-PLA$_2$ (2) and *Bl*D-PLA$_2$ (3). (**C**) Reactivity of anti *Bl*K-PLA$_2$ IgG against several snake venoms examined by ELISA. 96-well microtitration plates were precoated with 0.5 µg/mL of *Bl*-PLA$_2$s (pool), *Bothrops* species, *L. muta*, *C. d. terrificus* and *Micrurus lemniscatus*. Anti *Bl*K-PLA$_2$ IgG was added at different dilutions. Binding was visualized by incubation with peroxidase-coupled anti-rabbit IgG (diluted 1:12,000) and subsequent peroxidase-catalyzed conversion of *O*-phenylenediamine (OPD). The absorbance of pre-immune serum (control) was subtracted. Data shown represent the average of two independent experiments, with error bars indicating the maximum and minimum deviation from the average.

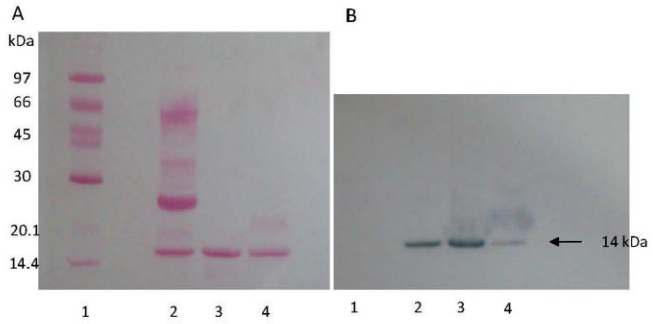

Figure 4. *Cont.*

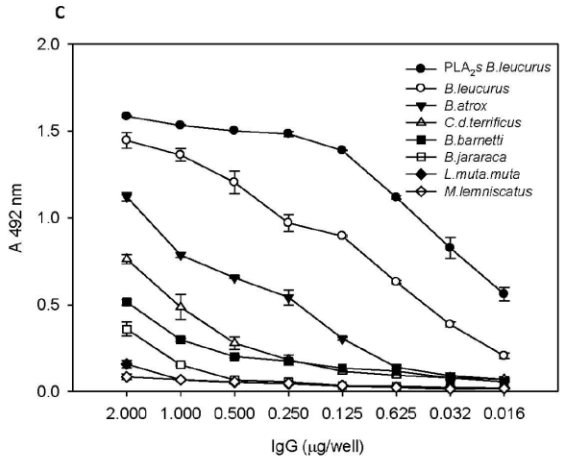

2.3. Phylogenetic Relationships among svPLA$_2$s

A phylogenetic tree (Figure 5) was obtained by the comparison of the sequences of representative mature proteins of group II (Viperidae) listed in Figure 2, and it also includes svPLA$_2$s of group I (Elapidae and Hydrophiidae) by the program phylogeny [34]. The most prominent characteristic of this tree is that the members of the different subfamilies are almost perfectly clustered and clearly separated from the other subgroup. This tree splits into two main branches, Viperidae PLA$_2$s (pit vipers and true vipers) and Elapidae together with Hydrophiidae (*Lapemis hardwickii* and *Aipysurus eydouxii*) PLA$_2$s, which are evidently divided. This suggests a possible evolutionary relationship between the different svPLA$_2$s. Thus, the *Bl*K49 PLA$_2$ (*B. leucurus*) was clustered in the same branch with homologous enzymes from *Bothrops* and *Deinagkistrodon* (formerly *Agkistrodon*) *acutus* snakes, while the *Bl*D49 isoform was clustered into the same branch with *Echis carinatus* (S49), *Protobothrops elegans* (R49), and with other Viperidae svPLA$_2$s. In some members of the group II svPLA$_2$s the D49 residue is replaced by serine, asparagine, or arginine and are identified as K49 [35,36]. This phylogenetic relationship appears to reflect the correlation of molecular properties and suggests that the two *Bl*-PLA$_2$s represent two fundamental PLA$_2$s species with different physiological activities. Phylogenetic differences of svPLA$_2$s is actually the result of two independent recruitment events, elapid (group I svPLA$_2$s) and viper venoms (group II svPLA$_2$s) [37]. Thus, the two independently recruited types of svPLA$_2$s have distinct activities, which the tissue-endogenous isoforms lacks (e.g., myotoxicity, antiplatelet effect, and neurotoxicity). In accordance with this, the toxic forms contain a positively charged hotspot on the surface that is lacking in the ancestral form from the pancreas [38].

Figure 5. Phylogenetic tree for the multiple-sequence alignment of svPLA$_2$s listed in Figure 2 (Viperidae), and some proteins from Elapidae and Hydrophiidae snakes. The length of the horizontal scale represents 30% divergence. Phylogenetic distances branch points are indicated.

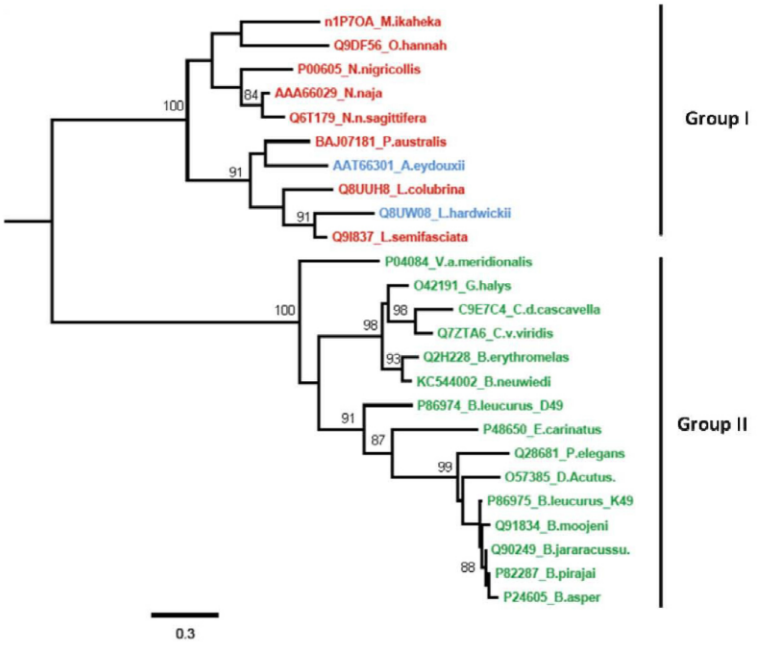

2.4. Antiviral Assays

In this study we evaluated the antiviral activity of two isolated svPLA$_2$s. To this end a one-step qRT-PCR was employed using a TaqMan technology with a probe for DENV detection and a probe for exogenous control (RNAseP) detection in a single multiplex assay. The use of qRT-PCR was performed in this study to avoid the risk of cross contamination and to increase the speed of the assay [39]. The addition of an amplification control (RNAseP) was particularly useful to monitor possible false negative results (due to RNA degradation) and to correct variations in the amounts of initial samples (due to different RNA recovery and samples loading), thus enabling PCR data normalization [40,41]. The PCR was calibrated *in vitro* RNAs transcripts of viral and exogenous control (RnaseP). The DENV and RnaseP standard curves were generated from five serial dilutions of transcribed RNAs from 10^7 copies/µL. The detection limit of the assay was 10^2 copies/reaction. Figure 6A shows amplification curves of DENV and RnaseP in five log dilutions. Figure 6B,C show the standard curves generated from the linear region of DENV and RnaseP amplification curves. The efficiency (E) and Pearson Correlation coefficient (R) value for both curves were: E_{DENV} = 91.34%, R_{DENV} = 0.999, E_{RnaseP} = 95%, R_{RnaseP} = 0.999. These high efficiencies (>90%) and r value (0.999) were important features of the quantitative Real-Time PCR strategy developed for our *in vitro* assays. High and similar PCR efficiencies of the target of interest and the normalization of reaction are important prerequisites for an accurate quantification, but not always considered in different studies using real-time PCR available in the scientific literature.

Figure 6. DENV and RnaseP standard curves generated from transcribed RNAs. (**A**) Curves were generated from seven serial dilutions of transcribed DENV and RnaseP RNAs from 10^7 copy number/µL. The black lines refer to DENV RNA and the gray lines to RnaseP RNA (exogenous control). (**B**,**C**) Standard curves were generated from the linear region of each amplification curve. Efficiency of amplification for each primer set was determined using the equation: Efficiency (E) = $10^{(-1/\text{slope})}$, being E_{DENV} = 91.34%, R_{DENV} = 0.999, E_{RnaseP} = 95%, R_{RnaseP} = 0.999.

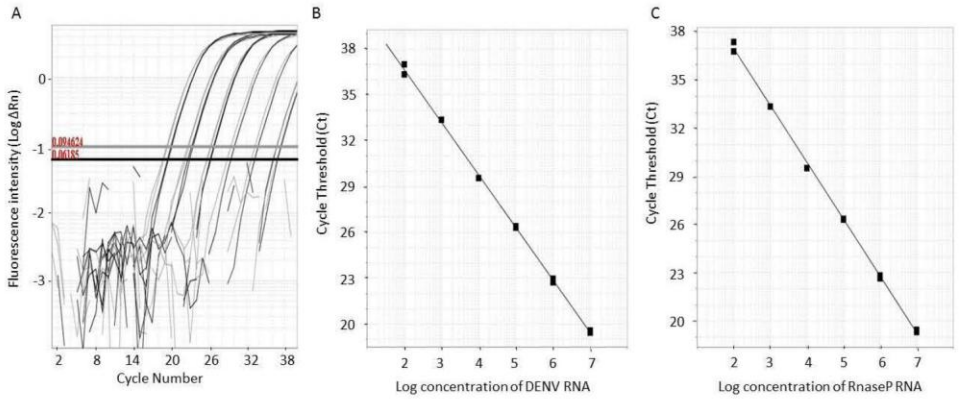

To carry out the *in vitro* antiviral assays, we first determined the concentration at which the *Bl*-PLA$_2$s and their isoforms could be used (to evaluate their antiviral effects) without causing damage to the cell culture. The maximum non-toxic concentration (MNTC) determined by cell viability was 40 µg/mL for *Bl*-PLA$_2$s (pool, partially purified fraction containing both PLA$_2$s isoforms) and 20 µg/mL for each enzyme *Bl*K- and *Bl*D-PLA$_2$ (Figure 7A). The lack of cytotoxicity of the pool fraction at 40 µg/mL may indicate the presence of any compounds that interfere with the activity of *Bl*-PLA$_2$s.Then, antiviral assays were conducted to evaluate the ability of *Bl*-PLA$_2$s (pool) and the enzymes, without catalytic (*Bl*K-) and with catalytic activity (*Bl*D-PLA$_2$) to inhibit the multiplication of DENV in LLC-MK2 cells compared to non-treated cells. The viral load was determined by qRT-PCR quantification of DENV RNA copies. Cells treated with *Bl*-PLA$_2$s (pool), as well as cells treated with each isoform (*Bl*K- and *Bl*D-PLA$_2$), showed a significant reduction ($p < 0.05$) in the number of DENV-1, DENV-2, and DENV-3 RNA copies when compared to non-treated infected cells. Similar results were obtained with all DENV used and no significant differences were observed ($p < 0.05$) in the antiviral assays of *Bl*-PLA$_2$s (pool), *Bl*K- and *Bl*D-PLA$_2$ (Figure 7B).

Brazil is the country with highest number of cases and highest cost, but the economic impact of dengue is substantial in many American countries, with the cost per capita greater than US$ 2.1 billion per year in four of the six American subregions (Andean region, Brazil, the Caribbean, and Central America and Mexico) [18,20]. Interestingly, treatment of the cell cultures after viral adsorption did not result in significant inhibitory effect on the viral replication (data not shown). This observation points to an effect of phospholipases in the cell membrane level, since svPLA$_2$-application after viral penetration into the cell did not reduce load in infected cells as compared to untreated cells. An antiviral effect showed by svPLA$_2$ from *C. d. terrificus* against DENV-2 and yellow fever virus (YFV) was recently reported [25].

Figure 7. (**A**) Cellular viability after the incubation of LLC-MK2 cells with different concentrations of *Bl*-PLA$_2$s (Pool) and their isoforms *Bl*K- and *Bl*D-PLA$_2$ for 48 h. The higher concentrations without significant toxicity ($p < 0.05$) were considered as the maximum non-toxic concentration (MNTC). Data represent the mean of three independent experiments performed in triplicate. Means with different symbols denote significant differences ($p < 0.05$). (**B**) Antiviral activity assessed by quantitative Real-Time PCR. Data represent the mean of two independent experiments performed in triplicate.

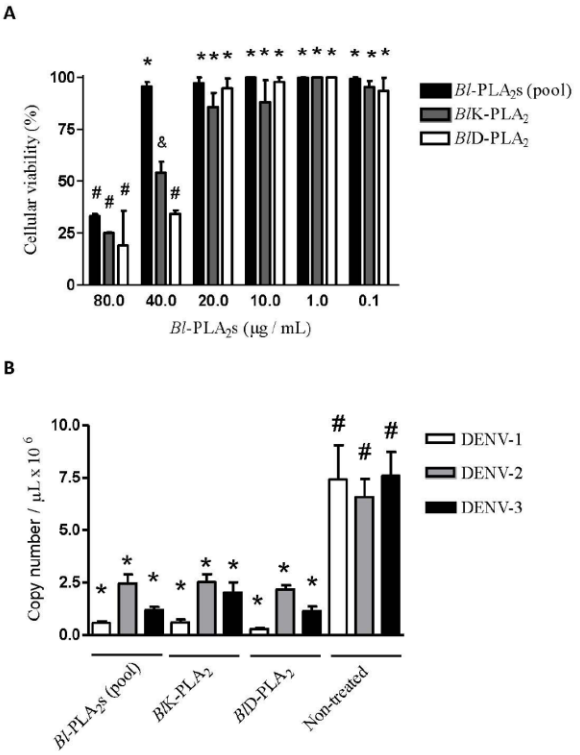

3. Materials and Methods

3.1. Purification of BlK-PLA$_2$ and BlD-PLA$_2$

Two *B.leucurus* snakes were captured in the north of the Minas Gerais State and kept at the serpentarium of the Ezequiel Dias Foundation (FUNED, Belo Horizonte, Brazil). Venoms from these captive specimens were collected manually by milking. The pooled samples of the freeze-dried venoms were stored at 4 °C. *Bl*-PLA$_2$s enzymes were purified as described in a previous work [24]. The homogeneity of purified svPLA$_2$s was determined by using MALDI-TOF mass spectrometry, SDS-PAGE under reducing and non-reducing conditions and by *N*-terminal sequence determination. All protein concentrations throughout this study were determined using a BCA assay kit (Pierce Chemical Company, Rockford, IL, USA). Anti-*BlK*-PLA$_2$ antiserum was raised in a rabbit (New Zealand 2.3 kg) using as antigen the isoform K49 as described [42]. The IgG fraction of immune rabbit serum was purified by affinity chromatography on protein A-Sepharose. The experiments reported

here were performed in accordance with the guidelines established by the Brazilian College for Animal Experimentation and approved by FUNED Animal Ethics Committee.

3.2. Protein Characterization

The molecular masses (*M*r) of purified *Bl*K- and *Bl*D-PLA_2s were determined by SDS-PAGE (15% gel) and by MALDI TOF mass spectrometry. The *N*-terminal and the complete amino acid sequence of each protein was determined by automated Edman degradation using a Shimadzu PPSQ-21A protein sequencer according to the manufacturer's instructions.

3.3. MALDI-TOF Mass Spectrometry

Protein masses were determined by Matrix assisted laser desorption/ionization-time-of flight (MALDI-TOF) mass spectrometry. Spectra were recorded and analyzed using a Bruker Autoflex III Smartbeam instrument in the linear positive mode controlled by the proprietary COMPASS™ 1.2 software package. The Nd-YAG-laser power (355 nm) was manually adjusted for optimal signal appearance. A freeze-dried salt- and detergent-free sample was dissolved in few microliters of 30% ACN in 0.1% TFA. 0.5 µL was spotted on a ground steel target plate, mixed with 0.5 µL matrix solution (10 mg/mL sinapinic acid in 50% ACN, 0.1% TFA) and left to dry at room temperature. Commercially available standard protein mixtures were spotted on the same target for calibration purposes prior to sample analyses.

3.4. 2D-Electrophoresis (2-DE) and Image Analysis

The proteins (60 µg) of *B. leucurus* venom were separated by 2-DE. Prior to running the first dimension, the IPG strips were placed in the rehydration tray and the proteins were dissolved in the De Streak Rehydrate solution (GE Health Care, Uppsala, Sweden), 0.5% IPG buffer pH 3–10 (GE Health Care). First dimension IEF was carried out in an Ettan IPGphor 3 (GE Health Care) as described by the manufacturer. Immobiline strips 7 cm, pH 3–10 linear (GE Health Care) were employed for the first dimension separation at 20 °C using a four-phase electrophoresis program: 300 V to reach 200 Vh; 1000 V to reach 300 Vh; 5000 V to reach 4000 Vh; and 5000 V to reach 1250 Vh (total accumulated 5800 Vh with 50 µA/strip). Prior to running the second dimension the proteins in the strip were reduced and alkylated by sequential incubation in the following solutions: 75 mM Tris pH 8.8, 6 M urea, 3% glycerol, 2% SDS, 0.002% bromophenol blue (equilibration buffer-EB), 10 mg/mL DTT for 20 min; and then a solution of 25 mg/mL iodoacetamide in EB for 20 min. In addition, SDS-PAGE was done in a mini gel 7.5 cm 15% polyacrylamide gel. Proteins were visualized using Coomassie blue staining. Direct scanning and image analysis was performed using an Image Master 2D Platinum 7 (GE Health Care).

3.5. Protein Sequencing

The thiol groups of purified proteins (1.5 mg each) were S-reduced and alkylated with vinyl pyridine as described [43]. The material was dissolved in 1 mL of 0.1 M Tris-HCl (pH 8.6), 6 M guanidine-HCl. After addition of 30 µl β-mercaptoethanol the samples were incubated first at 50 °C

for 4 h under nitrogen, then with 40 µL of 4-vinyl pyridine in the dark at 37 °C for 2 h and subsequently desalted on a Vydac C4 column with a gradient of 0%–60% acetonitrile in 0.1% TFA. The *S*-pyridylethylated (PE) proteins were digested with trypsin (2% *w*/*w*, enzyme:substrate in 1 mL of 0.1 M ammonium bicarbonate, pH 7.9) for 3.5 h at 37 °C. The cleavage products were separated on a Vydac C18 small pore column (4.6 × 250 mm) in a linear gradient of 0%–50% acetonitrile in 0.1% aqueous TFA and sequenced using a Shimadzu PPSQ 21A protein sequencer. The primary structures of *Bl*K- and *Bl*D-PLA_2s were compared with the sequences of other related proteins in the SWISS-PROT/TREMBL data bases using the FASTA and BLAST programs.

3.6. Immunoblot and Enzyme-Linked Immunoabsorbent Assay (ELISA)

For analysis of immunological reactivity of several different snake venoms against the anti-*BlK*-PLA_2 IgG, western immunoblotting and ELISA were used. The *Bl*K- and *Bl*D-PLA_2s isoforms (4 µg each) was subjected to SDS-PAGE (15% gel) under reducing conditions, then eletrophoretically transferred onto a nitrocellulose membrane according to the manufacturer's (Bio-Rad, Richmond, CA, USA) instructions. One gel of 2-DE containing separated proteins from *B. leucurus* venom was also used for immunoblot assay under similar experimental conditions. ELISA plate was coated with 100 µL of 0.5 µg/well of each antigen (*Bl*-PLA_2s or crude venoms) in 0.05 M carbonate buffer, pH 9.6. After washing with 0.05% Tween-saline, a blocking solution (2% casein in phosphate buffered saline-PBS) was added (1 h at room temperature). After two washes with the same solution, anti-*BlK*-PLA_2 antibody previously diluted in PBS containing 0.25% casein and 0.05% Tween 20 (0.015 to 2 µg/well) was added and incubated for 1 h at 37 °C. After six washes, peroxidase-coupled anti-rabbit IgG (Sigma, St. Louis, MO, USA, diluted 1:12,000) was added and incubated for 1 h at room temperature. The wells were washed and 100 µL of peroxidase substrate OPD (0.33 mg/mL in citrate buffer, pH 5.2, in the presence of 0.012% H_2O_2) was added and the color reaction developed for 1 h in the dark. Absorbance was read with a micro-plate reader at 492 nm.

3.7. Cells and Viruses

Aedes albopictus cells (C6/36 Line, mosquito cells) were maintained in Leibovitz's medium (L-15, Gibco/Invitrogen) supplemented with 10% fetal bovine serum (FBS) (Gibco/Invitrogen), 100 U/mL penicillin G, and 100 µg/mL streptomycin (Gibco/Invitrogen) at 28 °C in a B.O.D. incubator. Rhesus Monkey Kidney Epithelial Cells (LLC-MK2 Line) were maintained with Dulbecco's modified Eagle's medium (DMEM) supplemented with 5% FBS, 100 U/mL penicillin G and 100 µg/mL streptomycin at 37 °C in a humidified 5% CO_2 atmosphere. The viruses DENV-1 (Brasil/98), DENV-2 (SpH 125367) and DENV-3 (RibH 1) were propagated in C6/36 cells and titrated using Dulbecco plaque technique [44] in LLC-MK2 cells. Aliquots were stored at −80 °C until required.

3.8. Determination of the Non-Cytotoxic Concentrations

The non-cytotoxic concentrations of the compounds *Bl*-PLA_2s (Pool, partially purified fraction containing both PLA_2s) and their isoforms *Bl*K- and *Bl*D-PLA_2s were determined by assessment of cell viability using the MTT [3-(4,5-dimethylthiazol-2-yl)-2,5-diphenyl tetrazolium bromide] assay

(Sigma). Confluent LLC-MK2 cells monolayers (4×10^4 cells/well) in 96-well microplates were exposed to different concentrations (0.1, 1.0, 10.0, 20.0, 40.0, and 80.0 μg/mL) of *Bl*-PLA$_2$s (Pool), and the purified enzymes for 48 h in a CO_2 incubator. After the incubation period, cells were observed using an inverted optical microscope (Nikon, Tokyo, Japan) and washed twice with PBS buffer (136.9 mM NaCl, 2.68 mM KCl, 8.1 mM Na_2HPO_4, 1.47 mM KH_2PO_4, pH 7.4). Then, 100 μL of MTT solution (0.5 mg/mL in DMEM) was added to each well and the plate was maintained in a CO_2 incubator. After 3 h of incubation at 37 °C the plates were centrifuged at 400 × *g* for 10 min. The supernatant was removed and 50 μL of dimethyl sulfoxide (DMSO) was added to each well to solubilize the formazan crystals. The absorbance was measured at 540 nm using an automated Microplate Reader, Pharmacia Biotech Ultrospec 1000. The cellular viability was calculated by comparison with untreated cells, which was set to 100% viability. Each data point was the mean value of triplicates from three independent experiments. The highest concentration of each compound without any significant toxicity ($p < 0.05$) was considered as the maximum non-toxic concentration (MNTC).

3.9. Antiviral Assay

Antiviral assays were conducted to evaluate whether any *Bl*-PLA$_2$s pool and/or isolated proteins could inhibit the multiplication of DENV in LLC-MK2 cells. *Bl*-PLA$_2$s was added at their maximum non-toxic concentrations (MNTCs) to confluent LLC-MK2 cells monolayers (1.9×10^5 cells/well) in 24-well plates. Afterwards, DENV-1 was added at a multiplicity of infection of 0.05 to treated and untreated cells, and the plates were incubated for 48 h in a 5% CO_2 humidified incubator. After this period, the cell supernatants were collected and submitted to RNA extraction for viral load quantification by quantitative Real-Time PCR (qRT-PCR). Two independent experiments were performed in triplicate. The antiviral assay was repeated using two different DENV serotypes (DENV-2 and DENV-3).

3.10. RNA Extraction

RNA was extracted from the supernatants (140 μL) of antiviral assays using QIAamp® Viral RNA Mini Kit (Qiagen, Hilden, Germany), following the manufacturer's protocol. An exogenous control (10 μL of cloned RNase P, corresponding to 1×10^5 RNA copies) was added to each sample prior to RNA extraction. Finally, the RNA was eluted in 60 μL of diethyl pyrocarbonate (DEPC) treated water (Sigma) and maintained at −80 °C.

3.11. Generation of RNA Standard

Using pGEM-T Easy vector (Promega, Madison, WI, USA), two plasmids were constructed by cloning the 67 bp amplicon of 3'UTR region from DENV-1, consensus to the four serotypes of DENV [45], and 64 bp amplicon from Human RNAseP [46]. The amplicons were generated by SuperScript® III Platinum One-Step qRT-PCR System (Invitrogen, Carlsbad, CA, USA) using the primers shown in Table 1, according to the manufacture's instructions. The presence and orientation of the insert DNA were confirmed by sequencing. The plasmids were linearized by digestion with Nde I and the target sequences were amplified using MEGAscript® High Yield Transcription Kit (Ambion,

Austin, TX, USA). The transcribed RNAs were treated with DNAse (Invitrogen) and purified using the MEGAclear™Kit (Ambion). The RNAs were quantified by spectrophotometry (Genequant, Amersham Pharmacia Biotec, Cambridge, England). The copy numbers of the RNAs were calculated based on the concentrations and their molecular weights and 10-fold serial dilutions of these RNAs, ranging from 10^7 to 10^3 copies/µL were used as standards in all qRT-PCRs. The detection limit of the assay was verified from successive dilutions of the standards until detection was impossible or inaccurate.

Table 1. Probes and primer sequences for Dengue virus, DENV (3'UTR) and exogenous control (RnaseP) used in quantitative Real-Time PCR assay.

Target	Sequence (5'-3')	Nucleotide position
3'UTR-F	GARAGACCAGAGATCCTGCTGTCT	10,647–10,670
3'UTR-R	ACCATTCCATTTTCTGGCGTT	10,714–10,694
3'UTR-Probe	VIC-AGCATCATTCCAGGCAC-MGB-NFQ	10,675–10,691
RnaseP-F	AGATTTGGACCTGCGAGCG	50–68
RnaseP-R	GAGCGGCTGTCTCCACAAGT	114–95
RnaseP-Probe	FAM-TTCTGACCTGAAGGCTCTGCGCG-BHQ1	71–91

3.12. Quantitative Real-Time PCR

Quantitative Real-Time PCR was performed using a Real-Time PCR System StepOnePlus (Applied Biosystems, Foster City, CA, USA) and SuperScript™ III Platinum® One-Step qRT-PCR System (Invitrogen). Amplifications were carried out in reaction mixtures containing 5 µL of transcribed or viral RNA, 0.5 µL of SuperScript™/Platinum® Taq Mix, 2x reaction mix buffer, 0.4 µM of primers to DENV, 0.2 µM of primers to RnaseP, 0.2 µM of TaqMan probe to DENV, 0.1 µM of TaqMan probe to RnaseP (Applied Biosystems) (see Table 1), 0.25 µL of ROX Reference Dye, 0.5 µL of RNaseOUT™ (Invitrogen), and DEPC-treated water to 25 µL final volume. The cycling program consisted of an RT step at 50 °C for 30 min, initial denaturation at 95 °C for 2 min, followed by 40 cycles at 95 °C for 15 s and 60 °C for 1 min. Each reaction set was checked for contamination using negative control (all reagents included and water instead of DNA). In addition to this negative control, cells not infected were included in the assay.

3.13. Statistical Analysis

Data were expressed as means ± standard error (SE). Statistical differences were determined by the nonparametric Tukey's Multiple Comparison Test. Pearson's correlation (R) was used to evaluate the relationship between Cycle threshold (Ct) and quantity of RNA on standard curves of qRT-PCR. Values of $p < 0.05$ were considered significant.

4. Conclusions

We have described the main structural properties of two basic svPLA$_2$s, *Bl*K- without and *Bl*D-PLA$_2$s with hydrolytic activity from *B. leucurus* venom. The promising results observed in our antiviral assays, with decreased amounts of viral RNA quantified in cells treated with *Bl*-PLA$_2$s, opening up possibilities for biotechnological applications of these molecules as research tools.

Furthermore, the data suggest that, in addition to catalytic activity, the physiological role of *Bl*PLA$_2$s can be mediated by ligation to specific receptors on the cell membrane, which is in accord with the higher penetrability of most basic svPLA$_2$s compared to neutral and acidic enzymes [36] and others. Thus, consistent with these findings, *Bl*-PLA$_2$s display cytotoxic properties against DENV *in vitro*, suggesting that they are useful tools against DENV or as a prototype to develop anti-dengue drug.

Acknowledgments

We thank Gena Medeiros for her collaboration. This work was supported by the Brazilian Agencies: Conselho Nacional de Desenvolvimento Científico e Tecnológico (CNPq, Grant No: 482502/2012-6 to EFS), Coordenação de Aperfeiçoamento de Pessoal de Nível Superior (CAPES, Grant No: 23038000825/2011-63), and Fundação de Amparo a Pesquisa do Estado de Minas Gerais (FAPEMIG, Grant No: CBB APQ 01791-10 to EFS), and Deustsche Forschungsgemeinschaft (DFG grant: SFB815, Project A6 to JAE).

Conflicts of Interest

The authors declare no conflicts of interest.

References

1. Koh, D.C.I.; Armugan, A.; Jeyaseelan, K. Snake venom components and their applications in biomedicine. *Cell. Mol. Life Sci.* **2006**, *63*, 3030–3041.
2. Kini, R.M. Toxins in thrombosis and haemostasis, potential beyond imagination. *J. Thromb. Haemost.* **2011**, *9*, 193–208.
3. Koh, C.Y.; Kini, R.M. From snake venom toxins to therapeutic-cardiovascular examples. *Toxicon* **2012**, *59*, 497–506.
4. Lomonte, B.; Sasa, A.Y.; Gutierrez, J.M. The phospholipase A$_2$ homologues of snake venoms, biological activities and their possible adaptative roles. *Protein Pept. Lett.* **2009**, *16*, 860–876.
5. Samy, R.P.; Gopalakrishnakone, P.; Kesturu, G.; Swamy, S.N.; Hemshekhar, M.; Tan, K.S.; Rowan, G.E.G.; Stiles, B.G.; Chow, V.T.K. Snake venom phospholipases A$_2$: A novel tool against bacterial diseases. *Curr. Med. Chem.* **2012**, *19*, 6150–6162.
6. Doley, R.; Zhou, X.; Kini, R.M. Snake Venom Phospholipase A$_2$ Enzymes. In *Handbook of Venoms and Toxins of Reptiles*; Mackessy, S.P., Ed.; CRC Press: New York, NY, USA, 2010; pp. 173–198.
7. Huang, P.; Mackessy, S.P. Biochemical characterization of phospholipase A$_2$ (trimorphin) from the venom of the Sonoran lyre snake *Trimorphodon biscutatus lambda* (family Colubridae). *Toxicon* **2004**, *44*, 25–43.
8. Six, D.A.; Dennis, E.A. The expanding of superfamily of phospholipase A$_2$ enzymes, classification and characterization. *Biochim. Biophys. Acta* **2000**, *1488*, 1–19.
9. Bazaa, A.; Luis, J.; Srairi-Abid, N.; Kallech-Ziri, O.; Kessentini-Zouari, R. MVL-PLA$_2$; a phospholipase A$_2$ from *Microvipera lebetine transmediterranea* venom; inhibits tumor cells adhesion and migration. *Matrix Biol.* **2009**, *28*, 188–193.

10. Bazaa, A.; Pasquier, E.; Defilles, C.; Limam, I.; Kessentini-Zouari, R.; Kallech-Ziri, O.; el Battari, A.; Braguer, D.; el Ayeb, M.; Marrakchi, N.; *et al*. MVL-PLA$_2$; a snake venom phospholipase A$_2$; inhibits angiogenesis through an increase in microtubule dynamics and disorganization of focal adhesions. *PLoS One* **2010**, 5, e10124.
11. Khunsap, S.; Pakmanee, N.; Khow, O.; Chanhome, L.; Sitprija, V.; Suntravat, M.; Lucena, S.E.; Perez, J.C.; Sánchez, E.E. Purification of a phospholipase A$_2$ from *Daboia russelli siamensis* venom with anticancer effects. *J. Venom. Res.* **2011**, *2*, 42–51.
12. Samy, R.P.; Pachiappan, A.; Gopalakrishnakone, P.; Thwin, M.M.; Hian, Y.E.; Chow, V.T.K.; Bow, H.; Weng, J.T. *In vitro* antimicrobial activity of natural toxins and animal venoms tested against *Burkholderia pseudomallei*. *BMC Infect. Dis.* **2006**, *6*, 1–16.
13. Vargas, L.J.; Londoño, M.; Quintana, J.C.; Rua, C.; Segura, C.; Lomonte, B.; Nuñez, V. An acidic phospholipase A$_2$ with antibacterial activity from *Porthidium nasutum* venom. *Comp. Biochem. Physiol. B* **2012**, *161*, 341–347.
14. Gunther, A.G.; Stegmann, T. How lysophosphatidylcholine inhibits cell-cell fusion mediated by the envelope glycoprotein of human immunodeficiency virus. *Virology* **1997**, *235*, 201–208.
15. Fenard, D.; Lambeau, G.; Valentin, E.; Lefebvre, J.C.; Lazdunski, M.; Doglio, A. Secreted phospholipases A$_2$; a new class of HIV inhibitors that block virus entry into host cells. *J. Clin. Invest.* **1999**, *104*, 611–618.
16. Ooi, E.E.; Gubler, D.J. Global spread of epidemic dengue, the influence of environmental change. *Future Virol*. **2009**, *4*, 571–580.
17. Hotez, P.J.; Bottazzi, M.E.; Franco-Paredes, C.; Ault, S.K.; Periago, M.R. The neglected tropical diseases of Latin America and the Caribbean, a review of disease burden and distribution of a roadmap for control and elimination. *PLoS Negl. Trop. Dis.* **2008**, *2*, e300.
18. World Health Organization (WHO). Impact of Dengue. Available online: http//www.who.int/csr/disease/dengue/impact/em (accessed on 31 May 2013).
19. Thomas, S.J.; Strickman, D.; Vuaghan, D.W. Dengue epidemiology; ecology; resurgence. *Adv. Virus Res.* **2003**, *61*, 235–289.
20. Shepard, D.S.; Coudeville, L.; Halasa, Y.A.; Zambrano, B.; Dayan, G.H. Economic impact of dengue illness in the Americas. *Am. J. Trop. Med. Hyg.* **2011**, *84*, 200–207.
21. Whitehead, S.S.; Blaney, J.E.; Durbin, A.P.; Murphy, B.R. Prospects for a dengue virus vaccine. *Nat. Rev. Microbiol.* **2007**, *5*, 518–528.
22. Porto, M.; Teixeira, D.M. *Bothrops leucurus* (White-tailed-lancehead). *Herpetol. Rev.* **1995**, *26*, 156.
23. Sanchez, E.F.; Eble, J.A. P-III Metalloproteinase (Leucurolysin-B) from *Bothrops Leucurus* Venom, Isolation and Possible Inhibition. In *Drug Design of Zinc-Enzyme Inhibitors*; Supuran, C.T., Winum, J.-Y., Eds.; John Wiley & Sons Inc: Hoboken, NJ, USA, 2009; pp. 789–812.

24. Higuchi, D.A.; Barbosa, C.M.V.; Bincoleto, C.; Chagas, J.R.; Magalhaes, A.; Richardson, M.; Sanchez, E.F.; Pesquero, J.B.; Araujo, R.C.; Pesquero, J.L. Purification and partial characterization of two phospholipases A_2 from *Bothrops leucurus* (white-tailed-jararaca) snake venom. *Biochimie* **2007**, *89*, 319–328.
25. Muller, V.D.M.; Russo, R.R.; Cintra, A.D.O.; Sartim, M.A.; Alves-Paiva, R.M.; Figueiredo, L.T.M.; Sampaio, S.V.; Aquino, V.H. Crotoxin and phospholipases A_2 from *Crotalus. durissus terrificus* showed antiviral activity against dengue and yellow fever viruses. *Toxicon* **2012**, *59*, 507–515.
26. Julander, J.G.; Perry, S.T.; Shresta, S. Important advances in the field of anti-dengue virus research. *Antivir. Chem. Chemother.* **2011**, *21*, 105–116.
27. Mattiazzi, M.; Sun, Y.; Wolinski, H.; Bavdek, A.; Petan, T.; Anderluh, G.; Kohlwein, S.D.; Drubin, D.G.; Krizaj, I.; Petrovic, U. A neurotoxic phospholipase A_2 impairs yeast amphiphysin activity and reduces endocytosis. *PLoS One* **2012**, *7*, e40931.
28. Petricevich, V.L.; Mendonça, R.Z. Inhibitory potential of *Crotalus durissus terrificus* venom on measles virus growth. *Toxicon* **2003**, *42*, 143–153.
29. Larkin, M.A.; Blackshilds, G.; Brown, N.P.; Chenna, R.; McGettigan, P.A.; McWilliam, H.; Valentin, F.; Wallace, I.M.; Wilm, A.; Lopez, R.; *et al*. Clustal and Clustal X version 2.0. *Bioinformatics* **2007**, *23*, 2947–2948.
30. Scott, D.L. Phospholipase A_2 Structure and Catalytic Properties. In *Venom Phospholipase A_2 Enzymes, Structure; Function and Mechanism*; Kini, R.M., Ed.; John Wiley & Sons: Chichester, UK, 1997; pp. 97–128.
31. Páramo, L.; Lomonte, B.; Pizarro-Cerda, J.; Bengoechea, J.A.; Gorvel, J.P.; Moreno, E. Bactericidal activity of Lys49 and Asp49 myotoxic phaspholipases A_2 from *Bothrops asper* snake venom. *Eur. J. Biochem.* **1998**, *253*, 452–561.
32. Watanabe, L.; Fontes, M.R.; Soares, A.M.; Giglio, J.R.; Arni, R.K. Initiating structural studies of Lys49-PLA_2 homologues complexed with an anionic detergent; a fatty acid and a natural lipid. *Protein Pep. Lett.* **2003**, *10*, 525–530.
33. Freedman, J.E.; Snyder, S.H. Vipoxin. A protein from Russell's viper venom with high affinity for biogenic amine receptors. *J. Biol. Chem.* **1981**, *256*, 13172–13179.
34. Guindon, S.; Dufayard, J.F.; Lefort, V.; Anisimova, M.; Hordijk, W.; Gascuel, O. New algorithms and methods to estimate maximum-likelihood phylogenies: Assessing the performance of PhyML 3.0. *Syst. Biol.* **2010**, *59*, 307–321.
35. Polgar, J.; Magnenat, E.M.; Peitsch, M.C.; Wells, T.N.; Clemetson, K.J. Asp-49 is not an absolute prerequisite for the enzymic activity of low-Mr phospholipase A_2, Purification; characterization and computer modelling of an enzymically active Ser-49 phospholipase A_2; ecarpholin S; from the venom of *Echis carinatus sochureki* (saw-scaled viper). *Biochem. J.* **1996**, *319*, 965–968.
36. Chijiwa, T.; Tokunaga, E.; Ikeda, R.; Tereda, K.; Ogawa, T.; Oda-Ueda, N.; Hattori, S.; Nozaki, M.; Ohno, M. Discovery of novel Arg49 phospholipase A_2 isozyme from *Phrotobothrops elegans* venom and regional evolution of *Crotalinae* snake venom phospholipase A_2 isozymes in the southwestern islands of Japan and Taiwan. *Toxicon* **2006**, *48*, 672–682.
37. Fry, B.G.; Wüster, W. Assembling an arsenal, Origin and evolution of the snake venom proteome inferred from Phylogenetic analysis of toxin sequences. *Mol. Biol. Evol*. **2004**, *21*, 870–883.

38. Fry, B.G.; Scheib, H.; van der Weer, L.; Young, B.; McNaughtan, J.; Ramjan, S.F.R.; Vidal, N.; Poelmann, R.E.; Norman, J.A. Evolution of an arsenal. *Mol. Cell. Proteomics* **2008**, *7*, 215–246.
39. Cummings, K.L.; Tarleton, R.L. Rapid quantitation of *Trypanosoma cruzi* in host tissue by real-time PCR. *Mol. Biochem. Parasitol.* **2003**, *129*, 53–59.
40. Trane, L.D.; Bedini, B.; Donatelli, I.; Campitelli, L.; Chiappini, B.; de Marco, M.A.; Delogu, M.; Buonaboglia, C.; Vaccari, G. A sensitive one-step real time PCR for detection of avian influence viruses using a MGB probe and an internal positive control. *BMC Infect. Dis.* **2006**, *6*, 87.
41. Caldas, S.; Caldas, I.S.; Diniz, L.F.; Lima, W.G.; Oliveira, R.P.; Cecílio, A.B.; Ribeiro, I.; Talvania, A.; Bahia, M.T. Real-Time PCR strategy for parasite quantification in blood and tissue samples of experimental *Trypanosoma cruzi* infection. *Acta Trop.* **2012**, *123*, 170–177.
42. Naumann, G.B.; Silva, L.F.; Silva, L.; Faria, G.; Richardson, M.; Evangelista, K.; Kohlhoff, M.; Gontijo, C.M.F.; Navdaev, A.; Rezende, F.F.; *et al*. Cytotoxicity and inhibition of platelet aggregation caused by an L-amino acid oxidase from *Bopthrops leucurus* venom. *Biochim. Biophys. Acta* **2011**, *1810*, 683–694.
43. Wilson, K.J.; Yuan, P.M. Protein and Peptide Purification. In *Protein Sequencing a Practical Approach*; Findlay, J.B.C., Geisow, M.J., Eds.; IRL Press: Oxford, UK, 1989; pp. 3–41.
44. Dulbecco, R. Microbiology. In *Evolution of Microbiology and Microbes*; Dulbecco, R., Ed.; Lippincott Company: Philadelphia, PA, USA, 1994; pp.769–795.
45. Gurukumar, K.R.; Priyadarshini, D.; Patil, J.A.; Bhagat, A.; Singh, A.; Shah, S.; Cecilia, D. Development of real time PCR for detection and quantitation of Dengue Viruses. *Virol. J.* **2009**, *6*, 10.
46. World Health Organization. CDC protocol of real time RT PCR for influenza A (H1N1). Version 2009, Swine Influenza. Available online: http://www.who.int/csr/resources/publications/swineflu/CDCrealtimeRTPCRprotocol20090428.pdf (accessed on 27 June 2013).

© 2013 by the authors; licensee MDPI, Basel, Switzerland. This article is an open access article distributed under the terms and conditions of the Creative Commons Attribution license (http://creativecommons.org/licenses/by/3.0/).